DYNAMIC ANALYSIS OF DAM-RESERVOIR-FOUNDATION COUPLED SYSTEMS WITH INCLINED RESERVOIR BED

Thesis submitted by

SANTOSH KUMAR DAS

DOCTOR OF PHILOSOPHY IN ENGINEERING

CIVIL ENGINEERING DEPARTMENT
FACULTY COUNCIL OF ENGINEERING & TECHNOLOGY
JADAVPUR UNIVERSITY
KOLKATA-700032, INDIA

2023

INDEX NO.: 146/17/E

1. Title of the Thesis:

DYNAMIC ANALYSIS OF DAM-RESERVOIR-FOUNDATION COUPLED SYSTEMS WITH INCLINED RESERVOIR BED

2. Name, Designation and Institution of the Supervisors:

(1) Prof. (Dr.) Kalyan Kumar Mandal,
Associate Professor,
Department of Civil Engineering,
Jadavpur University,
Kolkata-700032, India.

(2) Prof. (Dr.) Arup Guha Niyogi,
Professor,
Department of Civil Engineering,
Jadavpur University,
Kolkata-700032, India.

3. List of Publications:

(i) Santosh Kumar Das, Kalyan Kumar Mandal and Arup Guha Niyogi (2022) Finite element-based direct coupling approach for dynamic analysis of dam–reservoir system. Innovative Infrastructure Solutions 8 (44):1-15. publisher-Springer.

(ii) Santosh Kumar Das, Kalyan Kumar Mandal and Arup Guha Niyogi (2022) A finite element based approach to observe hydrodynamic pressure in reservoir adjacent to concrete gravity dam. Ocean Systems Engineering 12(4): 385-402. publisher-Techno press.

4. List of Presentations in National/International Conferences/Workshops:

(i) Santosh Kumar Das, Kalyan Kumar Mandal and Arup Guha Niyogi (2020) Earthquake induced Hydrodynamic Pressure in Reservoir adjacent to Concrete Gravity Dam. Presented in Second ASCE India Conference on Challenges of Resilient and Sustainable Infrastructure Development in Emerging Economies (CRSIDE 2020).

(ii) Santosh Kumar Das, Kalyan Kumar Mandal and Arup Guha Niyogi (2020) Evaluation of Hydrodynamic Pressure on concrete Gravity Dam considering Reservoir-Dam interaction. Presented in International conference on Sustainable water resource management under changed climate, Organized by School of Water resource Engineering, Jadavpur University, Kolkata.

(iii) Santosh Kumar Das, Kalyan Kumar Mandal and Arup Guha Niyogi, (2022) Evaluation of Hydrodynamic Pressure in Reservoir Adjacent to Concrete Gravity Dam using Finite Element Technique. Presented in Second International Conference on Research Trends in Engineering and Management (ICRTEM 2022), Organized by R R Institute of Technology, Bangalore, India with IFERP.

STATEMENT OF ORIGINALITY

I, Santosh Kumar Das, registered on 07.04.2017 do hereby declare that this thesis entitled "**Dynamic Analysis of Dam-Reservoir-Foundation Coupled Systems with Inclined Reservoir Bed**" contains literature survey and original research work done by the undersigned candidate as part of Doctoral studies.

All information in this thesis have been obtained and presented in accordance with existing academic rules and ethical conduct. I declare that, as required by these rules and conduct, I have fully cited and referred all materials and results that are not original to this work.

I also declare that I have checked this thesis as per the "Policy on Anti Plagiarism, Jadavpur University, 2019", and the level of similarity as checked by iThenticate software is 4%.

Santosh kumar Das.
Signature of Candidate:

Date: 8/6/23

Certified by Supervisor(s):

(Signature with date, seal)

1. Kalyan kr. Mandal 08/06/2023
Associate Professor
Department of Civil Engineering
Jadavpur University
Kolkata-700 032

2. 08/06/2023
Professor
CIVIL ENGINEERING DEPARTMENT
JADAVPUR UNIVERSITY
KOLKATA-32

CERTIFICATE FROM THE SUPERVISOR(S)

This is to certify that the thesis entitled "**Dynamic Analysis of Dam-Reservoir-Foundation Coupled Systems with Inclined Reservoir Bed**" submitted by **Shri Santosh Kumar Das**, who got his name registered on 07.04.2017 for the award of Ph.D. (Engineering) degree of Jadavpur University is absolutely based upon his own work under the supervision of **Prof. (Dr.) Kalyan Kumar Mandal**, Associate Professor, Department of Civil Engineering, Jadavpur University & **Prof. (Dr.) Arup Guha Niyogi**, Professor, Department of Civil Engineering, Jadavpur University and that neither his thesis nor any part of the thesis has been submitted for any degree/ diploma or any other academic award anywhere before.

1. Kalyan Kr. Mandal 08/06/2023
Signature of the Supervisor
and date with Office Seal

Associate Professor
Department of Civil Engineering
Jadavpur University
Kolkata-700 032

2. 08/06/2023
Signature of the Supervisor
and date with Office Seal

Professor
CIVIL ENGINEERING DEPARTMENT
JADAVPUR UNIVERSITY
KOLKATA-32

ACKNOWLEDGEMENTS

I feel proud to express my profound and heartfelt gratitude to my research supervisors, Prof. (Dr.) Kalyan Kumar Mandal & Prof. (Dr.) Arup Guha Niyogi, without whose constant source of inspiration throughout my study, I am not able to complete this thesis. I am grateful to them for their valuable guidance, encouragement and continuous support throughout my research work.

I would like to offer thanks to Prof. (Dr.) Partha Bhattacharya (Present HOD, Civil Engineering Department) and my colleagues of the Civil Engineering Department, Jadavpur University for their valuable support and cooperation in my research work.

I am extremely thankful to my friends for their continuous encouragement and support during the time of my research.

My deepest gratitude goes to my respected parents, my lovely wife and my dear son for supporting me throughout my life. Their love and understanding have allowed me to make it successfully.

Finally, I bow down before the Almighty who had made everything possible.

Place: Jadavpur University

Santosh kumar Das.

Santosh Kumar Das

8/6/23

ABSTRACT

Concrete gravity dam should be designed considering dynamic exciting force so that it can sustain earthquake excitations. Hydrodynamic pressure develops at the face of the gravity dam during the earthquake. Variation of hydrodynamic pressure depends on the geometrical parameters of the adjacent reservoir. Inclination of the reservoir bed, inclined length of the reservoir base and reflection coefficient of the reservoir bottom are examples of such parameters influencing the hydrodynamic pressure of the reservoir and stresses of the gravity dam. In this study, the focus has been given to the variation of hydrodynamic pressure and stresses in the gravity dam for those parameters by applying dynamic excitations.

Fluid is considered compressible and inviscid and its motion is irrotational with small amplitude. Two-dimensional geometry of the dam, reservoir and foundation has been modelled using finite element. Standard eight-node isoparametric element has been used for the discretization of the dam, reservoir and foundation domain. Pressure is considered as nodal variable in the fluid domain following the Eulerian approach and displacement is considered as nodal variable for the gravity dam and foundation following the Lagrangian approach. Both dam and foundation are in plane strain condition. Length of the reservoir has been truncated to a suitable distance for saving computational time. A suitable non-reflecting boundary condition is applied along the truncated face of the reservoir. Similarly, along the truncated face of the foundation viscous boundary condition has been implemented. The effect of the surface wave is neglected. However, reservoir bottom absorption is considered in the study.

In the present study, dam-reservoir and dam-foundation interactions are included for the dynamic analysis of dam-reservoir-foundation systems. Analysis has been carried out by direct coupling approach of dam-reservoir-foundation coupled systems. A MATLAB code has been generated for numerical simulation. Hydrodynamic pressure of the reservoir and major and minor principal stresses of the dam and foundation have been observed by applying harmonic and earthquake excitations.

From the present study, it is clear that when the bed slope of the reservoir is in the anticlockwise direction the hydrodynamic pressure and stresses at the heel of the dam always increased due to an increase in slope angle. The stress of the foundation under the heel decreased with the increase of bed slope when aligned in anticlockwise direction. When the slope of the reservoir bed is in anticlockwise direction, the inclined reservoir bed is towards

the concrete gravity dam. Hence, the reservoir bed reflects the wave towards the gravity dam and enhances the hydrodynamic pressure and stresses at the heel of the dam. Again, due to the reduction in stiffness of the soil for the reduction in volume, the stress below the heel of the dam is decreasing for an anticlockwise slope. It is also observed that when the bed slope of the reservoir is in the clockwise direction the hydrodynamic pressure and stresses at the heel of the dam always decreased due to an increase in slope angle. The stress of the foundation under the heel increased with the increase of bed slope for clockwise slope. In the case of clockwise slope, the reflecting wave from the bed of the reservoir is going away from the gravity dam and decreases the pressure and stress at the heel of the dam. The stiffness of soil is increased due to an increase in volume in the case of clockwise slope. Hence, the stress in the foundation below the heel is decreasing.

Keywords: *Dam-reservoir-foundation coupled system; Non-reflecting boundary condition; viscous boundary condition; Inclined reservoir bottom; Hydrodynamic pressure; Earthquake Excitation*

CONTENTS

Chapter 3: THEORETICAL FORMULATION

Chapter 4: RESULTS AND DISCUSSION

LIST OF FIGURES

LIST OF TABLES

LIST OF SYMBOLS

$[M_d]$	Mass matrix of structure
$[C_d]$	Damping matrix of structure
$[K_d]$	Stiffness matrix of structure
$\{F_d\}$	Nodal force of Finite element model of structure
$\{\ddot{u}_d\}$	Nodal acceleration of Finite element model of structure
$\{\dot{u}_d\}$	Nodal displacement of Finite element model of structure
$\{u_d\}$	Nodal velocity of Finite element model of structure
$[D]$	Elasticity matrix of the structure
E	Young's modulus
ν	Poisson's ratio
$N_{1,2\ldots8}$	Shape functions of eight-node isoparametric element
B	Strain displacement matrix
J	Jacobian matrix
ξ, η	Local coordinate axis of finite element
a' and b'	Proportional damping constant
ξ'	Damping constant
ω	Angular frequency
T_{ij}	Total stress of fluid
T'_{ij}	Viscous stress tensor
p	Hydrodynamic pressure
δ_{ij}	Kronecker delta
μ	Coefficient of viscosity
λ	Material constants
D_{ij}	Rate of deformation tensor
B_i	Body force of fluid
c	Velocity of sound wave in the fluid domain
∇^2	Laplacian operator in two dimensions

g	Gravitational acceleration
H_f	Depth of the reservoir
$ae^{i\omega t}$	Horizontal component of the ground motion
n	Outwardly directed normal to the interface of dam and reservoir
α	Reflection coefficient of the reservoir bottom
q	Quantity related to reflection coefficient
ξ_m	Coefficient of boundary condition of Gogoi and Maity
$I_m, \Psi_m, \lambda_m, \beta_m, K_m, \Omega, \chi$	Quantities related to boundary condition of Gogoi and Maity
N_{rj}	Interpolation functions of the fluid domain
Ω	Region of fluid
$\boldsymbol{\Gamma}$	Boundary of fluid
$[J]$	Matrix analogous to mass matrix for equation of fluid motion
$[A]$	Matrix analogous to damping matrix for equation of fluid motion
$[H]$	Matrix analogous to stiffness matrix for equation of fluid motion
$\{F_f\}$	Force component at top surface of the reservoir
$\{F_{fs}\}$	Force component at dam-reservoir interface
$\{F_{fb}\}$	Force component at reservoir-bed interface
$\{F_t\}$	Force component at truncation surface of reservoir
$[R_f]$	Matrix related to $\{F_f\}$
$[R_{fs}]$	Matrix related to$\{F_{fs}\}$
$[R_{fb}]$	Matrix related to $\{F_{fb}\}$
$[R_t]$	Matrix related to $\{F_t\}$
t	Time step of dynamic excitation
v_t	Velocity of fluid at time *t*
u_t	Displacement at time *t*
Δt	Time difference between two steps of excitation
$[Q]$	The coupling term between dam and reservoir

$\ddot{u}_g$	Horizontal component of ground acceleration
N_{dr}	Interpolation function of line element at the dam-reservoir interface
F_r	Force on reservoir
β and γ	Coefficient of Newmark's integration method
σ and τ	Normal and shear stresses at the truncated boundary of the soil medium
c_n and c_t	damping coefficient in normal and tangential directions
G	Shear modulus
c_s and c_p	Compression wave and shear wave velocity
A_1 and A_2	Areas governed by the direction of wave propagation
$[Q_d]$	Coupling matrix connected with the nodes of the dam body
$[Q_c]$	Coupling matrix connected with the nodes of common nodes at the junction of the dam and soil foundation
M_{dd}	Mass matrix of dam related to dam other than common node
M_{dc}	Mass matrix of dam related to common node
M_{fc}	Mass matrix of foundation related to common node
M_{ff}	Mass matrix of foundation related to foundation other than common node
M_{cd}	Mass matrix at common node related to dam
M_{cc}	Mass matrix at common node only
M_{cf}	Mass matrix at common node related to foundation
K_{dd}	Stiffness matrix of dam related to dam other than common node
K_{dc}	Stiffness matrix of dam related to common node
K_{fc}	Stiffness matrix of foundation related to common node
K_{ff}	Stiffness matrix of foundation related to foundation other than common node
K_{cd}	Stiffness matrix at common node related to dam
K_{cc}	Stiffness matrix at common node only
K_{cf}	Stiffness matrix at common node related to foundation

C_{dd}	Damping matrix of dam related to dam other than common node
C_{dc}	Damping matrix of dam related to common node
C_{fc}	Damping matrix of foundation related to common node
C_{ff}	Damping matrix of foundation related to foundation other than common node
C_{cd}	Damping matrix at common node related to dam
C_{cc}	Damping matrix at common node only
C_{cf}	Damping matrix at common node related to foundation
$\ddot{P}$	Double derivative of nodal pressure of fluid
$\ddot{U}_{ad}, \ddot{U}_{ac}$and $\ddot{U}_{af}$	Acceleration component (absolute response) related to dam, common node of dam-foundation and foundation**.**
$\dot{P}$	Derivative of nodal pressure of fluid
$\dot{U}_{ad}, \dot{U}a_c\ and \dot{U}_{af}$	Velocity component (absolute response) related to dam, common node of dam-foundation and foundation**.**
P	Nodal pressure of fluid
U_{ad},Ua_c and U_{af}	Displacement component (absolute response) related to dam, common node of dam-foundation and foundation**.**
$\ddot{P}^{ff}$	Free field part of Double derivative of nodal pressure of fluid
$\ddot{u}_d^{ff}, \ddot{u}_c^{ff}, \ddot{u}_f^{ff}$	Free field part of acceleration component related to dam, common node of dam-foundation and foundation**.**
$\ddot{P}^a$	Added part of Double derivative of nodal pressure of fluid
$\ddot{u}_d^a, \ddot{u}_c^a\ and \ddot{u}_f^a$	Added part of acceleration component related to dam, common node of dam-foundation and foundation**.**
$\dot{P}^{ff}$	Free field part of derivative of nodal pressure of fluid
$\dot{u}_d^{ff}, \dot{u}_c^{ff} and \dot{u}_f^{ff}$	Free field part of velocity component related to dam, common node of dam-foundation and foundation**.**
$\dot{P}^a$	Added part of derivative of nodal pressure of fluid
$\dot{u}_d^a, \dot{u}_c^a\ and \dot{u}_f^a$	Added part of velocity component related to dam, common node of dam-foundation and foundation**.**

P^{ff}	Free field part of Nodal pressure of fluid
$u_d^{ff}, u_c^{ff} and u_f^{ff}$	Free field part of displacement component related to dam, common node of dam-foundation and foundation.
P^a	Added part of nodal pressure of fluid
$u_d^a, u_c^a \ and u_f^a$	Added part of displacement component related to dam, common node of dam-foundation and foundation.
$\ddot{U}_d^g, \ddot{U}_c^g and \ddot{U}_f^g$	Horizontal component of ground acceleration related to dam, common node of dam-foundation and foundation
R	Reaction due to free field portion
F	Force due to ground acceleration
C_p	Coefficient of pressure (ratio of hydrodynamic pressure to hydrostatic pressure)
T	Time period of vibration
a	Ground acceleration
L	Length of the reservoir
N_h	Number of divisions in horizontal direction of finite element mesh
N_v	Number of divisions in vertical direction of finite element mesh
θ_b	Slope angle of reservoir bottom with respect to horizontal base
Li	Inclined length of reservoir base
ρ_f	Density of fluid
q	Variable used for Newmark's method

CHAPTER 1

INTRODUCTION

1.1 GENERAL

Concrete gravity dam is an important structure for civilization. The structure holds huge amount of water necessary for cultivation, flood protection, and hydropower generation, etc. The design and construction of a gravity dam should be done cautiously laying utmost importance to their safety and sustainability. Accounting seismic response of concrete gravity dam precisely is very important for safeguarding dam structures. Gravity dam has to sustain hydrodynamic pressure originating due to earthquakes along with the other critical loads. A thorough study on the hydrodynamic pressure and responses of a gravity dam is essential for a safe design of the dam. The hydrodynamic behaviour of the adjacent reservoir depends on quite a few geometrical parameters, namely, bed slope, length of reservoir bed, inclination of the upstream face of the dam, etc. Seismic response of the dam-reservoir system must be assessed for these geometrical parameters to understand the interactive behaviour. Very few literatures are found to exist in open sources that deal with hydrodynamic studies of any reservoir due to changes in the bottom slope of the reservoir and its inclined length. Hence, in the present work the focus has been laid on studying the variations of hydrodynamic pressure and responses of the gravity dam for variation of slope angle of reservoir bottom and inclined length of reservoir base. Change in pressure is also observed for variation of the reflection coefficient of the reservoir bottom.

Fluid has been considered to be compressible, inviscid and irrotational, while showing up small amplitude waves when excited. The geometry of the reservoir, dam and foundation are considered two-dimensional. The irregular geometry of the dam and reservoir has been modelled using finite element technique. In the present study, eight-node isoparametric serendipity elements have been used for discretisation of the dam, reservoir, and foundation system. Most of the previous researchers have modelled the fluid domain using finite element along with different field variables such as displacement and pressure, etc. Among them, the displacement-based formulation may create circulation modes. These circulation modes are meaningless and subject to zero frequencies. In the present study, pressure has been considered as an unknown variable following the Eulerian approach to overcome the problem related to

the displacement-based formulation. As a result, the number of unknowns at every node is reduced to a single variable for the reservoir domain and computation time has reduced. However, displacement is considered as nodal variable for the dam and foundation following Lagrangian approach. Rayleigh damping has been used as structural damping for the dam and foundation. The dissipation of energy in form of waves influences the hydrodynamic behaviour of the reservoir and dam. Proper absorbing boundary must be ensured along the truncation surface of the reservoir and foundation to make them finite. Reservoir bottom absorption is also an important parameter for the hydrodynamic study of the dam-reservoir system. Behaviour of the reservoir for a change of reflection coefficient has also been studied in the present research.

Fluid-structure interaction and soil-structure interaction are of enormous importance in the assessment of seismic response of any dam-reservoir system. In the present study, both dam-reservoir and dam-foundation interactions have been employed through the direct coupling method to obtain the responses of the structure and the reservoir. The present work has been divided into three parts. In the first part, the reservoir has been modelled using finite element considering the dam and foundation as being rigid. The effect of surface wave is neglected and reservoir bottom absorption has been considered. Suitable truncation boundary condition is applied along the truncated length of the fluid domain. Variation of hydrodynamic pressure has been observed for change of bottom slope and inclined length of the reservoir base for harmonic and earthquake excitation. In the second portion of the work, the reservoir is modelled following the Eulerian approach while the dam is being modelled using Lagrangian approach. Dynamic analysis of the dam-reservoir system has been performed using the direct coupling method including the fluid-structure interaction. Once again, response of the dam and hydrodynamic pressure therein are evaluated for variations in bottom slope and inclined length of reservoir base. Finally, the finite element model of the dam-reservoir-foundation coupled system has been analyzed using the direct coupling method. Fluid-structure interaction and soil-structure interaction have been included. Stresses on the dam and hydrodynamic pressure have been studied for change of different parameters by applying harmonic and earthquake excitations. Significant changes in hydrodynamic pressure and stresses of the dam have been observed for change of reservoir bottom slope in all cases.

1.2 OBJECTIVE OF WORK

The main objective of the present study is to investigate the dynamic response of dam-reservoir-foundation coupled systems having inclined reservoir bed using appropriate non-reflecting boundary conditions for the infinite reservoir and soil foundation adopting finite element technique.

1.3 SCOPE OF WORK

The scopes of the work are as follows:

- Finite element modelling of concrete gravity dam, adjacent reservoir and soil foundation, respectively
- Numerical modelling of the reservoir with efficient artificial non-reflecting boundary conditions
- Study the dynamic responses of a dam-reservoir coupled system using direct coupling approach
- Numerical modelling of dam-reservoir-foundation coupled system with direct coupling approach
- Determination of responses of the concrete gravity dam considering dam-reservoir-foundation interaction with inclined reservoir bed
- Study on responses of dam-reservoir-foundation coupled system with absorptive and inclined reservoir bottom

1.4 ORGANIZATION OF THESIS

The entire research work is presented in five chapters.

In **Chapter 1**, a brief general introduction to the present research work has been furnished along with the scope and objective of the work. The organization of the thesis has been given at the end of this chapter.

In **Chapter 2**, a detailed review of existing literature related to the present research work has been written. Observations on the past literature have been given at the end of this chapter.

In **Chapter 3**, theoretical formulations used for the present work have been provided along with necessary derivations and explanations.

In **Chapter 4**, numerical results along with graphs and tables have been provided. Entire chapter has been divided into three sections. In **section I,** numerical results of the infinite reservoir have been discussed. In **section II,** numerical results of dam-reservoir coupled systems have been dealt with, while in **section III,** numerical results of dam-reservoir-foundation coupled systems have been taken care of. All the results have been presented along with discussions.

Finally, in **Chapter 5**, a summary of the present research is furnished. The conclusions based on the major findings of the present study have been provided. Suggestions for future scope of work have been given at the end of this chapter.

A list of references of relevance is presented at the end of the thesis.

CHAPTER 2

LITERATURE REVIEW

2.1 GENERAL

The seismic design of a concrete gravity dam depends on the behaviour of the adjacent reservoir and the foundation below the structure. Fluid-structure interaction and soil-structure interaction influence the responses of the dam when subjected to dynamic excitation. Modelling of the dam, reservoir and foundation and their analysis is a very complex problem. Previous researchers used different tools like finite difference, finite element method or boundary element method for modelling the geometry of the dam, reservoir and foundation systems. Many authors developed their analytical techniques for the analysis of dam-reservoir-foundation systems. Fluid-structure and soil-structure reactions are also considered for their studies. Previous research works relevant to the present studies are reviewed in this chapter. Finally, the summary of observations on the past work from the perspective of the present research is given at the end of this chapter.

2.2 ANALYSIS OF RESERVOIR

The reservoir adjacent to the gravity dam has a major impact on the structure. The effect of the reservoir should be considered at the time of designing the concrete gravity dam. The most vulnerable condition occurs during an earthquake. Hydrodynamic pressure develops on the face of the gravity dam due to seismic excitation. Therefore, hydrodynamic analysis of the reservoir is very much important. Different geometrical parameters of the reservoir should be studied during the analysis of the reservoir. Several researchers studied the behaviour of the reservoir due to dynamic excitations.

Chwang (1979) presented the effect of vertical and horizontal ground excitation on the development of hydrodynamic pressure in finite reservoir. It was seen that hydrodynamic pressure decreased as the size of the reservoir decreased for horizontal acceleration. Hydrodynamic pressure was adjusted by the application of vertical acceleration on the dam. The author suggested the criteria to understand whether cavitation will develop or not at the dam-water interface due to an earthquake. The stratification effect on hydrodynamic pressure due to horizontal ground motion was evaluated by Chwang (1981). The author found that

hydrodynamic pressure contains in-phase and out-of-phase components with respect to the applied excitation. It was also reported that the gravitational constant, oscillation frequency and height of the fluid are the functions of wave-effect.

The length of the reservoir is required to truncate at a suitable distance to make the reservoir finite. An appropriate truncation boundary condition is very much important for the analysis of the infinite reservoir. Sharan (1985) proposed a technique for modelling the radiation damping along the truncation surface. The finite element method was adopted for the determination of hydrodynamic pressure. Fluid was assumed as compressible. The vibration was assumed as of small amplitude and two-dimensional. It was found that the boundary condition proposed by him was suitable for the truncated reservoir for a very short distance from the upstream face of the dam.

The geometry of the reservoir and the boundary conditions are important for the analysis of the reservoir. Tsai (1992) determined the hydrodynamic pressure considering the arbitrary dam-reservoir interface assuming the fluid as compressible. A new boundary condition was suggested by Zhao (1994) at the surface of sediment at the reservoir bottom depending on the P-wave propagation theory. A rigid gravity dam was analyzed with the new proposed boundary condition at the reservoir bottom.

Gao et al. (2019) developed a model for the analysis of a semi-infinite reservoir using a high-order doubly asymptotic open boundary (DAOB). A high-order DAOB was formulated and coupled with the finite element method for the analysis. From numerical results, it was obtained that the proposed method has high accuracy and computational efficiency.

2.3 ANALYSIS OF DAM-RESERVOIR COUPLED SYSTEM USING FINITE ELEMENT METHOD

The actual behaviour of the dam and reservoir may be understood if both systems are coupled and analyzed as a single system. Most of the authors coupled the fluid and structure as a single unit and analyzed the coupled system considering the dam-reservoir interaction. Several researchers reported the analysis of dam-reservoir coupled systems with different approaches. Most of the researchers used the finite element technique and some researchers developed different numerical approaches for the analysis of dam-reservoir systems.

Zienkiewicz and Bettess (1978) introduced two approaches used for the solution of fluid-structure coupled problems excluding the effects of large-scale flow. The first approach was known as the Lagrangian approach. The second approach was known as the Eulerian approach where the pressure was assumed as a single variable in the fluid medium. In the Eulerian approach for frequency domain analysis, it was very easy to include the effects of fluid compressibility and surface wave simultaneously. In the Lagrangian approach, fluid displacement was assumed as the primary variable. The authors described the methodology of both approaches that are widely used for solving engineering problems.

Saini et al. (1978) analyzed the fluid-structure system using the finite element technique. The authors assumed the fluid as compressible and included the interaction effect of fluid and structure. The coupled infinite element and finite element were used to model the reservoir, on the other hand the dam was discretized by regular finite element. Structural damping for dam and radiation damping for the infinite reservoir were considered. It was found that radiation damping has a remarkable effect at high frequencies of excitation. The proposed method was suitable for the arbitrary geometry of the system and quite economical from the computational point of view.

Bathe and Hahn (1979) analyzed the fluid-structure system assuming the fluid as non-viscous. The fluid domain was discretized by finite element with lumped or consistent mass idealization. The incremental equilibrium equations were solved by the use of explicit or implicit time integration techniques. Similarly, an approximate method was suggested by Muller (1981) for the analysis of the fluid-structure interaction problem. Eigenvalue solution for the coupled system for compressible and incompressible fluid was performed to compare the results.

A procedure was proposed by Hall and Chopra (1982) for two-dimensional analysis of the dam and reservoir. The dam was assumed as elastic and water was assumed as linearly compressible. The dam and the fluid domain were assumed to be two substructures and discretized both domains using the finite element method. The authors assumed the dam-foundation interface as rigid and solved several problems to demonstrate the accuracy of the procedure.

Humar and Roufaiel (1983) used the finite element method for the estimation of hydrodynamic pressure adjacent to the gravity dam subjected to horizontal exciting force and

proposed a new radiation boundary condition that gives better results over the Sommerfeld boundary condition. The inclination at the downstream side of the dam was considered and the results established that the inclination of the dam reduced the hydrodynamic pressure.

Olson and Bathe (1985) used the finite element technique for the fluid-structure interaction problem. Pressure was assumed as the nodal variable for the reservoir domain and displacement was assumed as the nodal variable for the structure. Their method performed well both for static and transient analysis.

A damping technique was suggested by Sharan (1987) for modelling radiation damping for solving the fluid-structure interaction problem. The fluid was assumed as non-viscous and compressible. The pressure was assumed as nodal unknown variable in finite element model and the equation of motion was solved by direct integration technique. Several examples were solved to show the efficiency of the proposed damping technique. It was proved that the technique is very effective in a wide range of time periods of excitation.

Das and Aki (1988) proposed a mathematical model for vibration analysis of gravity dam considering the dam-reservoir interaction. Fluid was assumed as compressible and the dam was assumed as elastic. Their results proved that the interaction between fluid and structure increases the time period of the gravity dam.

Fenves and Loli (1988) developed a numerical procedure for the determination of the response of fluid-structure coupled systems subjected to dynamic excitations. The procedure involved cavitation of fluid and a nonlinear model of the structure. The fluid was modelled as a bilinear compressible material. A mixed displacement-pressure model was developed to simulate fluid motion. Displacement-based standard finite element model was used for the structure. The coupled equations of motion were solved by implicit time integration. Another numerical procedure was suggested by Loli and Fenves (1989) for the determination of the non-linear dynamic response of the dam-reservoir system. The water was assumed as compressible and fluid-structure interaction was considered. The responses of the gravity dam along with the tensile cracking of concrete were evaluated due to earthquake excitations.

Hung and Chen (1990) proposed a finite element model for the dynamic interaction of hydrodynamic pressure and vibration of a gravity dam. Euler's equation was used for analysing the systems. Both horizontal and vertical components of earthquake were considered

to be external excitation. From the numerical analysis, it was found that a strong nonlinear effect on hydrodynamic pressure and hazards of surface wave occurs due to the rise of water surface at the face of the dam.

Chen and Taylor (1990) suggested a finite element-based solution for the fluid-structure interaction problems. The analysis was based on the displacement-based formulation for a non-viscous fluid medium and submerged structure. The proposed approach fulfils the compatibility and equilibrium condition along the interface of a fluid-structure coupled system. A reduced integration technique was used for the determination of the stiffness of fluid to suppress the circulation modes.

Bougacha and Tassoulas (1991) determined the responses of gravity dam subjected to earthquake excitations. The authors evaluated the effect of sedimentary material at the reservoir bottom and established that saturated sediment had minor effects on the maximum value of tensile stress and crest displacement of the gravity dam.

Tsai and Lee (1991) proposed a formulation for the nonlinear analysis of dam-reservoir systems assuming the dam as flexible and the reservoir as infinite. The authors solved problems for simple geometry and for arbitrary geometry of the reservoir to show the accuracy of the method and developed an exact radiation condition for the reservoir.

A radiation boundary condition was developed by Sharan (1992). The proposed boundary condition was effective for energy dissipation of the infinite reservoir and absorption of the wave at the reservoir bed. The geometry of the dam was assumed as two-dimensional and subjected to horizontal ground motion. The geometry at the near-field of the reservoir was assumed as arbitrary. However, the reservoir bottom at the far field was assumed as horizontal. A parametric study was performed to show the effectiveness of the boundary condition for the vertical and non-vertical faces of the dam. The proposed boundary condition was accurate if the boundary was located very near the face of the dam.

A semi-analytical solution developed by Yang et al. (1993) for dynamic analysis of fluid-structure coupled problem. The proposed transmitting boundary condition governs the wave equation of the far field of the reservoir. This study included the radiation condition and assumed the water to be compressible. The finite element method was used for analysis of the

dam-reservoir system considering the semi-infinite reservoir maintaining the efficiency of the boundary condition in the time domain.

Sandberg (1995) suggested an approach for treating unsymmetrical coupled domains like fluid-structure coupled systems. Discretization of the whole system was done by the finite element technique. The displacement-based formulation was used for the structure and pressure or displacement was assumed as potential for the fluid domain. The problem was converted to a standard eigenvalue problem through some simple steps based on the eigenvalues of each subdomain.

Li et al. (1996) suggested an exact far boundary condition for analysis of the fluid-structure coupled problem. The proposed boundary condition was effective and accurate for the analysis of an infinite reservoir having constant depth considering the flexibility of the foundation.

Calayir et al. (1996) presented a procedure for two-dimensional analysis of dam-reservoir systems subjected to earthquake excitations. Both Eulerian and Lagrangian approaches for the analysis of fluid-structure coupled systems had been employed and the variation of compressibility of fluid on modal behaviour was examined. Further, the earthquake responses of the dam-reservoir system using the Lagrangian approach were determined. The results were compared with the Eulerian solutions depending on the assumption of compressible fluid.

A numerical model was suggested by Hatami (1997) to show the absorption effect of the reservoir bottom for earthquake analysis of concrete gravity dam. The absorption of the pressure wave at the base of the reservoir has a significant effect on the response of the dam subjected to earthquake excitations. The wave reflection coefficient approach for the analysis was used.

Aviles and Li (1998) proposed a numerical technique for the estimation of hydrodynamic pressure on the non-vertical face of rigid dam. The fluid was considered to be compressible and viscous and the study suggested the solution with a special boundary method employing Trefftz functions.

Ghaemian and Ghobarah (1998) developed a stable solution for the dam-reservoir interaction problem. The coupling of the dam and reservoir was done in a way that the two fields interact at the interface only. Two methods of staggered solutions for the analysis of fluid-structure interaction problems were suggested. Ghaemian and Ghobarah (1999) also determined the fracture response of the dam considering the fluid-structure interaction effect due to earthquake. The analysis was performed in the time domain employing similar staggered solution technique.

Maity and Bhattacharya (1999) proposed a far-boundary condition at the truncation surface of an infinite reservoir for analysis of the dam-reservoir system in the time domain. The finite element technique was used for the discretization of the fluid domain considering pressure to be unknown nodal variable. The compressibility of fluid was incorporated in this study.

Cetin and Mengi (2003) established a new transmitting boundary condition. The boundary condition was appropriate for finite element analysis. The transmitting boundary condition was based on the spectral properties of radiating waves. The analysis was performed on two simple benchmark problems and the results indicate that the proposed boundary condition reduced the computational load of analysis.

Maity and Bhattacharya (2003) presented another procedure for the analysis of a fluid-structure coupled system using the finite element technique. The fluid was non-viscous and compressible and the pressure was assumed as unknown variable in the fluid medium. Elastic structure and the fluid domain were modelled separately and discretized with finite element. The problem was solved by considering the interaction effect at the interface of fluid and structure by forming an iterative scheme.

Gogoi and Maity (2005) suggested an approach for the determination of time dependent degradation of concrete gravity dam. A technique for earthquake study of the dam adjacent to a reservoir with the application of damage mechanics was proposed. The study included the fluid-structure interaction effect and the responses of aged dams with a percentage of isotropic or orthotropic damage were determined for earthquake excitations.

A procedure was suggested by Kucukarslan et al. (2005) for time domain analysis of a dam-reservoir coupled system using the finite element method. The reservoir bottom effect in

the transient analysis of the coupled system was included in this study. Kucukarslan (2005) again performed the dynamic analysis of a dam structure submerged in an unbounded fluid medium including the dam-reservoir interaction. The fluid was considered as incompressible and inviscid and the finite element technique was used. An exact far boundary condition at the truncation surface of the reservoir domain was developed. The vibration was assumed as in the perpendicular direction of the dam-reservoir interface. The reservoir base was considered rigid and horizontal. The obtained results were compared with the existing truncation boundary condition and found that the proposed boundary was very efficient than the others.

Sesli and Altunisik (2005) used different mathematical and analytical approaches for the determination of hydrodynamic pressure on concrete gravity dam. The model of the Sariyer gravity dam was used for analysis purposes using different approaches such as Westergaard, Lagrange and Euler. Finite element modelling was done using ANSYS software. The dynamic analysis was performed by applying Erzincan earthquake ground motion. Newmark's method was adopted for the solution of the dynamic equation.

A new truncation boundary was suggested by Gogoi and Maity (2006) to evaluate the hydrodynamic pressure. The proposed boundary condition included the effect of the absorptive bottom. The reflection coefficient of sedimentary material at the reservoir bottom is responsible for the absorption of the hydrodynamic pressure wave. The thickness of the sediment layer and the properties of the sediment material influence the reflection coefficient at the bottom of the reservoir. The proposed boundary condition was effectively used for the infinite reservoir.

A new analytical approach was applied by Coskun (2007) along the truncated boundary of the reservoir for finite element analysis of the fluid-structure system. The unbounded fluid was assumed as incompressible and inviscid. For the derivation of the truncation boundary condition, the reservoir domain was divided into two regions. The regions are the near-field region with Complex geometry and far-field region having uniform cross-section.

Samii and Lotfi (2007) used modal approaches for solving the dam-reservoir problems. The coupled modal approaches include complications due to an unsymmetrical Eigen problem. However, the responses can be determined very efficiently from this method. The decoupled modal approach can be solved by a standard Eigen solver. Dynamic equation of motion can

be solved easily in this approach. The dam-reservoir problem had been solved by both methods and the results were compared for accuracy and efficiency point of view.

Aviles and Suarez (2010) presented the effect of surface waves on hydrodynamic pressure generated along the face of the dam. The fluid was assumed as compressible and viscous. A closed-form solution considering Trefftz's numerical approach was obtained. A short-term Fourier transform-based solution was proposed by Gogoi and Maity (2010) for solving the dam-reservoir problem against earthquake excitations and found that there was frequency-dependent interaction at the reservoir bottom and that may be solved by frequency domain analysis.

Attarnejad and Bagheri (2011) performed the transient analysis for the dam-reservoir problems considering the interaction effect. The hydrodynamic pressure was determined by applying the Sommerfeld boundary condition at the truncated surface by the application of El-Centro earthquake excitation. Gao et al. (2011) proposed a numerical technique for solving the dam-reservoir problem. High-order doubly asymptotic open boundary (DAOB) for solving the fluid-structure coupled problem was applied.

Ghorbani and Khiavi (2011) employed the Galerkin technique to develop the equation for a dam-reservoir coupled system. The responses of dam-reservoir coupled system were determined due to the horizontal and vertical components of the earthquakes. A new truncation boundary condition was proposed along the truncation surface of the infinite reservoir to model the energy dissipation in the upstream direction.

Heydari and Mansoori (2011) solved the dam-reservoir coupled problems using finite element software. The impedance option for the boundary condition of the absorbent reservoir and wave was employed. Suitable elements for structure and fluid were selected and seismic analysis was performed to determine the pressure and displacement.

A procedure was suggested by Hojati and Lotfi (2011) for dynamic analysis of the concrete gravity dam using two-dimensional semi-infinite fluid elements. A modified efficient procedure that makes the analysis simple and more time-saving than the existing procedure was proposed.

Wang et al. (2011) suggested a procedure for the analysis of dam-reservoir systems in the time domain. The finite element method was used for the modelling of the dam and a part of the reservoir having irregular geometry. A commercial software ABAQUS was used to model the coupled system. The observed results show the stability and high accuracy of the proposed method.

Zhang et al. (2012) performed the dynamic analysis of a concrete gravity dam. A subspace iterative method was used for modal analysis of concrete gravity dam after the development of a three-dimensional finite element model. Natural frequency, time period and corresponding modes were determined. The response spectrum method was implemented for the dynamic analysis of the gravity dam.

Neya and Ardeshir (2013) solved the dam-reservoir problem by performing the dynamic analysis in the frequency domain. The viscosity of the fluid and bottom absorption for horizontal and vertical excitation was considered. The obtained results were compared with the results of non-viscous fluid. A numerical method was proposed by Pelecanos et al. (2013) for solving the dam-reservoir problems. The analysis was done using a two-dimensional displacement-based formulation. Both stiff and flexible dam considering the upstream face of the dam vertical and sloped under different types of loading conditions were studied.

A new radiation boundary condition was suggested by Samii and Lotfi (2013) for solving unbounded reservoir problems. The proposed boundary condition was a high-order-based absorbing boundary. This new boundary condition included the absorption effect of the reservoir bed and far-field base excitation.

Mandal and Maity (2015) determined the responses of the aged concrete dam using the degradation index. The finite element method was used to model the dam and reservoir. Displacement was considered as the nodal variable for the structure and pressure was considered as the variable at nodes of the fluid region. The responses of the dam-reservoir coupled system were determined through a direct coupling approach.

Tarinejad and Pirboudaghi (2015) performed the dynamic analysis of the dam-reservoir coupled system using Legendre spectral element method (SEM). The results show the accuracy of the analysis. Altunisik and Sesli (2015) executed the dynamic analysis of gravity dam by Wstergaard, Lagrange and Euler approaches. The finite element model of the

system was generated using ANSYS software. Linear transient analysis was performed to determine the structural responses of the dam. Element matrices were determined using the Gauss integration technique. Equations of motion were solved by Newmark's method.

Vani and Babu (2017) performed an earthquake analysis of a concrete gravity dam considering the compressibility of water. The finite element method for modelling the dam-reservoir system following the Lagrange-Lagrange approach was used. The nine-node quadrilateral element was used for modelling the complete system. Responses of compressible water were compared to the responses of incompressible water modelled by the Westergaard approach.

A frontal solution method was proposed by Golchin et al. (2018) for solving the dam-reservoir problem. The structure and fluid were analyzed separately after having the solution of degrees of freedom at the interface. A combination of Lagrange and Eulerian formulas were used for solid and fluid regions.

Wang et al. (2018) performed the dynamic analysis of a gravity dam of different heights using a fluid-structure coupling model. From the obtained results, it was found that maximum hydrodynamic pressure occurred in the case of the Westergaard formula. A correction factor to the Westergaard formula having the influence of elasticity and height of the dam and absorbing characteristics of the reservoir bottom was suggested. The solution of the corrected formula is more efficient than the old one.

Mandal and Aziz (2019) executed dynamic analysis of unbounded reservoir using the finite element method. Pressure based Eulerian approach was used for the simulation of the fluid domain. The analysis was carried out with and without the compressibility of water. It was found that the magnitude of hydrodynamic pressure changes if the inclination of the upstream face of the dam is considered.

2.4 ANALYSIS OF DAM-RESERVOIR COUPLED SYSTEM USING BOUNDARY ELEMENT METHOD

Most of the researchers have used finite element method for modelling the geometry of dam and reservoir. Some authors used the boundary element method for the analysis of dam-reservoir coupled systems.

Antes and Estorff (1987) used boundary integral equations for solving wave propagation problems through elastic and isotropic media and compressible and non-viscous fluid in the time and frequency domain by employing the reciprocal theorem of boundary value problem. Appropriate boundary conditions were developed along the fluid-soil and fluid-structure interface. The boundary integral equations were solved by a point of collocation and discretization of the boundary. The boundary element procedure was used to solve the dam-reservoir problem due to horizontal and vertical ground motion. Fluid-structure interaction was included and absorption of pressure waves at the reservoir bottom was also considered.

A displacement-based formulation was suggested by Wepf et al. (1988) for the analysis of the dam-reservoir system. The hydrodynamic stiffness matrix using the boundary element method in the frequency domain was determined. Authors assumed the arbitrary shape of the upstream face of the dam and reservoir bed including a constant depth of reservoir extended to infinity. The analytical solution was used for the semi-infinite reservoir. The stiffness matrix from frequency domain to time domain was transformed and the results of time domain were matched well with the results obtained from frequency domain.

Tsai and Lee (1989) suggested a boundary integral equation and applied it to the determination of hydrodynamic pressure acting on the face of the dam. The fluid was assumed to be compressible. The obtained results were compared with available analytical solutions.

Cho and Liu (2002) developed a model of boundary integral equations for three-dimensional potential problems. The model was applied for the determination of hydrodynamic pressure. The area integrals were converted into line integrals and then integrated analytically. The model was also used for the three-dimensional problem of the dam-reservoir system.

Seghir et al. (2009) presented a numerical model for solving the fluid-structure interaction problem. Finite element was used for the modelling of the dam and boundary element formulation was used for the modelling of the unbounded reservoir. Displacement was the nodal variable for the dam and pressure was the variable for the fluid medium. Dam and reservoir were coupled through the equilibrium along the dam-reservoir boundary.

2.5 ANALYSIS OF DAM-RESERVOIR COUPLED SYSTEM USING FINITE DIFFERENCE METHOD

The finite difference method is a useful technique for solving the structural problem by solving differential equations. Most of the researchers used the finite element method for solving fluid-structure interaction problems. Some of them used the boundary element technique. Very few researchers used finite difference technique for solving the problem of the reservoir.

Chen and Hung (1992) proposed a two-dimensional model for the evaluation of the seismic response of the reservoir. For the pore water and sediment at the bottom, the equation of pressure wave was solved by a finite difference method. The augmentation of pore pressure was caused by the inertia of sediment. Pressures on the face of the dam exceed significantly those calculated for compressible fluid for ideal liquefied sediment.

2.6 ANALYSIS OF DAM-RESERVOIR COUPLED SYSTEM BY ANALYTICAL METHODS

The finite element method and boundary element method are famous tools for numerical analysis. Most of the researchers used these tools for the analysis of dam-reservoir coupled problems. Few researchers reported some new analytical solutions for solving the fluid-structure problem. Some of them are reviewed in this section relevant to the present study.

An analytical solution proposed by Avelis et al. (1986) for the calculation of earthquake-induced hydrodynamic pressure on the upstream face of the dam having an inclined fluid-structure interface. The solution was done with the linear combination of functions. These functions fulfil all the boundary conditions excluding the fluid-structure interface.

A semi-analytical procedure was developed by Tsai et al. (1990) for analysis of the dam-reservoir system in the time domain including the dam-reservoir interaction. In this study, the reservoir domain was divided into near-field and far-field. The obtained results were compared with the analytical solution.

For an incompressible fluid, Miquel and Bouaanani (2010) proposed a closed-form solution for the fundamental time period of the dam-reservoir system. The fundamental time period was found by solving a cubic equation. The proposed solution was compared with

existing analytical and finite element solutions for solving dam-reservoir problems. A good agreement of accuracy was observed by validating the obtained results.

Eftekhari and Jafari (2018) proposed a variational approach for dynamic analysis of the dam-reservoir system. For the implementation of boundary conditions at the interface of the dam and reservoir, an analogue procedure was adopted. Newmark's time integration method was used to solve ordinary differential equations. The proposed method was compared with the finite element approach and show better accuracy with less computational time.

2.7 ANALYSIS OF GRAVITY DAM USING SOIL-STRUCTURE INTERACTION

The seismic responses of the gravity dam are highly influenced by the soil foundation below the structure. The effect of the foundation should be considered for designing the concrete gravity dam. The soil-structure interaction plays an important role in the earthquake behaviour of the structure. Several researchers performed the dynamic analysis of the structure and foundation considering soil-structure interaction.

Guttierrez and Chopra (1978) proposed a method for the soil-structure interaction problem. The method was suitable for the structure modelled by finite element and the region of soil was either treated as a continuum such as viscoelastic half-space, or idealized as a finite element system. Half space concept is suitable for the region where similar soil is extended to greater depth. Finite element idealization is suitable for the region where soft soil is underlying by the rock at shallow depth. It has been seen that the substructure method is computationally efficient as the soil and structure are analyzed separately.

Fenves and Chopra (1987) suggested a procedure for seismic analysis of the dam including the effect of dam-foundation interaction. Effects of reservoir bottom sediment were also included. Water was assumed as compressible. Responses of dam were determined considering dam-water interaction.

Chavez and Fenves (1995) suggested a hybrid frequency-time domain procedure for earthquake analysis of the concrete gravity dam including dam-foundation interaction. The procedure included the sliding of the structure along the soil-structure interface.

Kontoe et al. (2009) used two absorbing boundaries for finite element analysis of geotechnical problems using the domain reduction method. Standard cone boundary was

implemented at the truncation of the soil surface to solve the problem. The results were compared with the results of viscous boundary. Some drawbacks of the absorbing boundaries were highlighted and a guideline for the proper use of absorbing boundaries in practical engineering problems was suggested.

Burman et al (2012) presented a time-domain transient analysis of dam-reservoir coupled systems considering soil-structure interaction. The finite element technique was employed for the analysis of dam-reservoir coupled systems using direct coupling approach. Time history analysis of the two-dimensional plain strain dam-foundation model was done considering soil-structure interaction. Necessary boundary condition was applied along the truncated surface and a material-damping factor was applied for the dam and foundation. Free field responses were added to those obtained from complete analysis of the dam-foundation system to achieve a higher degree of accuracy.

Yang et al. (2018) presented the formulation of different boundary conditions used for finite element analysis of the Soil-Structure interaction (SSI) problem with the help of ABAQUAS software. The effectiveness of all the boundaries was compared by solving a few numerical problems.

Mohammadnezhad et al. (2020) investigated the frequency content on the dynamic response of the gravity dam. Frequency content is an important parameter of the seismic response of the dam. A comparative analysis was done on the Pine flat dam with different earthquake excitation records having different frequency content. The obtained results illustrated that frequency content has a major impact on the seismic response of the gravity dam. The same geometrical model was analyzed for different modular ratios to get the effect of soil-structure interaction. The results indicated that different modular ratios have a significant effect on the dynamic response of the gravity dam.

2.8 ANALYSIS OF DAM-RESERVOIR-FOUNDATION SYSTEMS

The actual behaviour of the concrete gravity dam can be understood if the effect of the adjacent reservoir and the foundation are considered during the earthquake analysis of the structure. When the dam, reservoir and foundations are coupled and analyzed as a single system then the responses of the structure will be authentic for the seismic design of gravity dam. Fluid-structure and soil-structure interaction should be considered for the dynamic analysis of dam-

reservoir-coupled systems. Several researchers performed the analysis of dam-reservoir-foundation systems with their respective approaches.

A procedure was presented by Chopra and Chakrabarti (1981) for the determination of responses of concrete gravity dam considering dam-water-foundation interaction. Both horizontal and vertical components of earthquake excitation were used for the evaluation of the responses of the dam. The system was assumed as linear and two-dimensional.

Lotfi et al (1987) developed a procedure for the analysis of dam-water-foundation systems. The procedure was based on the finite element technique. The whole system was assumed as two-dimensional. Water-foundation interaction was incorporated in this study. The method was applied to various dam-water-foundation interaction problems and the efficiency was evaluated from the obtained results.

El-Aidi and Hall (1989) determined the seismic behaviour of the dam-reservoir-foundation system. The nonlinear behaviour of the dam associated with the cracking of concrete and water cavitation was evaluated due to the earthquake. It was seen that water cavitation has a minor effect on the earthquake response of gravity dam. Concrete cracking plays an important role in the failure of the dam. A possible failure mode was described associated with inclined cracks.

Medina et al. (1990) performed earthquake analysis of dam-water-sediment-foundation systems using the boundary element method in two dimensions. The foundation was considered both a deep stratum and a half-space region. Dam-water and dam-foundation interaction was considered in their analysis.

Valliappan and Zhao (1992) suggested a model for the analysis of the dam-water-foundation systems. The authors included the physical and mechanical properties of sediment at the reservoir bottom. The sediment was assumed as a viscoelastic medium. It was stated that the soft sediment layer is responsible for energy dissipation and amplification of incident waves at the interface water-sediment that may affect the responses of the gravity dam.

Chandrasekhar and Humar (1993) presented a procedure for the determination of the response of the gravity dam including fluid-foundation interaction and suggested that the hydrodynamic pressure was affected by the radiation of energy waves towards the infinite

direction of the reservoir, absorption of the wave at the reservoir bed and cross-coupling between the foundation and reservoir bottom. It was also stated that the analysis could be made simple through the wave propagation model by ignoring the cross-coupling approach.

Guan et al. (1994) proposed a method for dynamic analysis of reservoir-dam-soil systems. The authors performed the analysis in the time domain and assumed the coupled system as two-dimensional. The reservoir was assumed as infinite and the dam was supported on unbounded soil. The structure was modelled by the finite element method. The soil was assumed as homogeneous, isotropic and elastic half-space.

A closed-form solution was suggested by Bouaanani et al. (2003) for the determination of hydrodynamic pressure on the gravity dam subjected to earthquake excitations. The dam, water and foundation were assumed as linear and two-dimensional. Fluid was assumed as compressible, inviscid and have irrotational motion with small amplitude. The effect of the surface wave was neglected. Applied ground acceleration was assumed as horizontal and harmonic. The proposed closed-form solution was made for eigenvalues originated when solving the dam-reservoir interaction problem.

Mohammadi et al. (2009) used Eulerian and Lagrangian approach for the analysis of gravity dam. The purpose of their study was to determine the advantages and disadvantages of both methods. A set of coupled equations was developed for the modelling of the reservoir using the Eulerian method. The same equation was used for the modelling of the dam and foundation in the Lagrangian method. The results of both methods were compared for different boundary conditions and the elasticity of the foundation with different frequencies of loading.

Papazafeiropoulos et al. (2011) presented a numerical simulation for the determination responses of dam-water-foundation systems. The finite element model was used to model the coupled system. Necessary boundary conditions and interactions were formulated. It was stated that the water level and thickness of the soil layer have a significant effect on the dynamic characteristics of gravity dam in terms of Eigen frequencies and damping.

Mandal and Maity (2016) proposed a direct coupling approach for the determination of responses of gravity dam. The fluid-structure and soil-structure interaction were considered simultaneously. The displacement-based formulation was used for the modelling of the dam and foundation. The pressure-based formulation was used for modelling the fluid domain.

Responses of dam, foundation and reservoir were determined with and without fluid-structure and soil-structure interaction and compared to study the interaction effects on the gravity dam. Mandal and Maity (2017) also determined responses of gravity dam considering the bottom absorption of the reservoir. The modelling of the dam-reservoir-foundation system was done using the finite element technique. Mandal and Maity (2017) evaluated the responses of gravity dam considering the ageing effect of concrete. Dam-reservoir and dam-foundation interaction effect was considered. It was observed that the fundamental frequency of the dam decreases with age. Displacement and stresses of the dam increase with the increase of the age of the dam.

Wang et al. (2017) proposed a method for dynamic analysis of dam-reservoir-foundation systems. Seismic responses of gravity dam were determined for different elastic modulus. It has been seen that the responses of the dam were increased with the increase of the elastic modulus of the foundation. An experimental work executed by Humaish et al. (2018) for the evaluation of dynamic response of concrete gravity dam considering dam-foundation and dam-reservoir interaction. Tests for two different cases were conducted and seismic behaviour was investigated during shaking by shake table. The failure mechanism of the structure was also examined during the shaking.

Mohammadnezhad et al. (2019) used the finite element (FE) approach for dynamic analysis of the dam-foundation-reservoir system with the help of well-known software. The authors presented different mechanisms for the input of earthquake excitation. A series of analysis was performed for different cases to validate their proposed method in the dam-foundation-reservoir system.

Gorai and Maity (2019) presented a time history analysis of the dam-reservoir-foundation system. The finite element method was employed for this purpose. The geometry of the Koyna dam was used for analysis purposes. A comparative analysis of the responses of the dam was performed.

Mandal and Maity (2019) performed an earthquake analysis of the dam-reservoir-foundation system to get the responses of the structure. The analysis was performed using a direct coupling approach. Effective absorbing boundary conditions were applied at the truncation boundary of the fluid and foundation domain. Parametric studies were performed to obtain the responses of the structure.

Sharma et al. (2019) presented a space-time finite element technique for analysis of the dam-reservoir-foundation system. Pressure and displacement were computed through a special numerical technique. The performance and accuracy of the proposed method were obtained by solving some benchmark problems.

A mesh-free numerical method was proposed by Behroozi and Vaghefi (2020) for the determination of earthquake responses of dam-reservoir-foundation systems. The numerical model was constructed on Radial basis functions. The upstream face of the dam was taken as inclined. Different formulations were used to provide boundary conditions at the far end of the unbounded domain. Fluid was taken as compressible and energy depreciation was considered at the reservoir boundaries. The proposed model was used to determine the hydrodynamic pressure due to earthquake excitation.

Haghani et al. (2020) used the extended finite element method (XFEM) for earthquake analysis of the dam-reservoir-foundation systems. XFEM was used to take care of displacement discontinuity along the developed crack due to seismic excitations.

Khiavi and Sari (2021) suggested an analytical technique for the determination of hydrodynamic pressure. The reservoir was assumed as rectangular and harmonic excitation was applied vertically at the base of the foundation. A new method was adopted for the solution of the hydrodynamic wave equation based on the separation of variables. The obtained results proved that the vertical component of earthquake has a significant effect on hydrodynamic pressure.

Dastgerdi et al. (2022) developed two-dimensional modelling of the dam-reservoir-foundation system using ABAQUS software. The effect of the change of cross-section of the dam and face angle at the upstream side on seismic damage of the gravity dam due to Koyna earthquake excitation was examined. It was suggested to minimize the seismic damage on the concrete gravity dam, the upstream face angle should be provided and change of cross section should be avoided as much as possible.

Rasa et al. (2022) proposed a technique for the analysis of dam-reservoir-foundation systems considering the radiation of waves through the foundation and reservoir domain. The system was analyzed using the direct coupling approach. A two-dimensional finite element

formulation was developed using FORTRAN 90 programing language. Seismic analysis was carried out to determine the responses of the dam-reservoir-coupled system.

2.9 OBSERVATIONS

Based on the above literature review the following critical points may raise.

- Finite element method has the distinct advantage of tackling irregular geometry. A displacement-based formulation is used to model the concrete gravity dam and it is considered to be in a plane strain state.
- Most of the previous researchers have modelled the fluid domain using the Finite element method with different field variables such as displacement, velocity potential, pressure etc. Out of these, the displacement-based formulation leads to the presence of spurious or circulation or rotational modes which have no physical meaning. These circulation modes may correspond to zero frequencies. To overcome this problem a number of researchers considered the hydrodynamic pressure as a principal unknown quantity.
- The main problem to simulate the fluid is to model the infinite domain to a finite one. Different authors have proposed different truncation boundary conditions and they have their respective advantages and disadvantages.
- Similar to infinite fluid, the infinite soil is also truncated at a certain distance to make it finite for finite element modelling. Various non-reflecting boundary conditions at this truncation surface are proposed to simulate the effect of the infinite extent of this domain.
- Distribution of hydrodynamic pressure on a concrete gravity dam is highly influenced by the inclination of the reservoir bottom.
- Hydrodynamic pressure will be more practical if the reservoir bottom absorption along with the inclination of the reservoir bed is considered.
- The responses of concrete gravity dam are determined considering dam-reservoir and dam-foundation interactions. The interactions of dam-reservoir and dam-foundation are incorporated either by direct coupling or indirect coupling.
- In a dam-reservoir system by indirect coupling methodology, the hydrodynamic pressure in fluid domain is first determined considering the structure as rigid. The resulting pressure exerts forces on the adjacent structure. Due to this additional force, the structure undergoes new displacement. The fluid domain is solved again with the

calculated displacement to get the response of the elastic structures. The process is continued until a desired level of convergence in both pressures and displacements is achieved.

- In the dam-foundation system by indirect coupling methodology, the displacement of the gravity dam is determined considering the base of the dam as rigid. The reaction force at this rigid bottom of the dam is calculated and the soil foundation is analyzed with this calculated reaction force. Next, the dam is again solved with the changed boundary conditions. The process is further continued until the desired accuracy is achieved.
- Similarly, the responses of the dam-reservoir and dam–foundation can be determined by direct coupling approach. In this method, subsystems are coupled and solved as a single system. However, the resulting equations lead to unsymmetrical matrices and require a special numerical technique to solve the coupled systems.
- Responses of concrete gravity dam due to earthquake depends on the characteristics of the soil foundation beneath the gravity dam.
- The responses of the gravity dam will be more realistic if soil-structure and fluid-structure interaction are accounted for simultaneously in the numerical model of the dam-reservoir-foundation system.
- Very little work has been carried out on Dam-reservoir-foundation coupled system with inclined reservoir bed. In most cases, the studies have been performed using popular software packages like ANSYS, ABAQUS etc. However, code development has its own justification, as it gives the researcher the right to modify it according to the problem.

2.10 RESEARCH GOAL

The main goal of this study is to determine the dynamic responses of dam-reservoir-foundation coupled system with inclined reservoir bed. For this purpose, finite element analysis of dam-reservoir-foundation system is carried out for different harmonic and seismic excitations. The present algorithm includes both fluid-structure and soil-structure interaction. The effects of bottom slope of reservoir on the responses of this coupled system are observed. Hydrodynamic pressure, movement of fluid within the reservoir and stresses of dam and foundation are studied for different slope angles of reservoir base.

CHAPTER 3

THEORETICAL FORMULATION

3.1 GENERAL

The behaviour of concrete gravity dam and adjacent reservoir with inclined base has been observed applying dynamic excitations. Two-dimensional modelling of the dam-reservoir-foundation system has been done using finite element technique. In the first portion of the work, only the reservoir is analyzed considering the adjacent dam is rigid. In the next portion of the work, the dam-reservoir coupled system has been analyzed by direct coupling approach. At the end of the work, dam-reservoir-foundation systems are analyzed using direct coupling approach considering fluid-structure and soil-structure interaction simultaneously. Detailed theoretical formulations have been given in this chapter.

3.2 THEORETICAL FORMULATION FOR THE STRUCTURE (DAM)

The dynamic equation for the dam subjected to some external force is expressed as:

$$[M_d]\{\ddot{u}_d\} + [C_d]\{\dot{u}_d\} + [K_d]\{u_d\} = \{F_d\} \tag{1}$$

Where $[M_d]$, $[C_d]$ and $[K_d]$ are mass, damping and stiffness matrix of the structure and $\{\ddot{u}_d\}$, $\{\dot{u}_d\}$ and $\{u_d\}$ are nodal acceleration, velocity and displacements. while $\{F_d\}$ is the array of nodal forces. The body of the structure is assumed to be following plane-strain condition with the following elasticity matrix (Cook et al., 2007):

$$[D] = \frac{E}{(1+\nu)(1-2\nu)}\begin{pmatrix} 1-\nu & \nu & 0 \\ \nu & 1-\nu & 0 \\ 0 & 0 & \frac{1-2\nu}{2} \end{pmatrix} \tag{2}$$

Here, E is Young's modulus of the material of the structure. ν the Poisson's ratio for the dam. The structure discretized by eight-node isoparametric element is shown in Fig. 3.1.

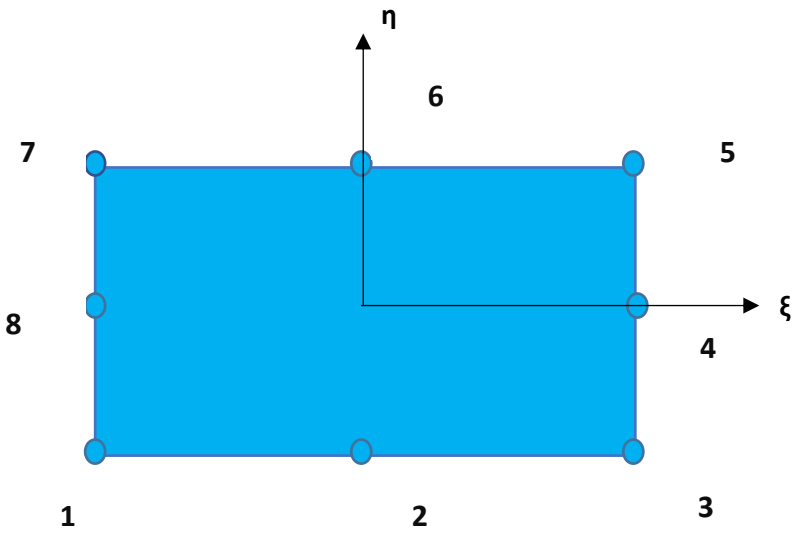

Fig. 3.1: Eight-node isoparametric element

The shape functions of the eight-node isoparametric element are as follows (Krishnamoorthy, 2004):

$$N_1 = (-0.25) \times (1-\xi) \times (1-\eta) \times (1+\xi+\eta)$$

$$N_2 = 0.5 \times (1-\xi^2) \times (1-\eta)$$

$$N_3 = (-0.25) \times (1+\xi) \times (1-\eta) \times (1-\xi+\eta)$$

$$N_4 = 0.5 \times (1+\xi) \times (1-\eta^2)$$

$$N_5 = (-0.25) \times (1+\xi) \times (1+\eta) \times (1-\xi-\eta)$$

$$N_6 = 0.5 \times (1-\xi^2) \times (1+\eta)$$

$$N_7 = (-0.25) \times (1-\xi) \times (1+\eta) \times (1+\xi-\eta)$$

$$N_8 = 0.5 \times (1-\xi) \times (1-\eta^2) \qquad (3)$$

The strain displacement matrix of the element is as follows (Krishnamoorthy, 2004):

$$B = \begin{pmatrix} \frac{\partial N_i}{\partial x} & 0 \\ 0 & \frac{\partial N_i}{\partial y} \\ \frac{\partial N_i}{\partial y} & \frac{\partial N_i}{\partial x} \end{pmatrix}_{i=1,8} \tag{4}$$

The stiffness matrix can be calculated as (Krishnamoorthy, 2004):

$$[K_d] = \iint [B]^T [D][B]|J| d\xi d\eta \tag{5}$$

The Jacobian matrix is given as follows (Cook et al., 2007):

$$J = \begin{bmatrix} \sum_{i=1}^{8} \frac{\partial N_i}{\partial \xi} x_i & \sum_{i=1}^{8} \frac{\partial N_i}{\partial \xi} y_i \\ \sum_{i=1}^{8} \frac{\partial N_i}{\partial \eta} x_i & \sum_{i=1}^{8} \frac{\partial N_i}{\partial \eta} y_i \end{bmatrix} \tag{6}$$

The numerical integration has been done by 2x2 Gauss quadrature values as follows:

Table 3.1: Two-point Gauss quadrature values

Sampling point	**ξ or η**	**Weightage function**
2	±0.57735027	1.000000

The mass matrix of the structure can be calculated as follows (Cook et al., 2007):

$$[M_d] = \int [N]^T \rho [N] \, d\xi d\eta \tag{7}$$

Here ρ denotes the density of the structure.

The Rayleigh damping model has been used for the structure and can be written as (Clough and Penzin, 1993)

$$[C_d] = a'[M_d] + b'[K_d] \tag{8}$$

a' and b' are defined as proportional damping constants. The relation between a' and b' can be expressed by the following equation.

$$\xi' = \frac{1}{2}\left(a'\omega + \frac{b'}{\omega}\right) \tag{9}$$

Values of a' and b' can be obtained by selecting the part of critical damping ξ_1' and ξ_2' for two different frequencies, ω_1 and ω_2 and solving the above equation for a' and b'.

$$a' = \frac{2(\xi_2'\omega_2 - \xi_1'\omega_1)}{({\omega_2}^2 - {\omega_1}^2)} \tag{10a}$$

$$b' = \frac{2\omega_1\omega_2(\xi_2'\omega_1 - \xi_1'\omega_2)}{({\omega_2}^2 - {\omega_1}^2)} \tag{10b}$$

3.3 THEORETICAL FORMULATION FOR THE FLUID DOMAIN (RESERVOIR)

The total stress of Newtonian fluid may be expressed by an isotropic tensor as follows:

$$T_{ij} = -p\delta_{ij} + {T'}_{ij} \tag{11}$$

Here T_{ij} presents the total stress and ${T'}_{ij}$ presents the viscous stress tensor. ${T'}_{ij}$ depends on the rate of deformation. Hydrodynamic pressure is denoted by p. δ_{ij} is Kronecker delta. The general form of ${T'}_{ij}$ for isotropic linearly elastic material can be written as below:

$${T'}_{ij} = \lambda\Delta\delta_{ij} + 2\mu D_{ij} \tag{12}$$

Here μ and λ are the material constants. Specifically, μ is the coefficient of viscosity, ($\lambda + 2\mu/3$) is the bulk viscosity, and D_{ij} is the rate of deformation tensor. D_{ij} can be expressed as:

$$D_{ij} = \frac{1}{2}\left(\frac{\partial V_i}{\partial y_j} + \frac{\partial V_j}{\partial x_i}\right) \quad \text{and } \Delta = D_{11} + D_{22} + D_{33} \tag{13}$$

Thus incorporating Eq. (12), Eq. (11) may be written as below.

$$T_{ij} = -p\delta_{ij} + \lambda\Delta\delta_{ij} + 2\mu D_{ij} \tag{14}$$

Bulk viscosity ($\lambda + 2\mu/3$) becomes zero for compressible fluid. Thus, the Eq. (12) modifies as follows.

$$T_{ij} = -p\delta_{ij} + \frac{2\mu}{3}\Delta\delta_{ij} + 2\mu D_{ij} \tag{15}$$

Now, if the viscosity of the fluid is neglected for simplicity, the total stress tensor reduces as below.

$$T_{ij} = -p\delta_{ij} \tag{16}$$

The Navier-Stokes equation of motion can be written as below (Jain, 2000):

$$\rho\left(\frac{\partial v_i}{\partial t} + V_j\frac{\partial v_i}{\partial x_j}\right) = \frac{\partial T_{ij}}{\partial x_j} + \rho B_i \tag{17}$$

Here ρ is the density of fluid and B_i is the body force. If Eq. (16) is substituted in Eq. (17), we obtain

$$\rho\left(\frac{\partial v_i}{\partial t} + V_j\frac{\partial v_i}{\partial x_j}\right) = \rho B_i - \frac{\partial p}{\partial x_i} \tag{18}$$

Disregarding the components of body forces and the convective terms, the following equations may be reached.

$$\frac{1}{\rho}\frac{\partial p}{\partial x} + \frac{\partial u}{\partial t} = 0 \tag{19}$$

$$\frac{1}{\rho}\frac{\partial p}{\partial y} + \frac{\partial v}{\partial t} = 0 \tag{20}$$

Here *u* and *v* are the components of velocity of the fluid along the orthogonal direction *x* and *y*, respectively. The continuity equation in two dimensions may be written as follows:

$$\frac{\partial p}{\partial t} + \rho c^2 \left(\frac{\partial u}{\partial x} + \frac{\partial v}{\partial y} \right) = 0 \tag{21}$$

Here *c* is the acoustic velocity of the wave in the fluid domain. Differentiating Eq. (19) and Eq. (20) with respect to *x* and *y*, respectively, the following equations can be obtained.

$$\frac{1}{\rho} \frac{\partial^2 p}{\partial x^2} + \frac{\partial}{\partial x} \left(\frac{\partial u}{\partial t} \right) = 0 \tag{22}$$

$$\frac{1}{\rho} \frac{\partial^2 p}{\partial y^2} + \frac{\partial}{\partial y} \left(\frac{\partial v}{\partial t} \right) = 0 \tag{23}$$

Adding Eq. (22) to Eq. (23), we obtain.

$$\frac{1}{\rho} \frac{\partial^2 p}{\partial x^2} + \frac{1}{\rho} \frac{\partial^2 p}{\partial y^2} + \frac{\partial}{\partial x} \left(\frac{\partial u}{\partial t} \right) + \frac{\partial}{\partial y} \left(\frac{\partial v}{\partial t} \right) = 0 \tag{24}$$

Now differentiating the terms in Eq. (21) with respect to time, *t*, the following equation can be obtained.

$$\frac{1}{\rho} \frac{\partial^2 p}{\partial t^2} + \rho c^2 \left\{ \frac{\partial}{\partial x} \left(\frac{\partial u}{\partial t} \right) + \frac{\partial}{\partial y} \left(\frac{\partial v}{\partial t} \right) \right\} = 0 \tag{25}$$

Combining Eq. (24) and Eq. (25), the following relation can be reached.

$$\frac{1}{\rho} \frac{\partial^2 p}{\partial x^2} + \frac{1}{\rho} \frac{\partial^2 p}{\partial y^2} - \frac{1}{\rho c^2} \left(\frac{\partial^2 p}{\partial t^2} \right) = 0 \tag{26}$$

Simplifying Eq. (26), the equation for compressible fluid can be obtained as follows.

$$\nabla^2 p(x, y, t) = \frac{1}{c^2} \ddot{p}\,(x, y, t) \tag{27}$$

Here ∇^2 is a two-dimensional Laplacian operator since we have considered a two-dimensional dam-reservoir coupled system for our analysis as shown in Fig. 3.2. Fluid is assumed as compressible and non-viscous. The fluid domain has been discretized by two-dimensional eight-node isoparametric element.

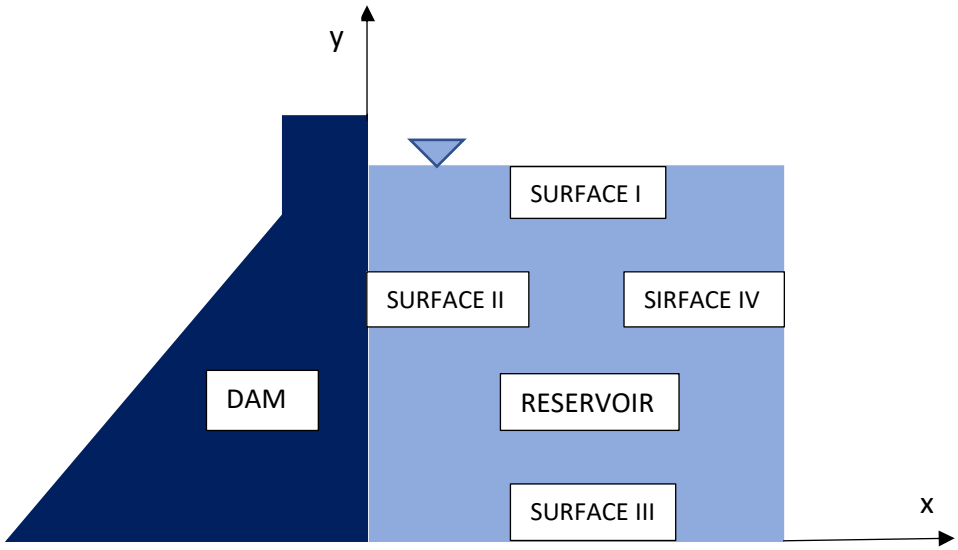

Fig. 3.2: Geometry of dam-reservoir system

Referring Fig. 3.2, the boundary conditions are set as follows:

- **Surface I**

At the top surface of the reservoir (**surface I**), the boundary condition considering the surface wave may be found below.

$$\frac{1}{g}\ddot{p} + \frac{\partial p}{\partial y} = 0 \tag{28}$$

If the surface wave is not considered, the boundary condition at top surface of the reservoir can be written as follows.

$$p\left(x, H_f\right) = 0 \tag{29}$$

H_f is the height of the unbounded reservoir.

- **Surface II**

At the interfacial surface of dam and reservoir (**surface II**), fluid pressure should satisfy the following expression.

$$\frac{\partial p}{\partial n}(0, y, t) = \rho_f a e^{i\omega t} \tag{30}$$

Here $ae^{i\omega t}$ is the ground acceleration, ω is the angular frequency, $i=\sqrt{-1}$ and n the outwardly directed normal to the elemental surface along the interface of the dam and reservoir. ρ_f is the density of the fluid.

- **Surface III**

At the bottom of the reservoir considering the absorption of seismic waves, fluid pressure has to follow the equation given below.

$$\frac{\partial p}{\partial n}(x,0,t) = i\omega q\dot{p}\,(x,0,t) \tag{31}$$

Here $i=\sqrt{-1}$

$$q = \frac{1}{c}\left(\frac{1-\alpha}{1+\alpha}\right) \tag{32}$$

α is the reflection coefficient of the reservoir bottom.

- **Surface IV**

At the truncated face (**surface IV**) of the reservoir, the boundary condition can be written as below.

$$\frac{\partial p}{\partial n} = \left(\xi_m - \frac{1}{c}\right)\dot{p} \tag{33}$$

According to Gogoi and Maity (2006), ξ_m is assumed as.

$$\zeta_m = -\frac{i\sum_{m=1}^{\infty}\frac{{\lambda_m}^2 I_m}{\beta_m}e^{(-k_m x)}(\Psi_m)}{\Omega c\sum_{m=1}^{\infty}\frac{{\lambda_m}^2 I_m}{\beta_m k_m}e^{(-k_m x)}(\Psi_m)} \tag{34}$$

Here

$$I_m = \frac{1}{H_f}\int_0^{H_f}\Psi_m\,dy \tag{35}$$

$$\Psi_m = \frac{1}{2\lambda_m}[(\lambda_m + \omega q)e^{i\lambda_m y} + (\lambda_m - \omega q)e^{-i\lambda_m y} \tag{36}$$

$$\lambda_m^2 = \left(\frac{(2m-1)\pi}{2H_f}\right)^2 + i2\omega q/H_f \tag{37}$$

$$\beta_m = (\lambda_m^2 - \omega^2 q^2)\left(H_f - \frac{\chi}{\lambda_m^2 - \chi^2}\right) + i\omega q \tag{38}$$

$$K_m = \sqrt{\lambda_m^2 - \Omega^2} \tag{39}$$

$$\Omega = \frac{\omega}{c} \quad \text{and} \quad \chi = \frac{\omega^2}{g} \tag{40}$$

If the surface wave is neglected, then χ can become zero.

Pressure is considered to be the nodal variable in the fluid medium. Now implementing the Galerkin approach, Eq. (27) can be discretized as given below.

$$\int_{\Omega} N_{rj}\left[\nabla^2 \sum N_{ri} p_i - \frac{1}{C^2}\sum N_{ri}\ddot{p}_i\right] d\Omega = 0 \tag{41}$$

N_{rj} are the shape functions of the reservoir domain and Ω is the region of fluid. Eq. (41) may be written below after the application of Green's theorem.

$$-\int_{\Omega}\left[\frac{\partial N_{rj}}{\partial x}\sum\frac{\partial N_{ri}}{\partial x}p_i + \frac{\partial N_{rj}}{\partial y}\sum\frac{\partial N_{ri}}{\partial y}p_i\right]d\Omega - \frac{1}{C^2}\int_{\Omega} N_{rj}\sum N_{ri}\, d\Omega\ddot{p}_i + \int_{\Gamma} N_{rj}\sum\frac{\partial N_{rj}}{\partial n}d\Gamma p_i = 0 \tag{42}$$

Here $\boldsymbol{\Gamma}$ is the boundary of the fluid domain. Eq. (42) can be expressed as follows.

$$[\bar{J}]\{\ddot{p}\} + [\bar{H}]\{p\} = \{F\} \tag{43}$$

where

$$[\bar{J}] = \frac{1}{C^2}\sum \int_{\Omega} [N_r]^T [N_r] d\Omega \tag{44}$$

$$[\bar{H}] = \sum \int_{\Omega} \left[\frac{\partial}{\partial x}[N_r]^T \frac{\partial}{\partial x}[N_r] + \frac{\partial}{\partial y}[N_r]^T \frac{\partial}{\partial y}[N_r] \right] d\Omega \tag{45}$$

$$\{F\} = \sum \int_{\Gamma} [N_r]^T \frac{\partial p}{\partial n} d\Gamma = \{F_f\} + \{F_{fs}\} + \{F_{fb}\} + \{F_t\} \tag{46}$$

The subscript *f, fs, fb* and *t* presents the top surface of the reservoir, dam-reservoir interface, reservoir-bottom interface and truncated surface respectively. At the top of the reservoir, $\{F_f\}$ can be expressed below.

$$\{F_f\} = -\frac{1}{g}[R_f]\{\ddot{p}\} \tag{47}$$

$$[R_f] = \sum \int_{\Gamma_f} [N_r]^T [N_r] d\Gamma \tag{48}$$

At the interface, if $\{a\}$ is the nodal acceleration vector in fluid, $\{F_{fs}\}$ may be written as given below.

$$\{F_{fs}\} = -\rho_f [R_{fs}]\{a\} \tag{49}$$

$$[R_{fs}] = \sum \int_{\Gamma_{fs}} [N_r]^T [T]\, [N_d] d\Gamma \tag{50}$$

$[T]$ is the transformation matrix along the dam-reservoir boundary and N_d is the shape function of the structure and N_r is the shape function of the reservoir along the fluid-structure interface.

Along the reservoir and bottom interface $\{F_{fb}\}$ may be written as given below.

$$\{F_{fb}\} = i\omega q [R_{fb}]\{p\} \tag{51}$$

$$\left[R_{fb}\right] = \sum \int_{\Gamma_{fb}} [N_r]^T \, [N_r] d\Gamma \tag{52}$$

At the truncated surface of the reservoir $\{F_t\}$ may be written as given below.

$$\{F_t\} = \zeta_m [R_t]\{p\} - \frac{1}{c}[R_t]\{\dot{p}\} \tag{53}$$

$$[R_t] = \sum \int_{\Gamma_t} [N_r]^T \, [N_r] d\Gamma \tag{54}$$

After writing all the terms, Eq. (43) becomes as below.

$$[J]\{\ddot{p}\} + [A]\dot{p} + [H]\{p\} = \{F_r\} \tag{55}$$

Here,

$$[J] = [\bar{J}] + \frac{1}{g}\left[R_f\right] \tag{56}$$

$$[A] = \frac{1}{c}[R_t] \tag{57}$$

$$[H] = [\bar{H}] + \zeta_m [R_t] - i\omega q\left[R_{fb}\right] \tag{58}$$

$$\{F_r\} = -\rho_f \left[R_{fs}\right]\{a\} \tag{59}$$

3.4 CALCULATION OF VELOCITY AND DISPLACEMENT OF FLUID

Acceleration of the fluid particles can be calculated after the determination of hydrodynamic pressure in the reservoir. Velocity of the fluid particle is determined using the value of acceleration with the help of Gill's time integration technique (Gill,1951). It is a systematic integration technique following the Runge-Kutta approach (Ralston and Wilf, 1965). At any instant of time *t*, velocity of fluid may be expressed as stated below.

$$v_t = v_{t-\Delta t} + \Delta t \dot{v}_t \tag{60}$$

Displacement of fluid particles in the reservoir can be determined at any instant of time by the following equation.

$$u_t = u_{t-\Delta t} + \Delta t v_t \tag{61}$$

3.5 THEORETICAL FORMULATION FOR DAM-RESERVOIR COUPLED SYSTEMS

The equation of the structure considering damping may be written as follows.

$$M_d \ddot{u}_d + C_d \dot{u}_d + K_d u_d - Qp - M_d \ddot{u}_g = 0 \tag{62}$$

$\ddot{u}_g$ is the ground acceleration. The coupling term $[Q]$ is generated due to the acceleration for the structure domain and pressure for the fluid domain at the interface of the dam and reservoir and can be stated as:

$$\int_{\Gamma_{dr}} N_{dr}^T n p d\Gamma = \left(\int_{\Gamma_{dr}} N_{dr}^T n N_{dr} d\Gamma \right) p = [Q]\{p\} \tag{63}$$

Here n is the direction vector between the boundary of dam and reservoir and N_{dr} is the interpolation function of line element at the dam-reservoir interface. The equation of the fluid domain can be expressed below.

$$J\ddot{p} + A\dot{p} + Hp + Q^T \ddot{u}_d - F_r = 0 \tag{64}$$

The pair of Eq. (62) and (64) are coupled in matrix form, which expressed the coupled equation of dam and reservoir is given below.

$$\begin{bmatrix} J & Q^T \\ 0 & M_d \end{bmatrix} \begin{Bmatrix} \ddot{p} \\ \ddot{u}_d \end{Bmatrix} + \begin{bmatrix} A & 0 \\ 0 & C_d \end{bmatrix} \begin{Bmatrix} \dot{p} \\ \dot{u}_d \end{Bmatrix} + \begin{bmatrix} H & 0 \\ -Q & K_d \end{bmatrix} \begin{Bmatrix} p \\ u_d \end{Bmatrix} = \begin{Bmatrix} F_r \\ M_d \ddot{u}_g \end{Bmatrix} \tag{65}$$

To solve Eq. (65), Newmark's integration method is used and given by the following equations (Bathe, 2009):

$$\{q\}_{j+1} = \{q\}_j + \Delta t \{\dot{q}\}_j + \frac{\Delta t^2}{2} \left[(1 - 2\beta)\{q\}_j + 2\beta \{\ddot{q}\}_{j+1} \right] \tag{66}$$

$$\{\dot{q}\}_{j+1} = \{\dot{q}\}_j + \Delta t\left[(1-\gamma)\{\ddot{q}\}_j + \gamma\{\ddot{q}\}_{j+1}\right] \tag{67}$$

Here, β and γ are chosen to maintain the accuracy and stability. The integration is stable if $2\beta \geq \gamma \geq 0.5$ and $\{q\} = \begin{Bmatrix} p \\ u_d \end{Bmatrix}$, $\{\dot{q}\} = \begin{Bmatrix} \dot{p} \\ \dot{u}_d \end{Bmatrix}$ and $\{\ddot{q}\} = \begin{Bmatrix} \ddot{p} \\ \ddot{u}_d \end{Bmatrix}$.

3.6 THEORETICAL FORMULATION FOR SOIL FOUNDATION

The soil foundation domain has been discretized using eight-node isoparametric element. Mass, stiffness and damping matrix of the soil medium has been calculated in the same manner as in the structure domain. Infinite soil medium is truncated to make it finite. The well-known viscous boundary condition (Kontoe, 2009) has been used in the present work. In two-dimensional modelling (Fig. 3.3), the absorbing boundary condition can be formulated from the following equations.

$$\sigma(s) + \rho c_p \dot{u}_{sl}(s) = 0 \tag{68}$$

$$\tau(s) + \rho c_s \dot{v}_{sl}(s) = 0 \tag{69}$$

Here, σ is the normal stress and τ is the shear stress at the truncation surface of the soil medium. u_{sl} is the normal displacement and v_{sl} is the shear displacement of soil and s denote the coordinate of artificial boundary. c_p and c_s are the compression wave and shear wave velocity, respectively. The normal and tangential damping coefficients $\boldsymbol{c_n}$ and c_t can be expressed as follows.

$$c_n = A_1 \rho c_p \tag{70}$$

$$c_t = A_2 \rho c_s \tag{71}$$

The coefficients c_s and c_p in two mutually orthogonal directions can be expressed below.

$$c_s = \sqrt{\frac{G}{\rho}} \tag{72}$$

$$c_p = \sqrt{\frac{E(1-\nu)}{(1+\nu)(1-2\nu)\rho}} \tag{73}$$

G is the shear modulus and is expressed as below.

$$G = \frac{1}{2(1+\nu)} \tag{74}$$

A_1 and A_2 are the areas influenced by wave propagation directions. Generally, they are assumed as unity. For an isotropic medium, they become as below (Kontoe, 2009).

$$A_1 = \frac{8}{15\pi}(5 + 2s - 2s^2) \tag{75}$$

$$A_2 = \frac{8}{15\pi}(3 + 2s) \tag{76}$$

Here, *s* can be expressed as below.

$$s = \sqrt{\frac{(1-2\nu)}{2(1-\nu)}} \tag{77}$$

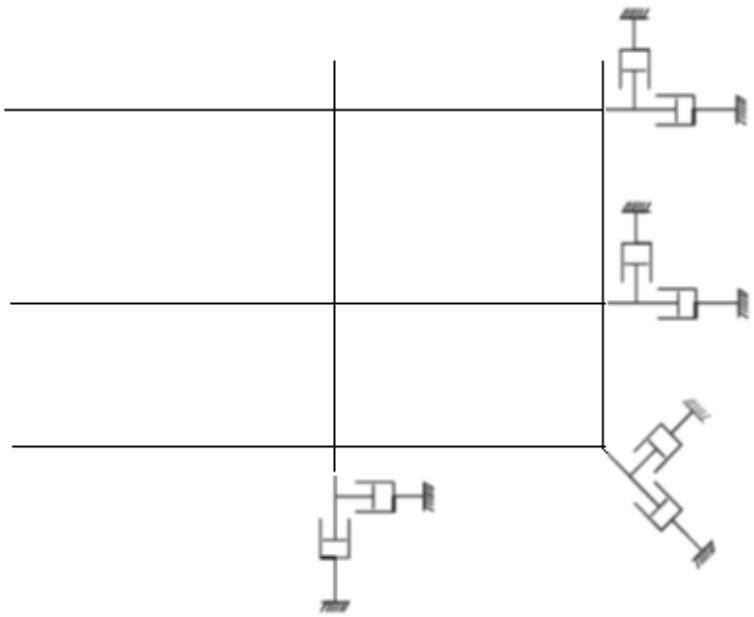

Fig 3.3 Schematic diagram of the standard viscous boundary

3.7 THEORETICAL FORMULATION OF DAM-RESERVOIR-FOUNDATION COUPLED SYSTEMS

The dam, reservoir and soil foundation systems are coupled using direct coupling approach. The coupling equation between dam and reservoir can be obtained by Eq. 65 considering fluid-structure interaction (FSI). Here "added motion" approach is followed to solve the soil-structure interaction (SSI) problem. Free field responses are determined at the base of the structure before the SSI analysis. Absolute responses of the dam-reservoir-foundation couple systems are assumed to be the sum of two parts, viz. free field responses and added part of the responses. The free field responses of the dam-reservoir-foundation system are obtained by analyzing the foundation alone due to external excitation without considering the dam and reservoir. Added part of the responses are found out by analyzing the dam-reservoir-foundation coupled model. The dynamic equilibrium equation for a coupled dam-reservoir-foundation system may be found in terms of absolute responses, U_a with the following equation.

$$\begin{bmatrix} J & Q_d^T & Q_c^T & 0 \\ 0 & M_{dd} & M_{dc} & 0 \\ 0 & M_{cd} & M_{cc} & M_{cf} \\ 0 & 0 & M_{fc} & M_{ff} \end{bmatrix} \begin{Bmatrix} \ddot{P} \\ \ddot{U}_{ad} \\ \ddot{U}_{ac} \\ \ddot{U}_{af} \end{Bmatrix} + \begin{bmatrix} A & 0 & 0 & 0 \\ 0 & C_{dd} & C_{dc} & 0 \\ 0 & C_{cd} & C_{cc} & C_{cf} \\ 0 & 0 & C_{fc} & C_{ff} \end{bmatrix} \begin{Bmatrix} \dot{P} \\ \dot{U}_{ad} \\ \dot{U}_{ac} \\ \dot{U}_{af} \end{Bmatrix} +$$

$$\begin{bmatrix} H & 0 & 0 & 0 \\ -\begin{bmatrix} Q_d \\ Q_c \end{bmatrix} & K_{dd} & K_{dc} & 0 \\ 0 & K_{cd} & K_{cc} & K_{cf} \\ 0 & 0 & K_{fc} & K_{ff} \end{bmatrix} \begin{Bmatrix} P \\ U_{ad} \\ U_{af} \\ U_{ac} \end{Bmatrix} = - \begin{bmatrix} I & 0 & 0 & 0 \\ 0 & M_{dd} & M_{dc} & 0 \\ 0 & M_{cd} & M_{cc} & M_{cf} \\ 0 & 0 & M_{fc} & M_{ff} \end{bmatrix} \begin{Bmatrix} F_r \\ \ddot{U}_d^g \\ \ddot{U}_c^g \\ \ddot{U}_f^g \end{Bmatrix} \quad (78)$$

Here subscript '*d*' indicates the nodes within the dam region, '*f*' signifies the nodes within the foundation region and '*c*' denotes the nodes along the interface of the dam and foundation. $\ddot{U}^g$ present the acceleration vector of ground motion. The mass damping and stiffness of the common nodes are the sum of the contributions from the dam (*d*) and foundation (*f*) and are expressed in Eq. 79. The coupling matrix $Q=\left[\begin{bmatrix} Q_d \end{bmatrix} \quad \begin{bmatrix} Q_c \end{bmatrix}\right]^T$, matrix $[Q_d]$ related to the body of the dam other than common nodes and matrix $[Q_c]$ is related to the common nodes at the interface of the dam and foundation. Absolute responses of the dam-reservoir-foundation

system are considered as the sum of the free field responses and added part of the responses response and expressed in Eq. 80.

$$M_{cc} = M_c^d + M_c^f, C_{cc} = C_c^d + C_c^f \text{ and } K_{cc} = K_c^d + K_c^f \tag{79}$$

$$\begin{Bmatrix} \ddot{P} \\ \ddot{U}_{ad} \\ \ddot{U}_{ac} \\ \ddot{U}_{af} \end{Bmatrix} = \begin{Bmatrix} \ddot{P}^{ff} \\ \ddot{u}_d^{ff} \\ \ddot{u}_c^{ff} \\ \ddot{u}_f^{ff} \end{Bmatrix} + \begin{Bmatrix} \ddot{P}^{a} \\ \ddot{u}_d^{a} \\ \ddot{u}_c^{a} \\ \ddot{u}_f^{a} \end{Bmatrix}, \quad \begin{Bmatrix} \dot{P} \\ \dot{U}_{ad} \\ \dot{U}_{ac} \\ \dot{U}_{af} \end{Bmatrix} = \begin{Bmatrix} \dot{P}^{ff} \\ \dot{u}_d^{ff} \\ \dot{u}_c^{ff} \\ \dot{u}_c^{ff} \end{Bmatrix} + \begin{Bmatrix} \dot{P}^{a} \\ \dot{u}_d^{a} \\ \dot{u}_c^{a} \\ \dot{u}_c^{a} \end{Bmatrix},$$

$$\text{and} \quad \begin{Bmatrix} P \\ U_{ad} \\ U_{ac} \\ U_{af} \end{Bmatrix} = \begin{Bmatrix} P^{ff} \\ u_d^{ff} \\ u_c^{ff} \\ u_f^{ff} \end{Bmatrix} + \begin{Bmatrix} P^{a} \\ u_d^{a} \\ u_c^{a} \\ u_f^{a} \end{Bmatrix} \tag{80}$$

Here superscripts 'ff' stands for free field responses and 'a' denotes added part responses. The free field responses are denoted by the free field displacements, u^{ff}, velocities, $\dot{u}^{ff}$ and accelerations, $\ddot{u}^{ff}$. The added parts of the responses are denoted by the displacements, u^a, velocities, $\dot{u}^a$and accelerations, $\ddot{u}^a$. The absolute responses are denoted by the displacements U_a, velocities, $\dot{U}_a$ and accelerations, $\ddot{U}_a$.Putting Eq. (80) in Eq. (78) we can get the following equations.

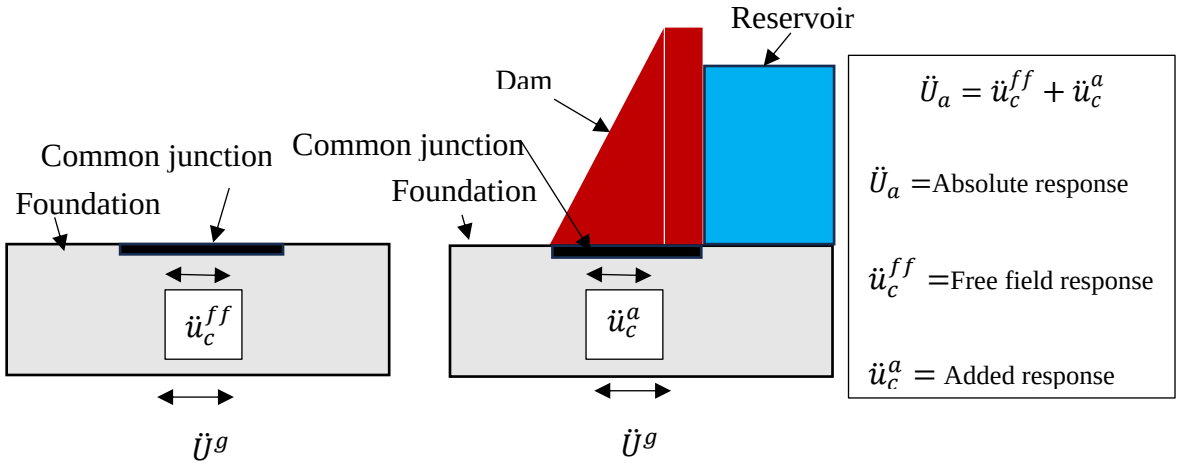

Fig. 3.4. Schematic diagram of dam-reservoir-foundation for application of ground motion

$$\begin{bmatrix} J & Q_d^T & Q_c^T & 0 \\ 0 & M_{dd} & M_{dc} & 0 \\ 0 & M_{cd} & M_{cc} & M_{cf} \\ 0 & 0 & M_{fc} & M_{ff} \end{bmatrix} \begin{Bmatrix} \ddot{P}^a \\ \ddot{u}_d^a \\ \ddot{u}_c^a \\ \ddot{u}_f^a \end{Bmatrix} + \begin{bmatrix} A & 0 & 0 & 0 \\ 0 & C_{dd} & C_{dc} & 0 \\ 0 & C_{cd} & C_{cc} & C_{cf} \\ 0 & 0 & C_{fc} & C_{ff} \end{bmatrix} \begin{Bmatrix} \dot{P}^a \\ \dot{u}_d^a \\ \dot{u}_c^a \\ \dot{u}_c^a \end{Bmatrix} +$$

$$\begin{bmatrix} H & 0 & 0 & 0 \\ -\begin{bmatrix} Q_d \\ Q_c \end{bmatrix} & K_{dd} & K_{dc} & 0 \\ 0 & K_{cd} & K_{cc} & K_{cf} \\ 0 & 0 & K_{fc} & K_{ff} \end{bmatrix} \begin{Bmatrix} P^a \\ u_d^a \\ u_c^a \\ u_f^a \end{Bmatrix} = R + F \tag{81}$$

Here

$$R = -\begin{bmatrix} J & Q_d^T & Q_c^T & 0 \\ 0 & M_{dd} & M_{dc} & 0 \\ 0 & M_{cd} & M_{cc} & M_{cf} \\ 0 & 0 & M_{fc} & M_{ff} \end{bmatrix} \begin{Bmatrix} \ddot{P}^{ff} \\ \ddot{u}_d^{ff} \\ \ddot{u}_c^{ff} \\ \ddot{u}_f^{ff} \end{Bmatrix} - \begin{bmatrix} A & 0 & 0 & 0 \\ 0 & C_{dd} & C_{dc} & 0 \\ 0 & C_{cd} & C_{cc} & C_{cf} \\ 0 & 0 & C_{fc} & C_{ff} \end{bmatrix} \begin{Bmatrix} \dot{P}^{ff} \\ \dot{u}_d^{ff} \\ \dot{u}_c^{ff} \\ \dot{u}_c^{ff} \end{Bmatrix} -$$

$$\begin{bmatrix} H & 0 & 0 & 0 \\ -\begin{bmatrix} Q_d \\ Q_c \end{bmatrix} & K_{dd} & K_{dc} & 0 \\ 0 & K_{cd} & K_{cc} & K_{cf} \\ 0 & 0 & K_{fc} & K_{ff} \end{bmatrix} \begin{Bmatrix} P^{ff} \\ u_d^{ff} \\ u_c^{ff} \\ u_f^{ff} \end{Bmatrix} \tag{82}$$

and

$$F = -\begin{bmatrix} I & 0 & 0 & 0 \\ 0 & M_{dd} & M_{dc} & 0 \\ 0 & M_{cd} & M_{cc} & M_{cf} \\ 0 & 0 & M_{fc} & M_{ff} \end{bmatrix} \begin{Bmatrix} F_r \\ \ddot{U}_d^g \\ \ddot{U}_c^g \\ \ddot{U}_f^g \end{Bmatrix} \tag{83}$$

A numerical technique is adopted to obtain the solution directly in terms of the absolute displacements of the entire system. Now, free field responses are determined by analyzing the soil foundation part separately. Therefore, the values of displacement, velocity and acceleration for the structure and fluid can be taken equal to zero. Hence, the equations can be written below.

$$\begin{Bmatrix} \ddot{P} \\ \ddot{U}_{ad} \\ \ddot{U}_{ac} \\ \ddot{U}_{af} \end{Bmatrix} = \begin{Bmatrix} 0 \\ 0 \\ \ddot{u}_c^{ff} \\ \ddot{u}_f^{ff} \end{Bmatrix} + \begin{Bmatrix} \ddot{P}^a \\ \ddot{u}_d^a \\ \ddot{u}_c^a \\ \ddot{u}_f^a \end{Bmatrix}, \quad \begin{Bmatrix} \dot{P} \\ \dot{U}_{ad} \\ \dot{U}_{ac} \\ \dot{U}_{af} \end{Bmatrix} = \begin{Bmatrix} 0 \\ 0 \\ \dot{u}_c^{ff} \\ \dot{u}_c^{ff} \end{Bmatrix} + \begin{Bmatrix} \dot{P}^a \\ \dot{u}_d^a \\ \dot{u}_c^a \\ \dot{u}_c^a \end{Bmatrix},$$

$$\text{and} \quad \begin{Bmatrix} P \\ U_{ad} \\ U_{ac} \\ U_{af} \end{Bmatrix} = \begin{Bmatrix} 0 \\ 0 \\ u_c^{ff} \\ u_f^{ff} \end{Bmatrix} + \begin{Bmatrix} P^a \\ u_d^a \\ u_c^a \\ u_f^a \end{Bmatrix} \tag{84}$$

Free field responses at the common and other nodes of the foundation are obtained by analyzing foundation only, i.e. no dam and reservoir are present on it. When the foundation is subjected to seismic excitation, the free field responses can be determined by solving the equation below.

$$\begin{bmatrix} M_{cc} & M_{cf} \\ M_{fc} & M_{ff} \end{bmatrix} \begin{Bmatrix} \ddot{u}_c^{ff} \\ \ddot{u}_f^{ff} \end{Bmatrix} + \begin{bmatrix} C_{cc} & C_{cf} \\ C_{fc} & C_{ff} \end{bmatrix} \begin{Bmatrix} \dot{u}_c^{ff} \\ \dot{u}_f^{ff} \end{Bmatrix} + \begin{bmatrix} K_{cc} & K_{cf} \\ K_{fc} & K_{ff} \end{bmatrix} \begin{Bmatrix} u_c^{ff} \\ u_f^{ff} \end{Bmatrix} = -\begin{bmatrix} M_{cc} & M_{cf} \\ M_{fc} & M_{ff} \end{bmatrix} \begin{Bmatrix} \ddot{U}_c^g \\ \ddot{U}_f^g \end{Bmatrix} \tag{85}$$

After getting the free field responses, the interaction force R can be determined by using Eq. (84) in the following simplified manner.

$$R = -\begin{bmatrix} 0 & 0 & 0 & 0 \\ 0 & M_{dd} & M_{dc} & 0 \\ 0 & M_{cd} & M_{cc}^{d} & 0 \\ 0 & 0 & 0 & 0 \end{bmatrix} \begin{Bmatrix} 0 \\ 0 \\ \ddot{u}_c^{ff} \\ 0 \end{Bmatrix} - \begin{bmatrix} 0 & 0 & 0 & 0 \\ 0 & C_{dd} & C_{dc} & 0 \\ 0 & C_{cd} & C_{cc}^{d} & 0 \\ 0 & 0 & 0 & 0 \end{bmatrix} \begin{Bmatrix} 0 \\ 0 \\ \dot{u}_c^{ff} \\ 0 \end{Bmatrix} - \begin{bmatrix} 0 & 0 & 0 & 0 \\ 0 & K_{dd} & K_{dc} & 0 \\ 0 & K_{cd} & K_{cc}^{d} & 0 \\ 0 & 0 & 0 & 0 \end{bmatrix} \begin{Bmatrix} 0 \\ 0 \\ u_c^{ff} \\ 0 \end{Bmatrix} \quad (86)$$

After getting the free field responses, the absolute responses of dam-reservoir-foundation coupled system are determined with the help of following steps.

Step I: the interaction force *R* in Eq. (86) is determined.

Step II: As per Eq. (81), the added responses of the dam, foundation and reservoir domain are calculated.

Step III: Free field response and these calculated added responses are needed to be sum up for getting absolute responses of dam-reservoir-foundation coupled systems.

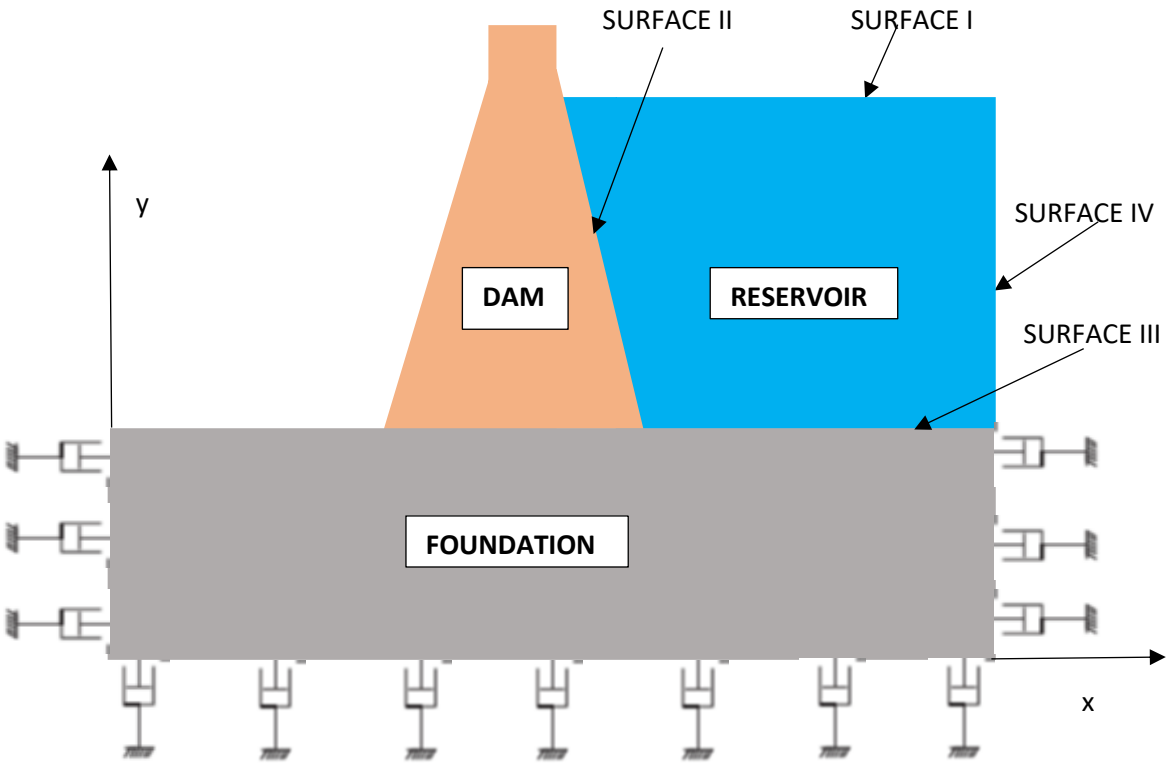

Fig. 3.5 Geometry of dam-reservoir-foundation coupled systems

CHAPTER 4

RESULTS AND DISCUSSION

4.1 GENERAL

Stability and sustainability of a concrete gravity dam depend upon the different parameters of the adjacent reservoir and the soil foundation beneath the dam structure. Gravity dams could be adversely affected by seismic waves. For the safety and stability of a dam, it should be designed against dynamic excitation. Hydrodynamic forces develop on the face of the dam due to earthquakes. Nature of hydrodynamic forces depends upon the physical behaviour of the adjacent reservoir and soil foundation. Different physical parameters of the adjacent reservoir and foundation of the gravity dam influence the hydrodynamic pressure on the dam as well as structural responses. Upstream slope of the reservoir, slope of the reservoir bed, inclined length and reflection coefficient of the reservoir bottom are important parameters that influence the hydrodynamic pressure. Along with these, seismic behaviour of the soil foundation has a high impact on the responses of the gravity dam. Effects of fluid-structure and soil-structure interactions are needed to be properly incorporated to understand the seismic behaviour of concrete gravity dam. A thorough study is required on the adjacent reservoir with different parametric changes. Understanding the behaviour of dam-reservoir coupled systems due to dynamic excitation including fluid-structure interaction is of utmost importance. The effect of soil foundation on the structure can be achieved by analyzing dam-reservoir-foundation coupled systems applying earthquake forces.

In the present work, the first analysis has been carried out on the reservoir considering the dam as rigid to understand the nature of hydrodynamic pressure for variation of different parameters of the reservoir. Bed slope of the reservoir, inclined length and reflection coefficient of the reservoir bottom are considered as variables during the parametric study. The study is continued to understand the nature of hydrodynamic pressure and responses of the gravity dam applying dynamic excitation on dam-reservoir coupled systems including the fluid-structure interaction. Different parametric studies are also executed for understanding the behaviour of these dam-reservoir coupled systems due to dynamic excitation. In the final step, the responses of dam-reservoir systems are studied considering the effect of soil foundation due to seismic excitations. Parametric studies on dam-reservoir-foundation coupled systems are also executed

to study the seismic performance of the concrete gravity dam. So, the entire chapter has been divided into three sections. In Section 1, analysis of infinite reservoir has been done. In Section 2, analysis of dam-reservoir coupled system has been carried out. In section 3, analysis of dam-reservoir-foundation systems has been carried out.

4.2 SECTION 1: ANALYSIS OF INFINITE RESERVOIR

Hydrodynamic pressure within the reservoir due to dynamic excitations is determined here. The foundation is considered as rigid. The fluid within the reservoir is assumed as compressible and its viscosity is neglected. The infinitely long reservoir is truncated at a suitable distance to save computational time. A suitable non-reflecting boundary condition, proposed by Gogoi and Maity (2006), is applied at this truncated surface. The fluid region is discretized and modelled by eight-node isoparametric element. A MATLAB code has been developed to analyze this unbounded reservoir.

4.2.1 VALIDATION OF THE DEVELOPED ALGORITHM

For the validation of the proposed algorithm, the results obtained from free vibration analysis are compared with the results of Samii and Lotfi (2007). Length (L) of the reservoir is taken as 200 m. and height (H_f) is assumed as 116.19 m. Velocity (c) of sound wave within the fluid is assumed as 1440 m/sec and unit weight (ρ_f) of water is taken as 9.81 kN/m^3. The natural frequencies of the reservoir are compared with the result obtained by Samii and Lotfi (2007) in Table 4.1. Since the deviations are quite insignificant, the developed program is deemed fit for further studies.

Table 4.1: Comparison of natural frequencies of first five modes of the reservoir

Mode Number	Natural frequency from present study in Hz	Natural frequency of Samii and Lotfi (2007) in Hz
1	3.188	3.115
2	4.881	4.749
3	7.924	7.796
4	9.330	9.300
5	10.036	9.958

4.2.2 SELECTION OF APPROPRIATE TRUNCATION BOUNDARY CONDITION

Selection of an efficient truncation boundary condition is one very important job for finite element analysis of infinite reservoir. In this section, the results obtained from different boundary conditions, such as Sommerfeld (1949), Sharan (1992), Maity and Bhattacharya (1999) and Gogoi and Maity (2006), are compared with the closed-form solution (exact C_p) achieved by Bouaanani et al. (2003) to obtain the suitable boundary condition for the analysis of unbounded reservoir. Depth (H_f) of the reservoir is considered as 70 m. Unit weight (ρ_f) of water is considered as 1000 kg/m^3 and velocity (c) of sound wave in water is set as 1440 m/sec. The reflection coefficient (α) of the reservoir bottom is taken as 0.95 and 0.5 respectively. The study has been done for two different exiting frequencies, such as, Tc/H_f =10 and 100. The amplitude of the applied excitations (a) is assumed equal to the gravitational acceleration of 1.0g. The values of pressure coefficients ($C_p = p/\rho_f a H_f$) at the heel of the dam are determined for different boundary conditions and presented in Table 4.2.

Table 4.2: Comparison of different truncation boundary conditions

Tc/H_f	L/H_f	α	Exact Cp (2003)	Sommer-feld (1949)	%Error	Sharan (1992)	%Error	Maity and Bhattacharya (1999)	%Error	Googol and Maity (2006)	%Error
10	0.1	0.95	0.8155	8.1721	902.10	0.6780	-16.9	0.7559	-7.30	0.75589	-7.31
10	0.2	0.95	0.8155	4.1341	406.94	0.7254	-11.0	0.7714	-5.40	0.77139	-5.41
10	0.5	0.95	0.8155	1.7794	118.20	0.8065	-1.1	0.8226	0.87	0.82253	0.86
10	1	0.95	0.8155	1.1217	37.55	0.9335	14.5	0.9348	14.63	0.93473	14.62
10	0.1	0.5	0.8097	8.1610	907.90	0.6573	-18.8	0.7344	-9.30	0.72717	-10.19
10	0.2	0.5	0.8097	4.1301	410.08	0.7209	-11.0	0.7669	-5.29	0.75903	-6.26
10	0.5	0.5	0.8097	1.7794	119.76	0.8065	-0.4	0.8226	1.59	0.81032	0.08
10	1	0.5	0.8097	1.0400	28.45	0.9335	15.3	0.9348	15.45	0.91878	13.47
100	0.02	0.95	0.7431	25.3642	3313.30	0.6555	-11.8	0.7417	-0.19	0.74170	-0.19
100	0.05	0.95	0.7431	10.1594	1267.17	0.6804	-8.4	0.7419	-0.17	0.74186	-0.17
100	0.1	0.95	0.7431	5.1042	586.88	0.7064	-4.9	0.7420	-0.15	0.74214	-0.13
100	0.02	0.5	0.7430	25.3642	3313.75	0.6555	-11.8	0.7417	-0.18	0.74164	-0.18
100	0.05	0.5	0.7430	10.1594	1267.35	0.6804	-8.4	0.7419	-0.15	0.74180	-0.16
100	0.1	0.5	0.7430	5.1042	586.97	0.7064	-4.9	0.7420	-0.13	0.74208	-0.12

From the above table, it is clear that the percentage error of pressure coefficient (C_p) at the heel of the dam is less for the boundary conditions proposed by Maity and Bhattacharya (1999) and Gogoi and Maity (2006). From the literature, it is observed that the boundary

condition proposed by Maity and Bhattacharya is applicable for Tc/H_f >4. However, the boundary condition proposed by Gogoi and Maity did not show such limitations and was found quite suitable for the present study. Hence, the boundary condition proposed by Gogoi and Maity (2006) has been used for the analysis of unbounded reservoir in the present study.

4.2.3 NUMERICAL RESULTS WITH DISCUSSION

In the present work, the behaviour of infinite reservoir adjacent to a concrete gravity dam has been observed considering the dam as rigid. Length of the infinite reservoir is truncated to make the reservoir finite and a non-reflecting boundary condition, proposed by Gogoi and Maity (2006), is applied at the truncated surface. The fluid medium has been discretized and modelled using eight-node isoparametric element (Fig. 4.1). For the convergence study for suitable mesh and time step, pressure coefficients (C_p) obtained at the heel of the dam are shown in Table 4.3 and Table 4.4 respectively. Here, the excitations are considered to be sinusoidal with Tc/H_f is equal to 100. The reflection coefficient (α) at the reservoir bottom is taken as 0.95. Height (H_f) of the reservoir is assumed as 100 m. and L/H_f is assumed as 0.5. Here T is the time period of vibration and L is the truncated length of the reservoir. Unit weight of water (ρ_f) is considered as 1000 kg/m^3 and velocity (c) of sound wave in water is assumed as 1440 m/sec. From Table 4.3 one may see that N_h =4 and N_v =8 is quite acceptable. Hence, N_h is the number of divisions in the horizontal direction and N_v is the number of divisions in the vertical direction. From Table 4.4 it is clear that time step $t = T/32$ is acceptable. In the rest of the work, time step t is taken as $T/32$ for the applied harmonic excitations.

Table 4.3: Convergence test for meshing of reservoir

N_h	N_v	C_p
2	8	0.74301
3	8	0.74303
4	8	0.74304
5	8	0.74304

Table 4.4: Convergence test for time step

T/t	C_p
16	0.75963
32	0.75597
48	0.75597

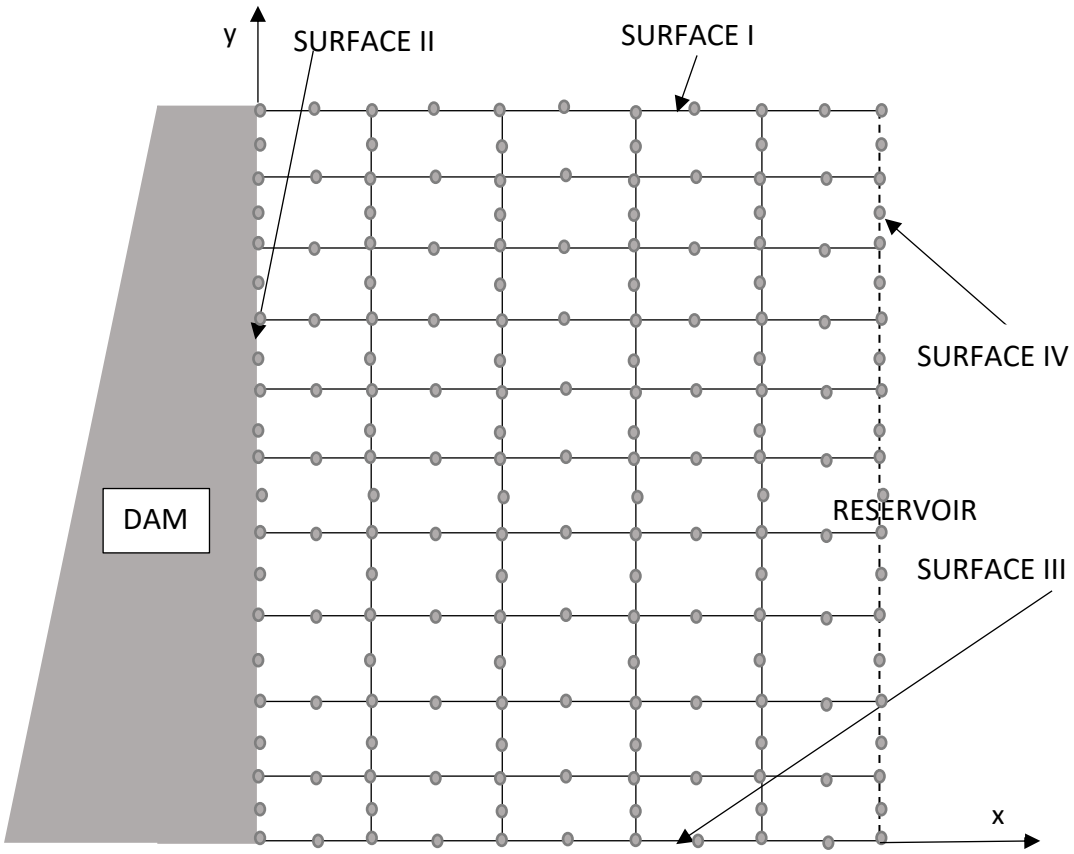

Fig. 4.1: Typical finite element mesh of reservoir

The present section of work has been divided into two parts. In Part I, analysis of the unbounded reservoir has been done for variation of inclination of the reservoir base. In Part II, analysis has been carried out for variation of inclined length of the reservoir.

4.2.3.1 PART I: ANALYSIS OF INFINITE RESERVOIR FOR VARIATION OF BED SLOPE

In this portion of the work, variation of hydrodynamic pressure has been studied with the variation of inclination angle (θ_b) of the reservoir bottom (Fig. 4.2). The angle (θ_b) is assumed as positive if it is anticlockwise with respect to the horizontal surface and considered to be negative when it is clockwise. Height of the reservoir (H_f) is assumed as 100 m, density (ρ_f) of fluid is assumed 1000 kg/m^3 and velocity of sound wave (c) is taken as 1440 m/sec. The upstream face of the dam is considered as vertical and rigid. L/H_f is assumed as 0.5 and the value of the reflection coefficient (α) is assumed as 0.95. Change of hydrodynamic pressure with different reservoir bed inclinations such as θ_b =+5^0, +10^0, 15^0, +20^0 and θ_b =-5^0, -10^0, -15^0, -20^0 is observed by applying harmonic load of Tc/H_f equal to 100 and earthquake excitation (Koyna Earthquake 1967, Fig. 4.3).

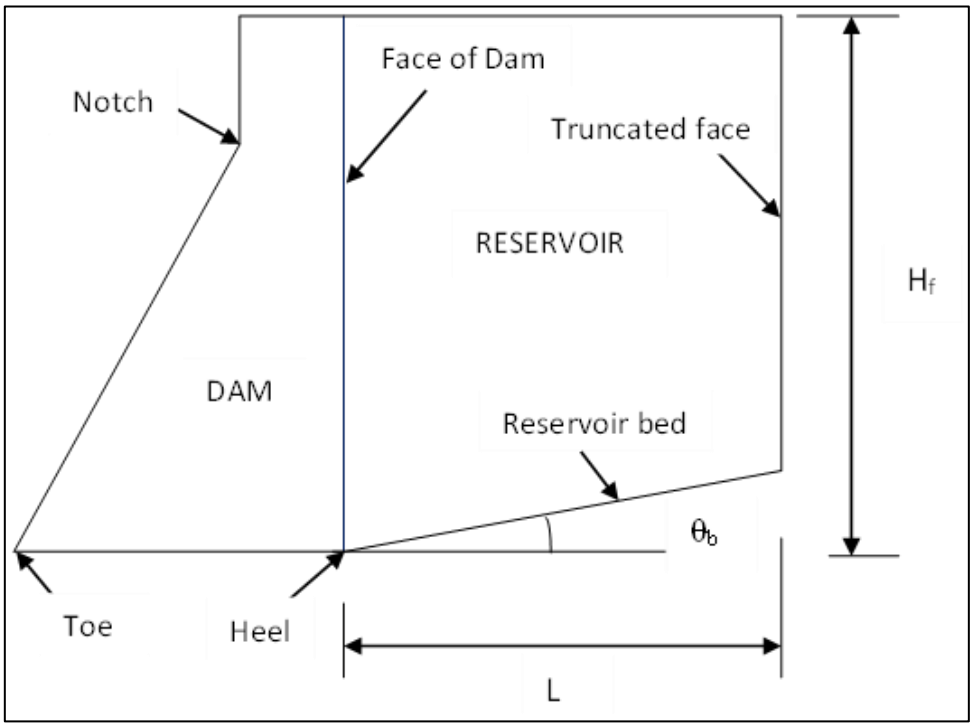

Fig. 4.2: Geometry of inclined bottom surface of the reservoir

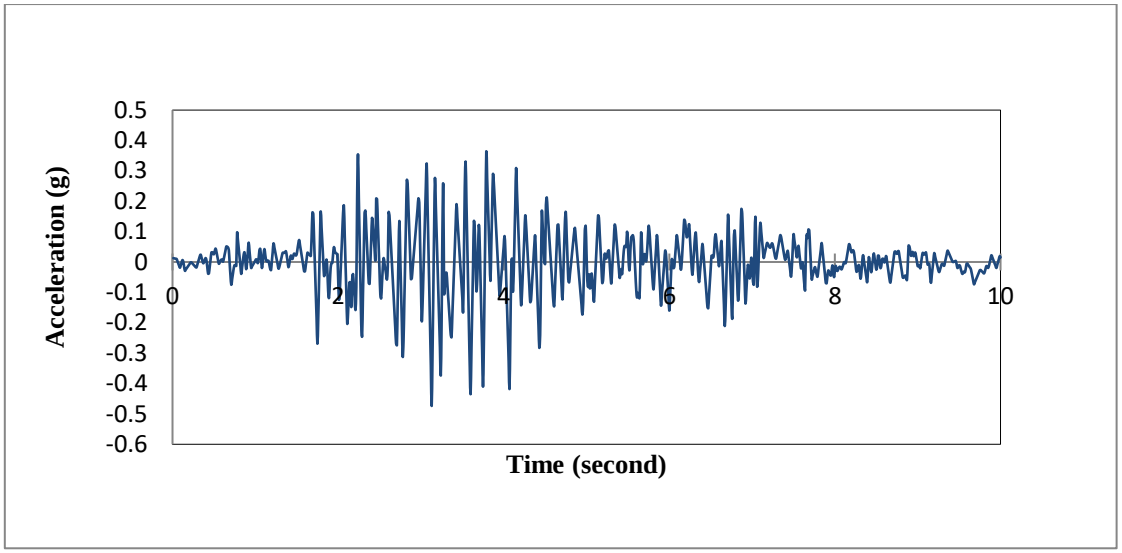

Fig. 4.3: Horizontal acceleration of Koyna earthquake (1967)

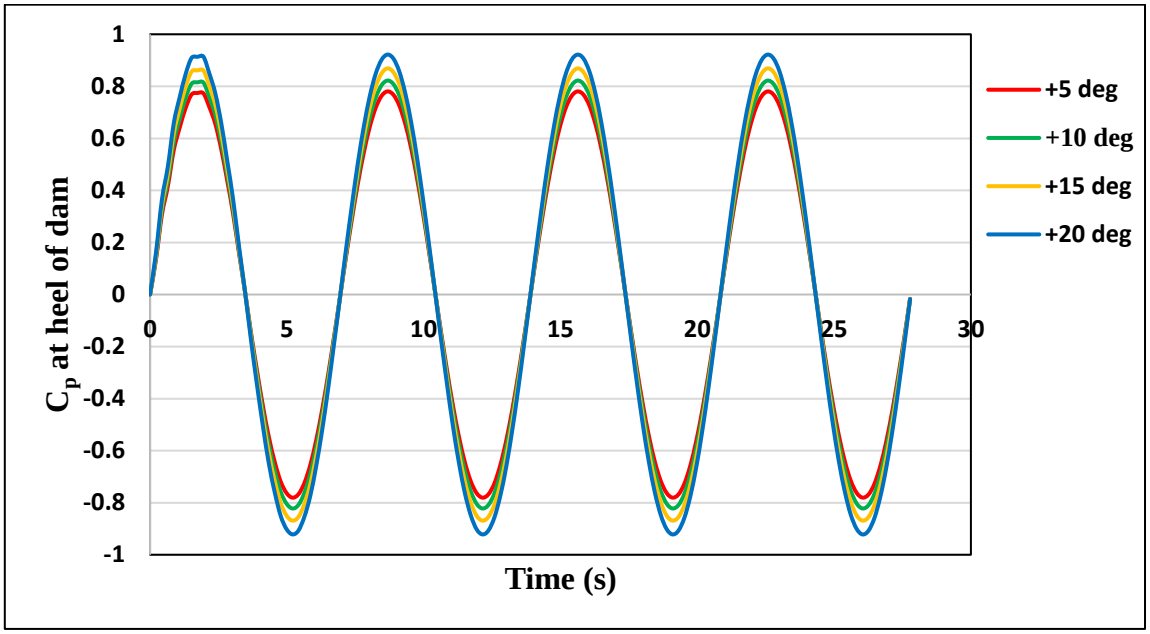

Fig. 4.4: Time history of pressure coefficient (C_p) at the heel of the dam with different bottom slopes θ_b (positive) due to harmonic loading

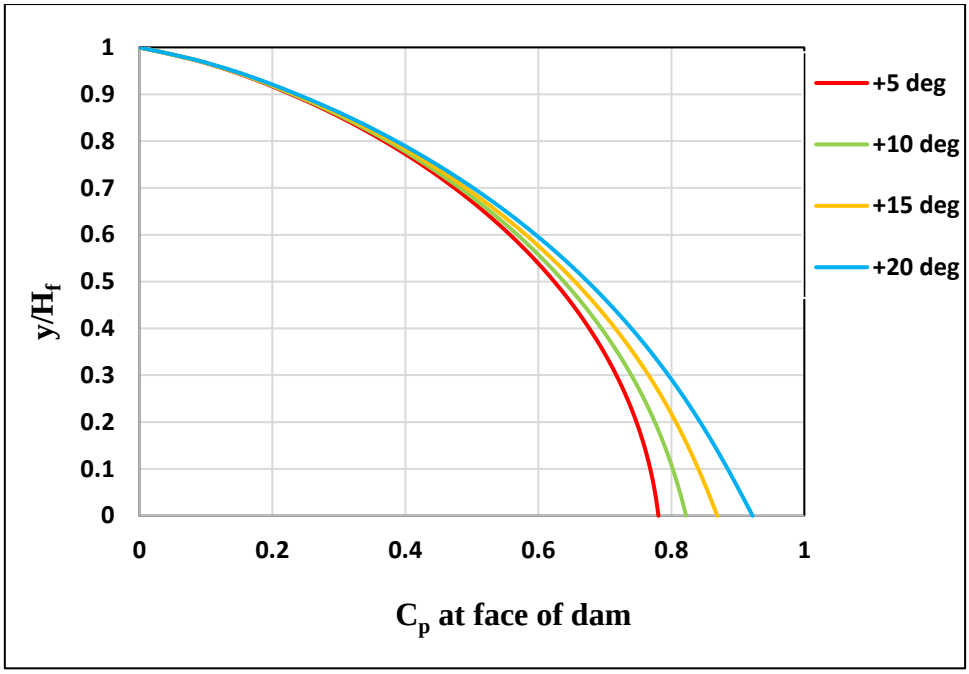

Fig. 4.5: Distribution of pressure coefficient (C_p) at the face of the dam with different bottom slopes θ_b (positive) due to harmonic loading

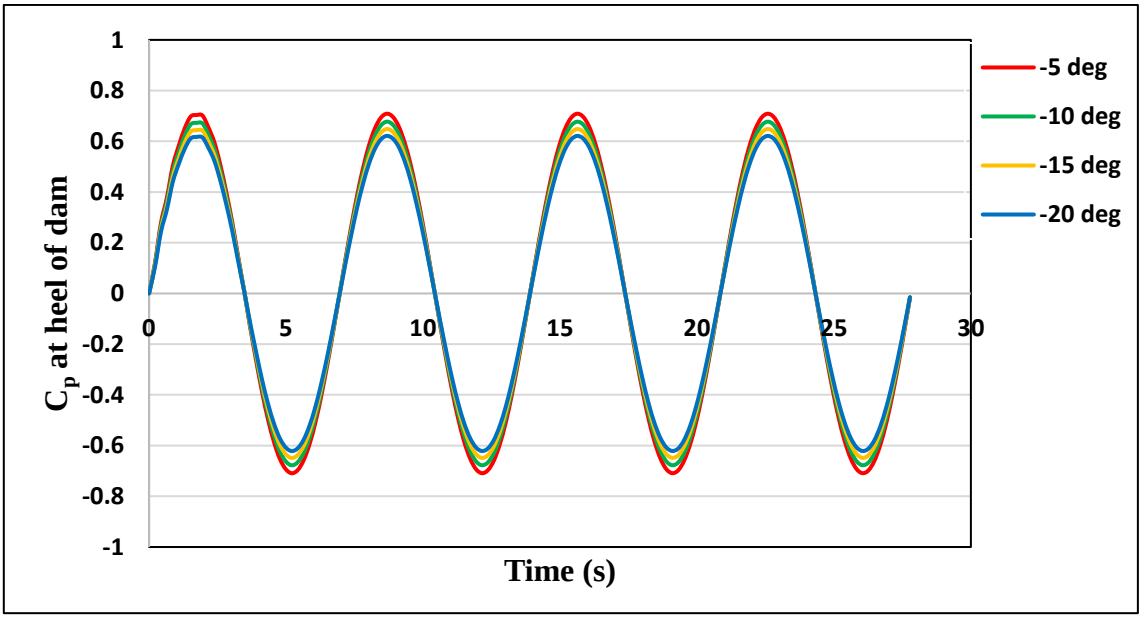

Fig. 4.6: Time history of pressure coefficient (C_p) at the heel of the dam with different bottom slopes θ_b (negative) due to harmonic loading

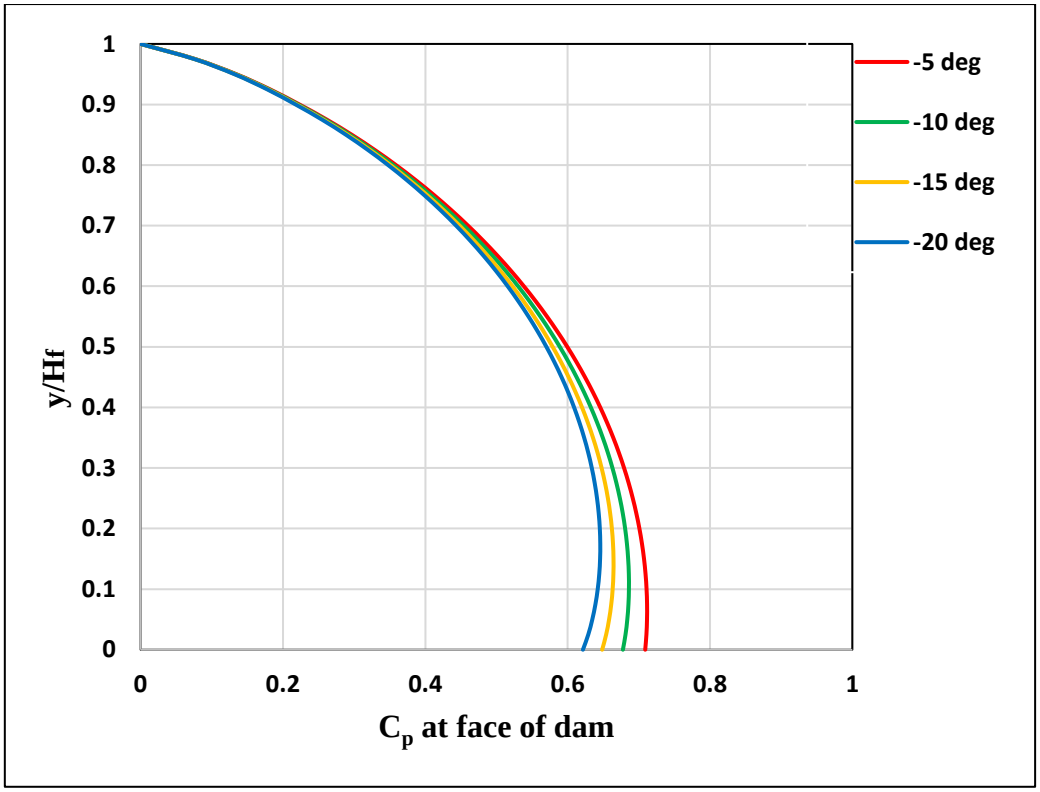

Fig. 4.7: Distribution of pressure coefficient (C_p) at the face of the dam with different bottom slopes θ_b (Negative) due to harmonic loading

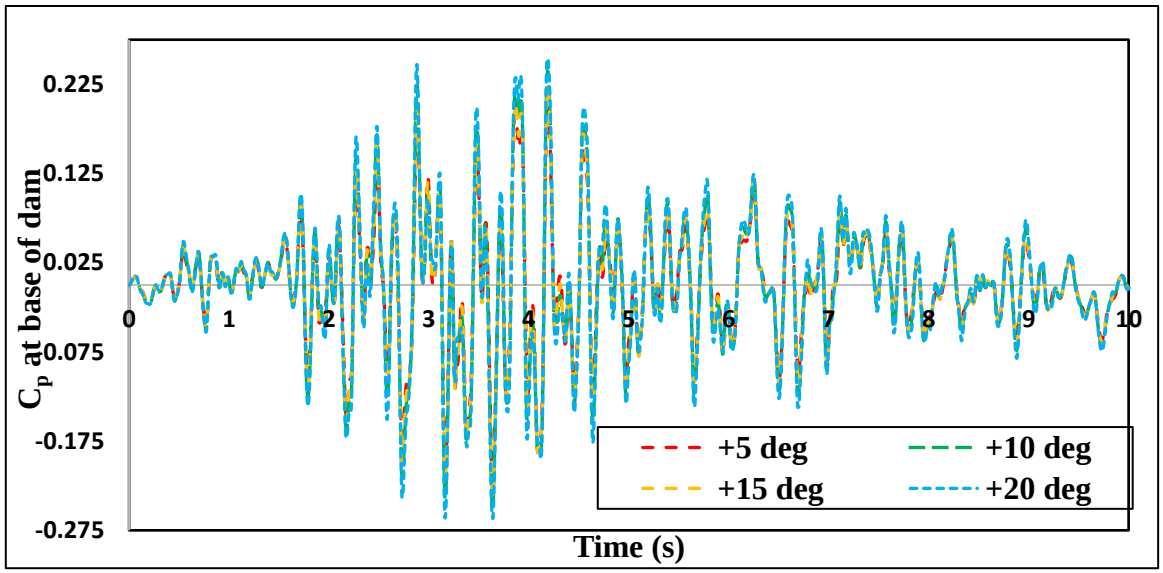

Fig. 4.8: Time history of pressure coefficient (C_p) at the heel of the dam with different bottom slopes θ_b (positive) due to Koyna earthquake

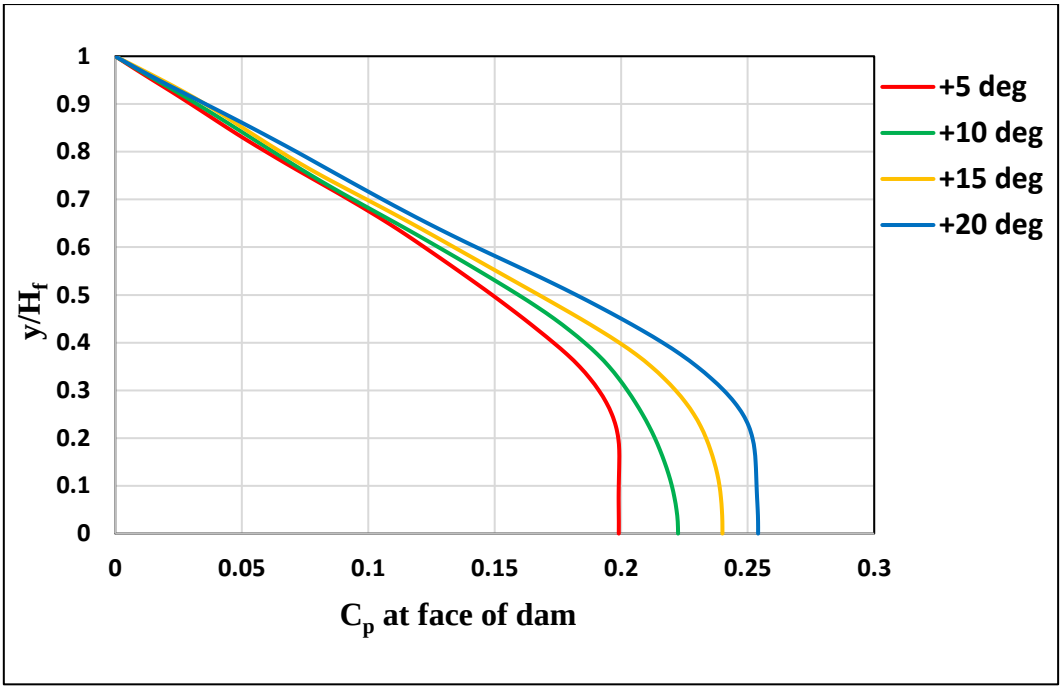

Fig. 4.9: Distribution of pressure coefficient (C_p) at the face of the dam with different bottom slopes θ_b (positive) due to Koyna earthquake

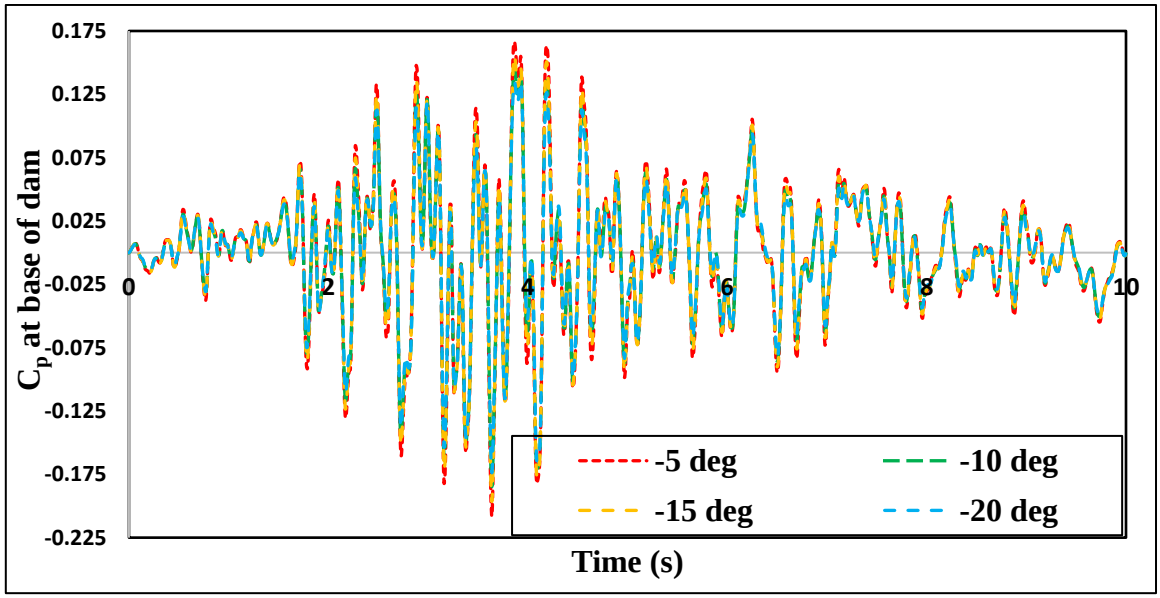

Fig. 4.10: Time history of pressure coefficient (C_p) the at heel of the dam with different bottom slopes θ_b (negative) due to Koyna earthquake

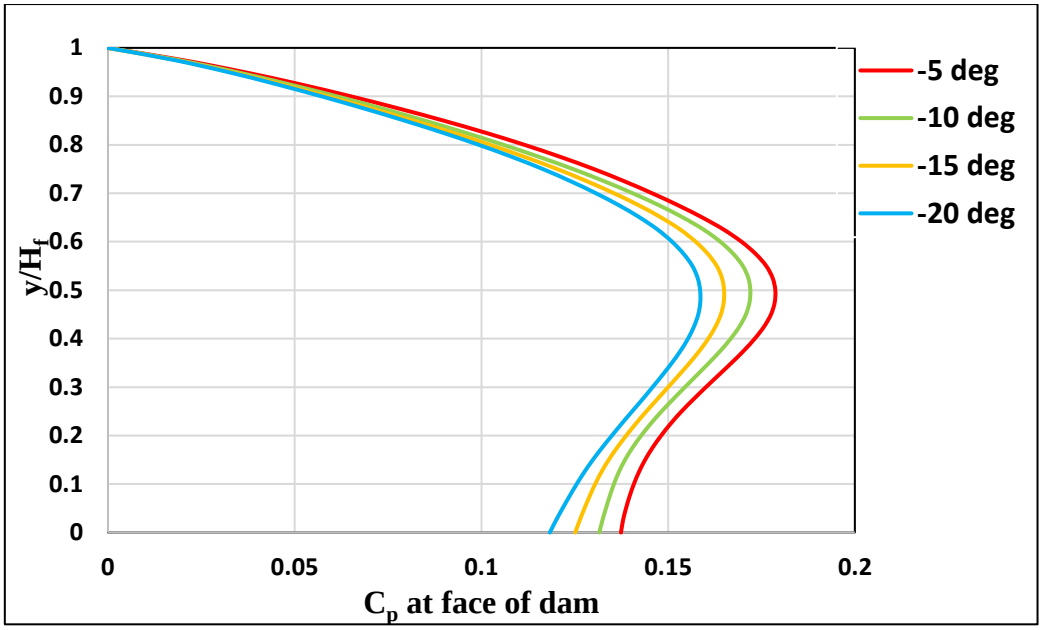

Fig. 4.11: Distribution of pressure coefficient (C_p) the at face of the dam with different bottom slopes θ_b (negative) due to Koyna earthquake

The Fig. 4.4 shows the time history plot of pressure coefficient (C_p) at the heel of the dam with different positive slope angles of the reservoir bottom and Fig. 4.5 shows the distribution of pressure coefficient (C_p) at the face of the dam with different positive slope angles of reservoir bed for harmonic excitation. From these figures, it is observed that hydrodynamic pressure at the base of the dam increases with the increase in positive magnitude of the bottom slope (θ_b) of the reservoir. Similarly, Fig. 4.6 shows the time history plot of the pressure coefficient (C_p) at the heel of the dam with different negative reservoir bed slopes. Fig. 4.7 shows the distribution of pressure coefficient (C_p) at the face of the dam with different negative slope angles of the reservoir bottom for harmonic excitation. From these figures, it may be inferred that hydrodynamic pressure at the heel of the dam decreases with the increase in negative magnitude of slope angle (θ_b) of the reservoir bottom. Fig. 4.8 and Fig. 4.10 show the time history plot of the pressure coefficient at the heel of the dam due to the Koyna earthquake (1967) with different bottom slope angles for positive and negative slopes respectively. Fig. 4.9 and Fig.4.11 present the distribution of pressure coefficient (C_p) at the face of the dam with different positive and negative bottom slopes (θ_b) respectively due to the earthquake. From these figures, it can be concluded that the value of hydrodynamic pressure increases with the increase in positive slope and decreases with the increase in negative slope at the reservoir bottom when subjected to seismic excitation.

When the slope of the reservoir bed is in positive (anticlockwise) direction, the inclined reservoir bed is towards the concrete gravity dam (Fig. 4.12). Due to this inclination, the reservoir bed reflects the wave towards the gravity dam and this is the main reason for obtaining the higher hydrodynamic pressure within the reservoir due to the comparatively higher value of positive (anticlockwise) slope. When the slope of the reservoir bed is in the negative (clockwise) direction, the inclined reservoir bed is away from the concrete gravity dam (Fig. 4.13). Due to this inclination, the reservoir bed reflects the wave that is going away from the gravity dam. This is the main reason for obtaining the lower value of hydrodynamic pressure within the reservoir due to the comparatively higher value of negative (clockwise) slope.

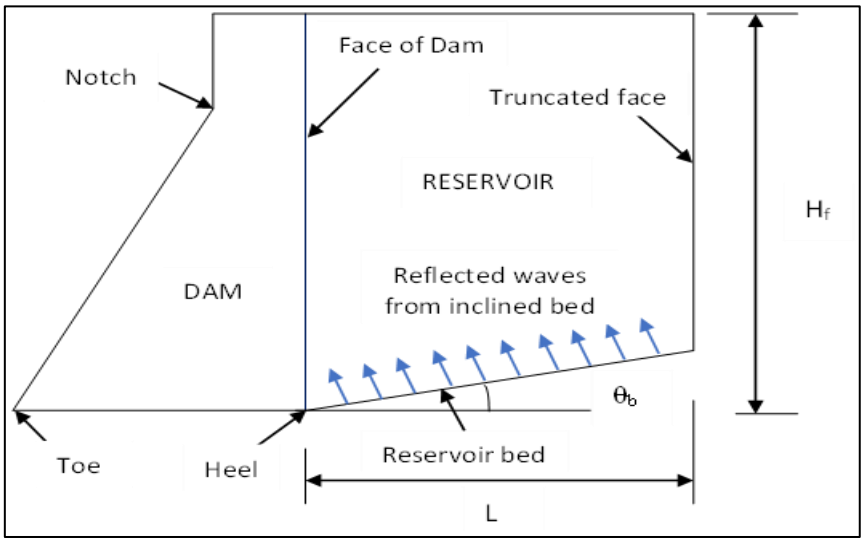

Fig. 4.12: Inclined reservoir bed (anticlockwise) with reflected waves

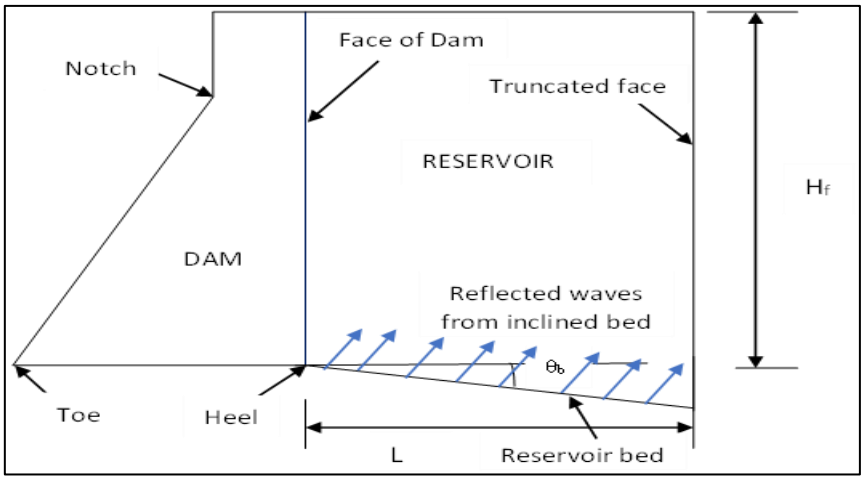

Fig. 4.13: Inclined reservoir bed (clockwise) with reflected waves

4.2.3.2 PART II: ANALYSIS OF INFINITE RESERVOIR FOR VARIATION OF INCLINED BOTTOM LENGTH

In this portion of work, variation of hydrodynamic pressure coefficient (C_p) at the face of the dam has been observed for different values of inclined length (L_i) of reservoir bed (Fig. 4.14). The height of the reservoir (H_f), velocity of acoustic wave in water (c) and density of fluid (ρ_f) have been taken as in subsection 4.2.3.1. We assume Tc/H_f = 100, L/H_f = 0.5 and reflection coefficient (α) of the reservoir bottom is equal to 0.95. Figs. 4.17 to Fig. 4.20 show the variation of pressure coefficient at the face of the dam with different values of inclined length L_i such as 0.25L, 0.5L and 0.75L with different positive slopes θ_b =+5^0, +10^0, +15^0 and +20^0 respectively. Similarly, Fig, 4.21 to Fig. 4.24 present the variation of pressure coefficient at the face of the dam with different values of inclined length (L_i= 0.25L,0.5L and 0.75L) with different negative slope angles (θ_b =-5^0, -10^0, -15^0, -20^0). From these figures, it is observed that hydrodynamic pressure increases with the increase of inclined length of the reservoir bottom for positive bed slope. It is also observed that pressure decreases with the increase of inclined length of the reservoir bottom for negative bed slope. Fig. 4.25 to Fig. 4.27 and Fig. 4.28 to Fig. 4.30 show the velocity profile of the reservoir with different inclined lengths of bottom of the reservoir for bed slope +15^0 and -15^0 respectively. The differences in the velocity profile of the reservoir are significant for different inclined lengths of the reservoir bed.

When the slope of the reservoir bed is in positive (anticlockwise) direction, the inclined reservoir bed is towards the concrete gravity dam (Fig. 4.15). Due to this inclination, the reservoir bed reflects the wave towards the gravity dam. When the inclined length increases, the amount of reflecting wave from the reservoir bed towards the gravity dam increases for positive slope. This is the main reason for obtaining the higher hydrodynamic pressure within the reservoir due to the increase of inclined length for positive (anticlockwise) slope. When the slope of the reservoir bed is in the negative (clockwise) direction, the inclined reservoir bed is away from the concrete gravity dam (Fig. 4.16). Due to this inclination, the reservoir bed reflects the wave that is going away from the gravity dam. When the inclined length increases, more amount of the reflecting wave from the reservoir bed is going away from the gravity dam for negative slope. This is the prime reason for obtaining the lower value of hydrodynamic pressure within the reservoir due to the increase of inclined length for negative (clockwise) slope. Hydrodynamic pressure changes due to changes in the inclined length of the reservoir

bed. For this reason, the velocity profiles of the reservoir are different for the different inclined lengths of the reservoir bed.

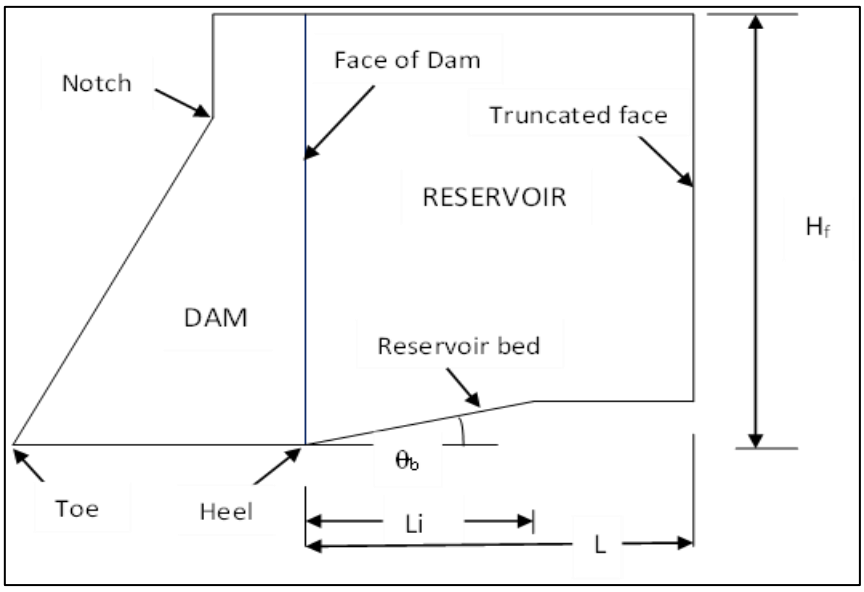

Fig. 4.14: Geometry with variable inclined length of reservoir bottom

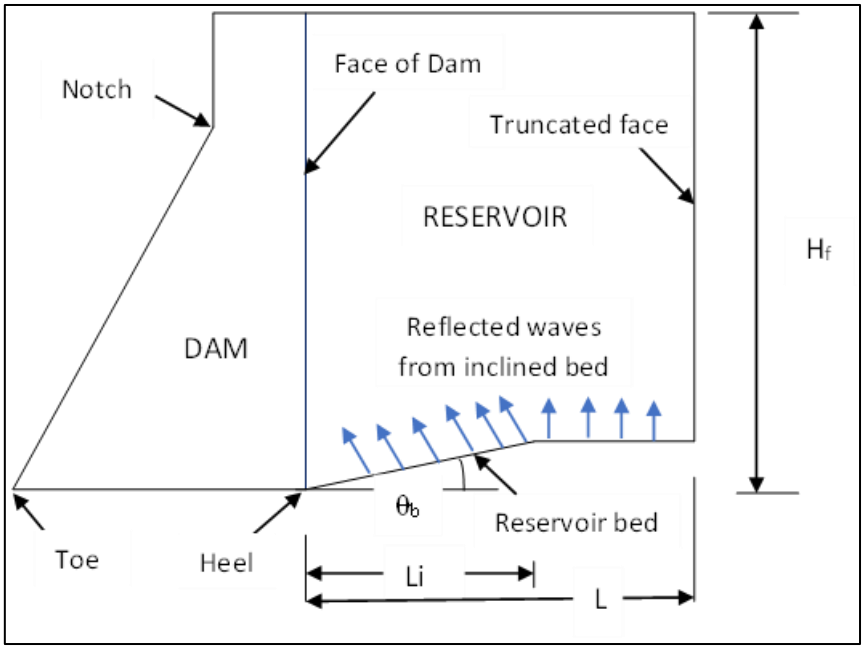

Fig. 4.15: Variable inclined length of reservoir bed (anticlockwise) with reflected waves

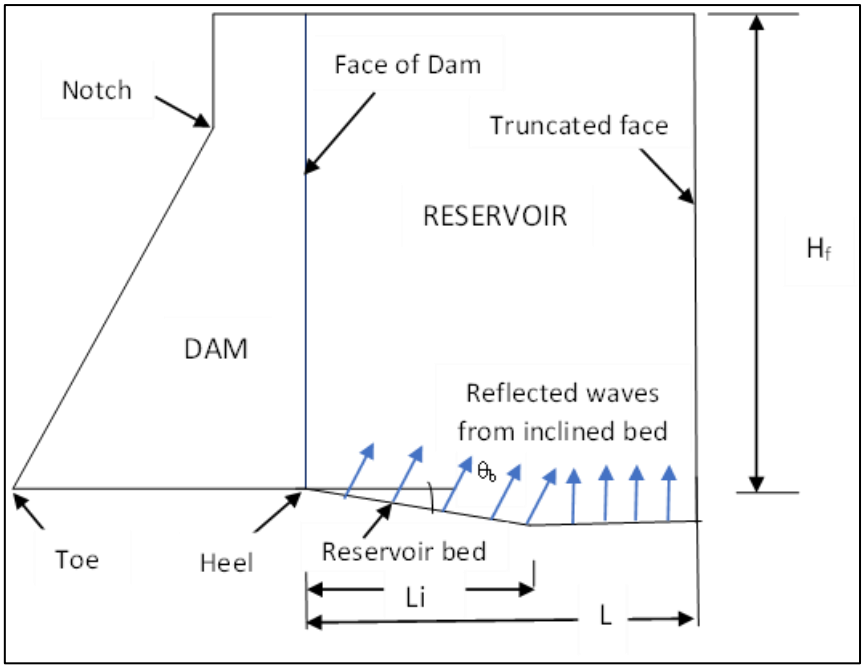

Fig. 4.16: Variable inclined length of reservoir bed (clockwise) with reflected waves

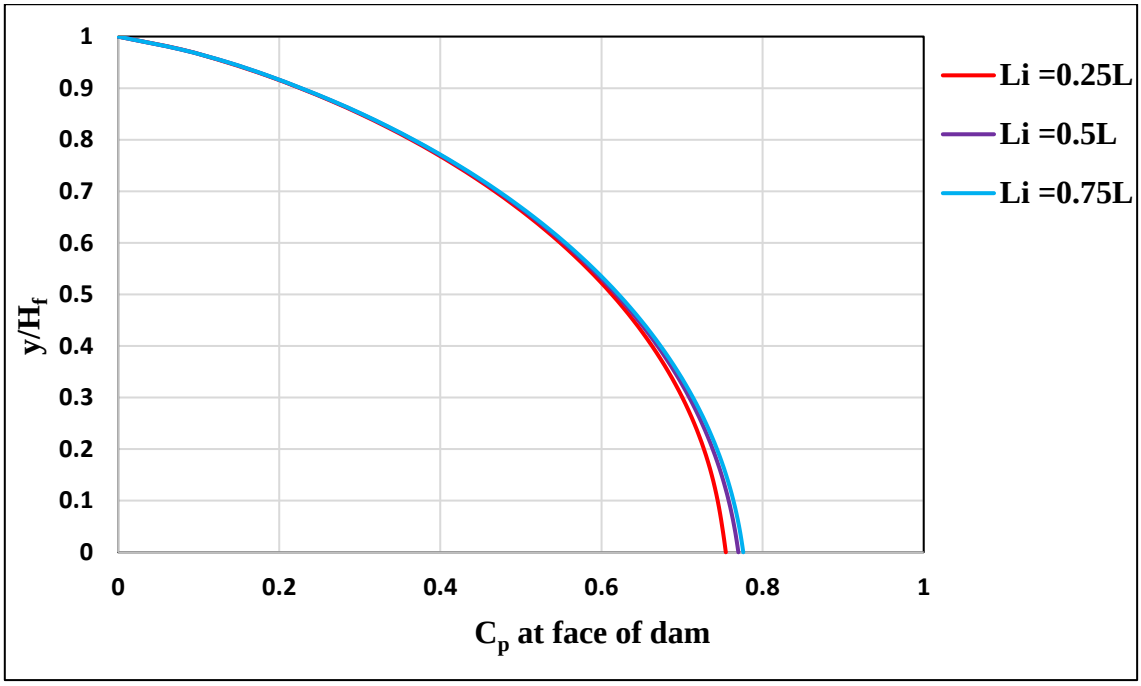

Fig. 4.17: Distribution of pressure coefficient (C_p) at the face of the dam for bottom slope (θ_b) = $+5^0$

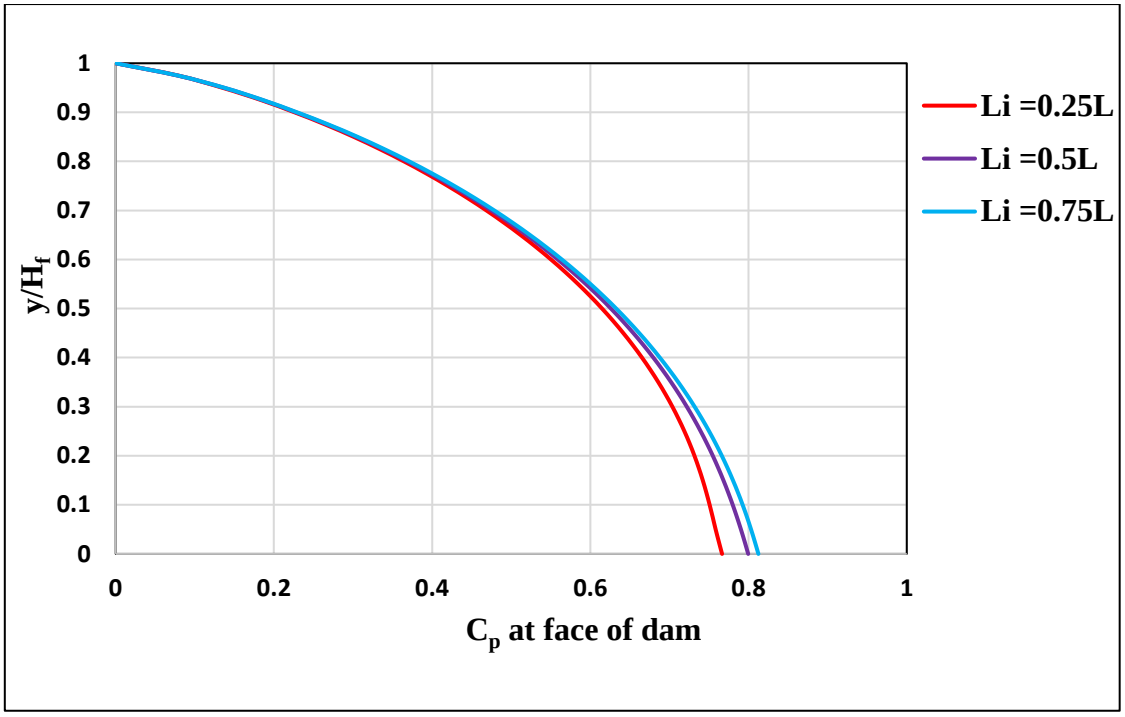

Fig. 4.18: Distribution of pressure coefficient (C_p) at the face of the dam for bottom slope (θ_b) = +10^0

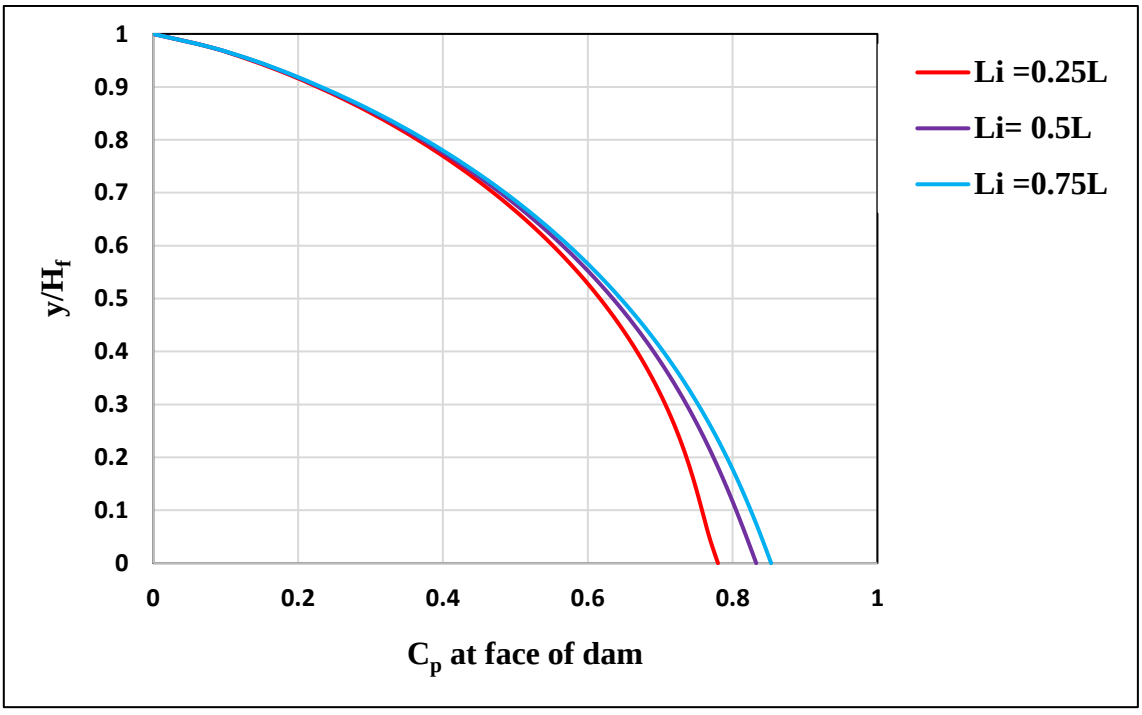

Fig. 4.19: Distribution of pressure coefficient (C_p) at the face of the dam for bottom slope (θ_b) = +15^0

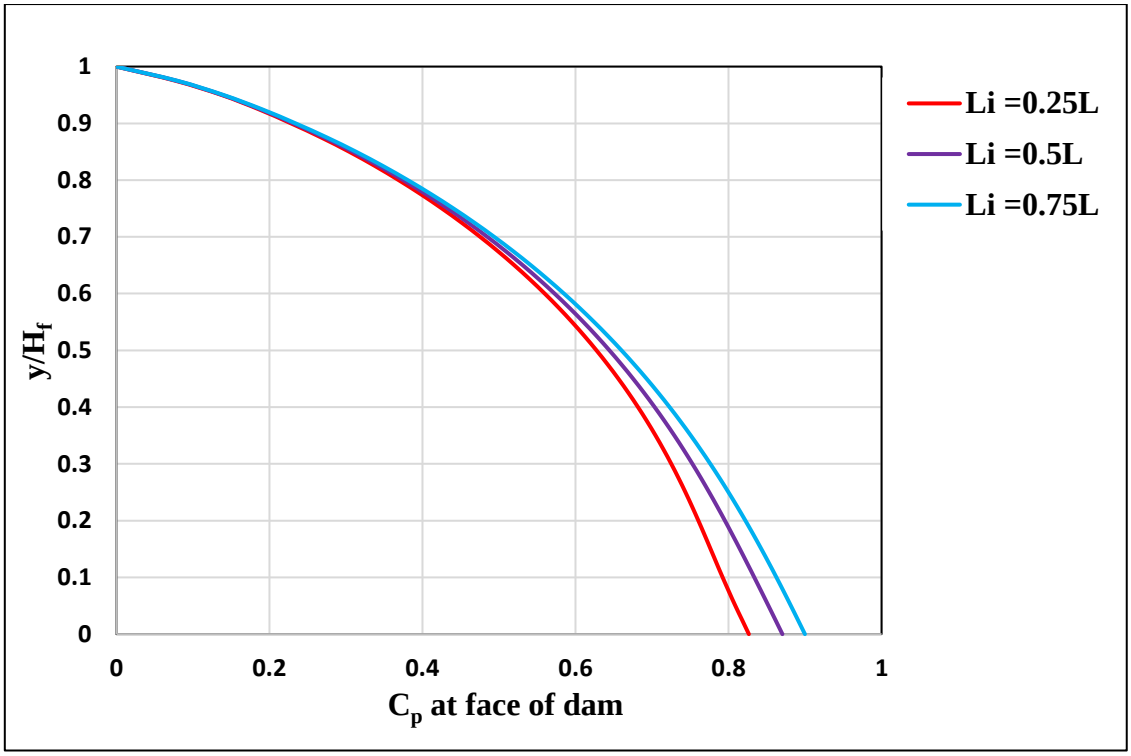

Fig. 4.20: Distribution of pressure coefficient (C_p) at the face of the dam for bottom slope (θ_b) = $+20^0$

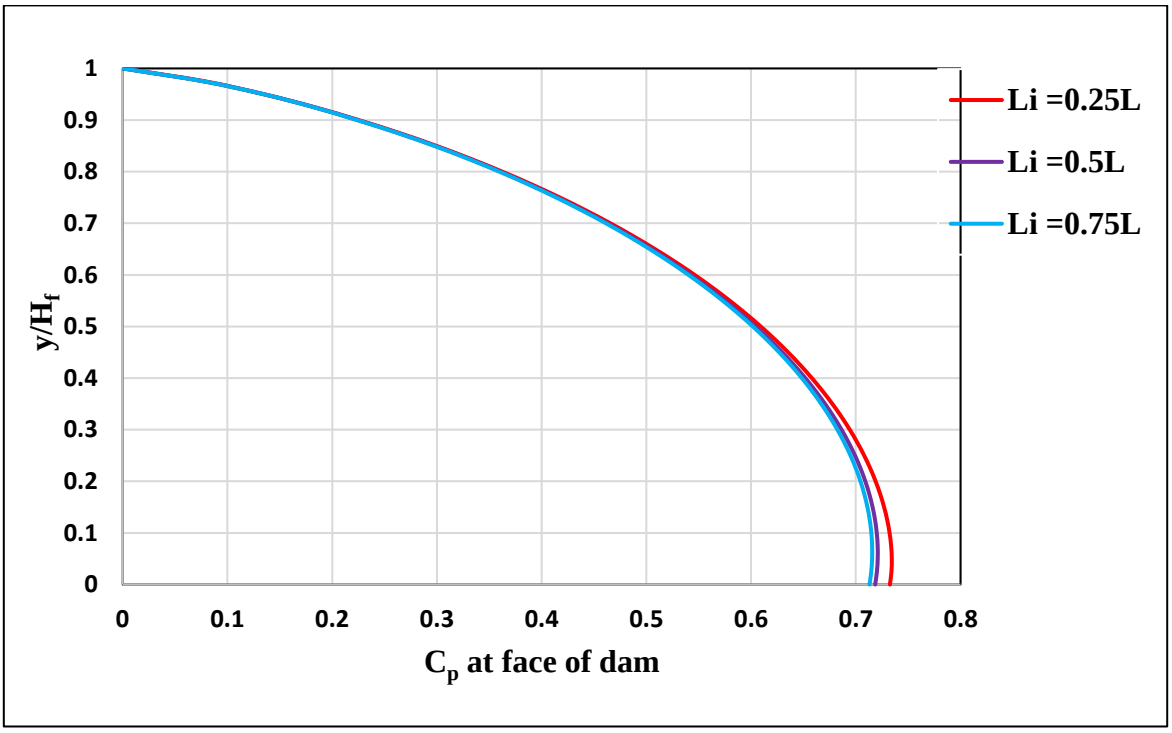

Fig. 4.21: Distribution of pressure coefficient (C_p) at the face of the dam for bottom slope (θ_b) = -5^0

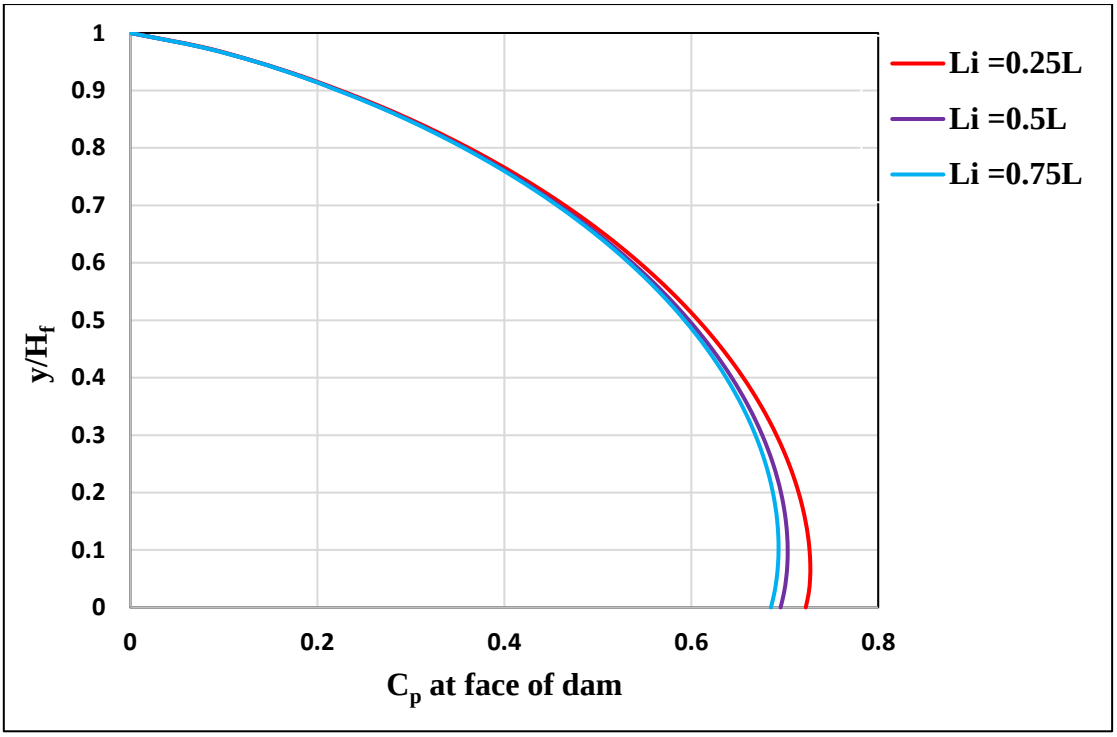

Fig. 4.22: Distribution of pressure coefficient (C_p) at the face of the dam for bottom slope (θ_b) = -10^0

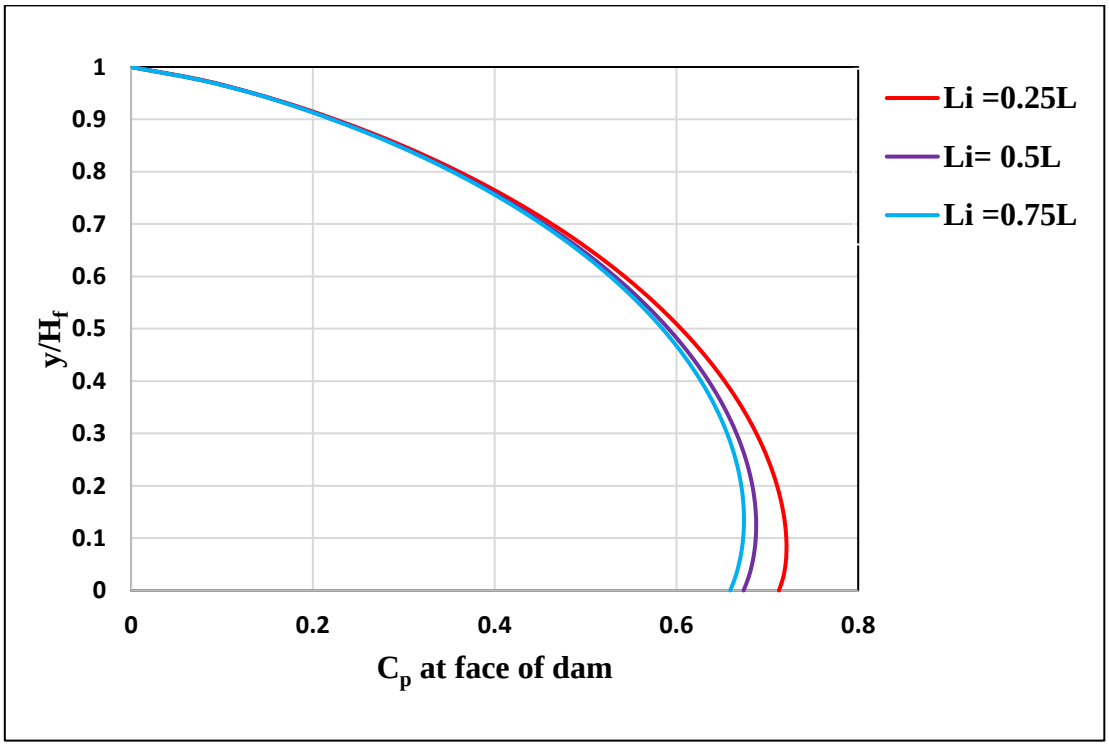

Fig. 4.23: Distribution of pressure coefficient (C_p) at the face of the dam for bottom slope (θ_b) = -15^0

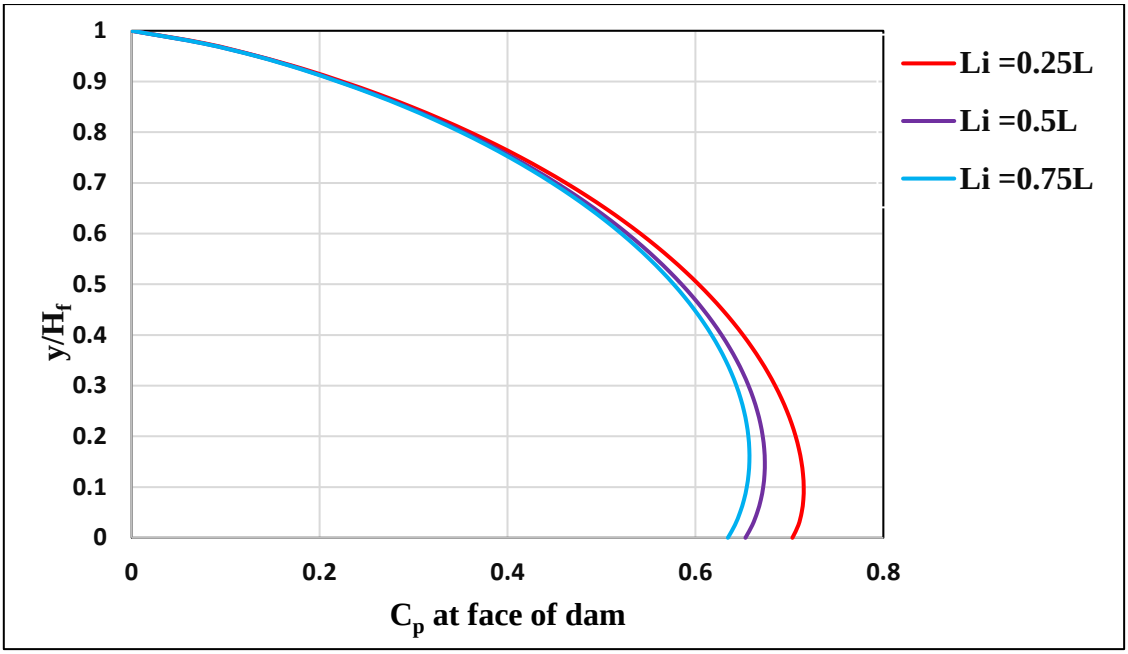

Fig. 4.24: Distribution of pressure coefficient (C_p) at the face of the dam for bottom slope (θ_b) = -20^0

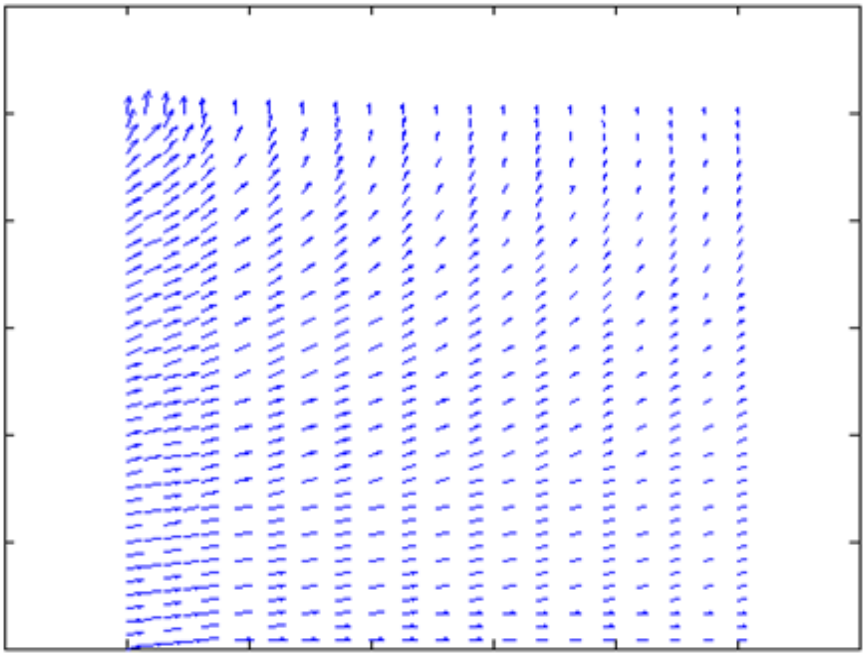

Fig. 4.25: Velocity profile of reservoir at 8.89 sec. for L_i=0.25L and θ_b = +15^0

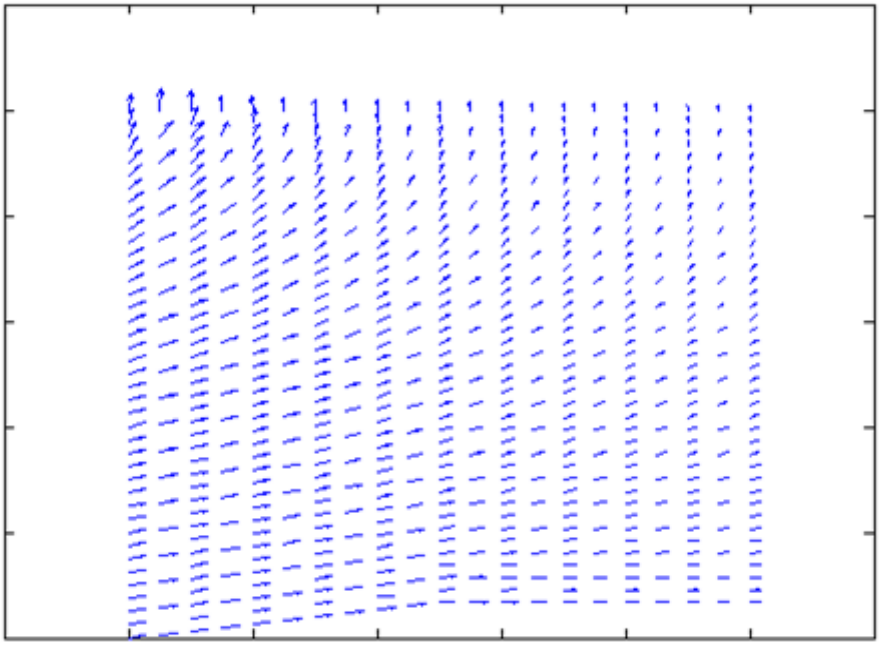

Fig. 4.26: Velocity profile of reservoir at 8.89 sec. for L_i=0.5L and θ_b = +15^0

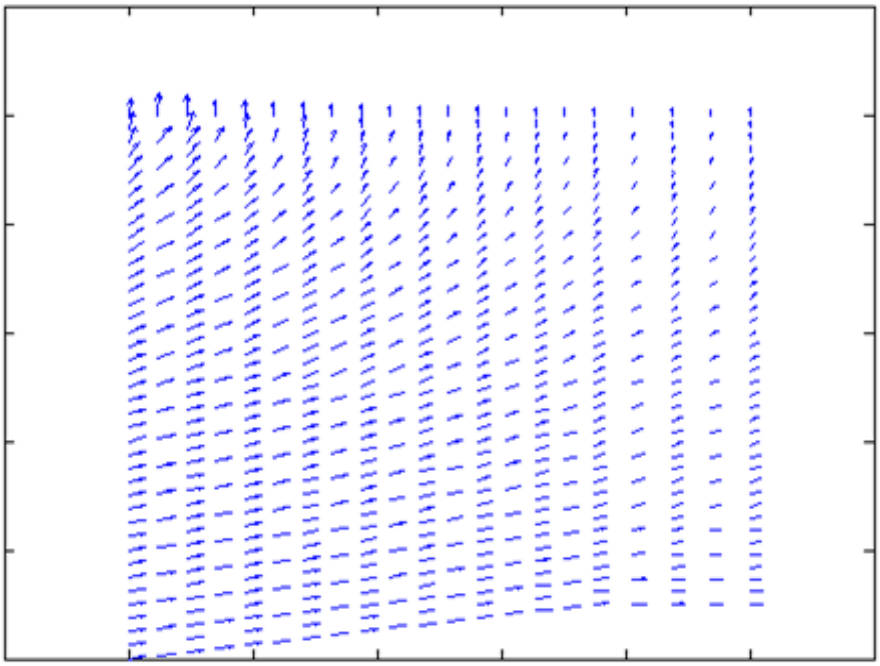

Fig. 4.27: Velocity profile of reservoir at 8.89 sec. for L_i=0.75L and θ_b = +15^0

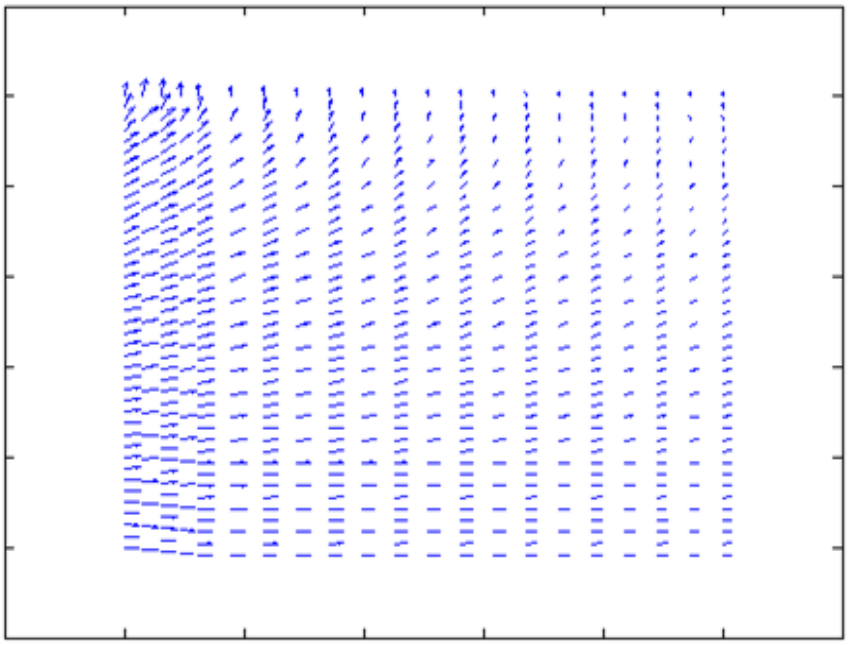

Fig. 4.28: Velocity profile of reservoir at 8.89 sec. for L_i=0.25L and θ_b = -15^0

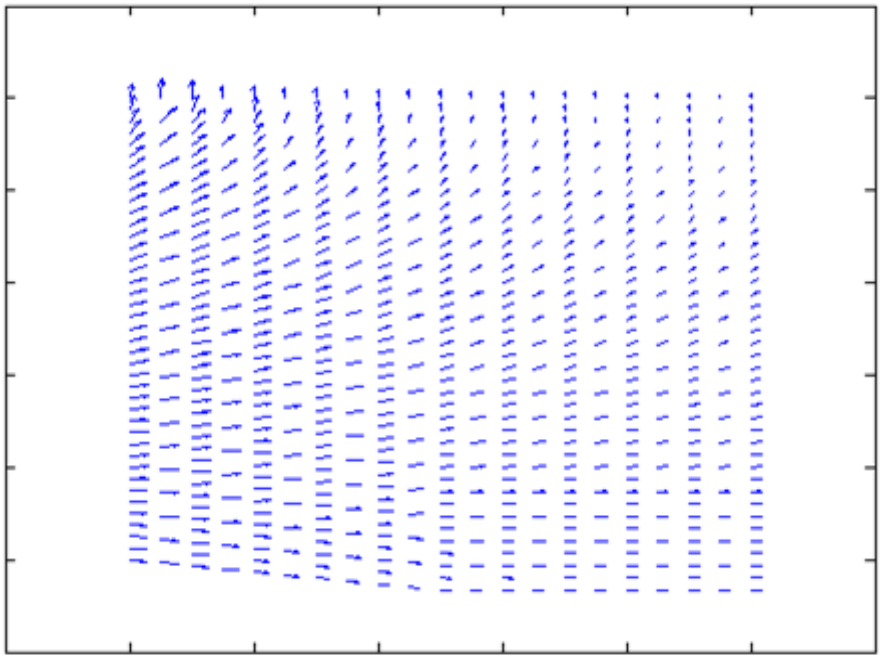

Fig. 4.29: Velocity profile of reservoir at 8.89 sec. for L_i=0.5L and θ_b = -15^0

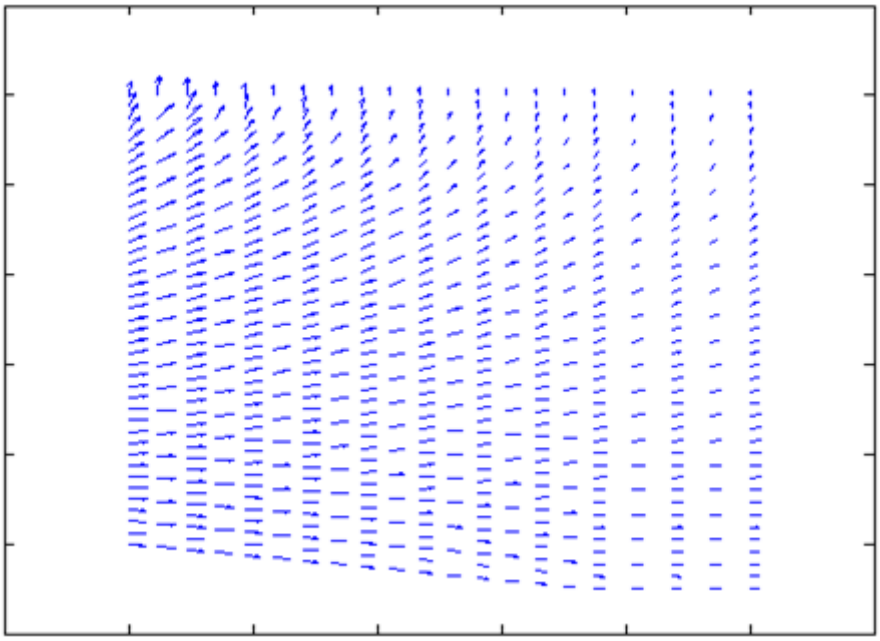

Fig. 4.30: Velocity profile of reservoir at 8.89 sec. for L_i=0.75L and θ_b = -15^0

4.3 SECTION 2: ANALYSIS OF DAM-RESERVOIR COUPLED SYSTEM

Proper modelling of Fluid-structure interaction reflects the actual behaviour of hydrodynamic pressure developed on the upstream face of the dam. Analysis of dam-reservoir coupled systems including the fluid-structure interaction is necessary to understand the responses of gravity dam and variation of hydrodynamic pressure. In the present section of work, the behaviour of hydrodynamic pressure and responses of gravity dam has been determined for several physical parameters considering fluid-structure interaction. The foundation below the gravity dam is considered rigid. The upstream face of the gravity dam is considered vertical and the effect of surface wave is neglected. The reservoir is truncated at $L=0.5H_f$ and an effective non-reflective boundary condition, proposed by Gogoi and Maity (2006), is applied at the truncated surface. Reservoir bottom absorption is considered. Analysis has been carried out for different inclinations, inclined lengths and different values of reflection coefficients of the reservoir bottom against sinusoidal and earthquake excitations.

4.3.1 VALIDATION OF THE DEVELOPED ALGORITHM

The proposed algorithm is validated with a similar type of dam-reservoir coupled problem considered by Samii and Lotfi (2007). The time periods of three modes of dam-reservoir systems are compared with time periods calculated from the literature of Samii and Lotfi (2007) in Table 4.5. The obtained results are nearly complying with the results of Samii and Lotfi (2007).

Table 4.5 Comparison of time periods of first three modes of dam-reservoir system

Mode no.	Time period from present study (Sec.)	Time period of Samii and Lotfi (2007) (Sec.)
1	0.360174	0.395773
2	0.322581	0.305988
3	0.227817	0.214293

4.3.2 NUMERICAL RESULTS AND DISCUSSION

In this portion of the work, behaviours of the infinite reservoir and concrete gravity dam have been observed considering the dam-reservoir interaction. Fluid is assumed as non-viscous and compressible. The effect of surface waves is neglected. The height of the reservoir is assumed as H_f=103 m and the reservoir is truncated at $L=0.5H_f$. A non-reflecting boundary condition, proposed by Gogoi and Maity (2006), is applied along the truncated face. Unit weight of water (ρ_f) is assumed as 1000 kg/m^3. The velocity of acoustic wave (c) is taken as 1438.7 m/sec and the reflection coefficient (α) of the reservoir bottom is considered as 0.95. The dam is considered to be the Koyna dam. Eight-node isoparametric element has been used for the discretization of the dam and reservoir (Fig. 4.31). The modulus of elasticity of concrete for the gravity dam is assumed as 3.15×10^{10} N/m^2 and Poisson ratio is taken as 0.235. Unit weight of concrete is taken as 2415.816 kg/m^3 and damping ratio for the dam is considered as 0.05. For the convergence study, the displacement at the tip of the dam is presented in Table 4.6. for various mesh sizes. The results are determined by applying sinusoidal excitation of frequency Tc/H_f=100. The amplitude of the applied excitations (a) is assumed equal to the gravitational acceleration of 1.0g. From this convergence study, the mesh size is taken as N_h= 3 and N_v=8

for the dam while for the reservoir N_h= 4 and N_v=8. Here N_h is the number of divisions in the horizontal direction N_v is the number of divisions in the vertical direction.

Hydrodynamic pressure at the face of the dam has been determined by applying harmonic excitation of Tc/H_f = 100 with the reservoir bottom slope (θ_b) as $+4^0$, $+12^0$, $+20^0$ and -4^0, -12^0, -20^0 respectively both for rigid dam i.e. without considering dam-reservoir interaction and considering dam-reservoir interaction. Fig. 4.32 to Fig 4.34 show the distribution of pressure coefficient (C_p) at the face of the dam for positive bottom slopes. Fig. 4.35 to Fig 4.37 show the distribution of pressure coefficient (C_p) at the face of the dam for negative bottom slopes. From these figures, it has been observed that the hydrodynamic pressure coefficient is slightly higher at the heel of the dam when dam is considered. This is due to the interaction effect between fluid and structure.

Table 4.6: Convergence study with various finite element meshes for the dam-reservoir coupled system

Mesh size for dam N_h **x** N_v	**Mesh size for reservoir** N_h **x** N_v	**Displacement at tip of dam (m)**
2 x 6	2 x 6	0.00303
3 x 6	3 x 6	0.00304
3 x 6	4 x 6	0.00305
3 x 8	4 x 8	0.00355
3 x 8	5 x 8	0.00355

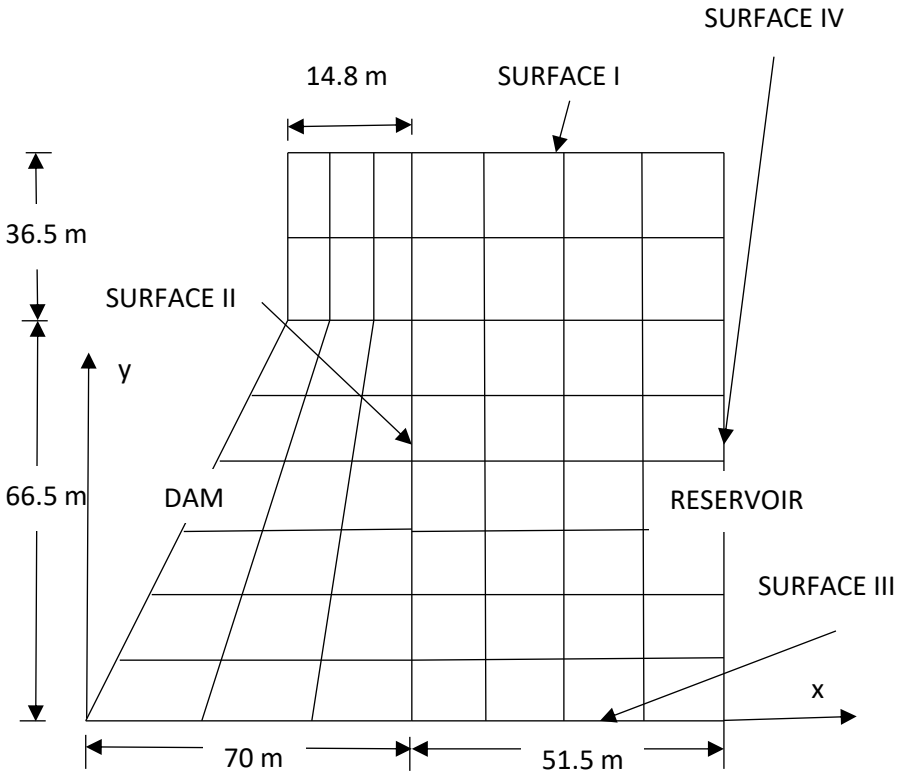

Fig. 4.31: Typical finite element model of Koyna dam and reservoir system

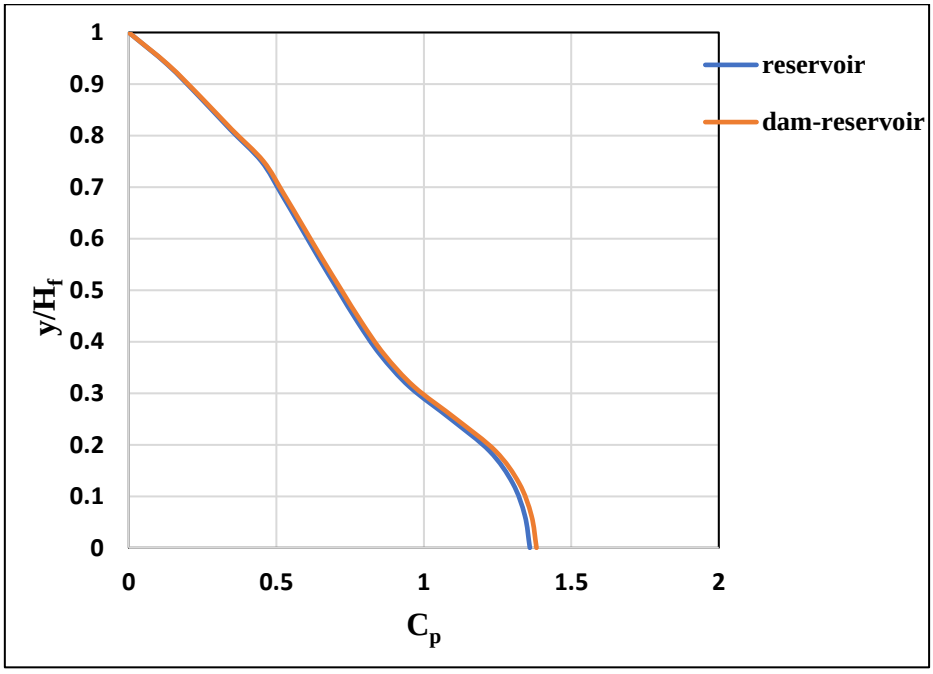

Fig. 4.32: Distribution of pressure coefficient (C_p) at the face of the dam for bottom slope $+4^0$

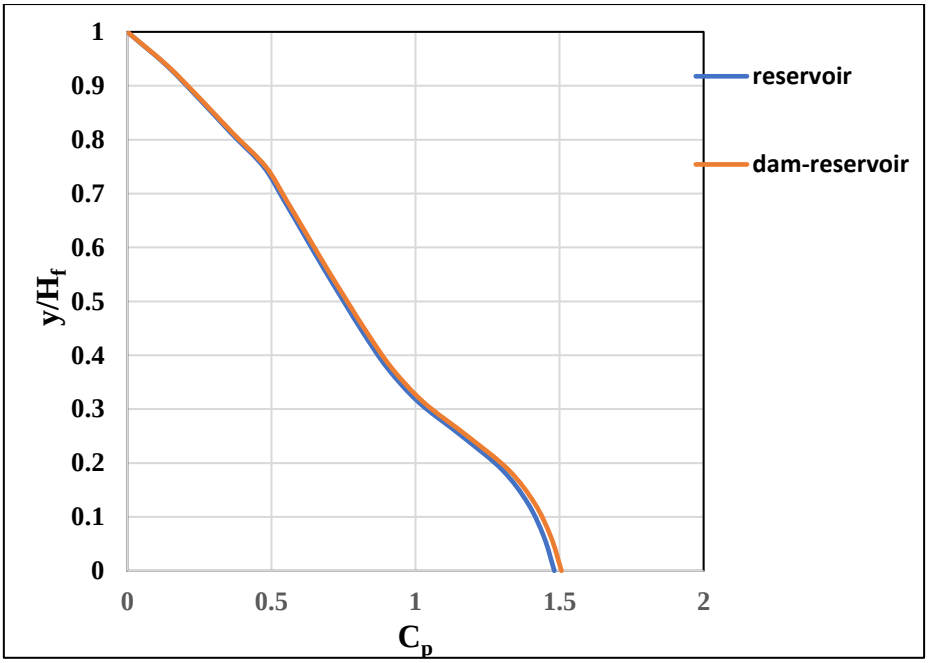

Fig. 4.33: Distribution of pressure coefficient (C_p) at the face of the dam for bottom slope $+12^0$

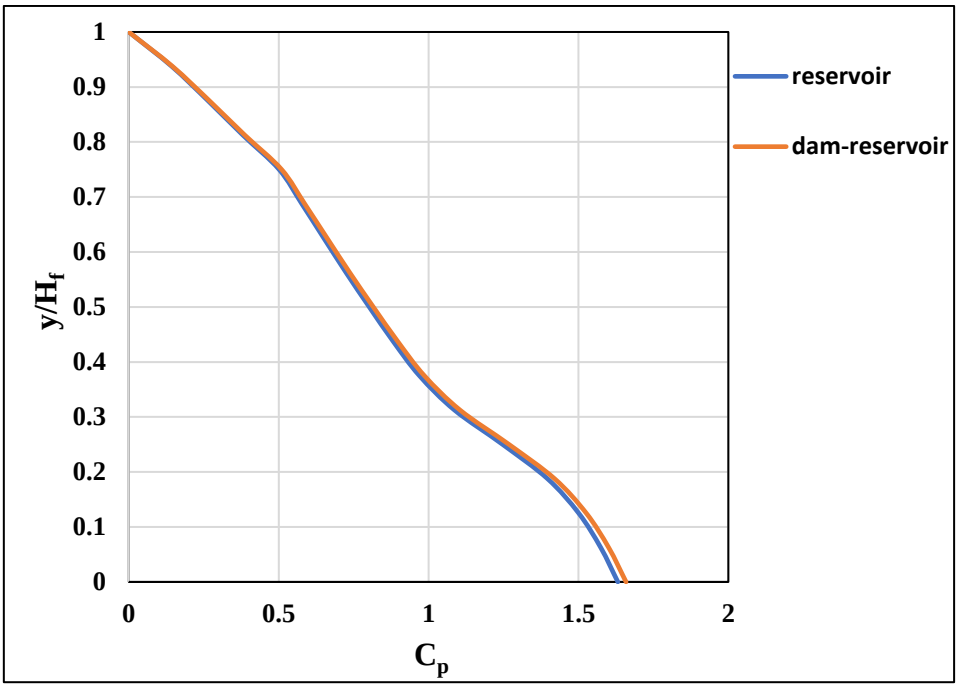

Fig. 4.34: Distribution of pressure coefficient (C_p) at the face of the dam for bottom slope $+20^0$

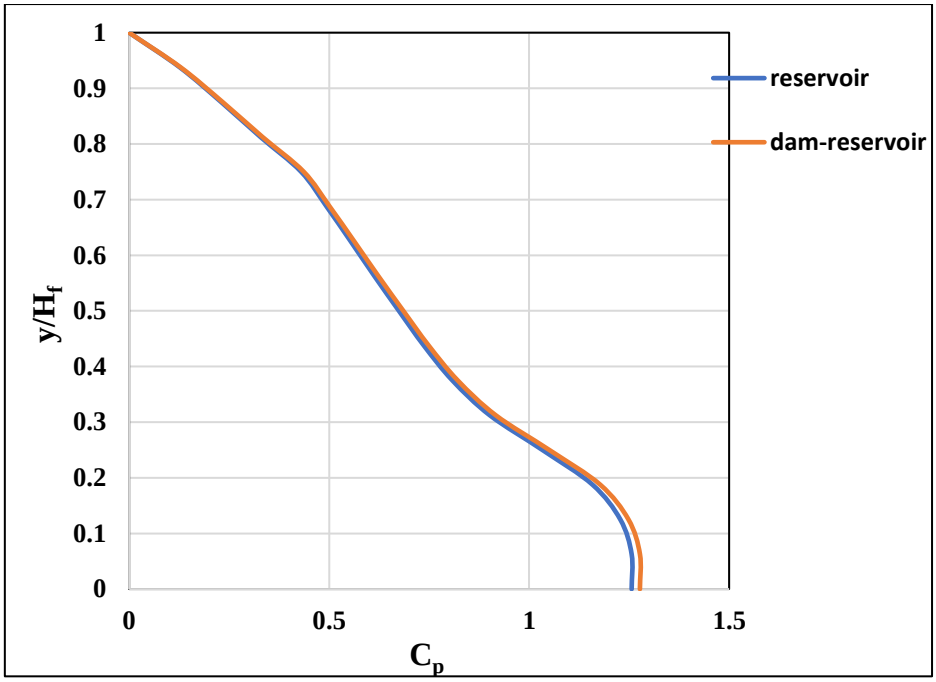

Fig. 4.35: Distribution of pressure coefficient (C_p) at the face of the dam for bottom slope -4^0

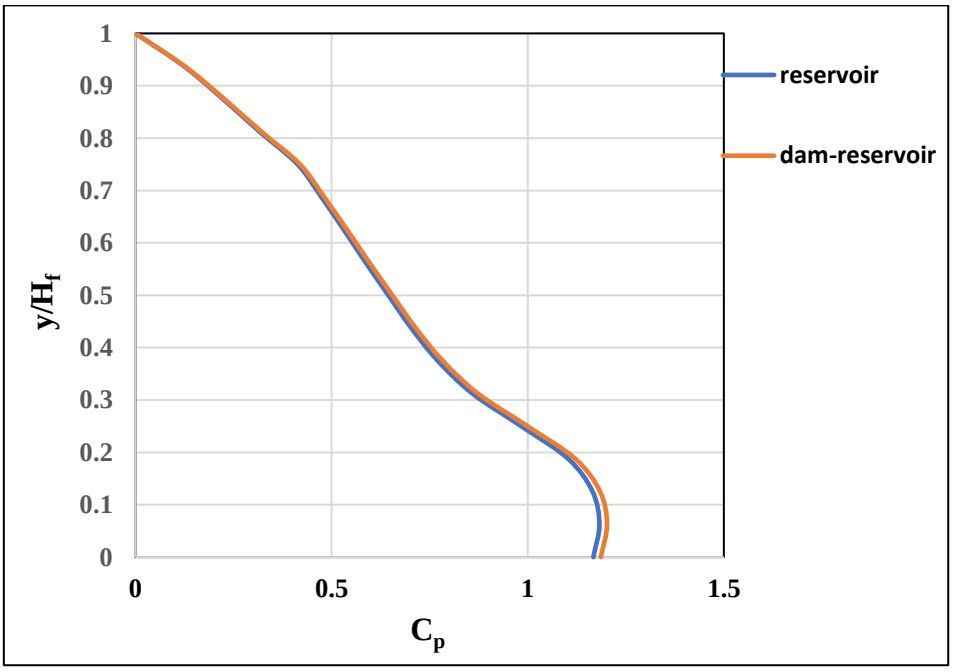

Fig. 4.36: Distribution of pressure coefficient (C_p) at the face of the dam for bottom slope -12^0

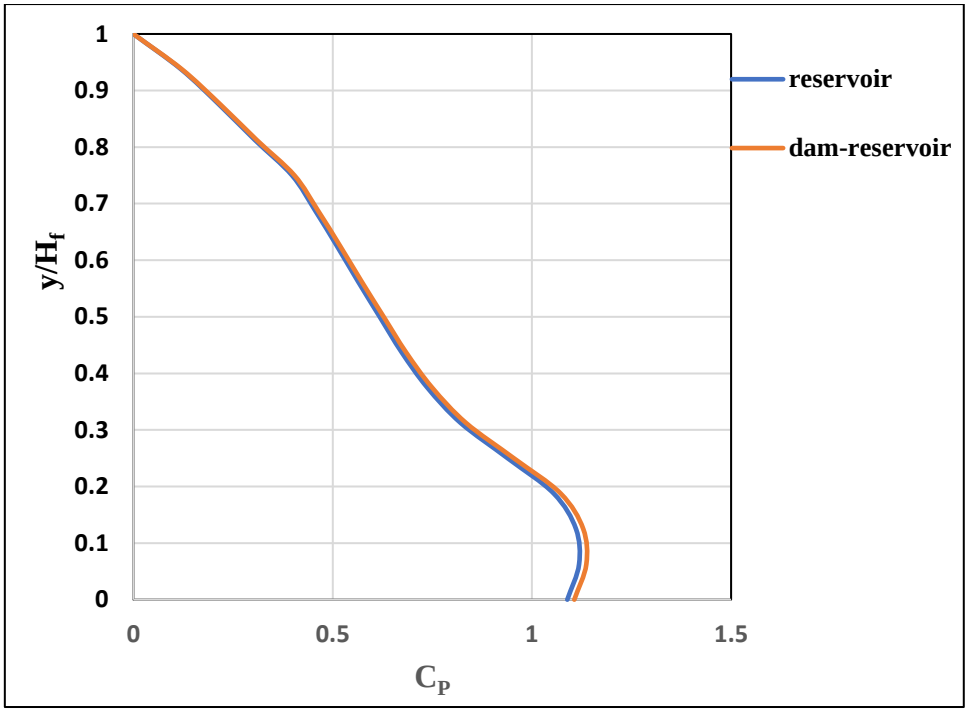

Fig. 4.37: Distribution of pressure coefficient (C_p) at the face of the dam for bottom slope -20^0

The present section of work has been divided into four parts. In Part I, analysis of the dam-reservoir system has been done for the variation of inclination of the reservoir base. In Part II, analysis of the fluid-structure system has been carried out for variation in inclined length of the reservoir. In Part III, analysis has been done for variation of the reflection coefficient of the reservoir bottom. In Part IV, earthquake analysis of the dam-reservoir coupled system has been carried out.

4.3.2.1 PART I: ANALYSIS OF DAM-RESERVOIR COUPLED SYSTEM FOR INCLINATION OF RESERVOIR BED

In this part of work, variation of hydrodynamic pressure at the face of the concrete gravity dam has been observed for different exciting frequencies along with the change in slope angle of the reservoir bed (Fig. 4.38). The height of the reservoir is assumed as H_f=103 m and L/H_f ratio is taken as 0.5. Unit weight of water (ρ_f) is assumed as 1000 kg/m^3. Velocity of acoustic wave (c) in water is taken as 1438.7 m/sec and the reflection coefficient (α) of the reservoir bottom is considered as 0.95. Geometry of the Koyna dam is adopted here for the analysis. Modulus of elasticity of concrete for the gravity dam is assumed as 3.15 × 10^{10} N/m^2 and Poisson ratio is taken as 0.235. Unit weight concrete is taken as 2415.816 kg/m^3 and damping

ratio is considered as 0.05. Change of pressure with different reservoir bottom slope (θ_b = 4^0,$12^0$and 20^0) is observed due to harmonic excitations of Tc/H_f = 4,10 and 100.

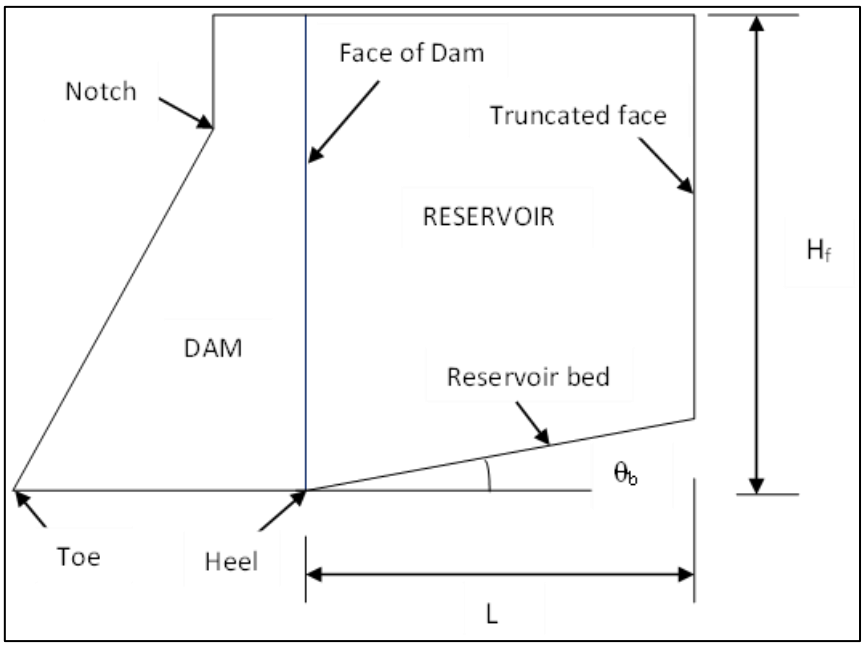

Fig. 4.38: Geometry of dam-reservoir coupled system with inclined bottom surface

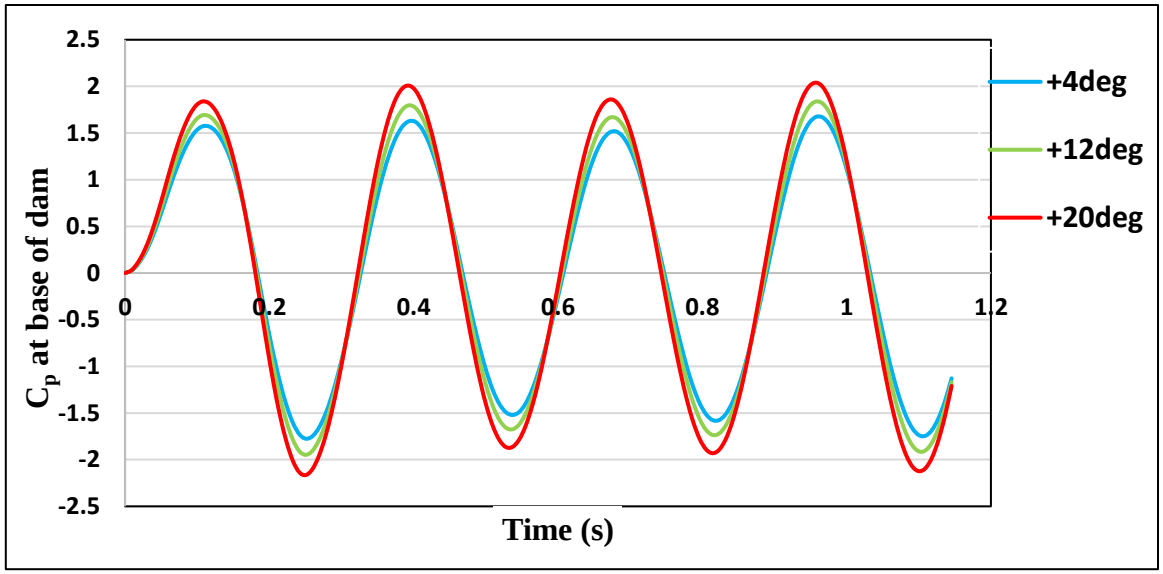

Fig. 4.39: Time history of pressure coefficient (C_p) at the heel of the dam for Tc/H_f =4 for positive bottom slopes

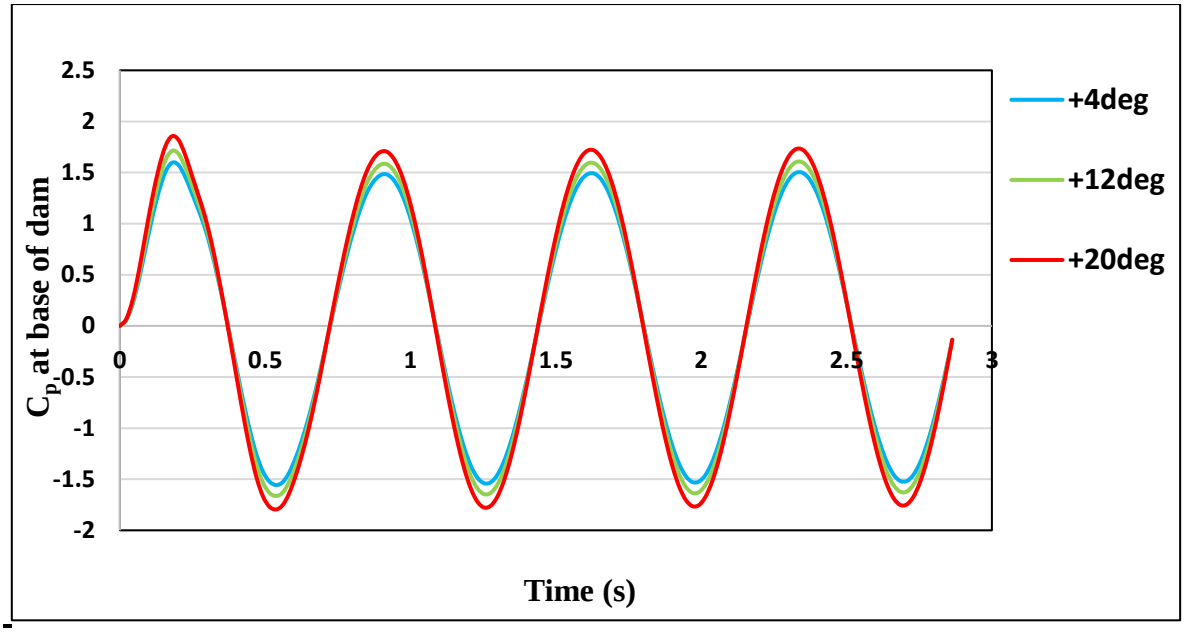

Fig. 4.40: Time history of pressure coefficient (C_p) at the heel of the dam for Tc/H_f =10 for positive bottom slopes

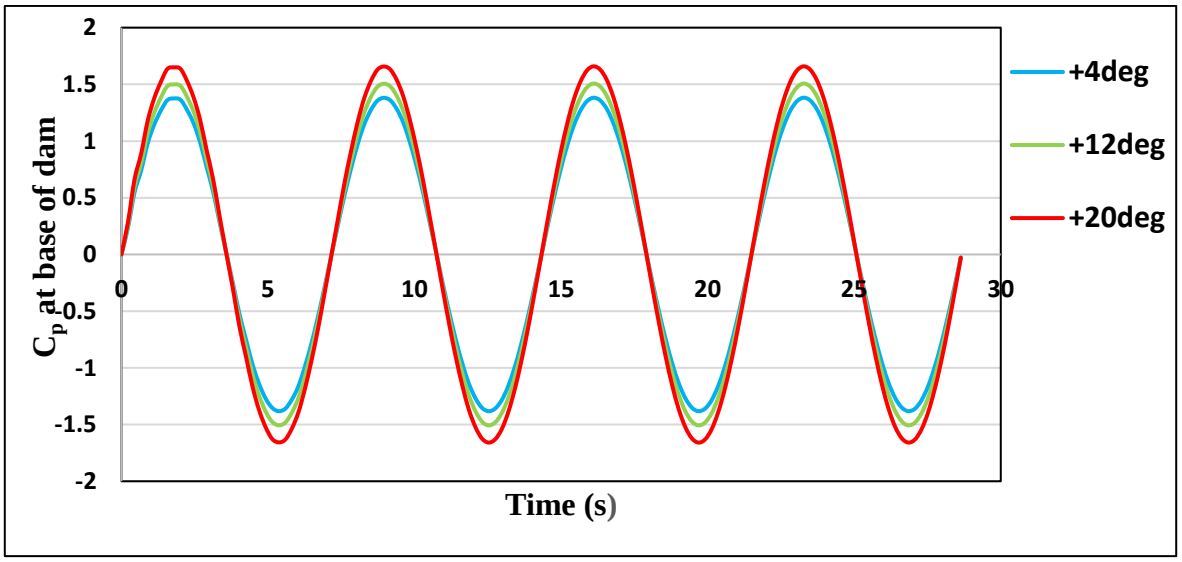

Fig. 4.41: Time history of pressure coefficient (C_p) at the heel of the dam for Tc/H_f =100 for positive bottom slopes

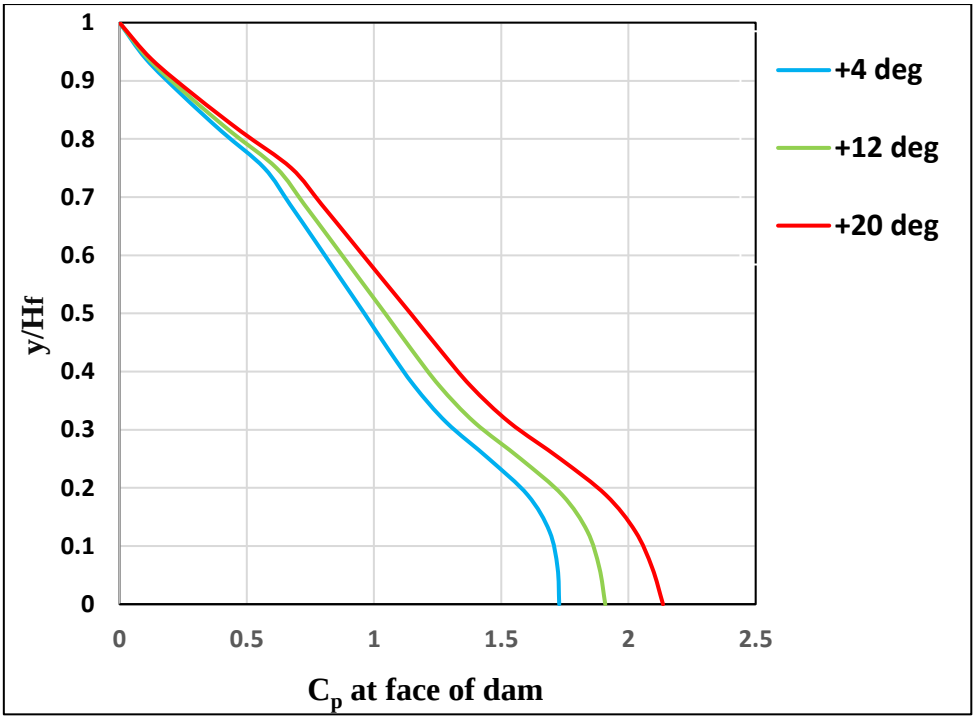

Fig. 4.42: Distribution of pressure coefficient (C_p) at the face of the dam Tc/H_f =4 for positive bottom slopes

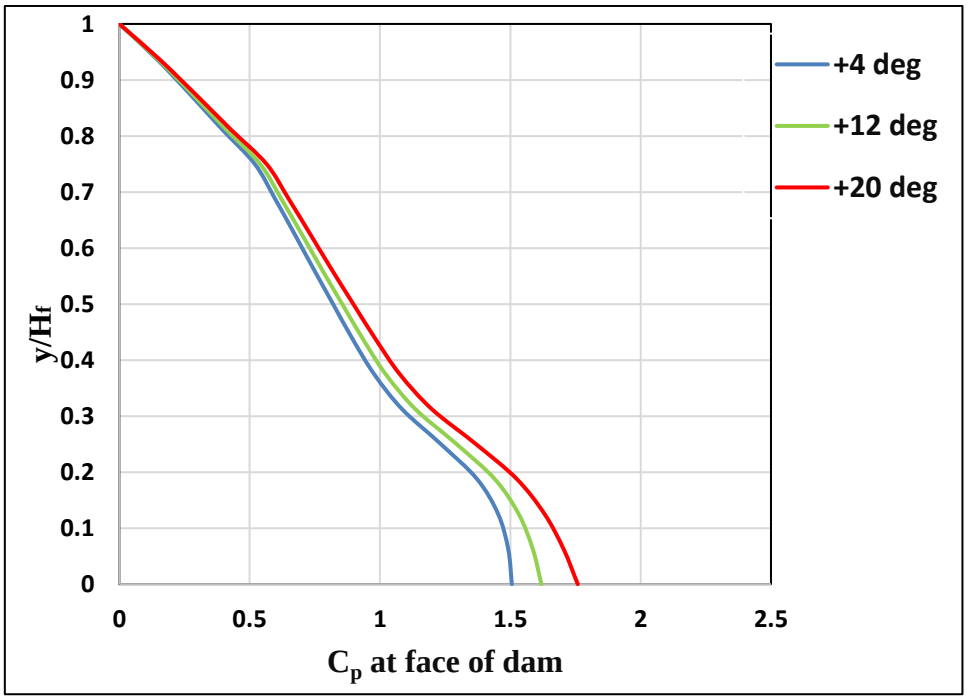

Fig. 4.43: Distribution of pressure coefficient (C_p) at the face of the dam Tc/H_f =10 for positive bottom slopes

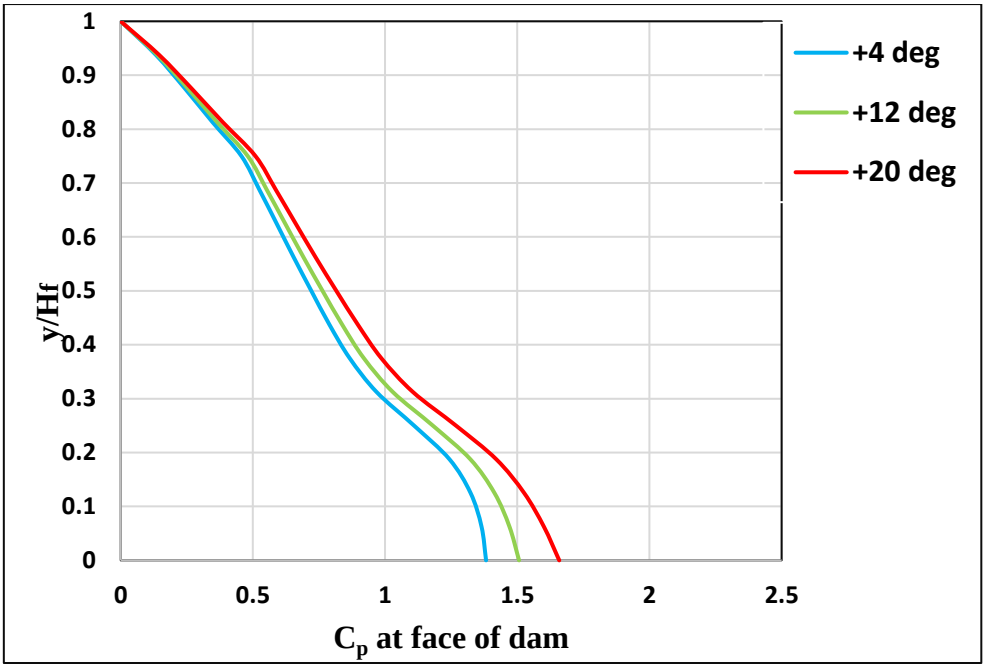

Fig. 4.44: Distribution of pressure coefficient (C_p) at the face of the dam Tc/H_f =100 for positive bottom slopes

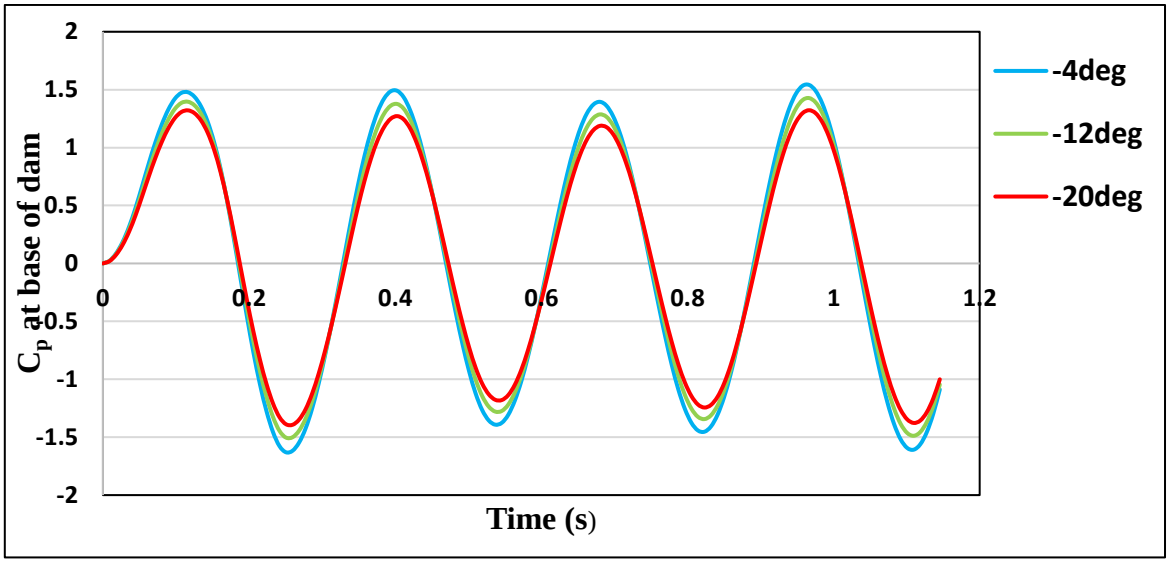

Fig. 4.45: Time history of pressure coefficient (C_p) at the heel of the dam for Tc/H_f =4 for negative bottom slopes

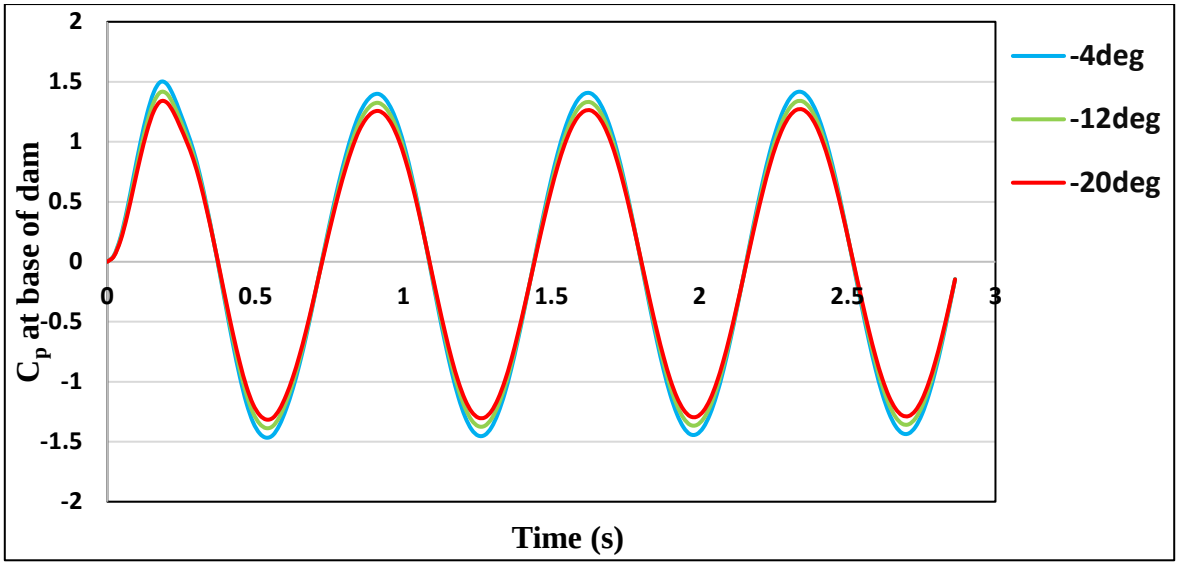

Fig. 4.46: Time history of pressure coefficient (C_p) at the heel of the dam for Tc/H_f =10 for negative bottom slopes

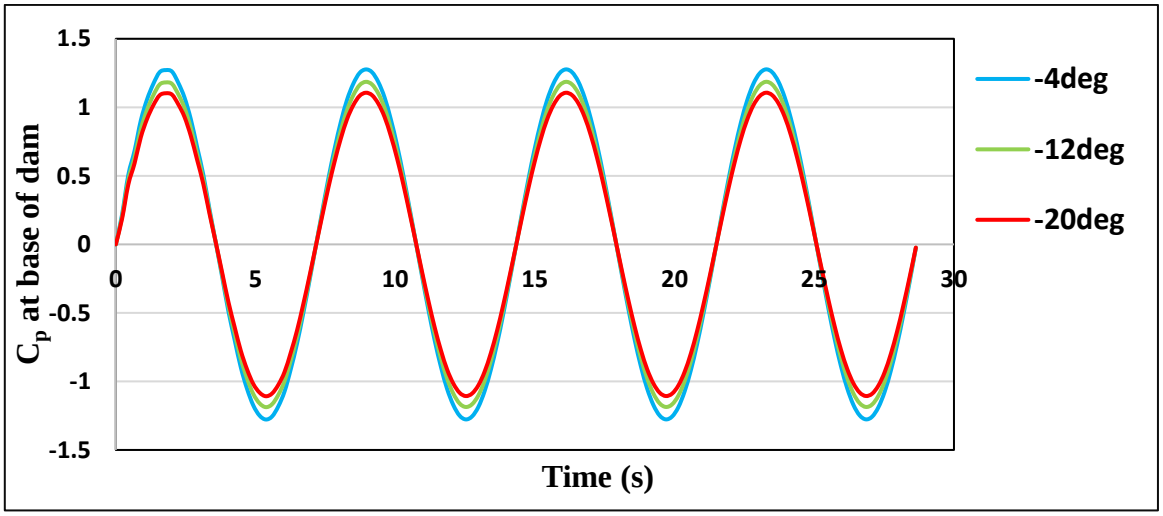

Fig. 4.47: Time history of pressure coefficient (C_p) at the heel of the dam for Tc/H_f =100 for negative bottom slopes

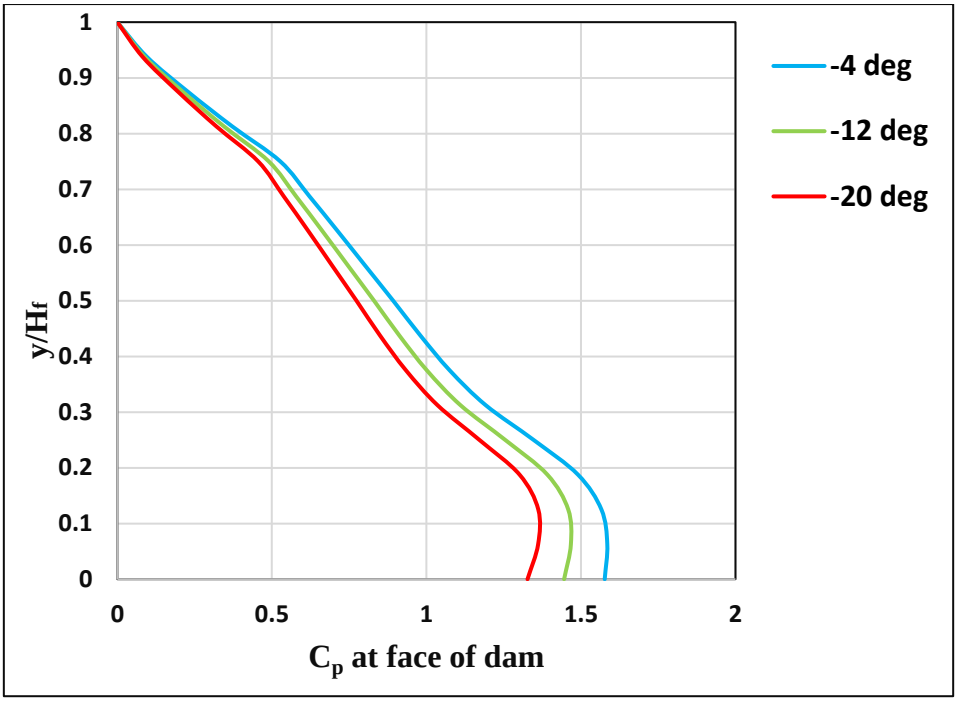

Fig. 4.48: Distribution of pressure coefficient (C_p) at the face of the dam Tc/H_f =4 for negative bottom slopes

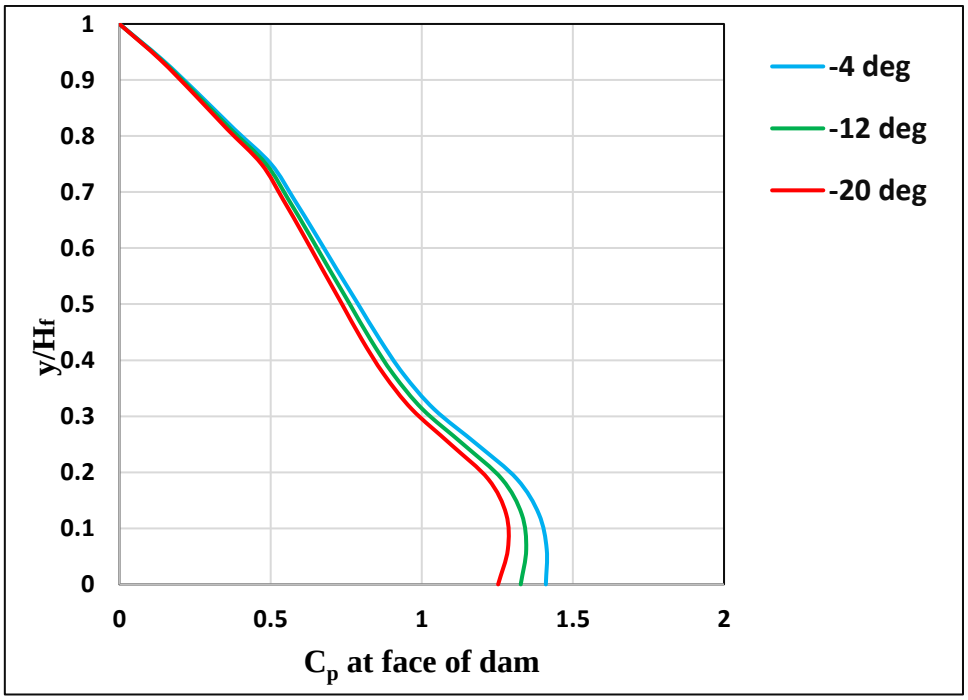

Fig. 4.49: Distribution of pressure coefficient (C_p) at the face of the dam Tc/H_f =10 for negative bottom slopes

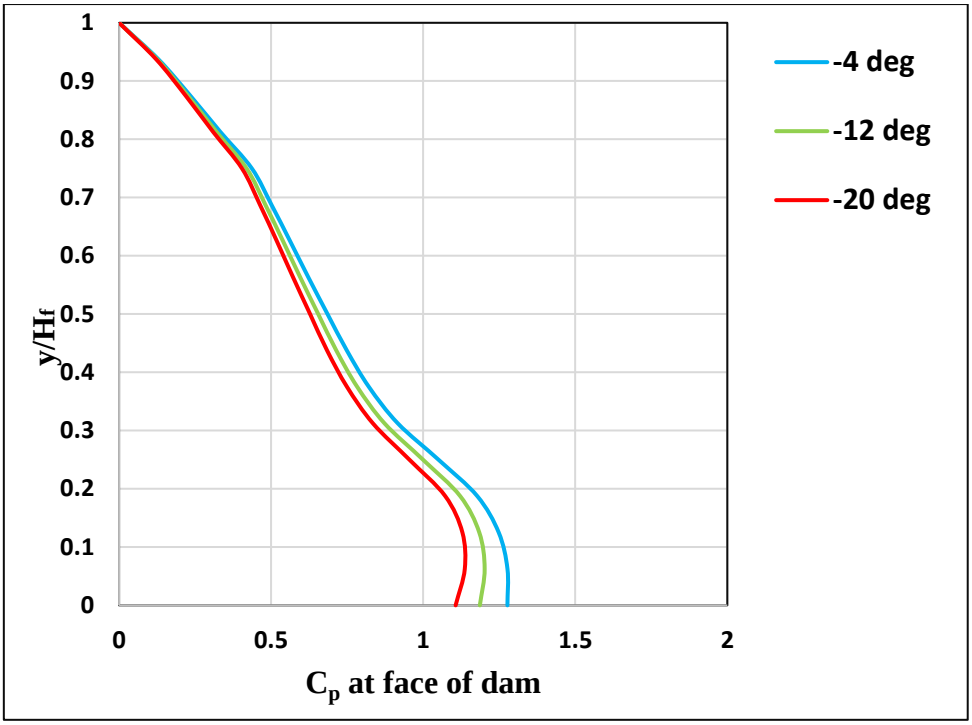

Fig. 4.50: Distribution of pressure coefficient (C_p) at the face of the dam Tc/H_f =100 for negative bottom slopes

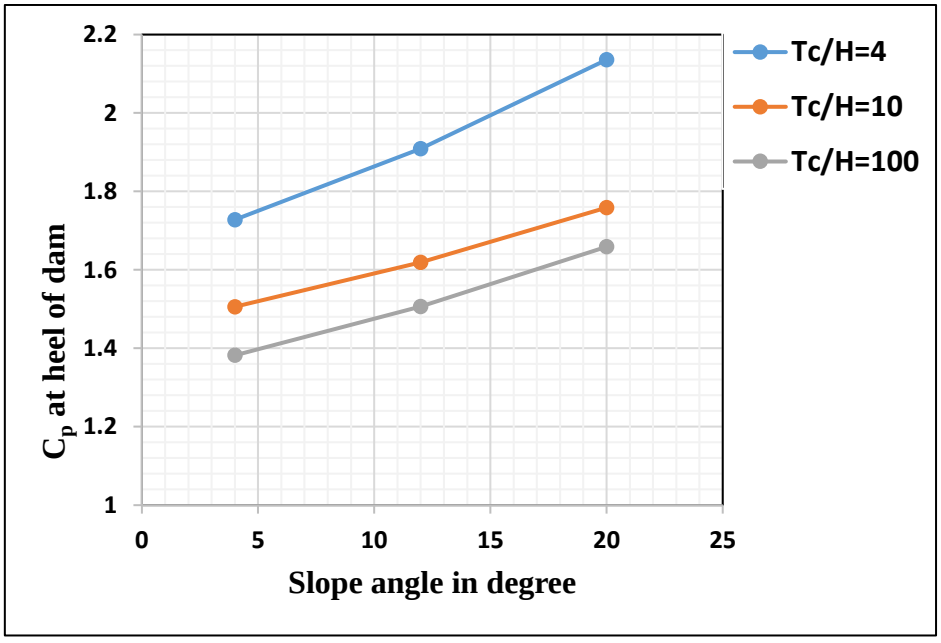

Fig. 4.51: Distribution pressure coefficient at heel of the dam for positive slope angles

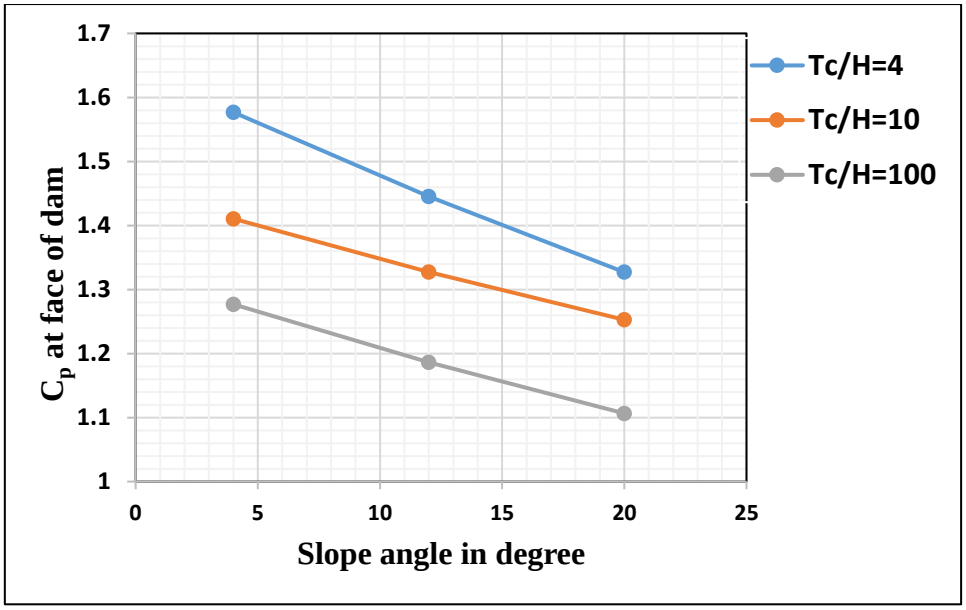

Fig. 4.52: Distribution Pressure coefficient at heel of the dam for negative slope angles

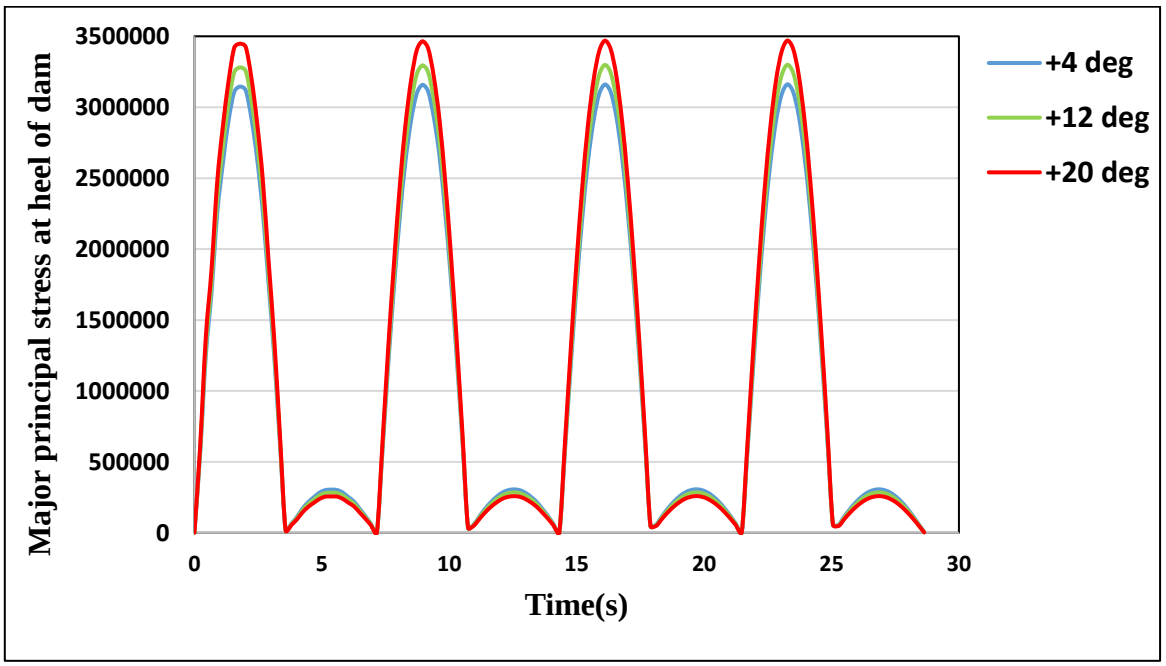

Fig. 4.53: Time history plot of major principal stress at the heel of the dam for positive slope angles of reservoir bottom

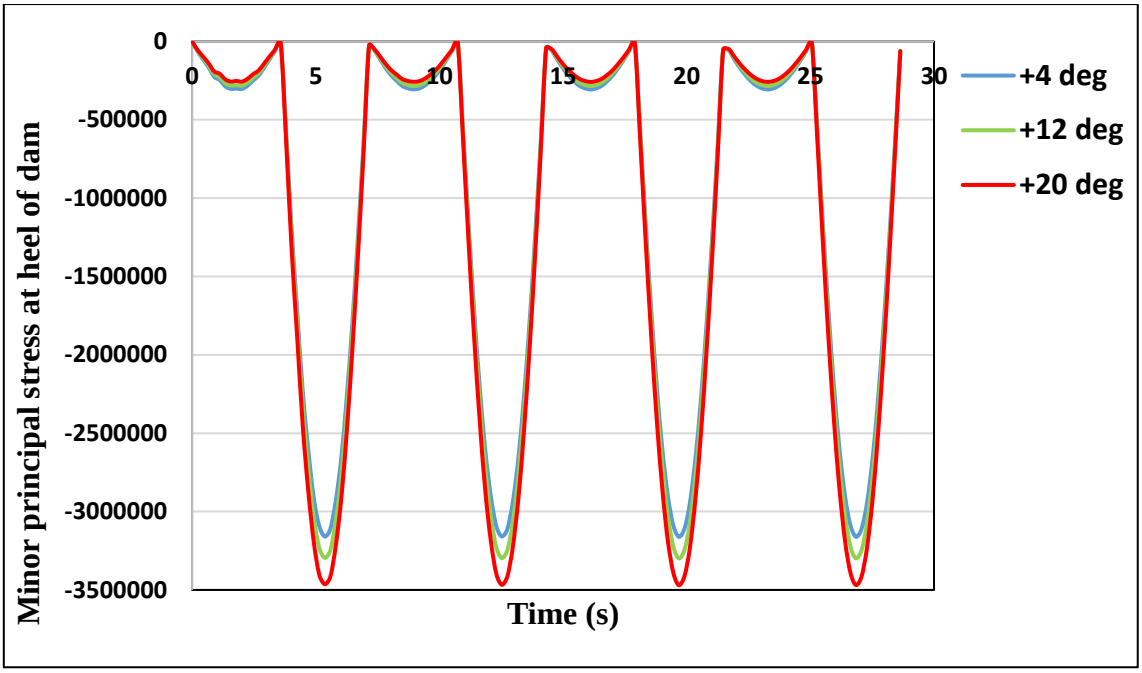

Fig. 4.54: Time history plot of minor principal stress at the heel of the dam for positive slope angles of reservoir bottom

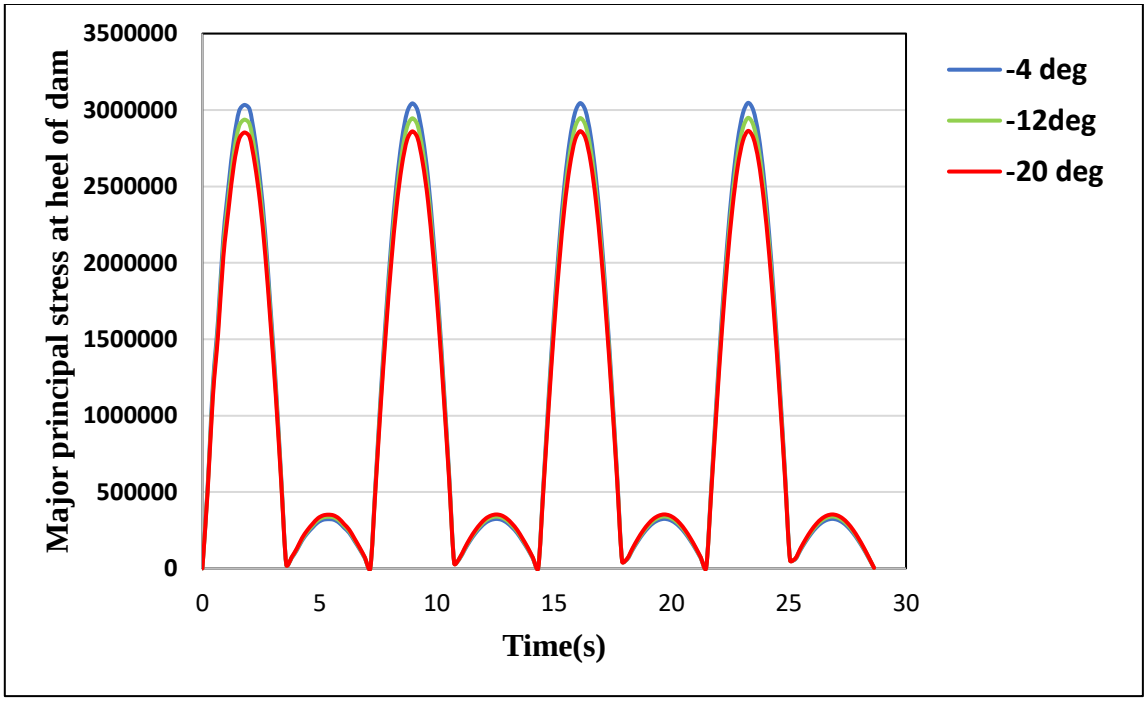

Fig. 4.55: Time history plot of major principal stress at the heel of the dam for negative slope angles of reservoir bottom

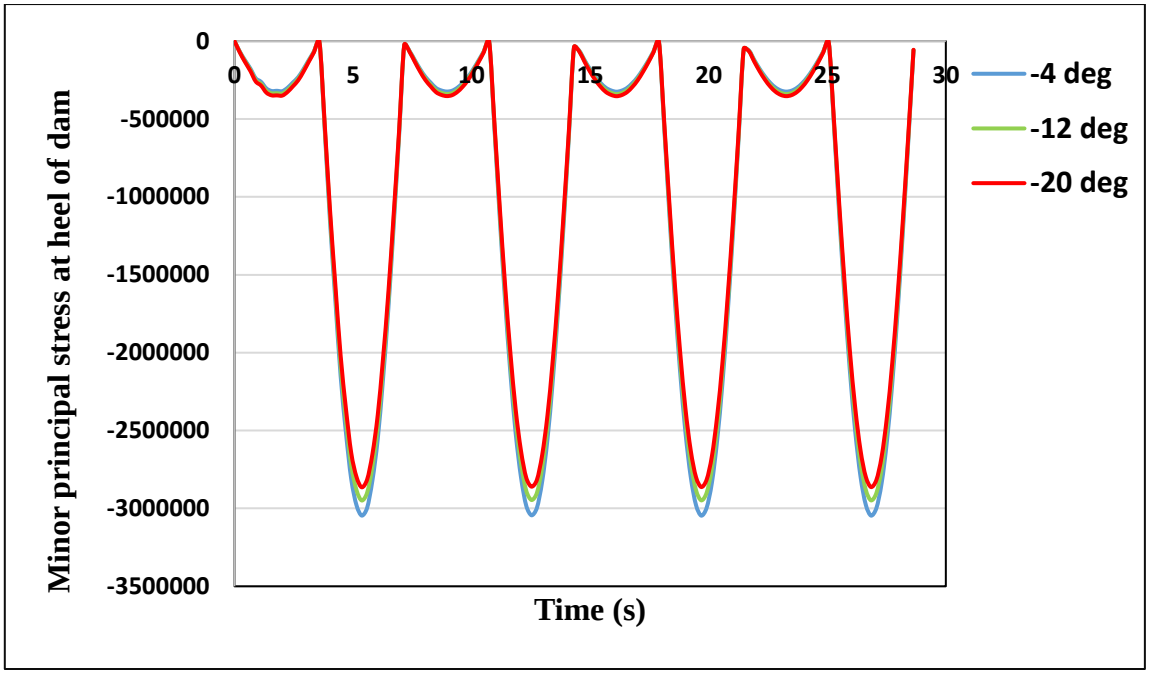

Fig. 4.56: Time history plot of minor principal stress at the heel of the dam for negative slope angles of reservoir bottom

Fig. 4.39 to Fig. 4.41 present the time history plot of pressure coefficient ($C_p = p/\rho_f a H_f$) at the heel of the dam for different bottom slope of the reservoir due to Tc/H_f = 4, 10 and 100 respectively. Fig. 4.42 to Fig. 4.44 show the distribution of pressure coefficient (C_p) at the face of the dam for Tc/H_f = 4, 10 and 100 respectively, for different positive slopes (θ_b) of the reservoir bottom. From these figures, it is clear that pressure at the heel of the dam increases with the increase of positive slope of the reservoir bed for all values of exciting frequencies. Pressure is higher at Tc/H_f = 4 compared to other frequencies for all values of positive bottom slope angles. Similarly, Fig. 4.45 to Fig. 4.47 illustrates the time history plot of pressure coefficient ($C_p = p/\rho_f a H_f$) at the heel of the dam for different negative slopes due to Tc/H_f = 4, 10 and 100 respectively. Fig. 4.48 to Fig. 4.50 present the distribution of pressure coefficient (C_p) at the face of the dam for Tc/H_f = 4, 10 and 100 respectively, for different negative slope (θ_b) of the reservoir bottom. From these figures, it has been observed that pressure at heel of the dam decreases with the increase of negative slope of the reservoir bottom for all values of exciting frequencies.

Fig. 4.51 presents the pressure coefficients at the heel of the dam for different positive slope angles of the reservoir bottom for different frequencies (Tc/H_f =4, 10 and 100). The rate of increment of pressure coefficient for the increase of positive slope angles (θ_b) is highest for Tc/H_f =4. Fig. 4.52 displays the pressure coefficients at the heel of the dam for different negative slope angles (θ_b) of the reservoir bottom for different frequencies (Tc/H_f =4, 10 and 100). The rate of decrement of pressure coefficient for the increase of negative slope angle is highest for Tc/H_f =4.

Fig. 4.53 displays the time history plot of major principal stress and Fig. 4.54 displays the time history plot of minor principal stress at the heel of the gravity dam for positive slope angle (θ_b) of the reservoir bottom. From both figures, it is evident that the maximum values of major and minor principal stresses at the heel of the dam increase with the increase of the positive slope angle (θ_b) of the reservoir bottom. Fig. 4.55 displays the time history plot of major principal stress and Fig. 4.56 displays the time history plot of minor principal stress at the heel of the dam for negative slope angle (θ_b) of the reservoir bottom. From both figures, it may be concluded that the maximum values of major and minor principal stresses at the heel of the dam decrease with the increase of the negative slope angle of the reservoir bottom.

When the slope of the reservoir bed is in positive (anticlockwise) direction, the inclined reservoir bed is towards the concrete gravity dam. Due to this inclination, the reservoir bed reflects the wave towards the gravity dam. For this reason, hydrodynamic pressure at the heel of the dam increases and the stresses at the heel of the dam increase with the increase of the positive slope angle (θ_b) of the reservoir bottom. When the slope of the reservoir bed is in the negative (clockwise) direction, the inclined reservoir bed is away from the concrete gravity dam. Due to this inclination, the reservoir bed reflects the wave that is going away from the gravity dam. For this reason, hydrodynamic pressure at the heel of the dam and the stresses at the heel of the dam decrease with the increase of the negative slope angle of the reservoir bottom.

4.3.2.2 PART II: ANALYSIS OF DAM-RESERVOIR COUPLED SYSTEM FOR VARIATION OF INCLINED LENGTH OF RESERVOIR

In this part of work, variation of pressure coefficient (C_p) at the face of the dam has been determined for different inclined lengths (L_i) of reservoir bed (Fig. 4.57) considering dam-reservoir interaction. The height (H_f) of the reservoir is taken as 103 m. and L/H_f ratio is assumed to be 0.5. Density of water (ρ_f), velocity of acoustic wave (c), reflection coefficient (α) of reservoir bottom, modulus of elasticity of concrete, unit weight of concrete, Poisson ratio and damping ratio are taken as considered in subsection 4.3.2.1.

Hydrodynamic pressure at the face of the dam has been observed for different inclined lengths of the reservoir (L_i = 0.25 L, 0.5 L, 0.75 L) with different positive inclinations ($+4^0$, $+12^0$, $+20^0$) as well as different negative inclinations (-4^0, -12^0, -20^0) of the reservoir bottom applying sinusoidal excitations. Fig. 4.58 to Fig. 4.60 display the hydrodynamic pressure distribution at the face of the dam for the reservoir bottom slope of $+4^0$, $+12^0$ and $+20^0$ respectively, with different values of inclined length of the reservoir such as L_i = 0.25 L, 0.5 L and 0.75 L. Similarly, Fig. 4.61 to Fig. 4.63 show the hydrodynamic pressure distribution at the face of the dam for L_i=0.25 L, 0.5L and 0.75L with different negative slopes -4^0, -12^0 and -20^0 respectively. From these figures, it has been found that pressure at the heel of the dam increases with the increase of inclined length (L_i) of the reservoir for positive slopes. It has been also found that pressure at the heel of the dam decreases with the increase of inclined length (L_i) of the reservoir for negative slopes.

Fig. 4.64 and Fig. 4.65 show the time history plot of major principal and minor principal stress at the heel of the dam for positive slope of $+20^0$ respectively. Similarly, Fig. 4.66 and Fig. 4.67 show the time history plot of major and minor principal stress at the heel of the dam for negative slope angle -20^0 respectively. From these figures, it is observed that the value of major and minor principal stresses at heel of the dam increases with the increase of inclined length for positive slope and decreases with the increase of inclined length for negative slope.

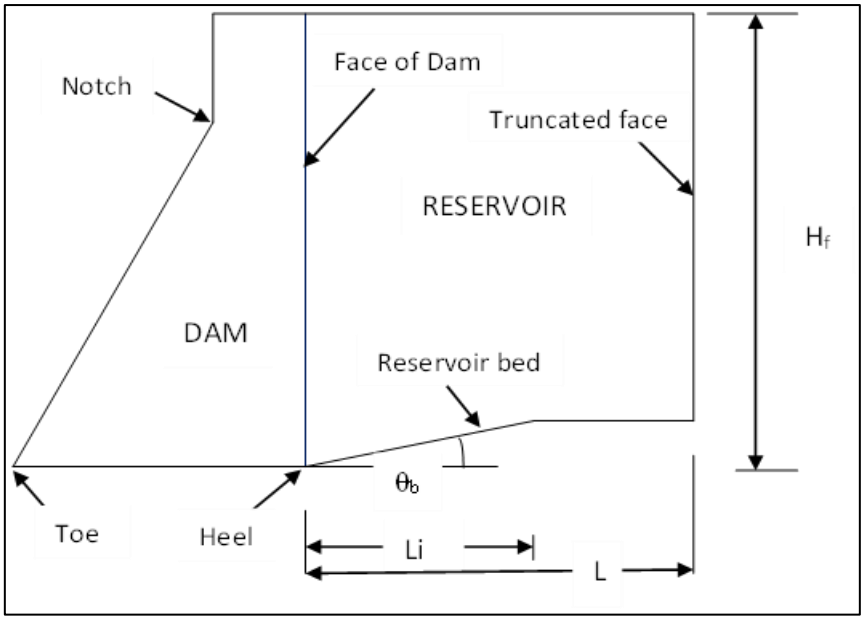

Fig. 4.57: Dam-reservoir coupled system with variable inclined bottom length

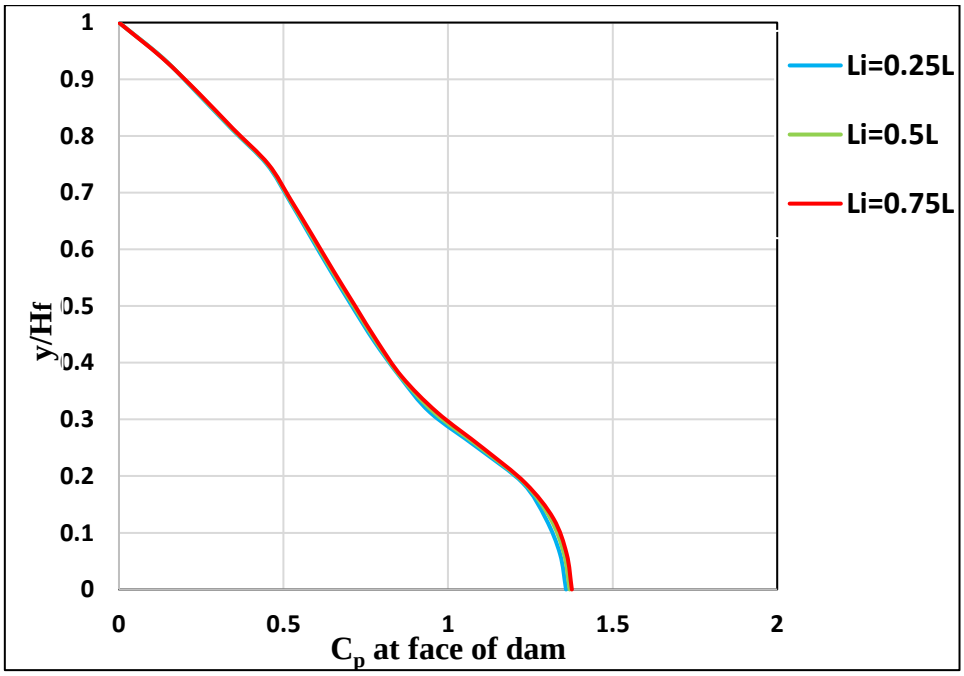

Fig. 4.58: Distribution of pressure coefficient (C_p) at the face of the dam for bottom slope $+4^0$

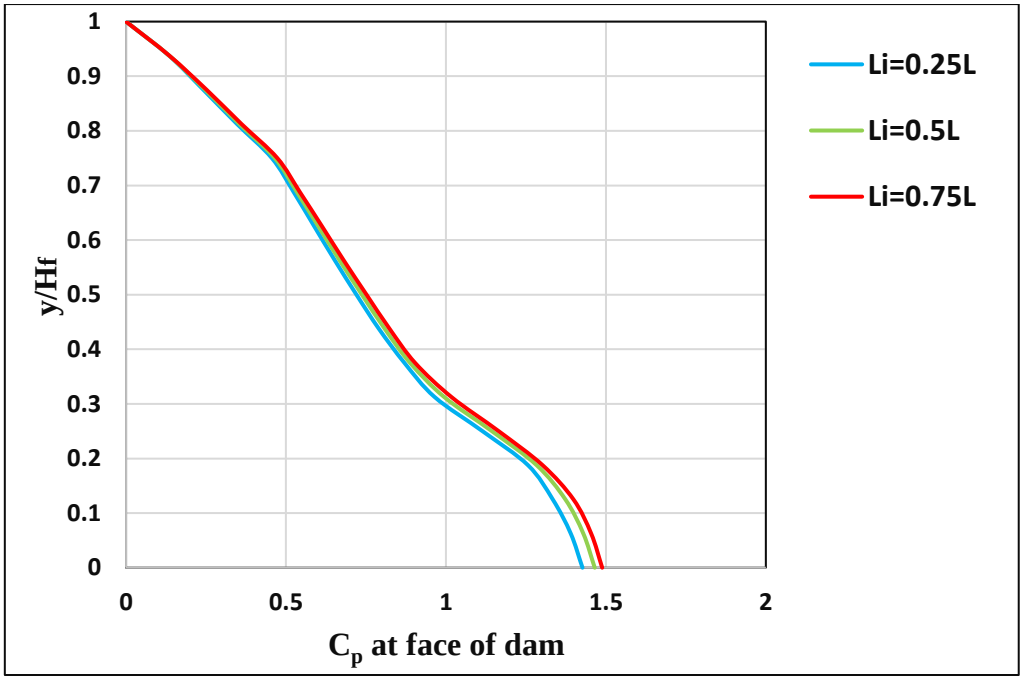

Fig. 4.59: Distribution of pressure coefficient (C_p) at the face of the dam for bottom slope $+12^0$

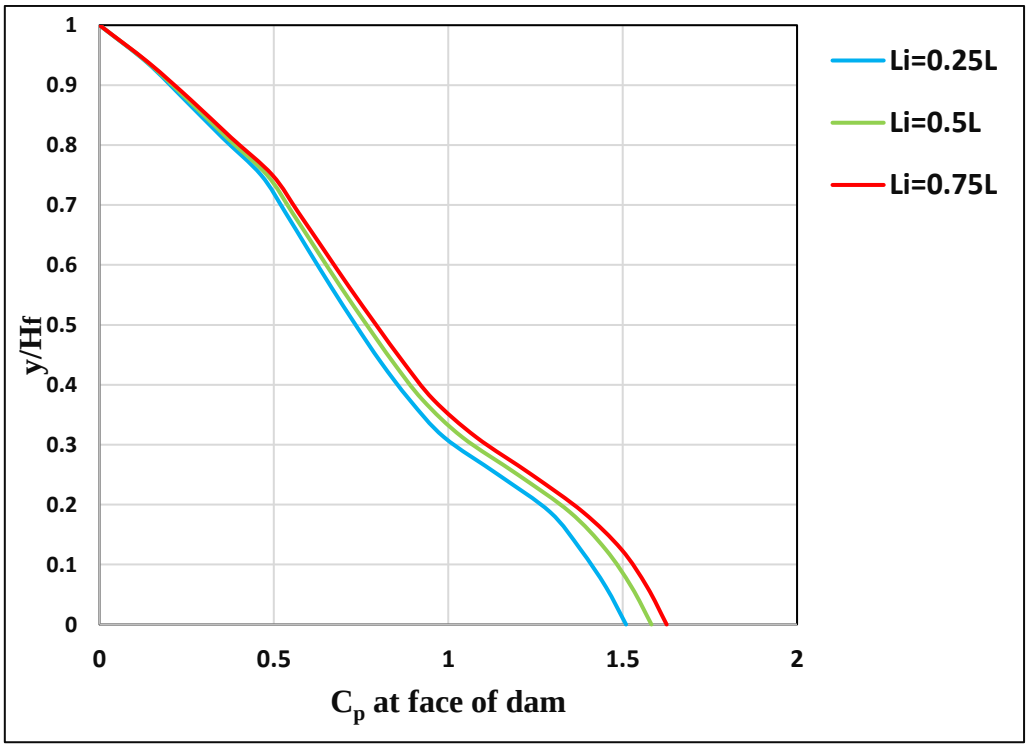

Fig. 4.60: Distribution of pressure coefficient (C_p) at the face of the dam for bottom slope $+20^0$

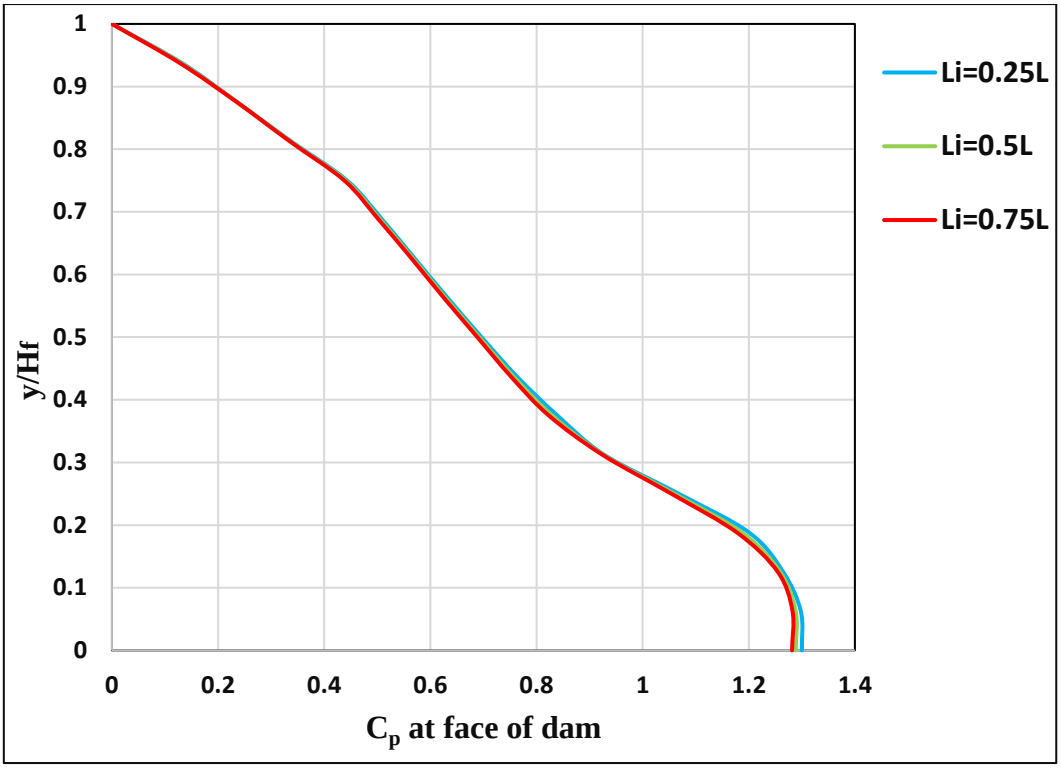

Fig. 4.61: Distribution of pressure coefficient (C_p) at the face of the dam for bottom slope -4^0

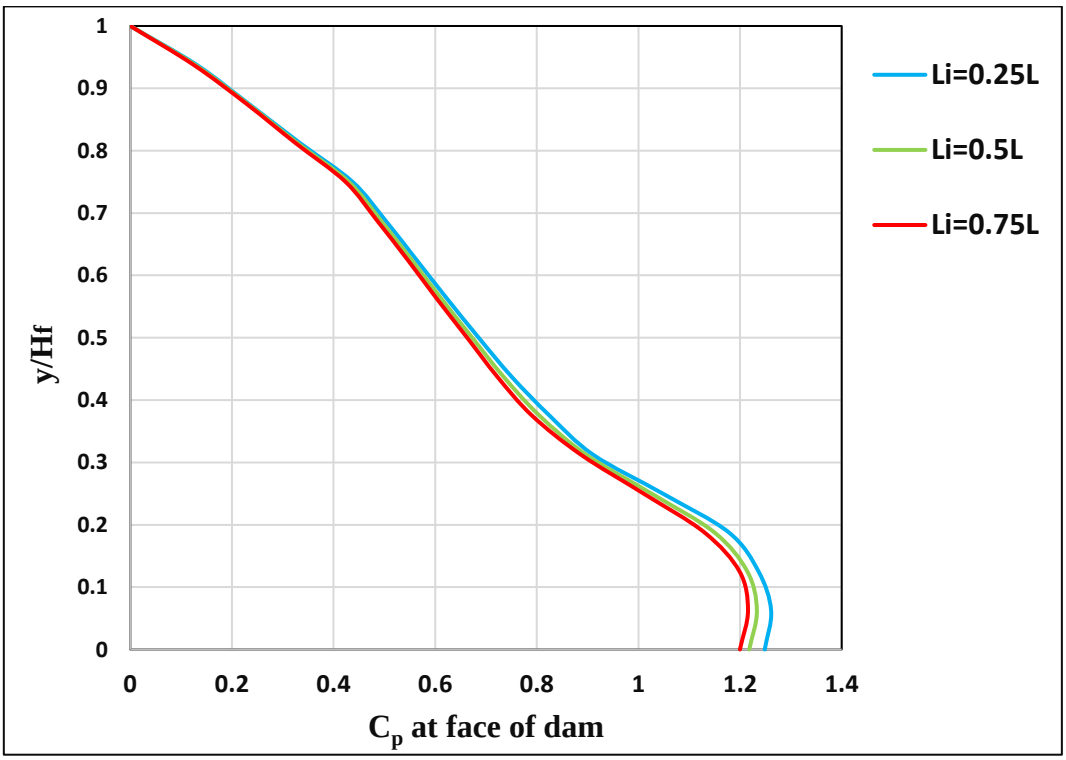

Fig. 4.62: Distribution of pressure coefficient (C_p) at the face of the dam for bottom slope -12^0

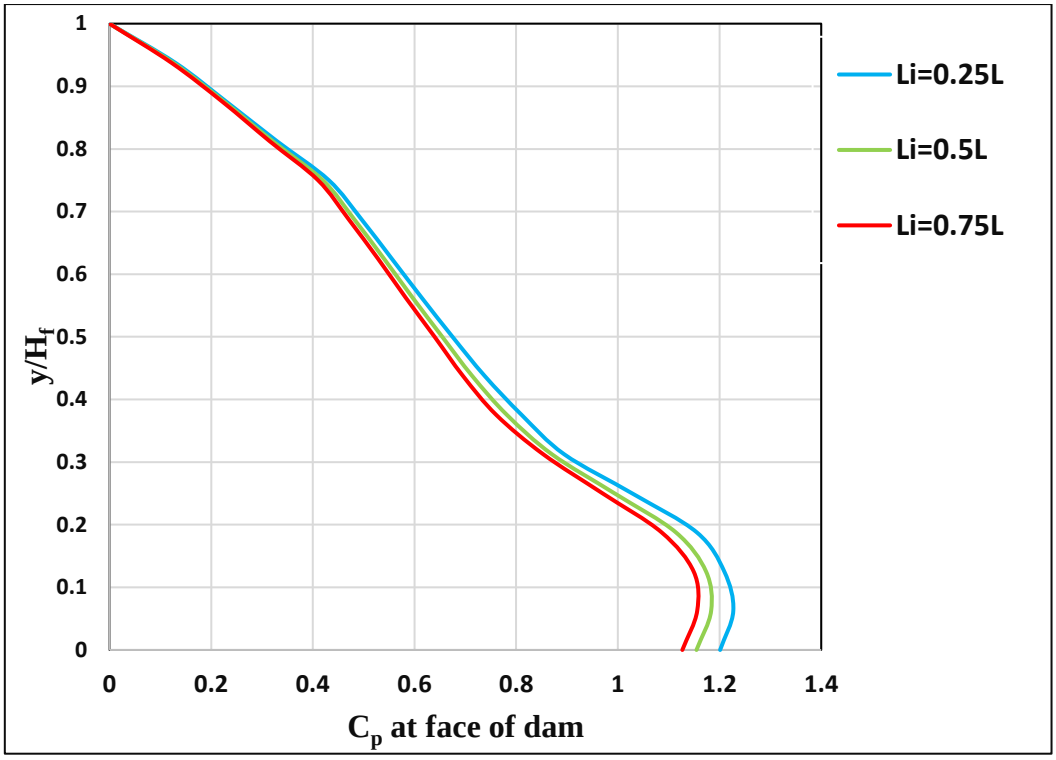

Fig. 4.63: Distribution of pressure coefficient (C_p) at the face of the dam for bottom slope -20^0

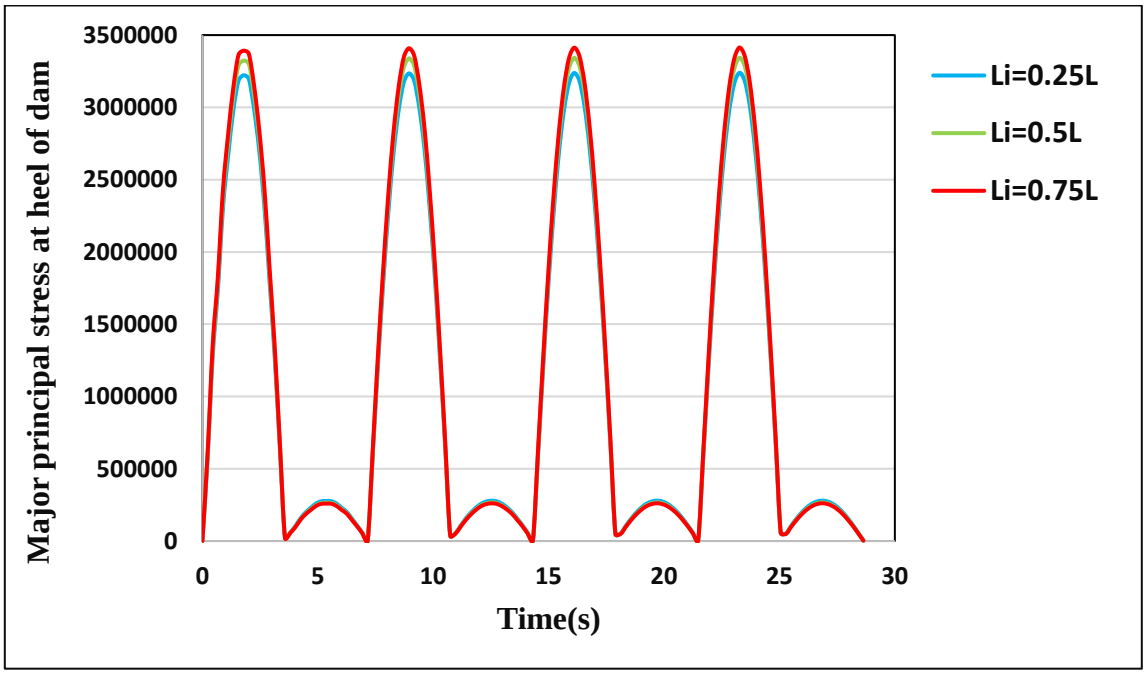

Fig. 4.64: Time history plot of major principal stress at the heel of the dam for slope angle +20^0

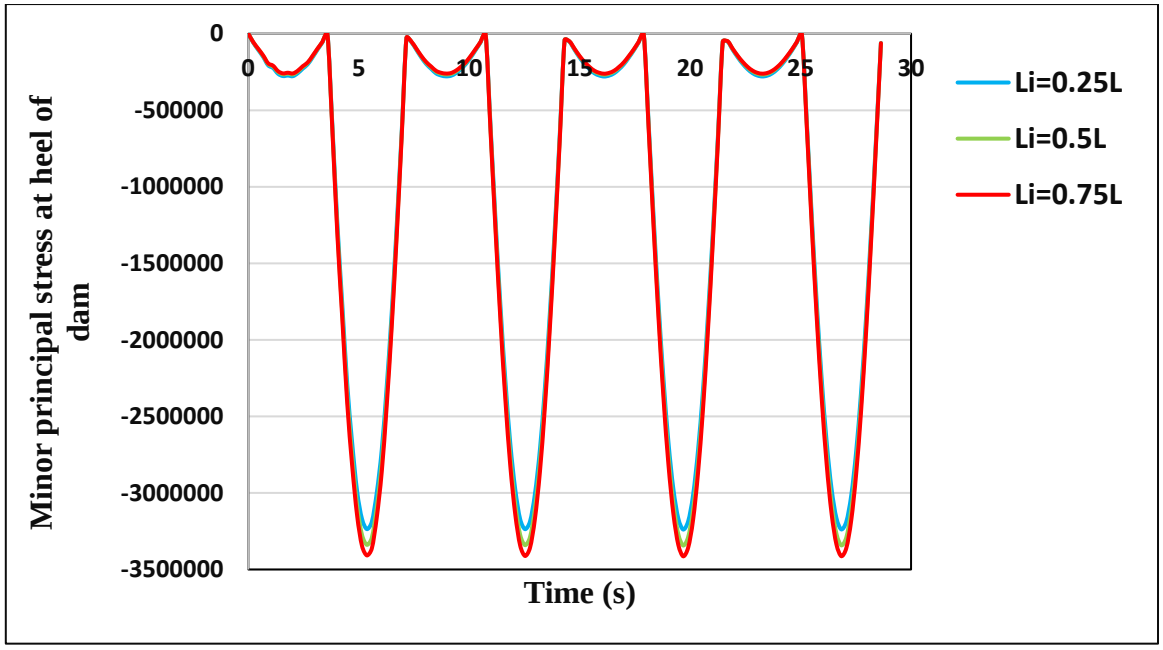

Fig. 4.65: Time history plot of minor principal stress at the heel of the dam for slope angle $+20^0$

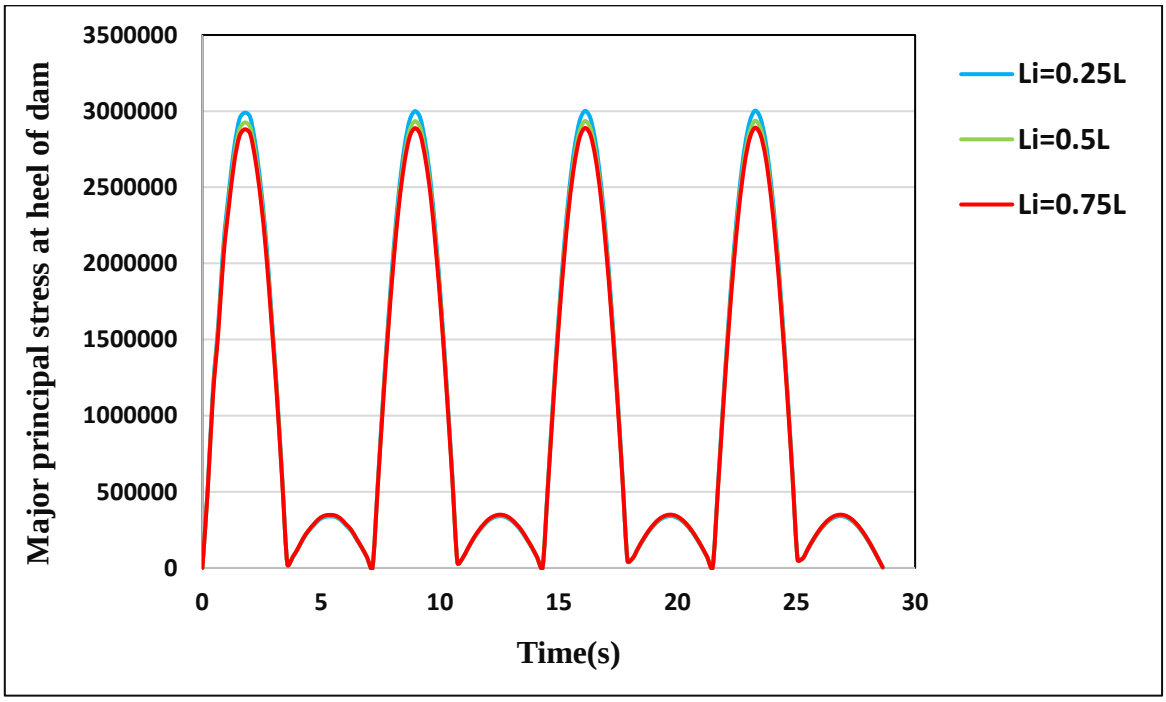

Fig. 4.66: Time history plot of major principal stress at the heel of the dam for slope angle -20^0

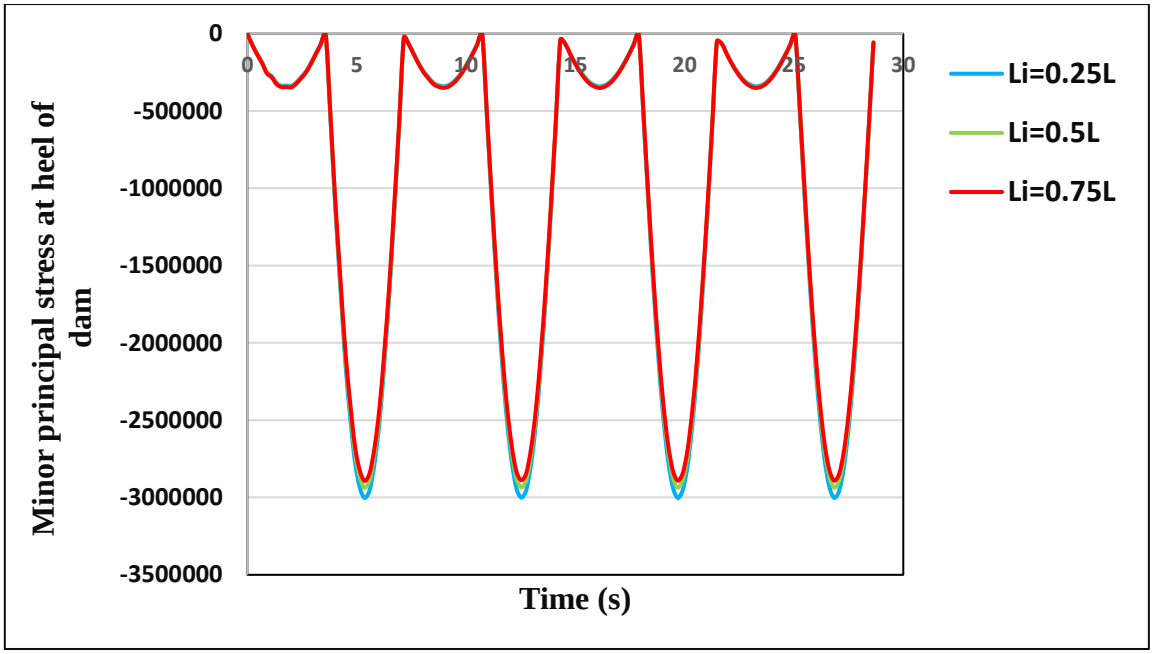

Fig. 4.67: Time history plot of minor principal stress at the heel of the dam for slope angle -20^0

4.3.2.3 PART III: ANALYSIS OF DAM-RESERVOIR COUPLED SYSTEM FOR VARIATION OF REFLECTION COEFFICIENT

In this article, the distribution of hydrodynamic pressure at the heel of the gravity dam has been observed for different reflection coefficients of the reservoir bed with different inclined length of the reservoir. The geometry and material properties of the dam and reservoir are considered as in subsection 4.3.2.1. In this part, L/H_f ratio is taken as 0.5 and L_i is considered as $0.5L$. Hydrodynamic pressure coefficients at heel of the dam are determined for different positive slope angles ($+4^0$, $+12^0$, $+20^0$) as well as different negative slope angles (-4^0, -12^0, -20^0) of the reservoir bottom. Fig. 4.68 presents the hydrodynamic pressure coefficient at the heel of the dam with different values of reflection coefficient for positive slope angles at the reservoir bottom as $+4^0$, $+12^0$ and $+20^0$ respectively due to sinusoidal excitation of frequency of Tc/H_f=100. Fig. 4.69 presents the hydrodynamic pressure coefficient at heel of the dam due to same sinusoidal excitation for different negative slopes -4^0, -12^0 and -20^0 respectively.

From Fig. 4.68 to Fig. 4.69, it is observed that the hydrodynamic pressure coefficient has a minimum value for α=0 for all the cases of slope angles. However, the pressure coefficient has maximum value when α=1 for all values of slope angles. Therefore, it can be concluded that pressure will increase at heel of the dam if the reflection coefficient is increased for any

values of slope angles. From the figures, it is also observed that the difference of pressure is high between α =0 to 0.5 and the difference of pressure is comparatively small between α =0.5 to 1.

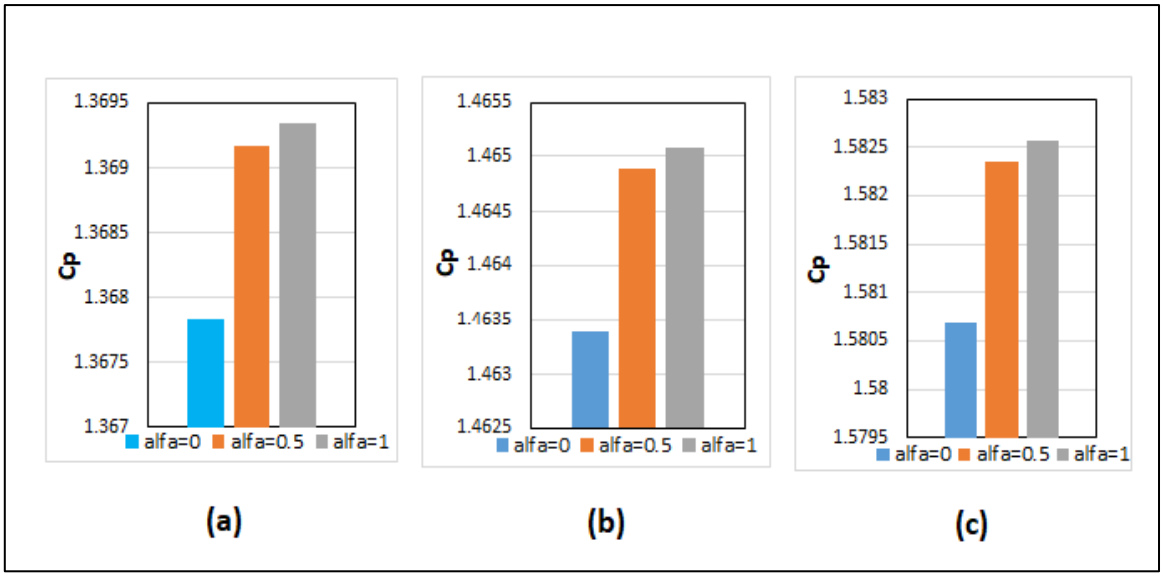

Fig. 4.68: Hydrodynamic pressure coefficient (C_p) at the heel of the dam for bottom slope angles of (a)+ 4^0, (b) + 12^0 and (c) +20^0

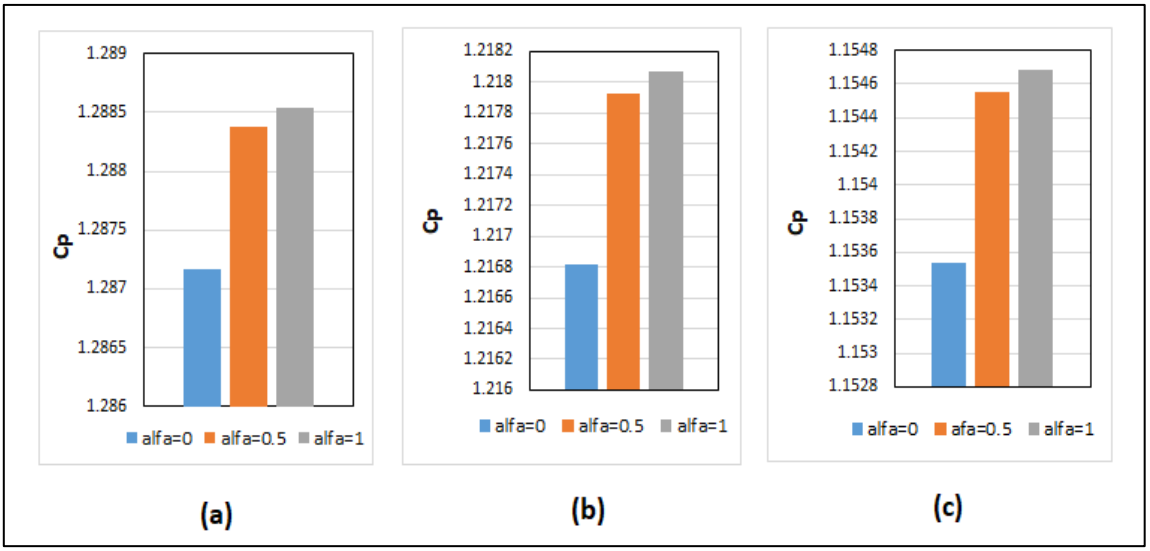

Fig. 4.69: Hydrodynamic pressure coefficient (C_p) at the heel of the dam for bottom slope angles of (a)- 4^0, (b) -12^0 and (c) -20^0

4.3.2.4 PART IV: ANALYSIS OF DAM-RESERVOIR COUPLED SYSTEM DUE TO EARTHQUAKE

In this part of work, variation of hydrodynamic pressure at the face of the dam has been observed for north-south component of El-Centro earthquake excitation (Fig. 4.70) with the change of slope angles both for negative and positive slope of reservoir bed considering dam–reservoir interaction. The Height of the reservoir (H_f) is considered as 103 m, L/H_f ratio is assumed as 0.5, inclined length is taken as L_i=0.5L and reflection coefficient (α) of reservoir bottom is taken as 0.95. The dam and reservoir geometry and their properties are taken as in subsection 4.3.2.1. Fig. 4.71 and Fig. 4.72 show the time history plot of pressure coefficient at the heel of the dam for positive bottom slope and negative bottom slope respectively. Fig. 4.73 shows hydrodynamic pressure at the face of the dam for positive slope and Fig. 4.74 shows hydrodynamic pressure at the face of the dam for negative bottom slope. Fig. 4.75 and 4.76 present the time history of major principal stress and minor principal stress at the heel of the dam for positive bottom slope respectively. Same ways, the major and minor principal stress at the heel of the dam for negative slope are presented in Fig. 4.77 and 4.78 respectively. Fig. 4.79 to Fig. 4.86 present the contours for different slope angles. From these figures, differences in stresses have been observed for changes in slope angle of reservoir bed both for positive and negative. It has been seen that maximum stress occurred at notch of the dam and maximum hydrodynamic pressure occurred at heel of the dam.

From this part of work, it is observed that maximum pressure occurred for higher value of positive slope angle of the reservoir bottom and it is also noted that maximum peak occurred for lower value of negative slope angle of the reservoir bottom. It is also observed that maximum stress at the heel of the dam occurred at higher value of positive slope angle of the reservoir base and maximum stress at the heel of the dam occurred at lower value of negative slope angle of the reservoir base.

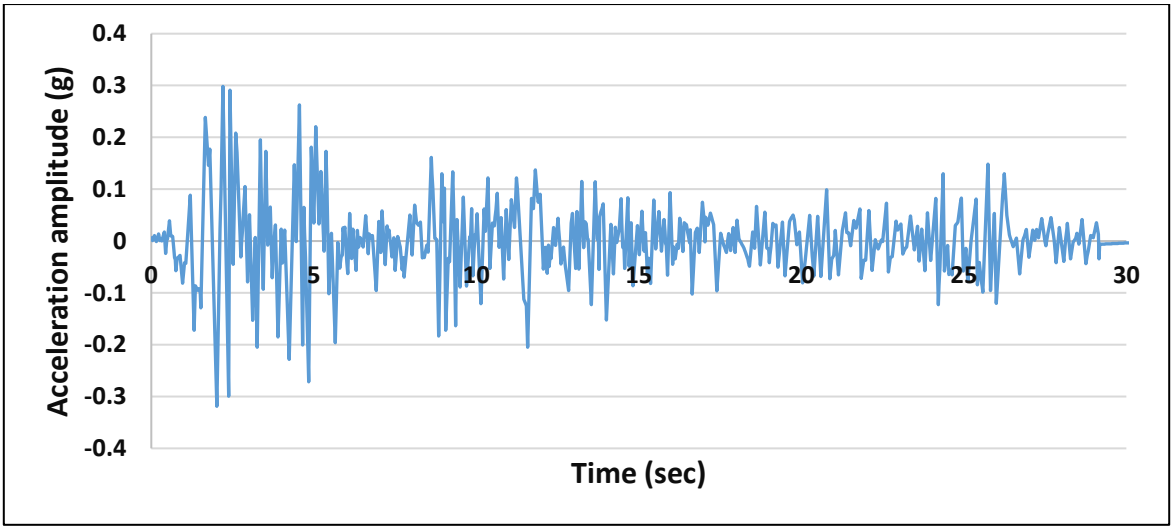

Fig. 4.70: North-south component of El-Centro earthquake (1940)

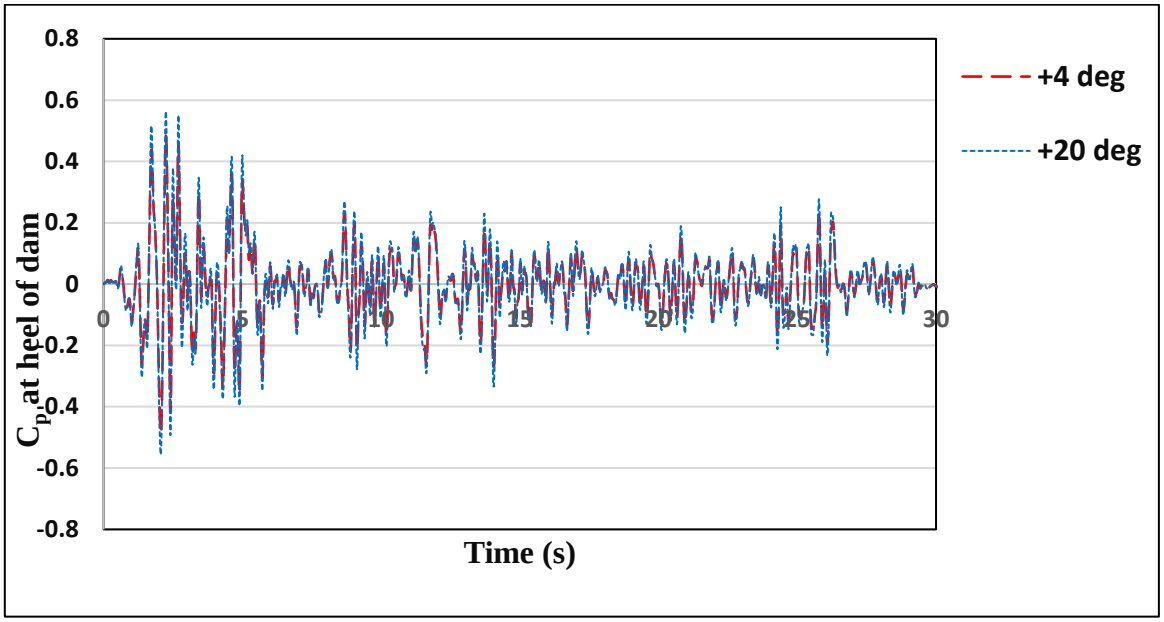

Fig. 4.71: Time history plot of pressure coefficient (C_p) at the heel of the dam for positive bottom slopes for North-south component of El-Centro earthquake

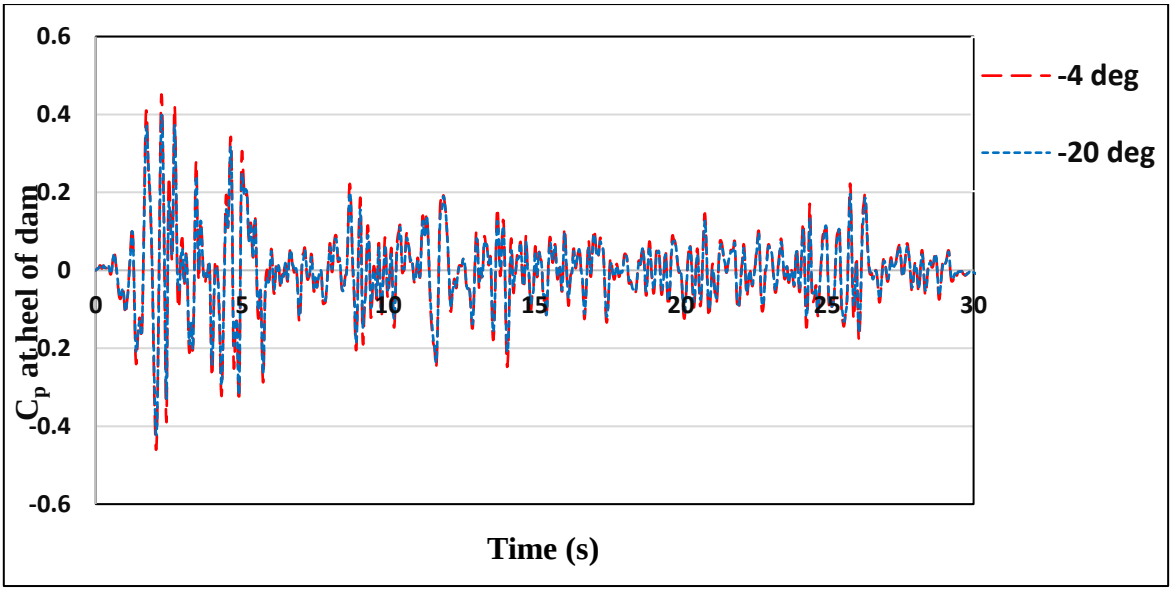

Fig. 4.72: Time history plot of pressure coefficient (C_p) at the heel of the dam for negative bottom slopes for North-south component of El-Centro earthquake

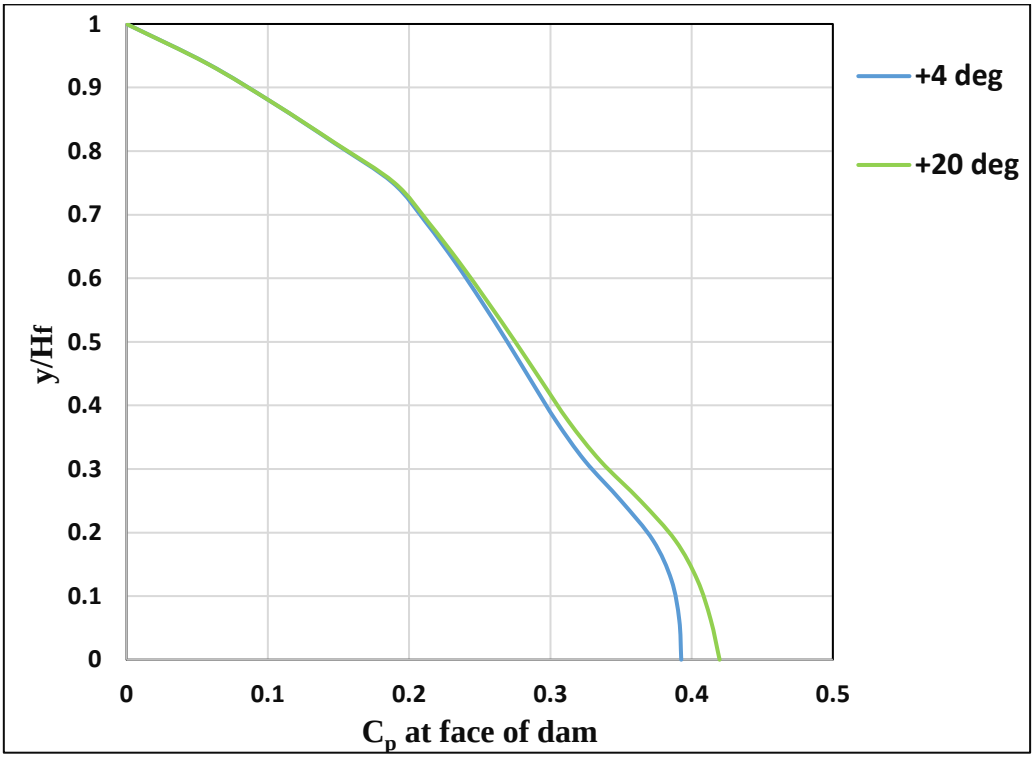

Fig. 4.73: Hydrodynamic pressure coefficient (C_p) at the face of the dam for positive bottom slopes for North-south component of El-Centro earthquake

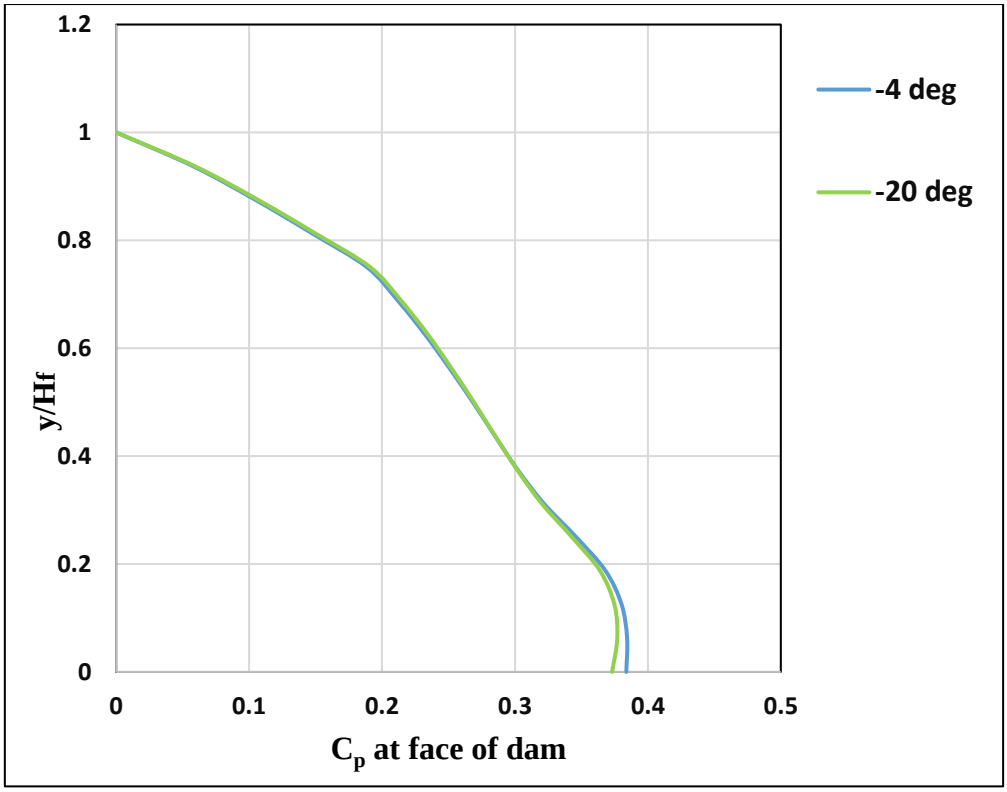

Fig. 4.74: Hydrodynamic pressure coefficient (C_p) at the face of the dam for negative bottom slopes for North-south component of El-Centro earthquake

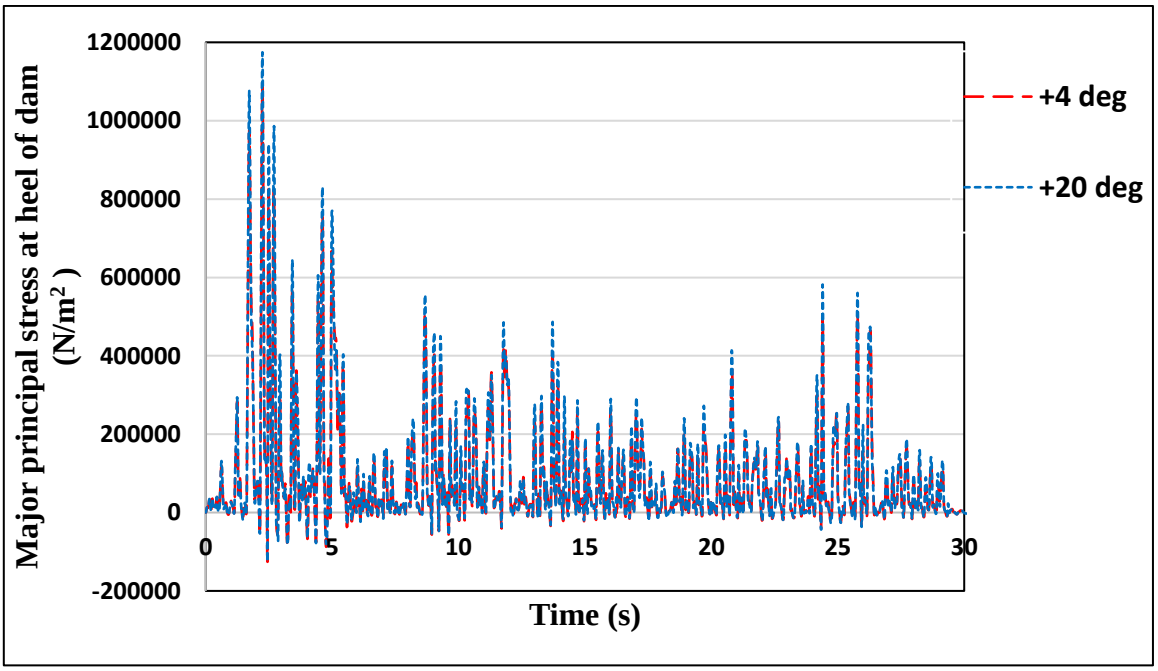

Fig. 4.75 Time history of major principal stress at the heel of the dam for positive bottom slopes for North-south component of El-Centro earthquake

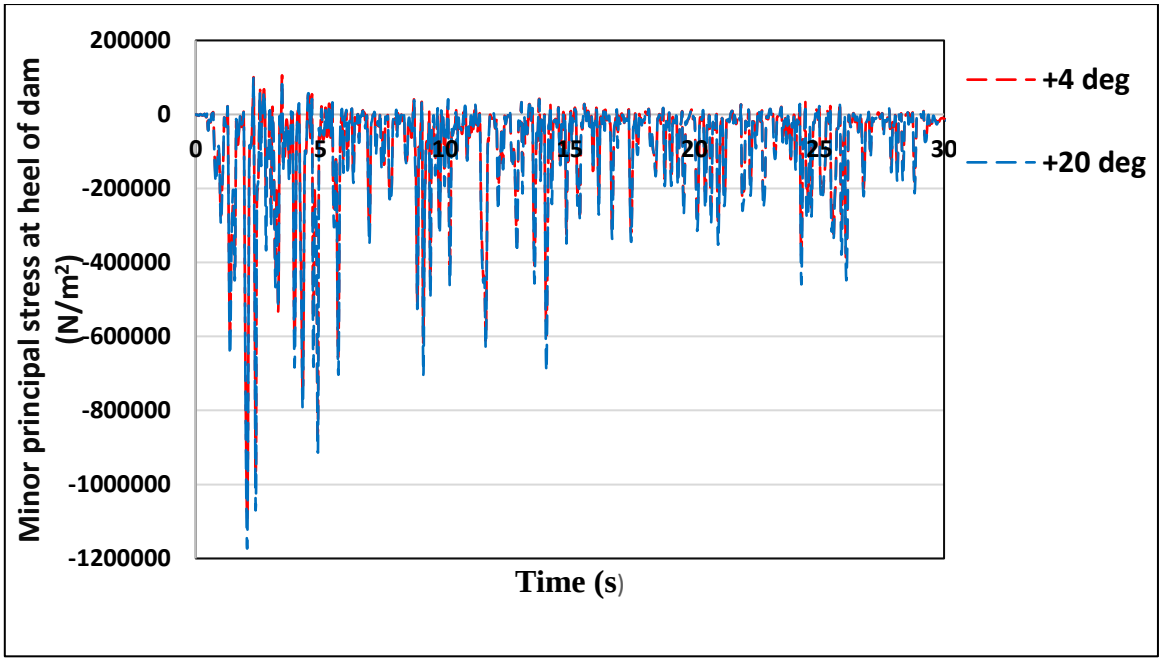

Fig. 4.76: Time history of minor principal stress at the heel of the dam for positive bottom slopes for North-south component of El-Centro earthquake

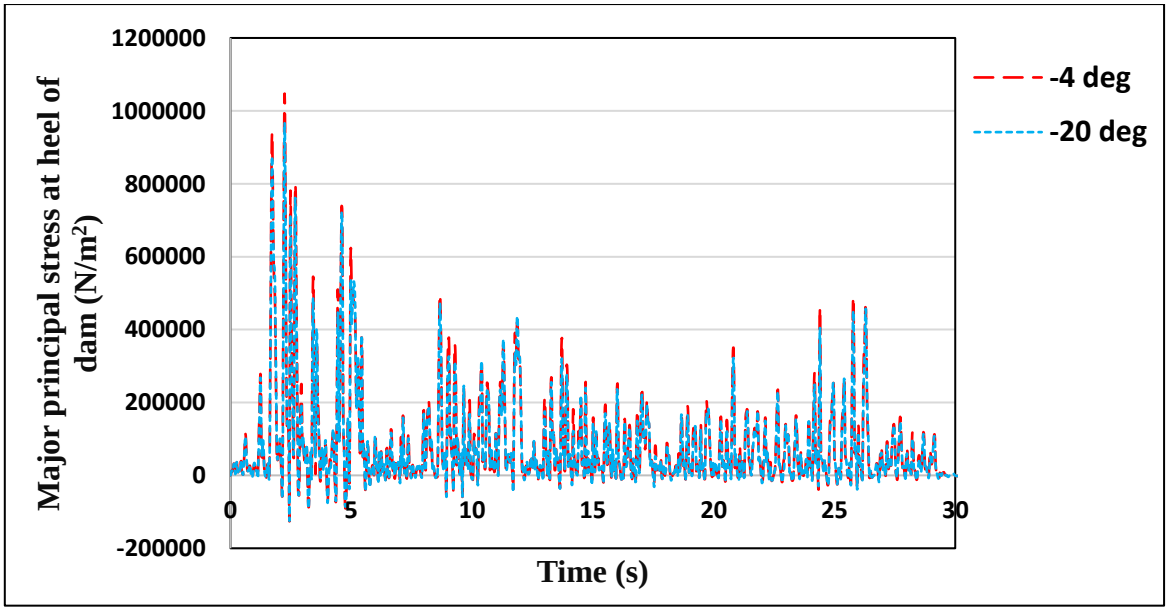

Fig. 4.77: Time history of major principal stress at the heel of the dam for negative bottom slopes for North-south component of El-Centro earthquake

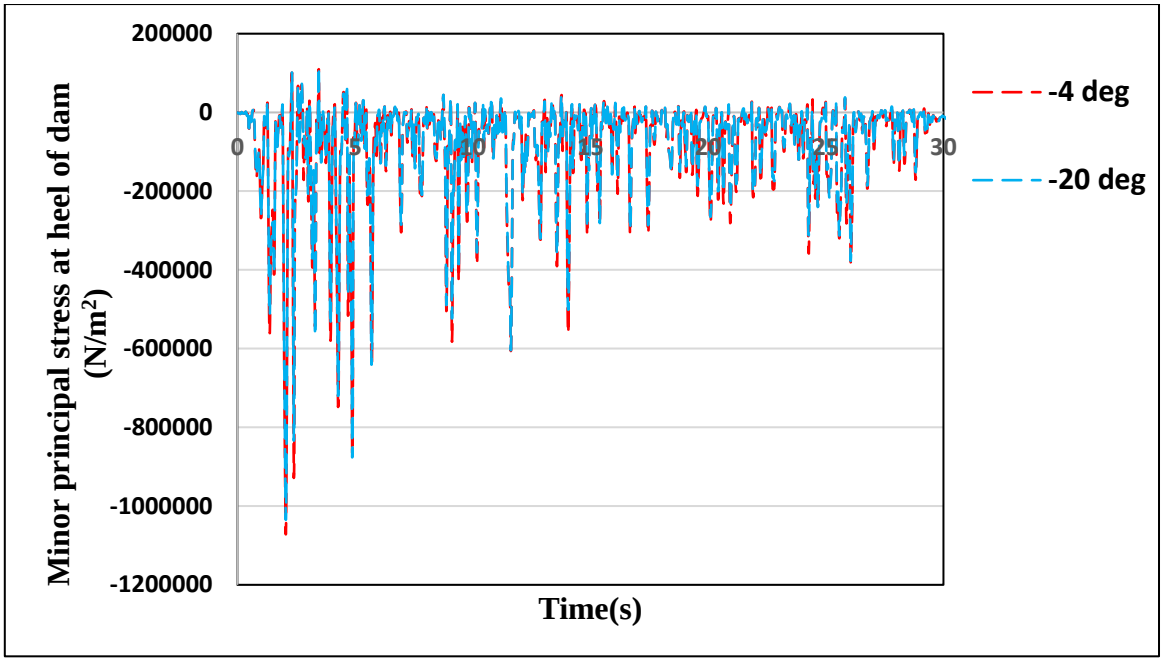

Fig. 4.78: Time history of minor principal stress at the heel of the dam for negative bottom slopes for North-south component of El-Centro earthquake

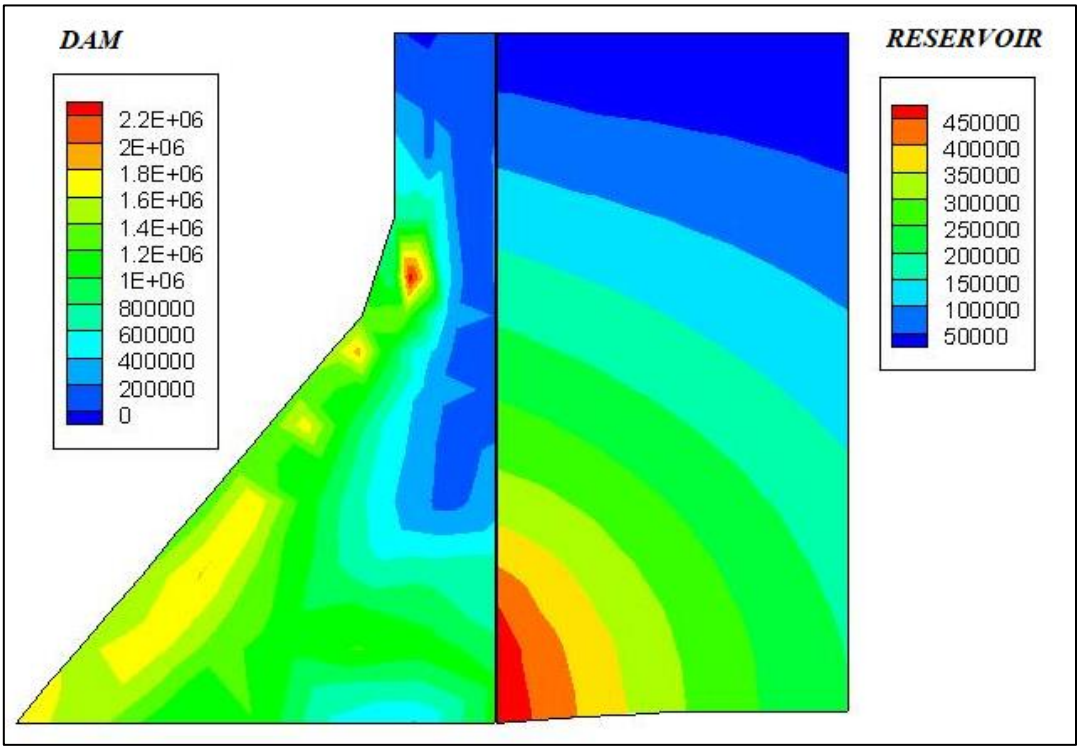

Fig. 4.79: Contour of major principal stress plot of dam and pressure of reservoir for base angle $+4^0$ due to North-south component of El-Centro earthquake

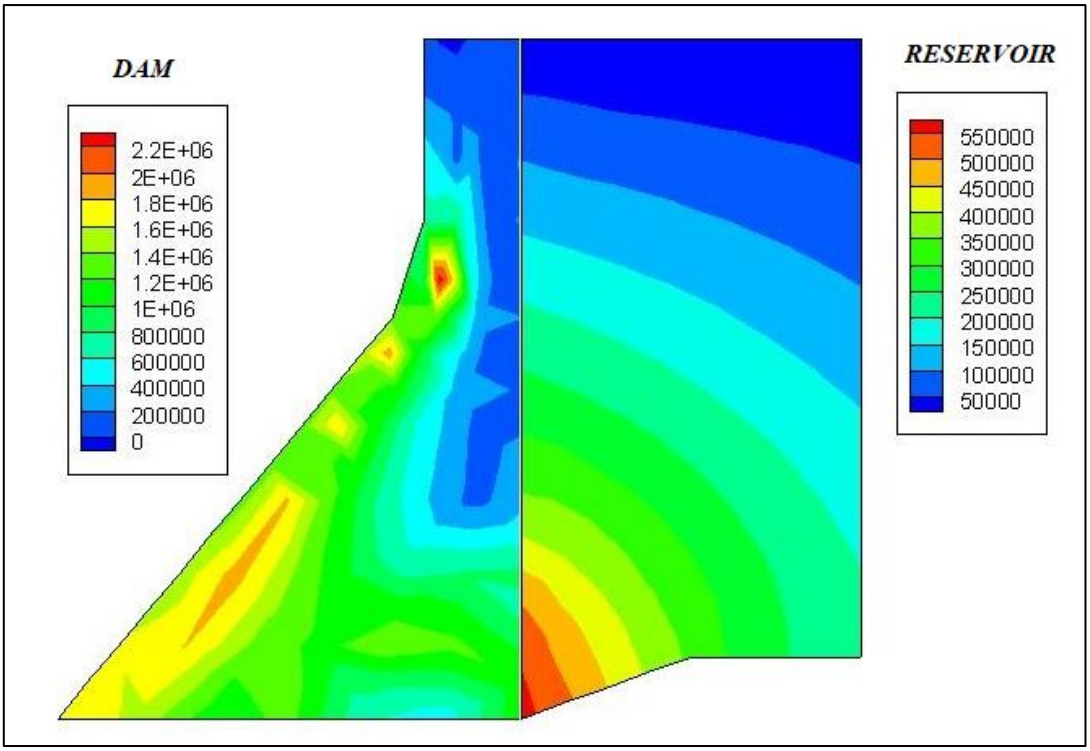

Fig. 4.80: Contour of major principal stress plot of dam and pressure of reservoir for base angle $+20^0$ due to North-south component of El-Centro earthquake

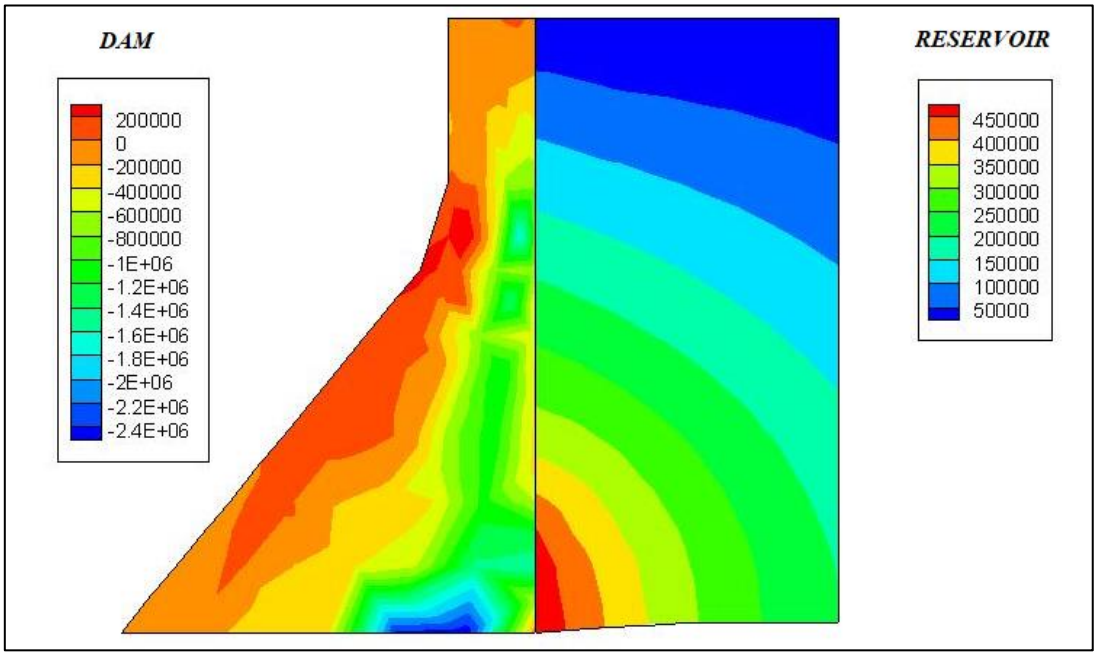

Fig. 4.81: Contour of minor principal stress plot of dam and pressure of reservoir for base angle $+4^0$ due to North-south component of El-Centro earthquake

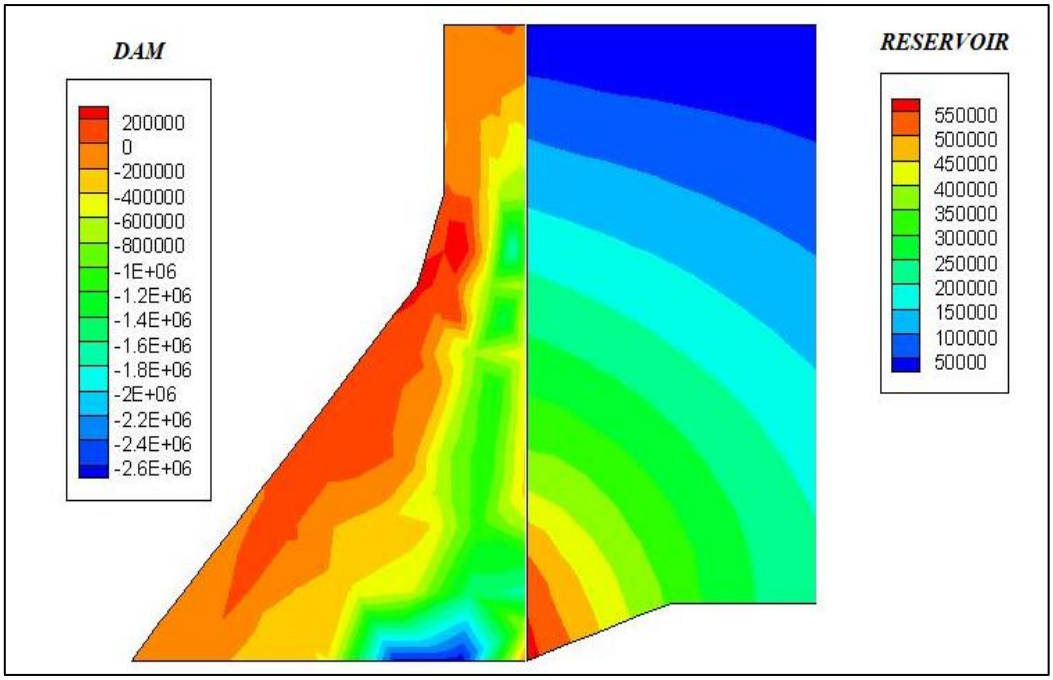

Fig. 4.82: Contour of minor principal stress plot of dam and pressure of reservoir for base angle $+20^0$ due to North-south component of El-Centro earthquake

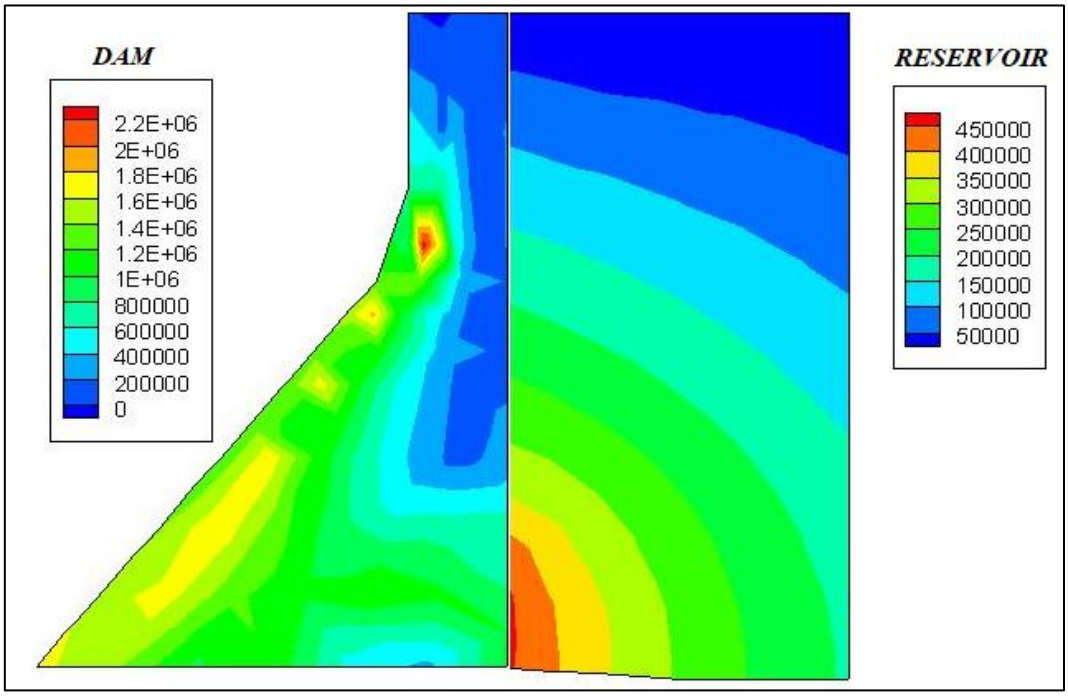

Fig. 4.83: Contour of major principal stress plot of dam and pressure of reservoir for base angle -4^0 due to North-south component of El-Centro earthquake

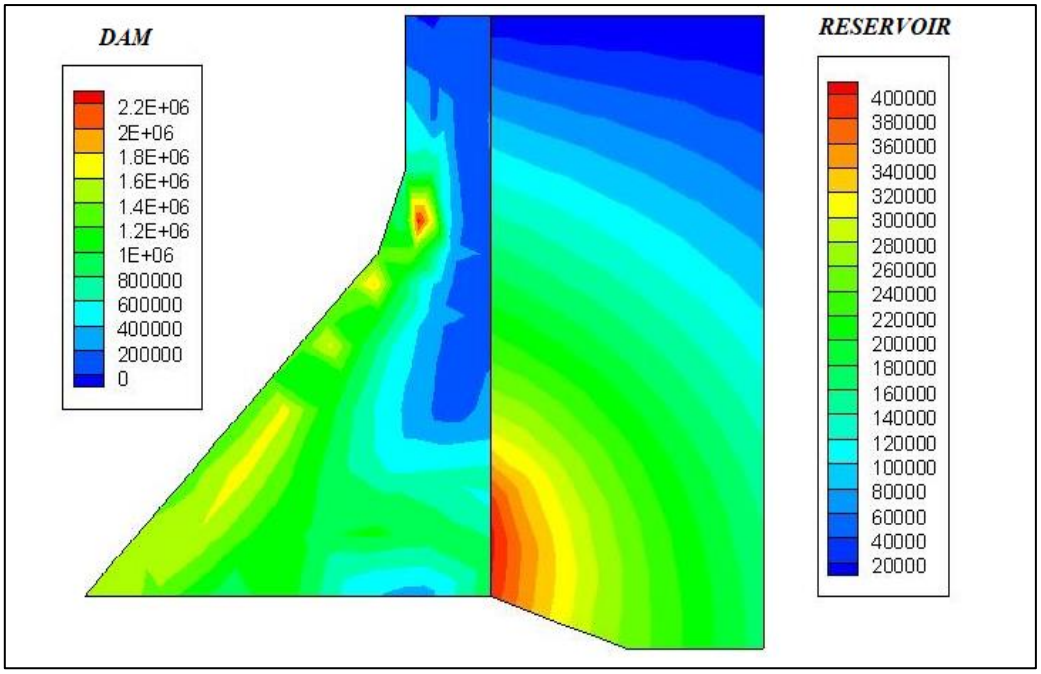

Fig. 4.84: Contour of major principal stress plot of dam and pressure of reservoir for base angle -20^0 due to North-south component of El-Centro earthquake

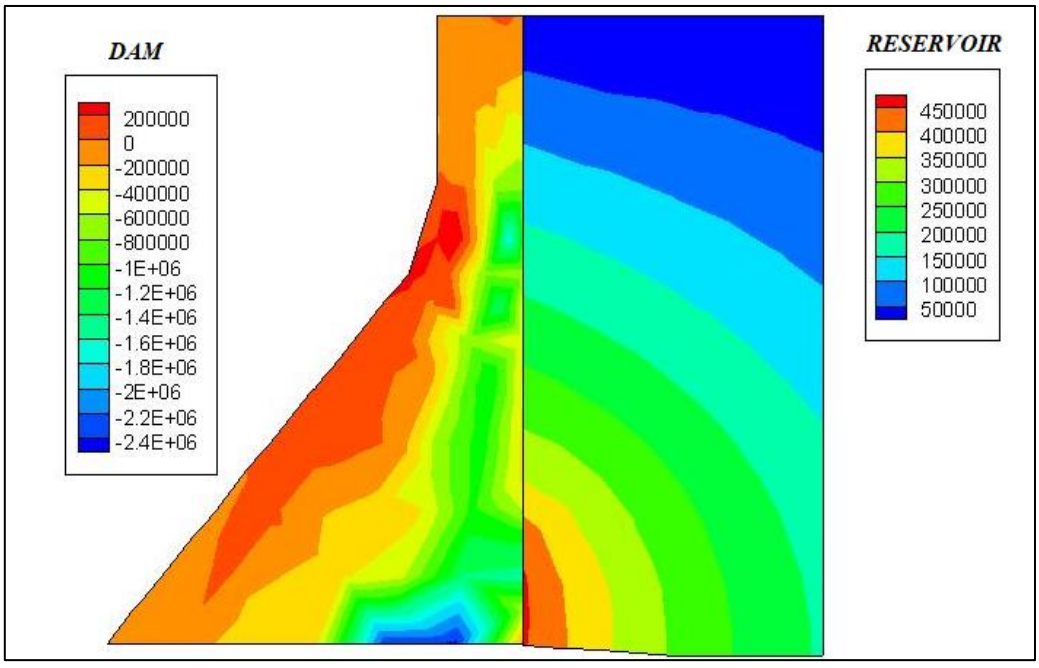

Fig. 4.85: Contour of minor principal stress plot of dam and pressure of reservoir for base angle -4^0 due to North-south component of El-Centro earthquake

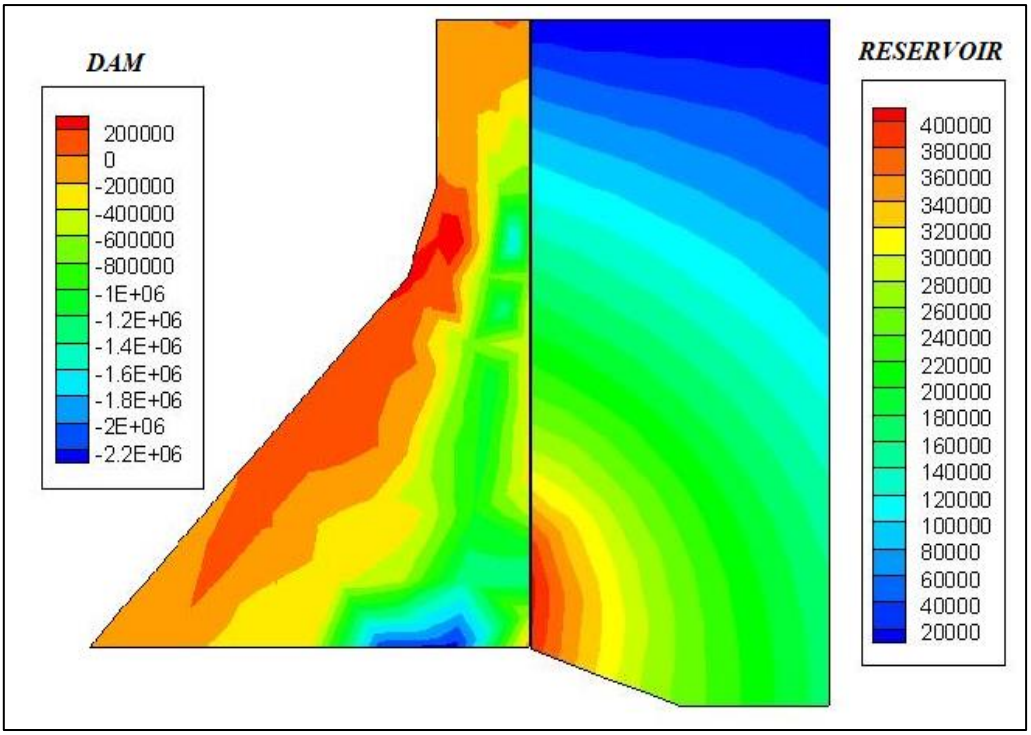

Fig. 4.86: Contour of minor principal stress plot of dam and pressure of reservoir for base angle -20^0 due to North-south component of El-Centro earthquake

4.4 SECTION 3: ANALYSIS OF DAM-RESERVOIR-FOUNDATION COUPLED SYSTEMS

Behaviour of concrete gravity dam during an earthquake is immensely important for the safe design of the structure. Behaviour of the adjacent reservoir and the foundation is also equally important. Determination of hydrodynamic pressure and stresses in gravity dam should be done considering fluid-structure and soil-structure interaction. The effect of the foundation should be included to obtain a clear idea about the seismic behaviour of the gravity dam. In the present section of work, two-dimensional geometry of dam, reservoir and foundation has been considered. Eight-node isoparametric element is used for the discretization of reservoir, dam and foundation domain. Pressure is assumed as nodal variable for fluid domain and displacement is considered as nodal variable for the dam and foundation. Fluid is truncated at a suitable distance and an effective truncation boundary condition, proposed by Gogoi and Maity (2006), is applied at the truncation surface. The effect of surface wave is neglected and reservoir bottom absorption is considered. The viscous boundary condition is applied along the truncated face of the foundation. Hydrodynamic pressure and stresses have been determined for harmonic and earthquake exiting forces. Effect of bottom slope of reservoir and reflection coefficient has been observed.

4.4.1 VALIDATION OF THE DEVELOPED ALGORITHM

The developed algorithm is validated with the problem carried out by Papazafeiropoulos et al. (2011). The geometry and material properties are adopted from Papazafeiropoulos et al. (2011). The density of water (ρ_f) is assumed as 1000kg/ m^3 and velocity of acoustic wave (c) is taken as 1440 m/s. Modulus of elasticity of the dam is taken as 3.15x 10^{10} N/m^2 and density of the gravity dam is assumed as 2400kg/m^3. Modulus of elasticity of the foundation is taken as 3.15x 10^{10} N/m^2 and density is assumed to be 2400kg/ m^3. At the truncated surface of the reservoir and foundation, non-reflecting boundary conditions proposed by Papazafeiropoulos et al. (2011) are applied. The hydrodynamic pressure at the face of the dam due to harmonic excitation of frequency of Tc/H_f=10 is presented in Fig. 4.87. The results of the present study are in conformity with Papazafeiropoulos et al. (2011).

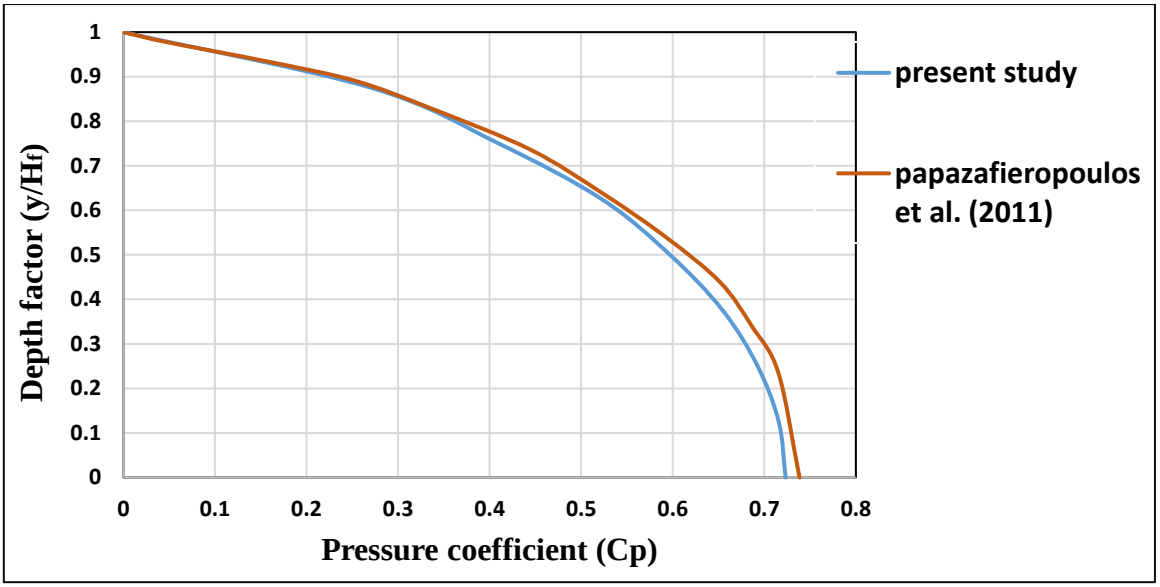

Fig. 4.87: Hydrodynamic pressure along the upstream face of the dam

4.4.2 NUMERICAL RESULTS AND DISCUSSION

In the present section of work, variations of hydrodynamic pressure and stresses of the gravity dam are observed from the dynamic analysis of dam-reservoir-foundation coupled systems considering fluid-structure and soil-structure interactions simultaneously. A typical dam-reservoir-foundation coupled system is shown in Fig. 4.88. The size of the soil foundation (length=350 m., height =100 m.) is taken as per the reference of Mandal and Maity (2017). Height of the reservoir (H_f) is considered as 103 m. Density of water (ρ_f) is considered as 1000kg/m^3 and velocity of the acoustic wave in water is assumed as 1438.7 m/s. Modulus of elasticity of the dam is taken as 3.15x 10^{10} N/m^2 and density of the structure is taken as 2415.816 kg/m^3. Poisson ratio is considered as 0.235. Modulus of elasticity of the foundation is taken as 1.75x 10^{10} N/m^2 and density is assumed as 1800kg/m^3. Poisson ratio for soil foundation is taken as 0.2. Hydrodynamic pressure and stresses of the dam and foundation are observed for various bottom slopes and reflection coefficients.

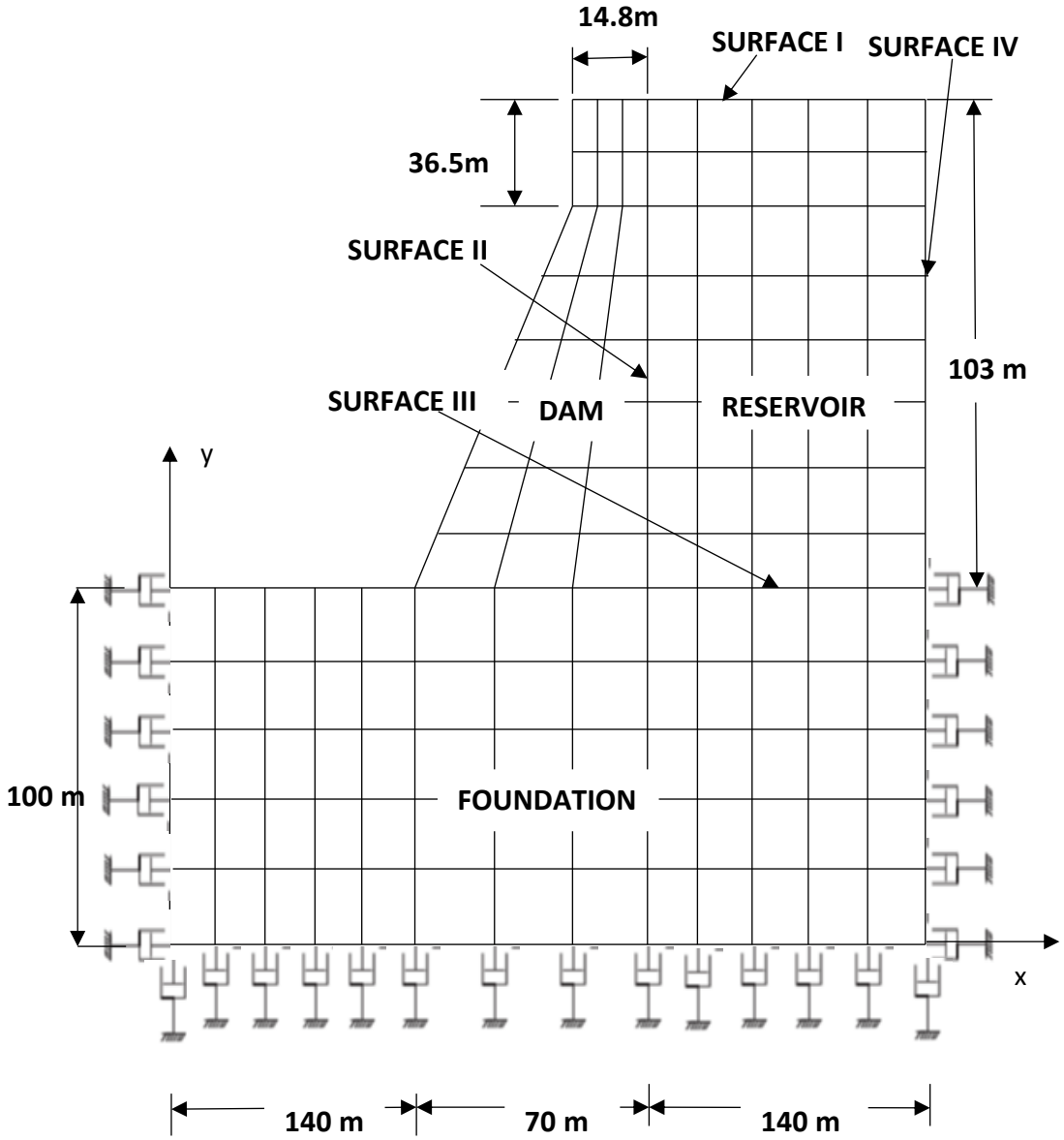

Fig. 4.88: Typical Finite element discretization of dam-reservoir-foundation coupled systems

The present section is divided into three parts. In Part I, analysis of dam-reservoir foundation-system is carried out for variation of bed slope of the reservoir applying harmonic excitation. In Part II, analysis has been done for variation of reflection coefficient of the reservoir bottom. In Part II, seismic analysis of dam-reservoir-foundation system has been carried out.

4.4.2.1 PART I: ANALYSIS OF DAM-RESERVOIR-FOUNDATION COUPLED SYSTEM FOR VARIATION OF RESERVOIR BED SLOPE

In this part of the work, changes in hydrodynamic pressure within the reservoir and stresses in the dam and foundation have been observed for different bottom slope angles (θ_b) of the reservoir. The external excitation is assumed to be harmonic of Tc/H_f equal to 100 and reflection coefficient (α) at the reservoir bottom is taken as 0.95. Fig 4.89 presents variation of coefficient (C_p) of hydrodynamic pressure at the face of the dam for positive bottom slope ($+5^0$, $+10^0$ and $+15^0$). Fig 4.90 shows the variation of coefficient (C_p) of hydrodynamic pressure at the face of the dam for negative bottom slope (-5^0, -10^0 and -15^0). Fig. 4.91 displays the time history plot of pressure coefficient (C_p) at the heel of the dam for positive angles at the reservoir base ($+5^0$, $+10^0$ and $+15^0$) and Fig. 4.92 presents the time history plot of pressure coefficient (C_p) at the heel of the dam for negative angles at the reservoir base (-5^0, -10^0 and -15^0). From these figures, it is clear that hydrodynamic pressure at the heel of the dam increases with the increase of base angle for positive slope and pressure at the heel of the dam decreases with the increase of base angle for negative slope. Fig 4.93 and Fig. 4.94 present major and minor principal stresses at the heel of the dam for positive bottom slope. Fig 4.95 and Fig. 4.96 present major and minor principal stresses at the heel of the dam for negative bottom slope of the reservoir. The maximum stress (major and minor) at the heel of the dam is increased for an increase in positive slope angle ($+5^0$, $+10^0$ and $+15^0$) and the maximum stress (major and minor) at the heel of the dam is decreased due to the increase in negative slope angle (-5^0, -10^0 and -15^0). Fig. 4.97 shows the time history plot of major principal stress and 4.98 presents the time history plot of minor principal stress of the foundation near the heel of the dam for positive slope angles ($+5^0$, $+10^0$ and $+15^0$). Fig. 4.99 shows the time history plot of major principal stress and 4.100 presents the time history plot of minor principal stress of the foundation near the heel of the dam for negative slope angles (-5^0, -10^0 and -15^0). From these figures, it is seen that the maximum stress both major and minor principal stress of the foundation near the heel of the dam is decreased with the increase of positive slope angle. This has also been observed that the maximum stress of the foundation near the heel of the dam is increased with the increase of negative slope angle.

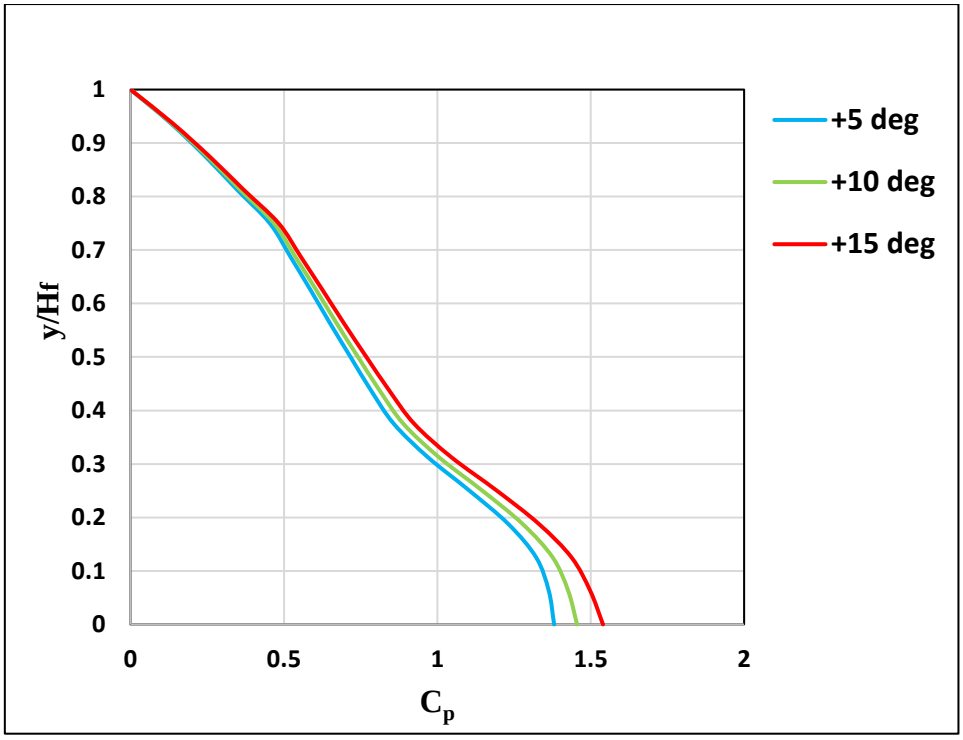

Fig. 4.89: Distribution of pressure coefficient (C_p) at face of the dam with different bottom slopes θ_b (positive) due to harmonic loading

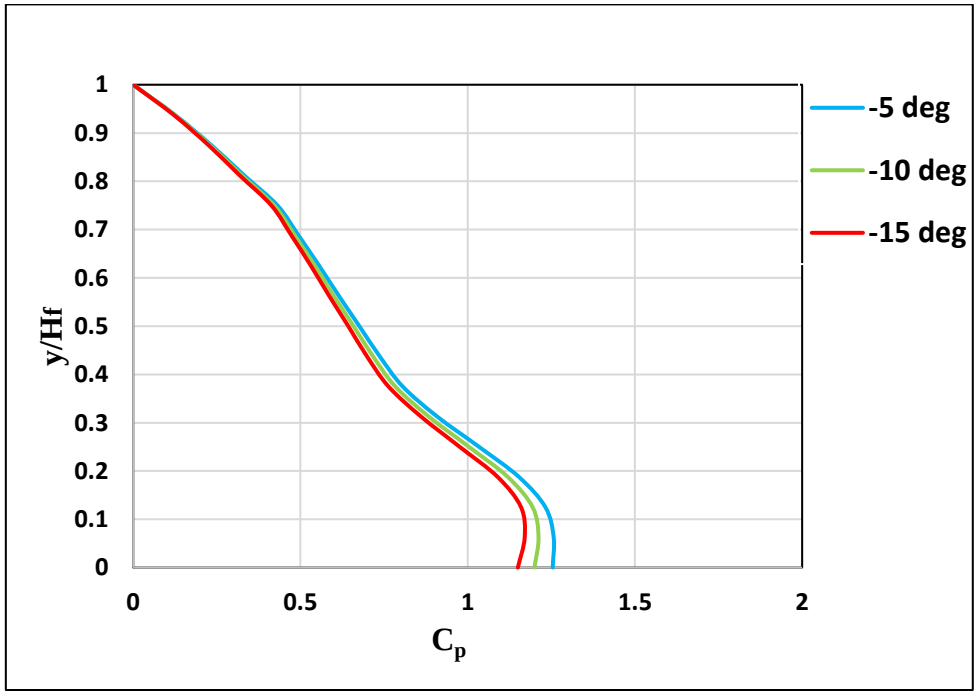

Fig. 4.90: Distribution of pressure coefficient (C_p) at face of the dam with different bottom slopes θ_b (negative) due to harmonic loading

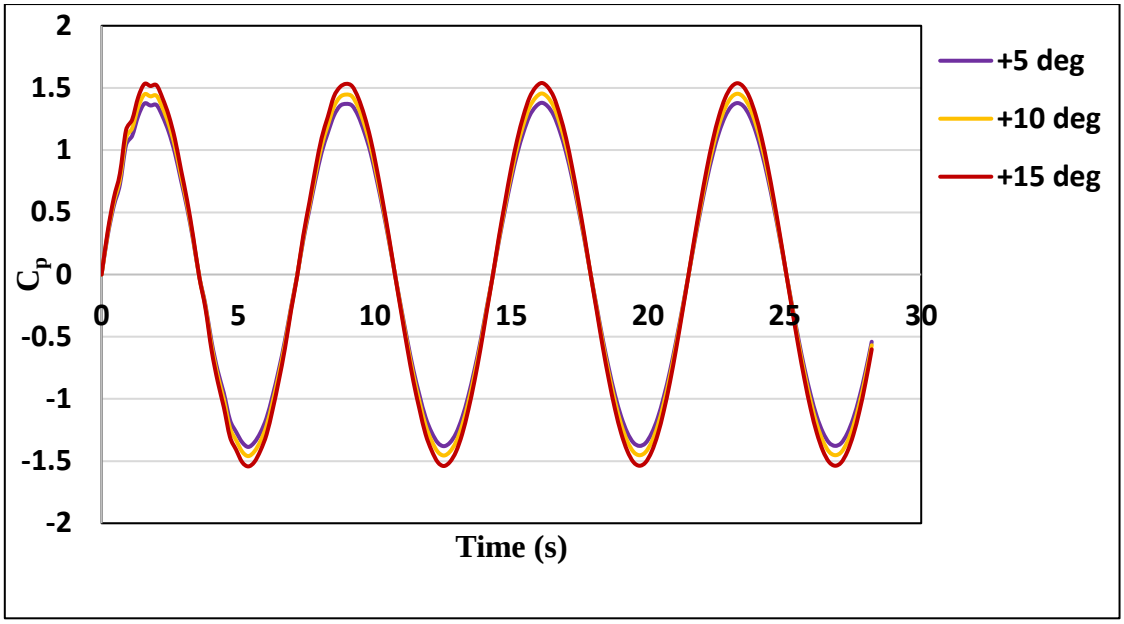

Fig. 4.91: Time history of pressure coefficient (C_p) at the heel of the dam for positive bottom slopes

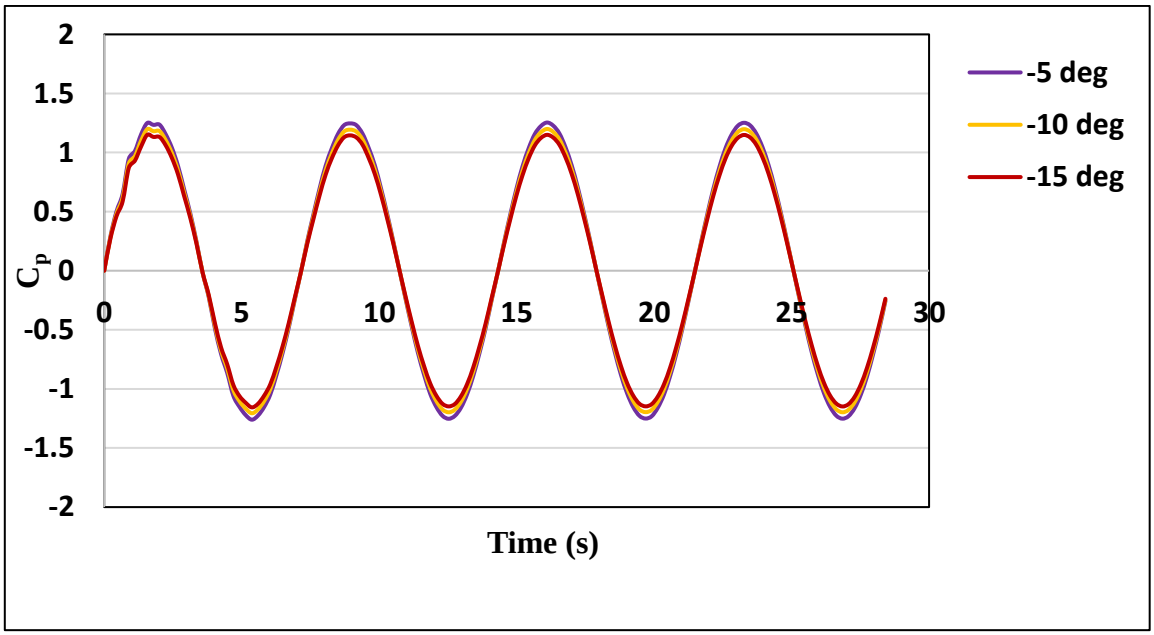

Fig. 4.92: Time history of pressure coefficient (C_p) at the heel of the dam for negative bottom slopes

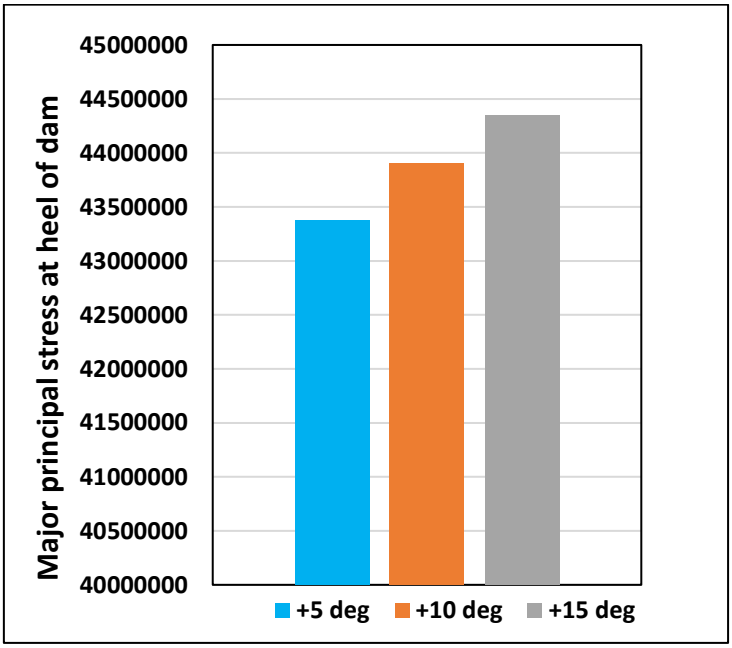

Fig. 4.93: Major principal stress at the heel of the dam for positive bottom slopes of reservoir

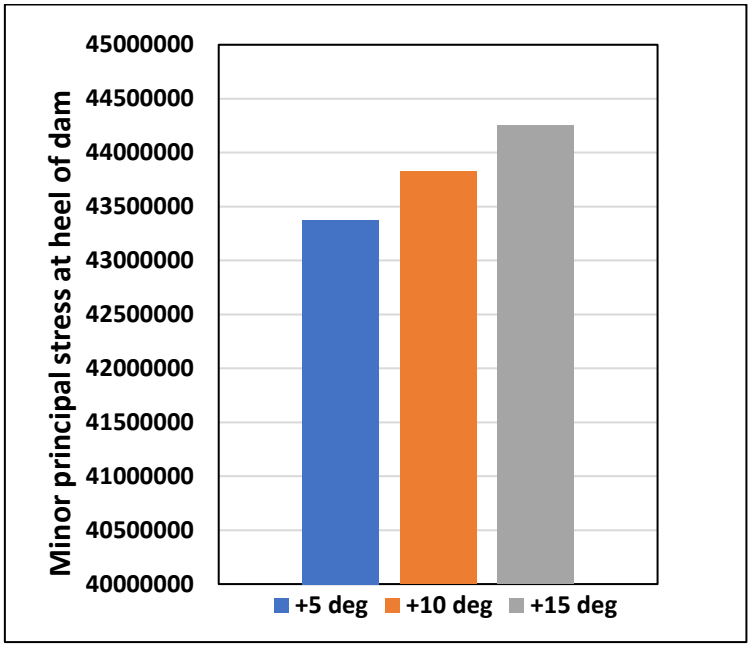

Fig. 4.94: Minor principal stress at the heel of the dam for positive bottom slopes of reservoir

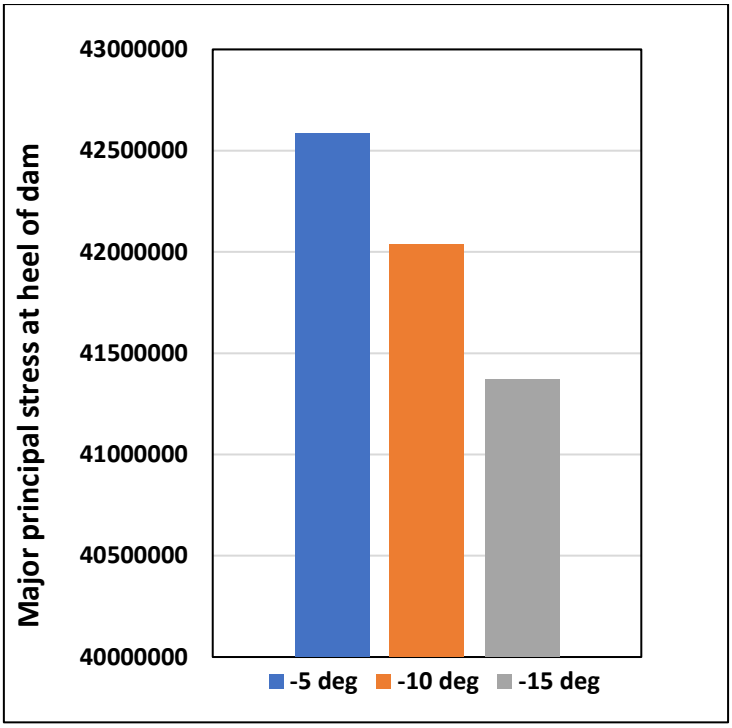

Fig. 4.95: Major principal stress at the heel of the dam for negative bottom slopes of reservoir

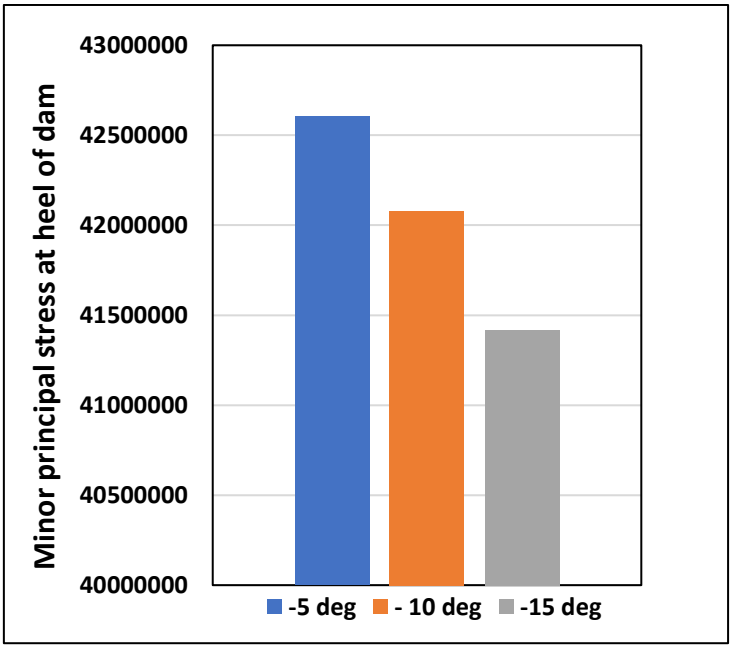

Fig. 4.96: Minor principal stress at the heel of the dam for negative bottom slopes of reservoir

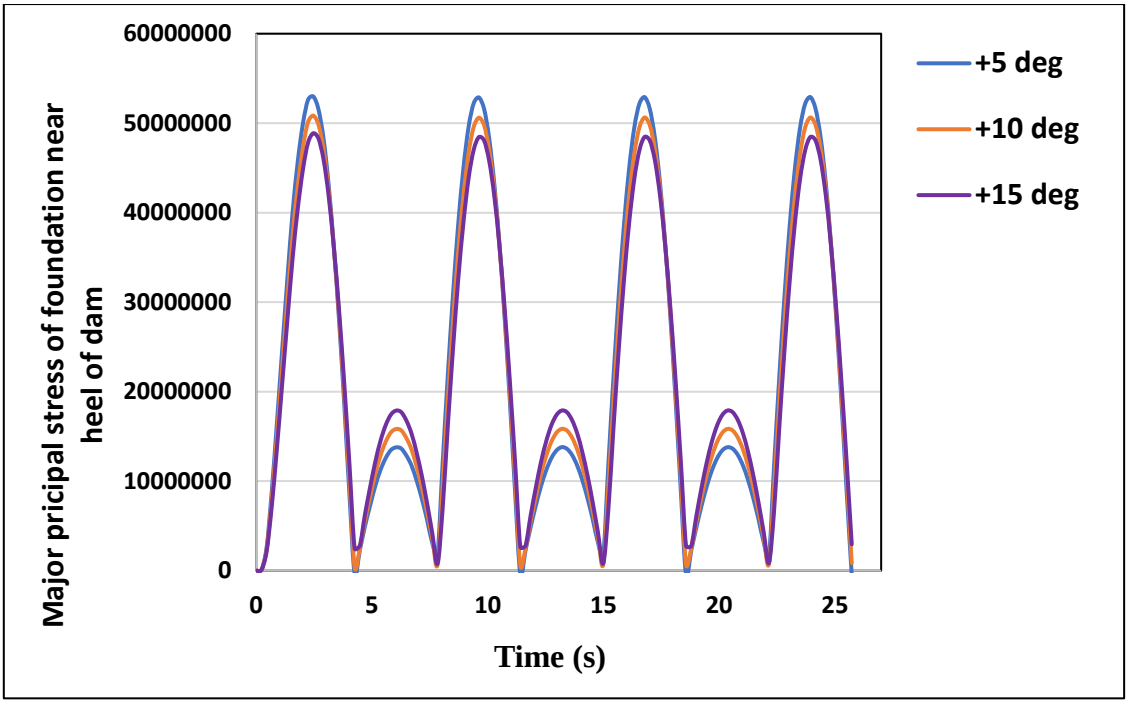

Fig. 4.97: Time history plot of major principal stress of foundation near heel of the dam for positive bottom slopes

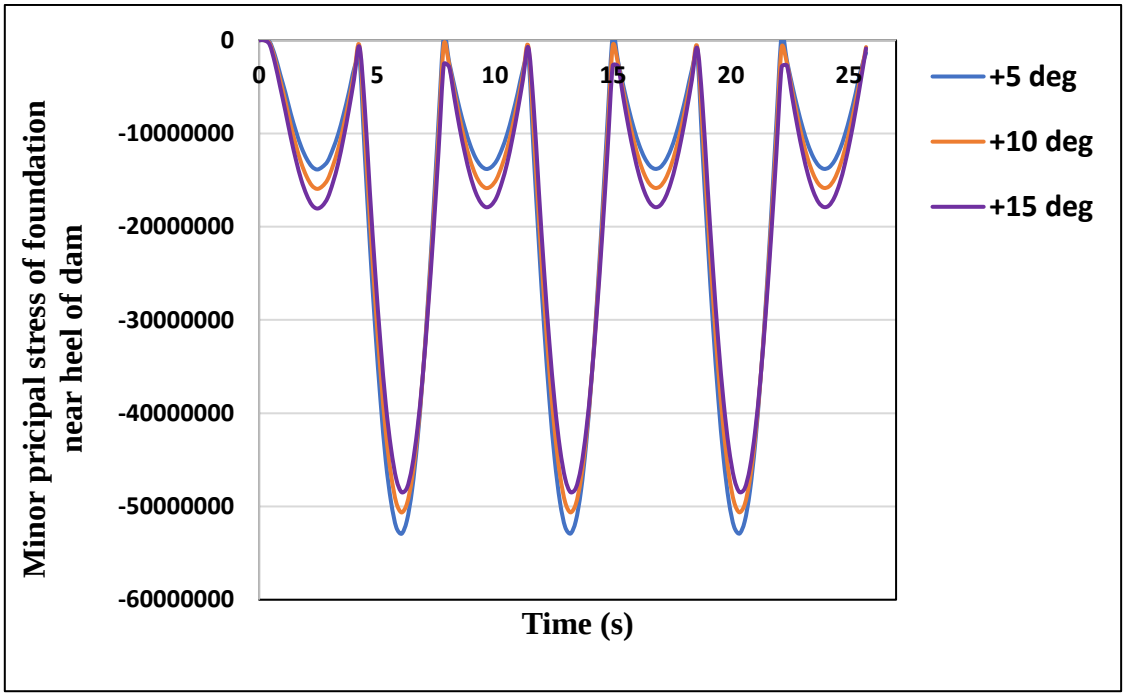

Fig. 4.98: Time history plot of minor principal stress of foundation near heel of the dam for positive bottom slopes

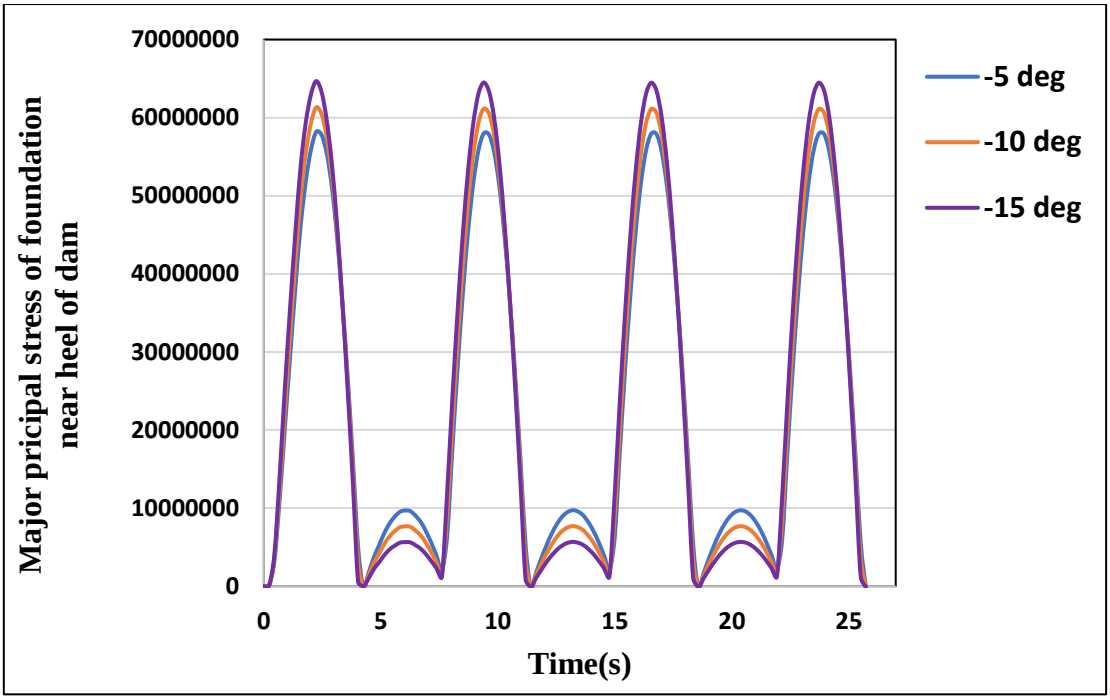

Fig. 4.99: Time history plot of major principal stress of foundation near heel of the dam for negative bottom slopes

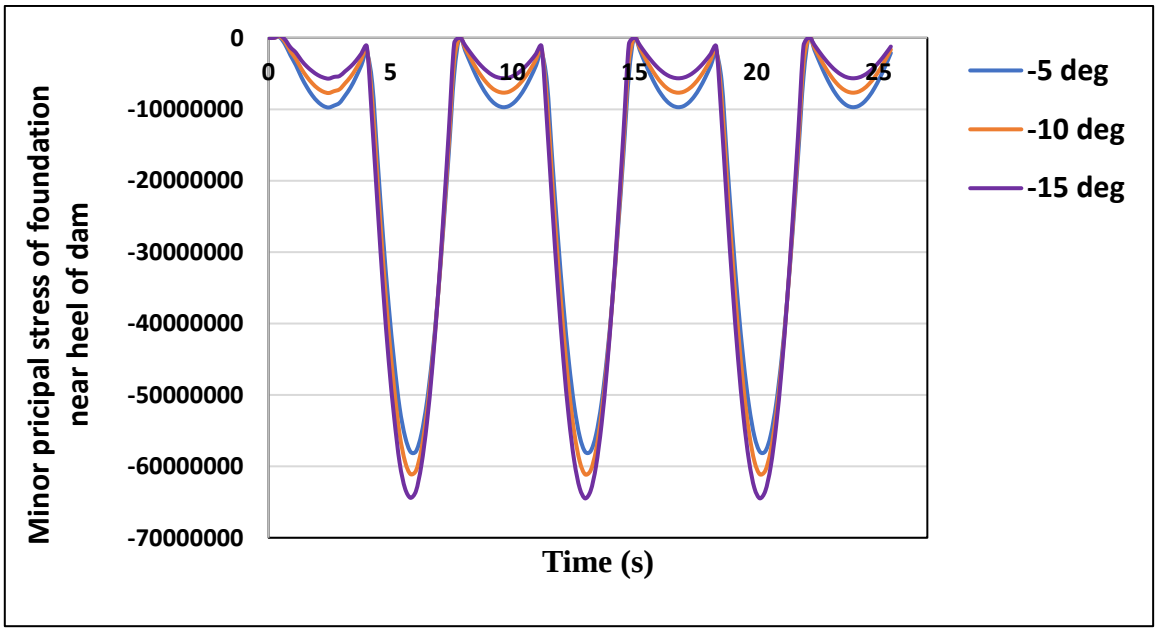

Fig. 4.100: Time history plot of minor principal stress of foundation near heel of the dam for negative bottom slopes

4.4.2.2 PART II: ANALYSIS OF DAM-RESERVOIR-FOUNDATION COUPLED SYSTEM FOR VARIATION OF REFLECTION COEFFICIENT OF RESERVOIR BED

In this part of the work, hydrodynamic pressure at the heel of the gravity dam has been observed for different values of reflection coefficient (α) with inclined reservoir bottom surface considering the dam-reservoir and dam-foundation interaction simultaneously. The geometry and properties of reservoir, dam and foundation are considered the same as in subsection 4.4.2. In this part of work Tc/H_f is taken as 100. Table 4.7 presents the pressure coefficient (C_p) at the heel of the dam for different reflection coefficients with different slopes (θ_b) of reservoir bottom. It has been seen that pressure is increased with the increase of reflection coefficient for any value of bottom slope.

Table 4.7: Pressure coefficient (C_p) at the heel of the dam for different reflection coefficient with inclined base

Slope angle (θ_b)	Reflection coefficient (α)	C_p
$+5^0$	0.0	1.37868
	0.5	1.38052
	1.0	1.38075
$+10^0$	0.0	1.45312
	0.5	1.45525
	1.0	1.45552
$+15^0$	0.0	1.53721
	0.5	1.53969
	1.0	1.54000
-5^0	0.0	1.25264
	0.5	1.25392
	1.0	1.25408
-10^0	0.0	1.19853
	0.5	1.19952
	1.0	1.19965
-15^0	0.0	1.14899
	0.5	1.14986
	1.0	1.14996

4.4.2.3 PART III: SEISMIC ANALYSIS OF DAM-RESERVOIR-FOUNDATION COUPLED SYSTEMS

In this part of work, hydrodynamic pressure at the face of the dam has been observed for earthquake excitation with change in slope angle (negative and positive) of the reservoir bottom considering dam-reservoir-foundation interaction. Stresses of the dam and foundation are observed for seismic excitation. Here, north–south component of El-Centro earthquake excitation (Fig. 4.70) is considered to be external excitation. Height of the reservoir (H_f) is considered as 103 m. and reflection coefficient (α) of the reservoir bottom is taken as 0.95. The geometry of the dam, reservoir and foundation and their properties are as taken as in subsection 4.4.2. Fig. 4.101 presents distribution of hydrodynamic pressure coefficient at the face of the dam for positive bottom slope ($+5^0$, $+10^0$ and $+15^0$). Fig. 4.102 presents distribution of hydrodynamic pressure coefficient at the face of the dam for negative bottom slope (-5^0, -10^0 and -15^0). Fig. 4.103 shows the time history plot of pressure coefficient at the heel of the dam for positive bottom slope. Fig. 4.104 shows the time history plot of pressure coefficient at the heel of the dam for negative bottom slope. From these figures, it is clear that pressure at the heel of the dam increases due to the increase in positive bottom slope and pressure at the heel of the dam decreases due to the increase in negative bottom slope. Fig. 4.105 to Fig. 4.110 show the velocity profile of the reservoir for different values of bed slope of the reservoir. Hydro dynamic pressure changes due to the change in bed slope. For this reason, difference in velocity profile of the reservoir has been seen for different values of bed slope of the reservoir. Fig 4.111 and Fig. 4.112 present major and minor principal stresses at the heel of the dam for positive bottom slopes. Fig 4.113 and Fig. 4.114 present major and minor principal stresses at the heel of the dam for negative bottom slopes. This has been clear that the maximum stress (major and minor) at the heel of the dam increased for increase in positive slope angle ($+5^0$, $+10^0$ and $+15^0$) at base of the reservoir and the maximum stress (major and minor) at the heel of the dam decreased for increase in negative slope angle (-5^0, -10^0 and -15^0) at base of the reservoir. Fig 4.115 and Fig. 4.116 present major and minor principal stresses at the notch of the dam for positive bottom slope of the reservoir bottom. Fig 4.117 and Fig. 4.118 present major and minor principal stresses at the notch of the dam for negative bottom slopes of the reservoir. This has been clear that the maximum stress (major and minor) at the notch of dam increased for increase in positive slope angle ($+5^0$, $+10^0$ and $+15^0$) at base of the reservoir and the maximum stress (major and minor) at the notch of the dam decreased for increase in negative slope angle (-5^0, -10^0 and -15^0) at base of the reservoir. It has been seen that stresses

at the heel of the dam are higher than the notch of the dam. Fig. 4.119 shows the time history plot major principal stress and 4.120 presents the time history plot of minor principal stress of the foundation near the heel of the dam for positive slope angles ($+5^0$, $+10^0$ and $+15^0$) due to earthquake excitation. Fig. 4.121 shows the time history plot major principal stress and 4.122 presents the time history plot of minor principal stress of the foundation near the heel of the dam for negative slope angles (-5^0, -10^0 and -15^0). From these figures, it has been seen that the maximum stress (major and minor) of the foundation near the heel of the dam decreased with increase in slope angle at the reservoir base for positive slope due to earthquake excitation. This has been also seen that the maximum stress (major and minor) of the foundation near heel of the dam increased with increase in slope of the reservoir base for negative slope due to earthquake excitation. Fig. 4.123 to Fig. 4.128 show the contour of pressure and stresses for different bed slope of the reservoir. From these figures, it has been seen that maximum hydrodynamic pressure in reservoir occurs at the heel of the dam and maximum stress occurs at the heel of the dam due to earthquake excitation.

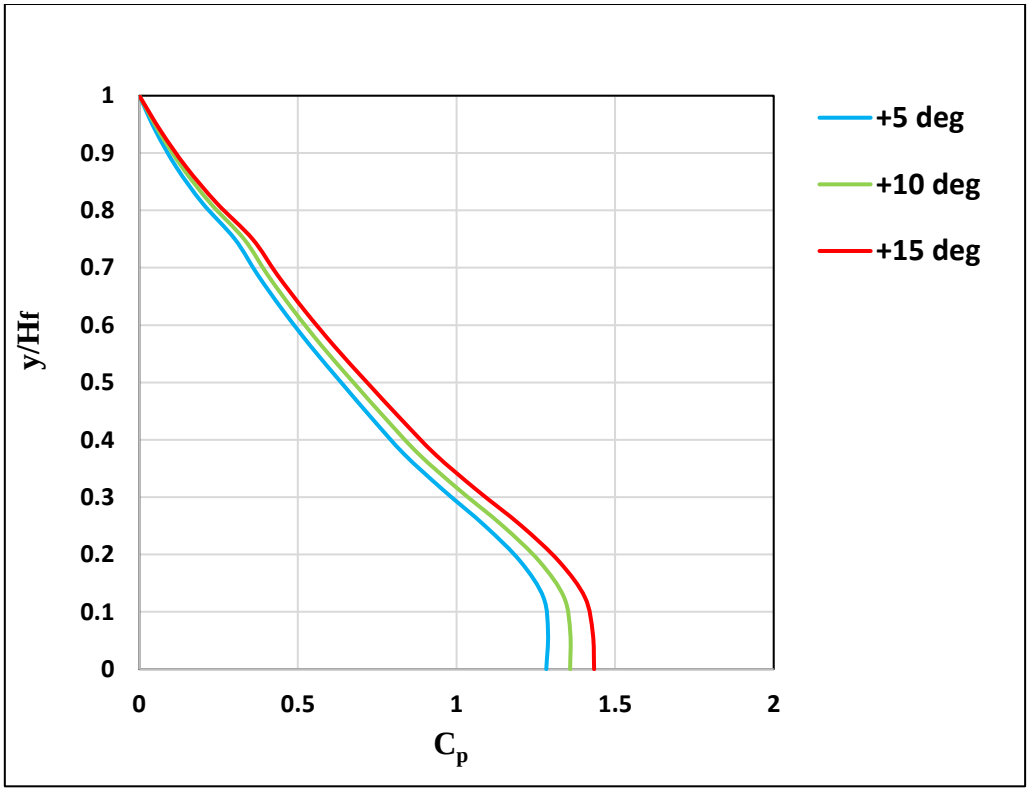

Fig. 4.101: Distribution of pressure coefficient (C_p) at face of the dam with different bottom slopes θ_b (positive) due to North–South component of El-Centro earthquake

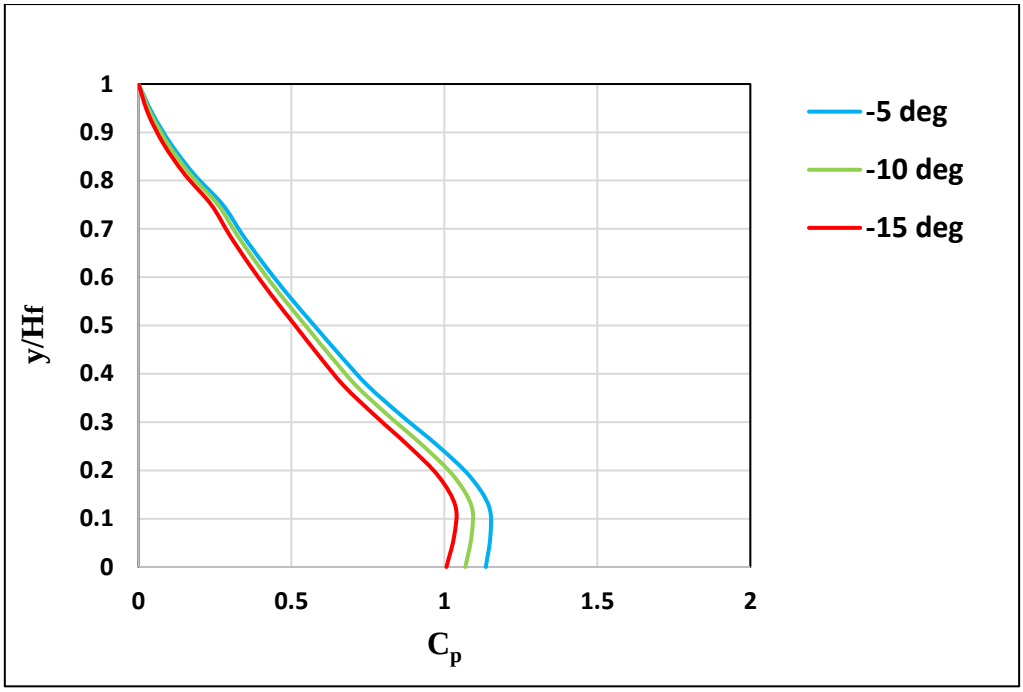

Fig. 4.102: Distribution of pressure coefficient (C_p) at face of the dam with different bottom slopes θ_b (negative) due to North–South component of El-Centro earthquake

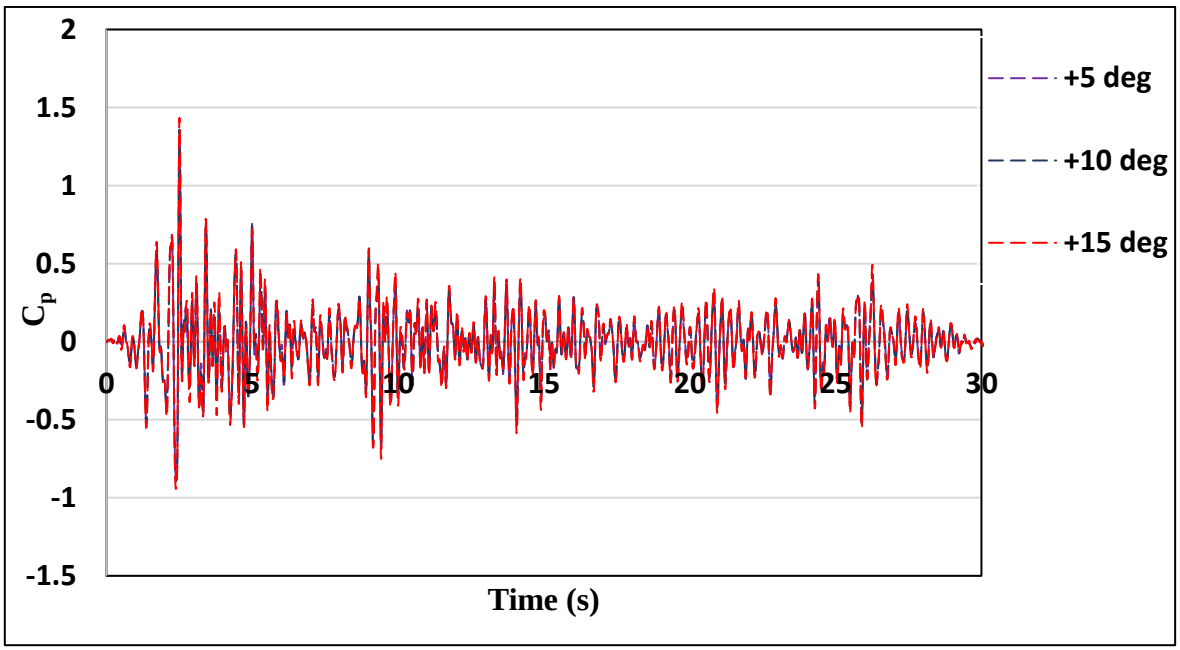

Fig. 4.103: Time history of pressure coefficient (C_p) at heel of the dam for positive bottom slopes for North–South component of El-Centro earthquake

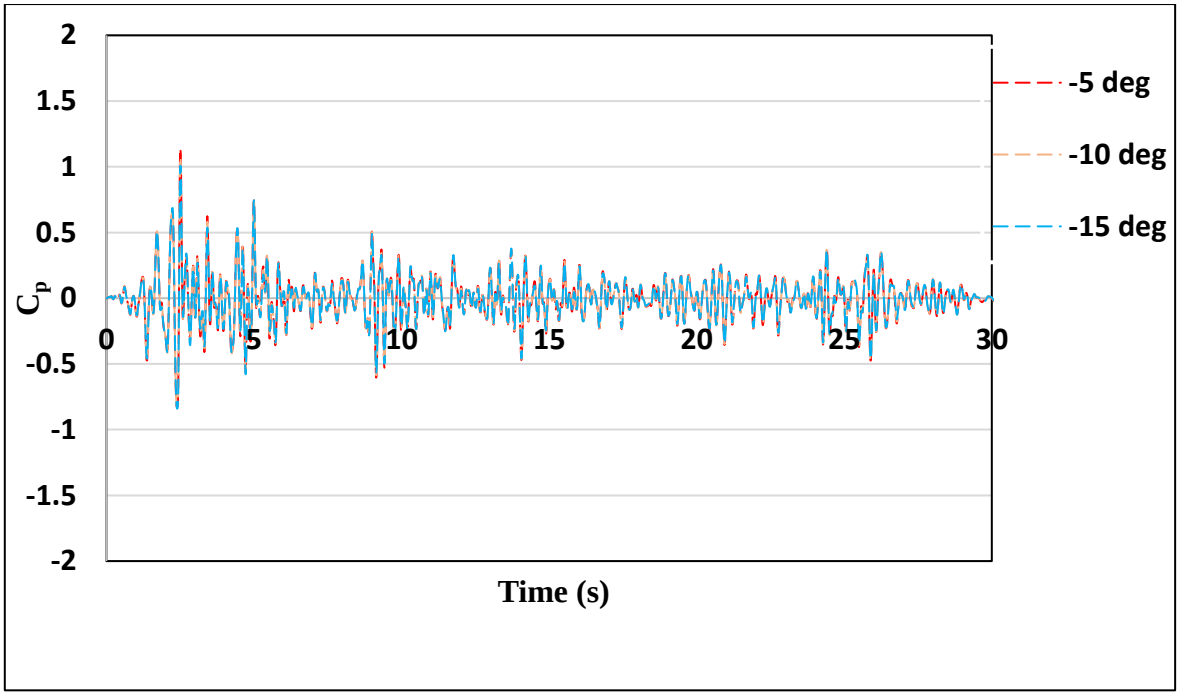

Fig. 4.104: Time history of pressure coefficient (C_p) at heel of the dam for negative bottom slopes for North–South component of El-Centro earthquake

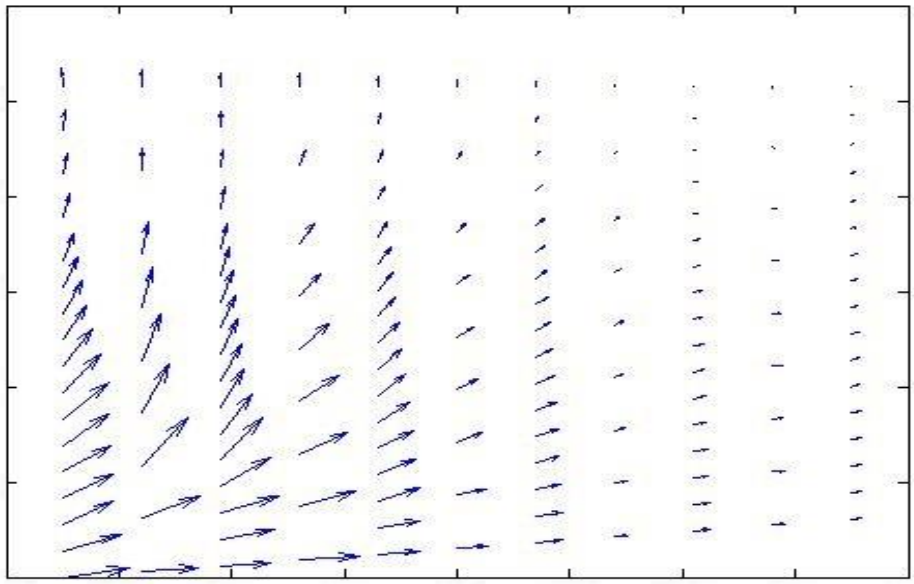

Fig. 4.105: Velocity profile of reservoir at 2.52 sec. for θ_b = $+5^0$ for North–South component of El-Centro earthquake

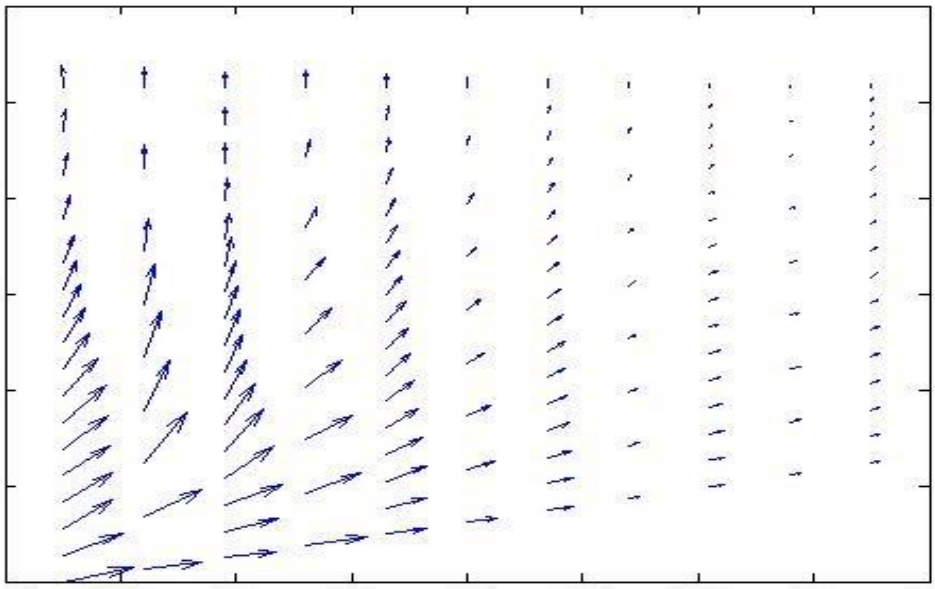

Fig. 4.106: Velocity profile of reservoir at 2.52 sec. for $\theta_b = +10^0$ for North–South component of El-Centro earthquake

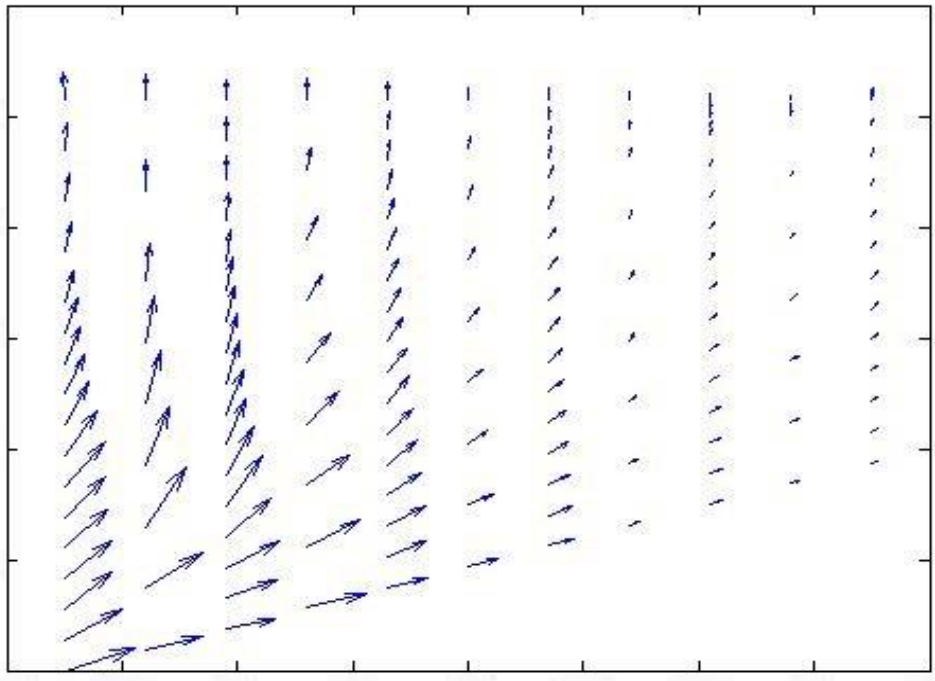

Fig. 4.107: Velocity profile of reservoir at 2.52 sec. for $\theta_b = +15^0$ for North–South component of El-Centro earthquake

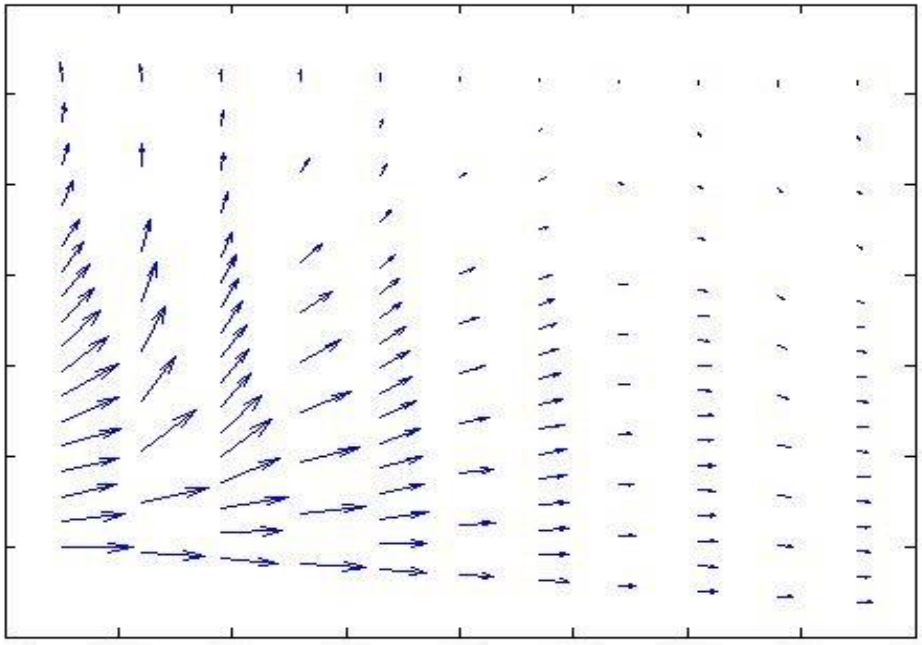

Fig. 4.108: Velocity profile of reservoir at 2.52 sec. for θ_b = -5^0 for North–South component of El-Centro earthquake

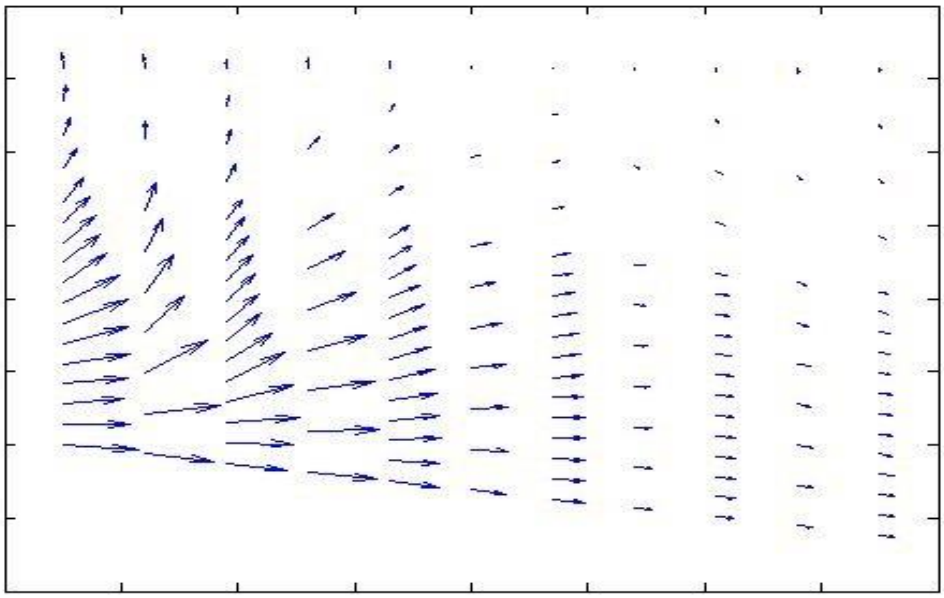

Fig. 4.109: Velocity profile of reservoir at 2.52 sec. for θ_b = -10^0 for North–South component of El-Centro earthquake

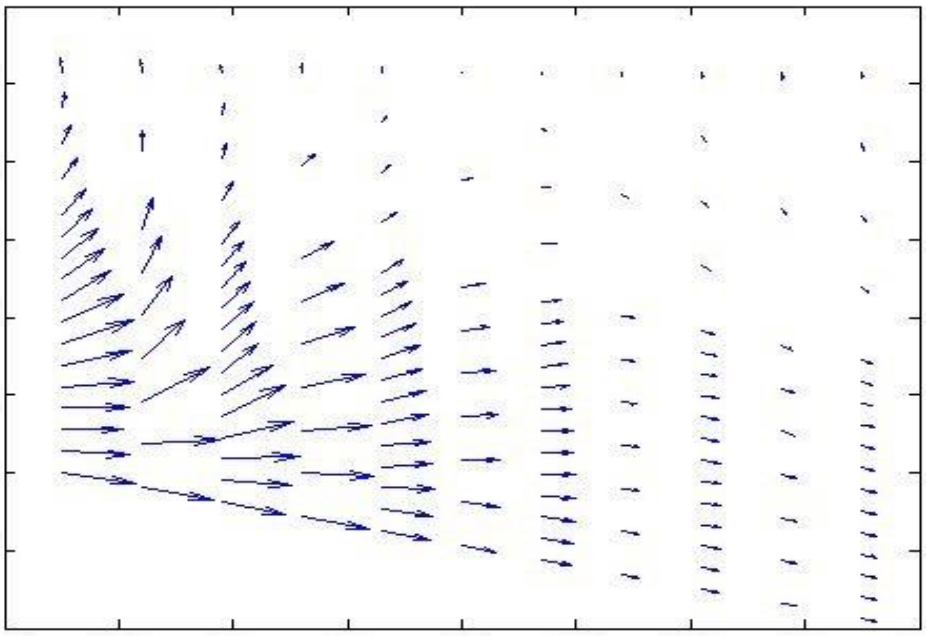

Fig. 4.110: Velocity profile of reservoir at 2.52 sec. for θ_b = -15^0 for North–South component of El-Centro earthquake

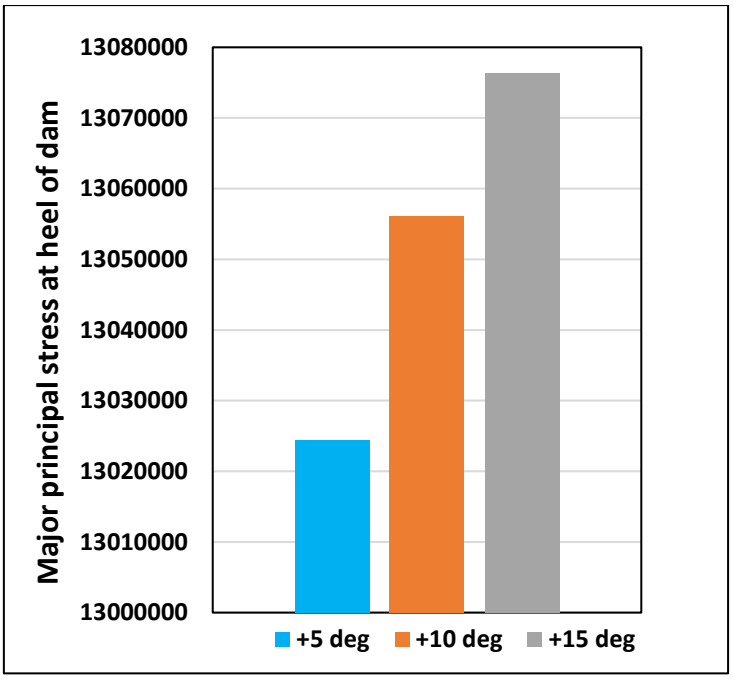

Fig. 4.111: Major principal stress at heel of the dam for positive bottom slopes of reservoir for North–South component of El-Centro earthquake

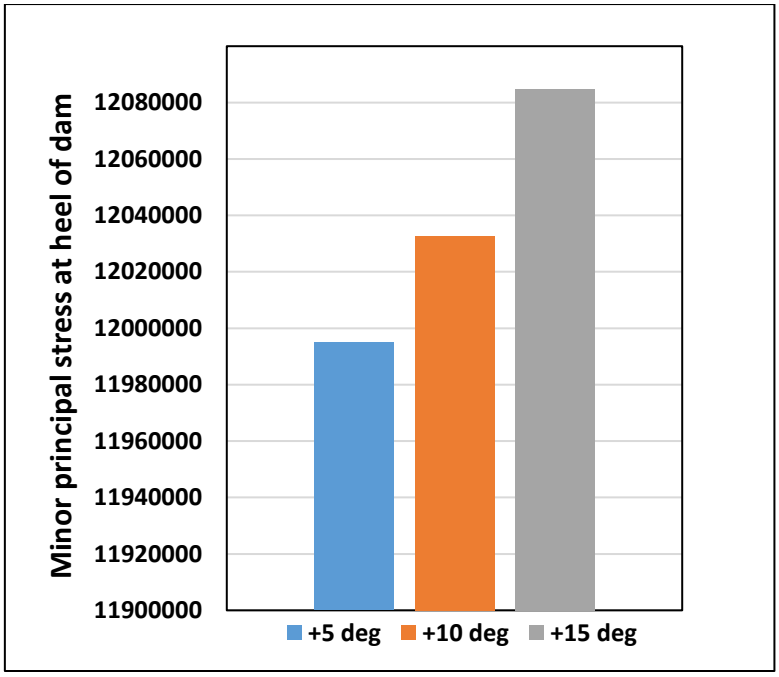

Fig. 4.112: Minor principal stress at heel of the dam for positive bottom slopes of reservoir for North–South component of El-Centro earthquake

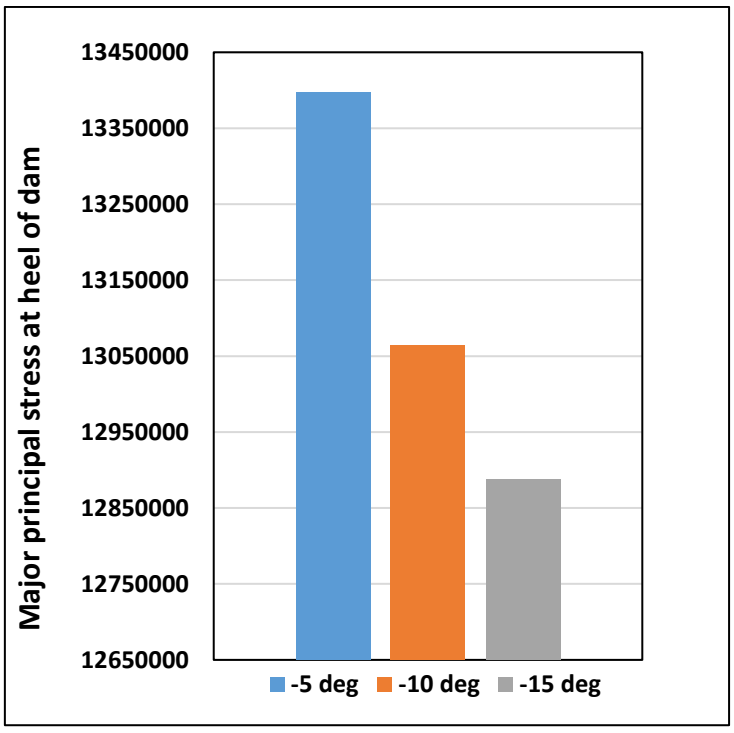

Fig. 4.113: Major principal stress at heel of the dam for negative bottom slopes of reservoir for North–South component of El-Centro earthquake

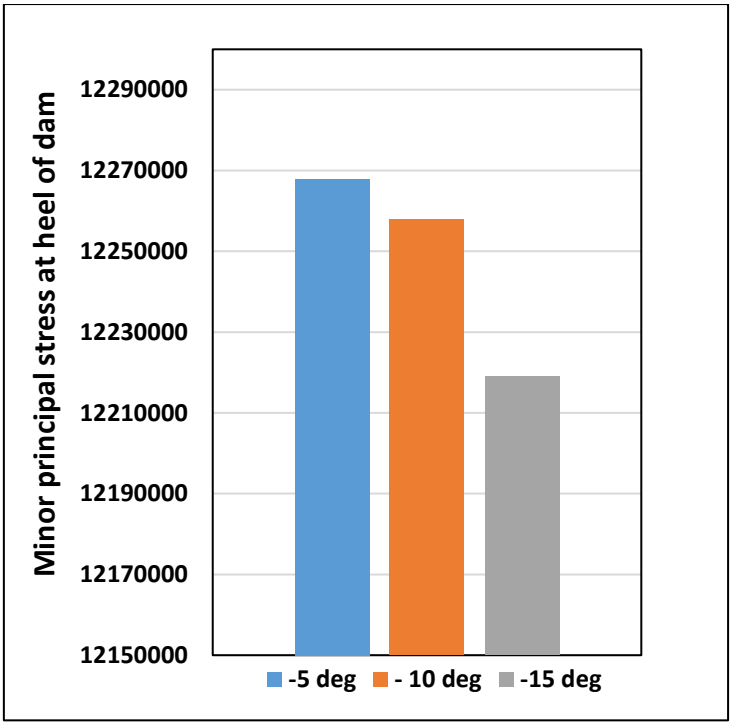

Fig. 4.114: Minor principal stress at heel of the dam for negative bottom slopes of reservoir for North–South component of El-Centro earthquake

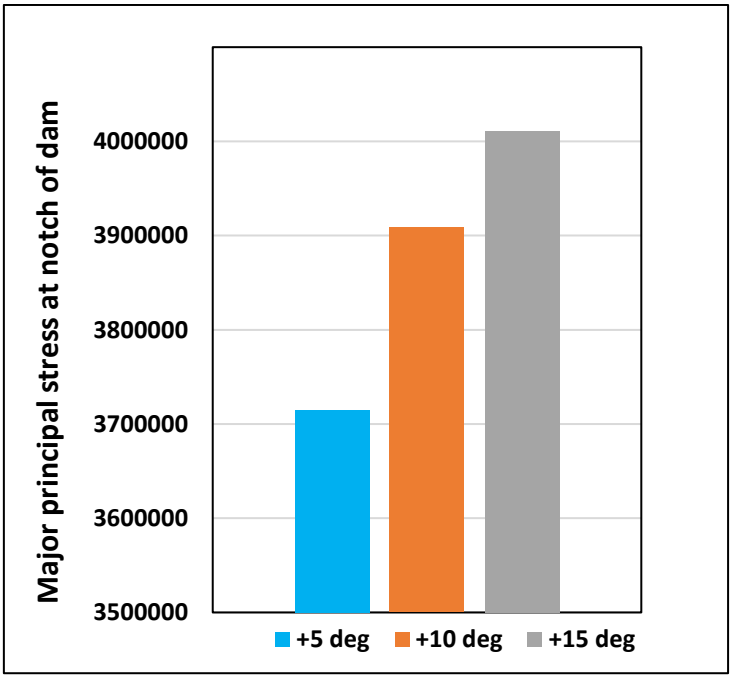

Fig. 4.115: Major principal stress at notch of the dam for positive bottom slopes of reservoir for North–South component of El-Centro earthquake

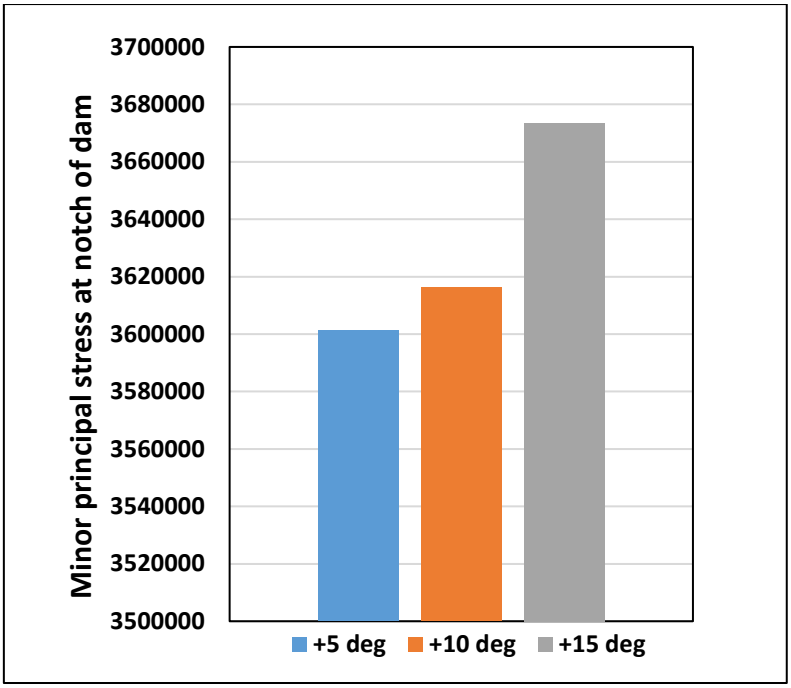

Fig. 4.116: Minor principal stress at notch of the dam for positive bottom slopes of reservoir for North–South component of El-Centro earthquake

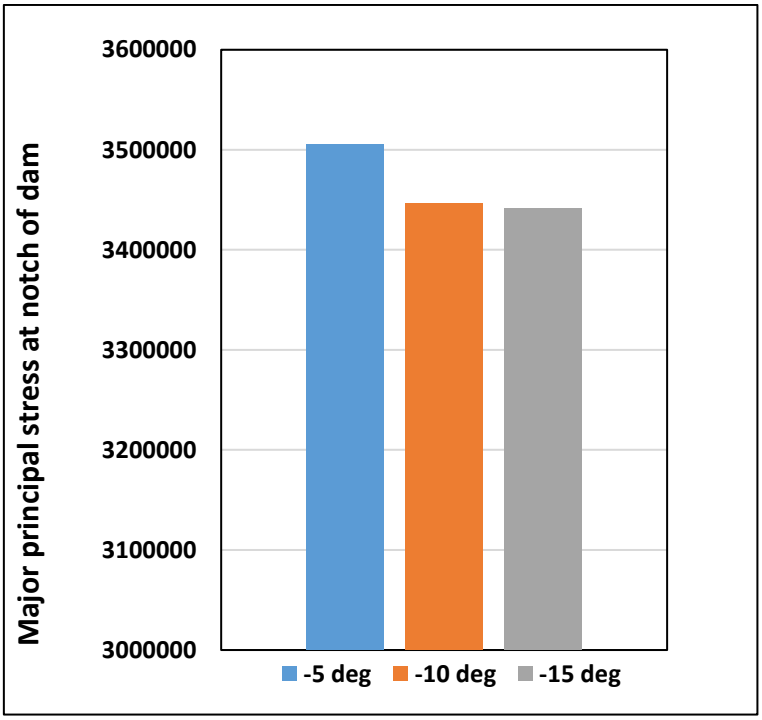

Fig. 4.117: Major principal stress at notch of the dam for negative bottom slopes of reservoir for North–South component of El-Centro earthquake

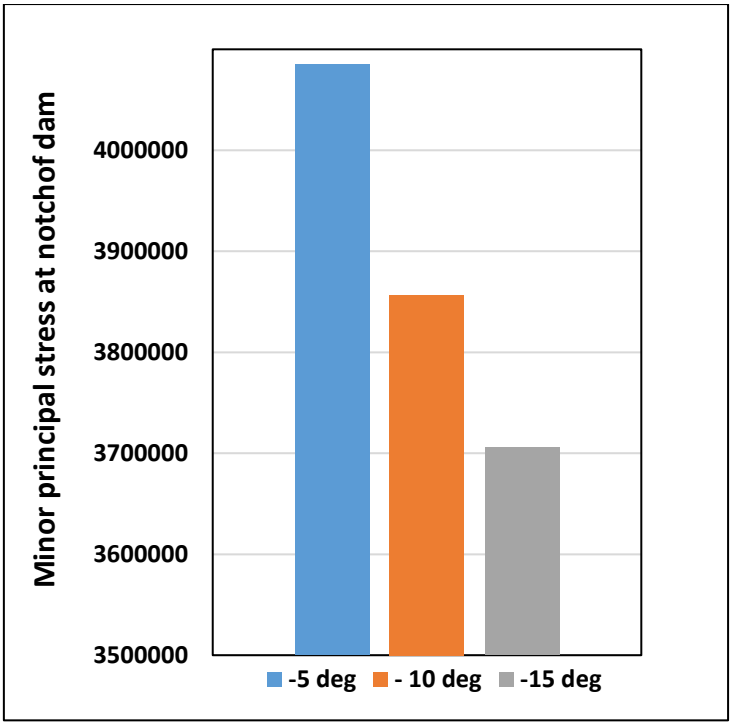

Fig. 4.118: Minor principal stress at notch of the dam for negative bottom slopes of reservoir for North–South component of El-Centro earthquake

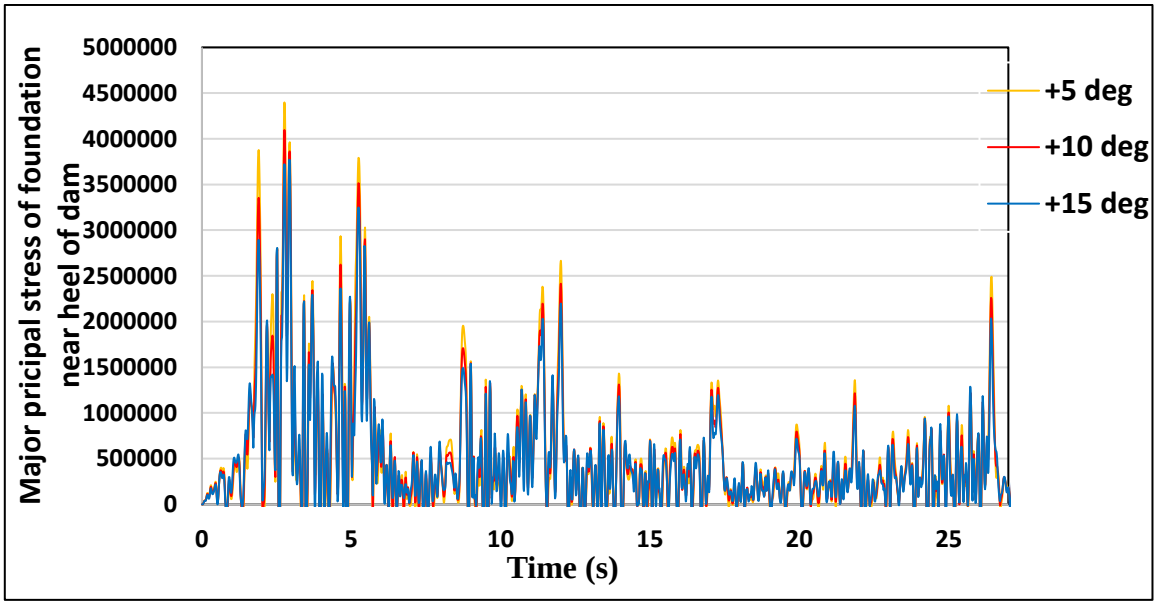

Fig. 4.119: Time history plot of major principal stress of foundation near heel of the dam for positive bottom slopes due to North–South component of El-Centro earthquake

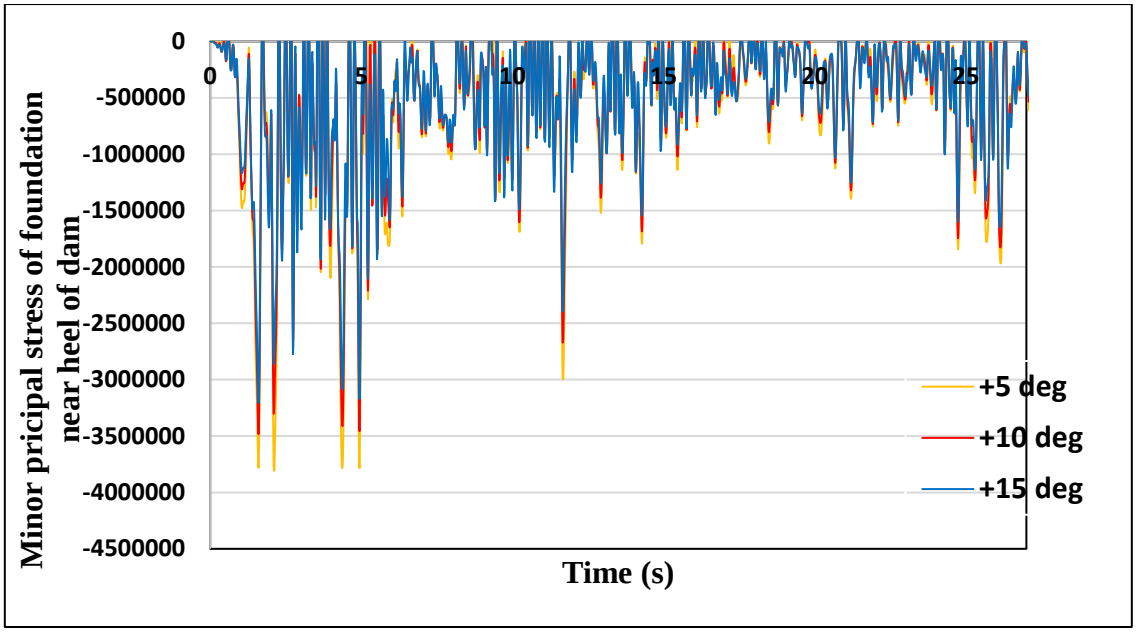

Fig. 4.120: Time history plot of minor principal stress of foundation near heel of the dam for positive bottom slopes due to North–South component of El-Centro earthquake

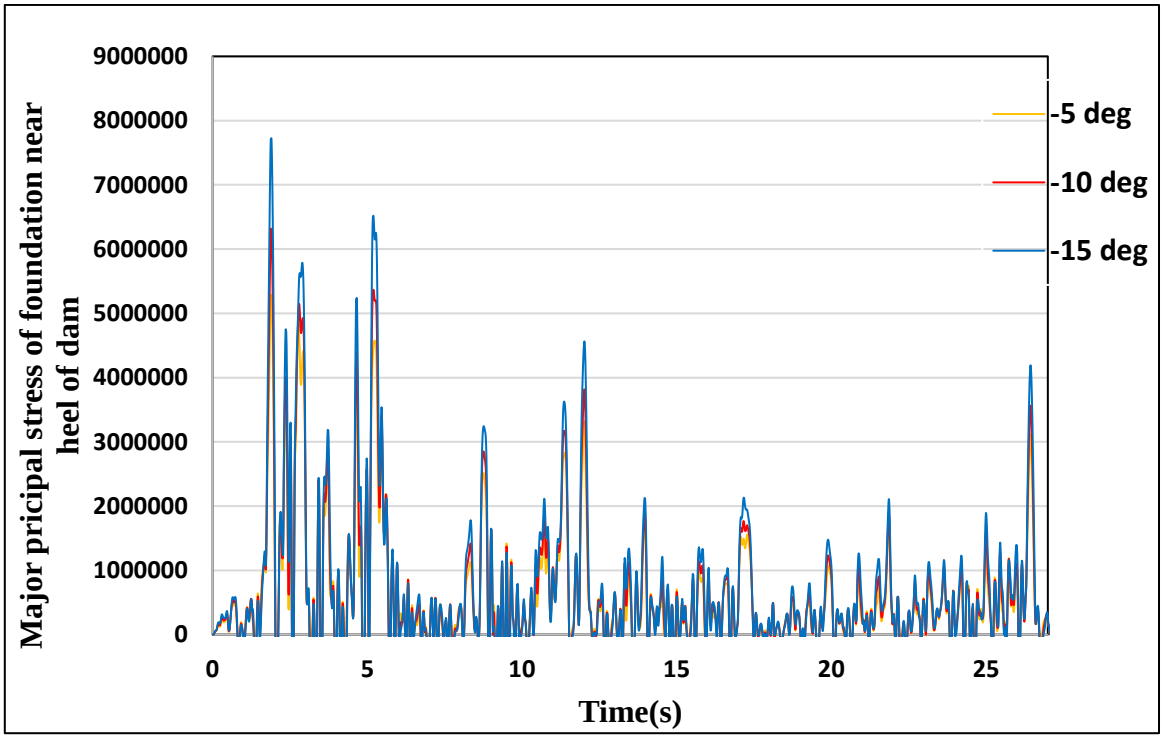

Fig. 4.121: Time history plot of major principal stress of foundation near heel of the dam for negative bottom slopes due to North–South component of El-Centro earthquake

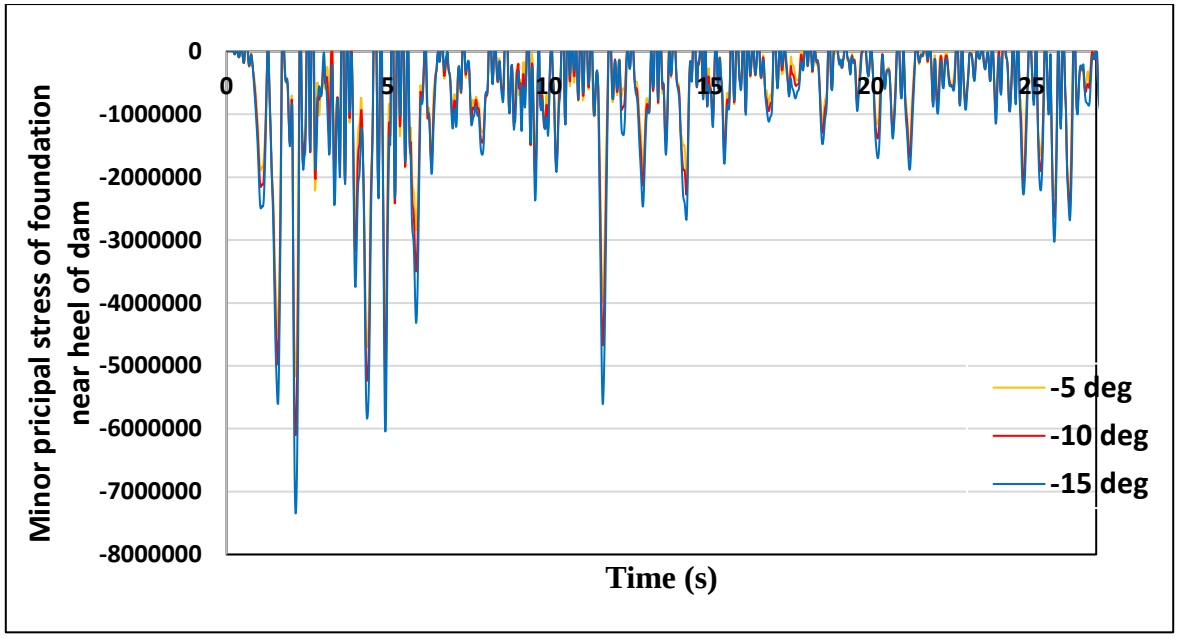

Fig. 4.122: Time history plot of minor principal stress of foundation near heel of the dam for negative bottom slopes due to North–South component of El-Centro earthquake

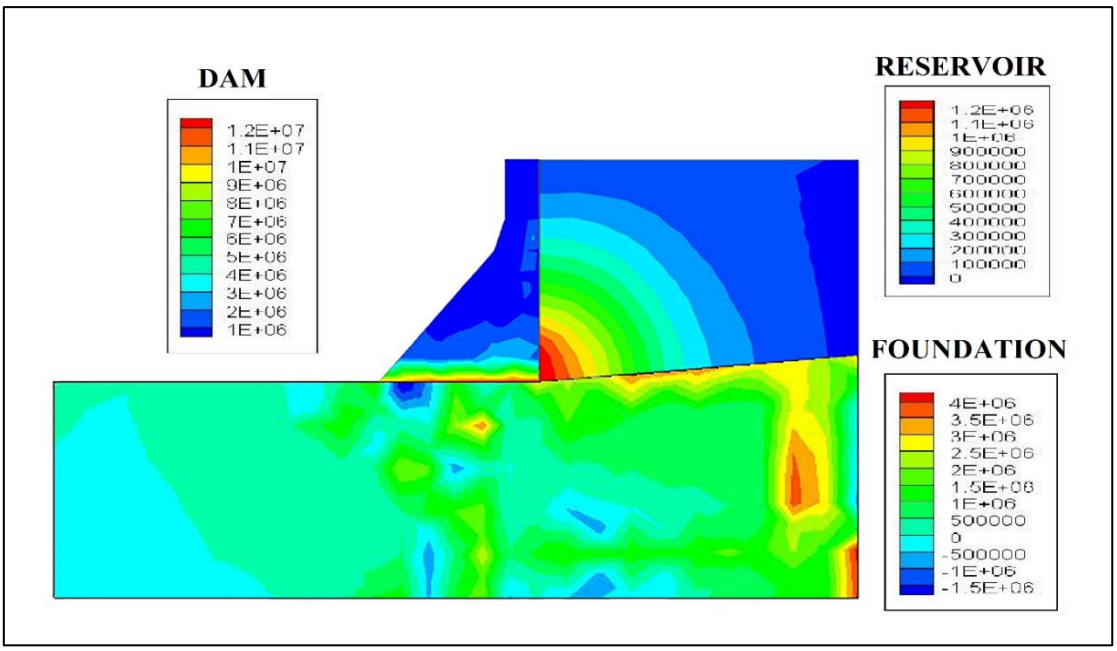

Fig. 4.123: Contour of pressure and stresses for bed slope $+5^0$ at 2.52 sec. due to North–South component of El-Centro earthquake

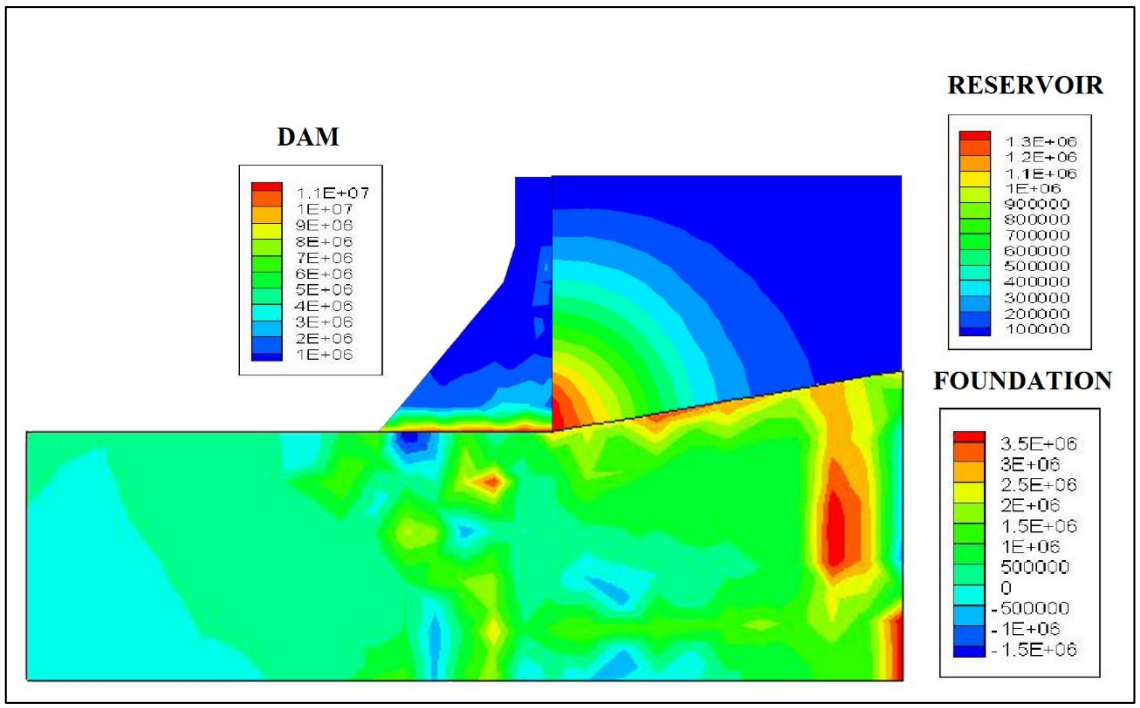

Fig. 4.124: Contour of pressure and stresses for bed slope $+10^0$ at 2.52 sec. due to North–South component of El-Centro earthquake

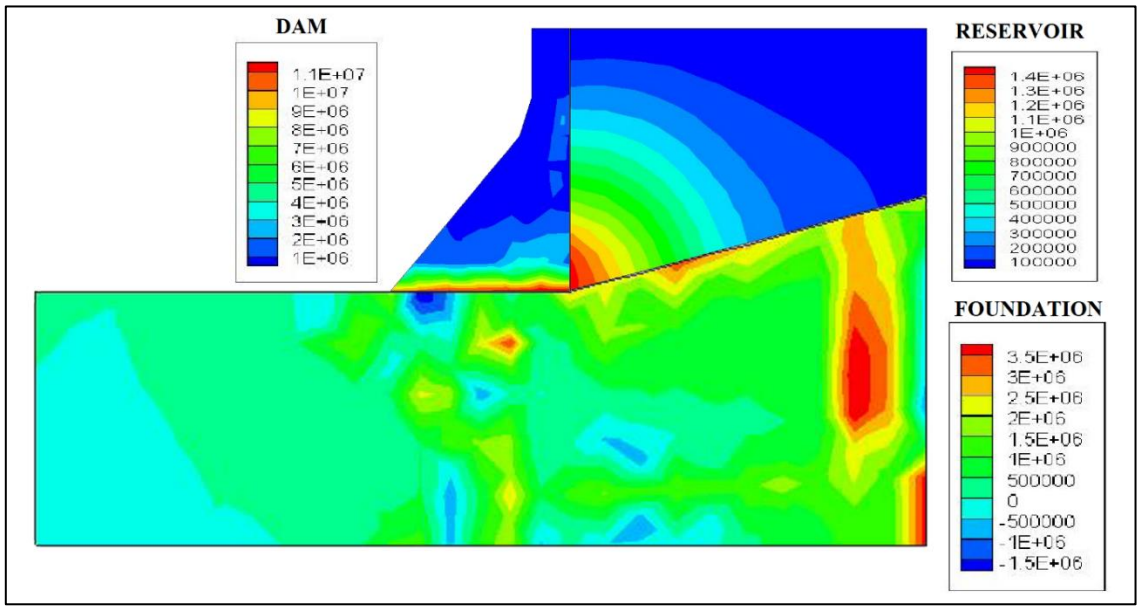

Fig. 4.125: Contour of pressure and stresses for bed slope $+15^0$ at 2.52 sec. due to North–South component of El-Centro earthquake

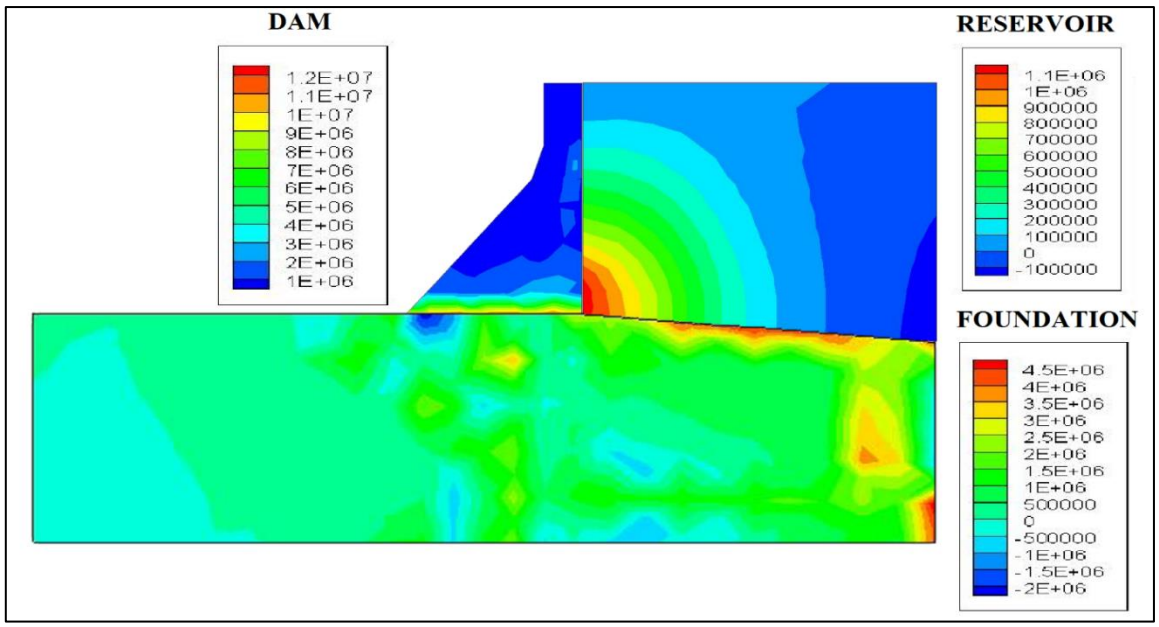

Fig. 4.126: Contour of pressure and stresses for bed slope -5^0 at 2.52 sec. due to North–South component of El-Centro earthquake

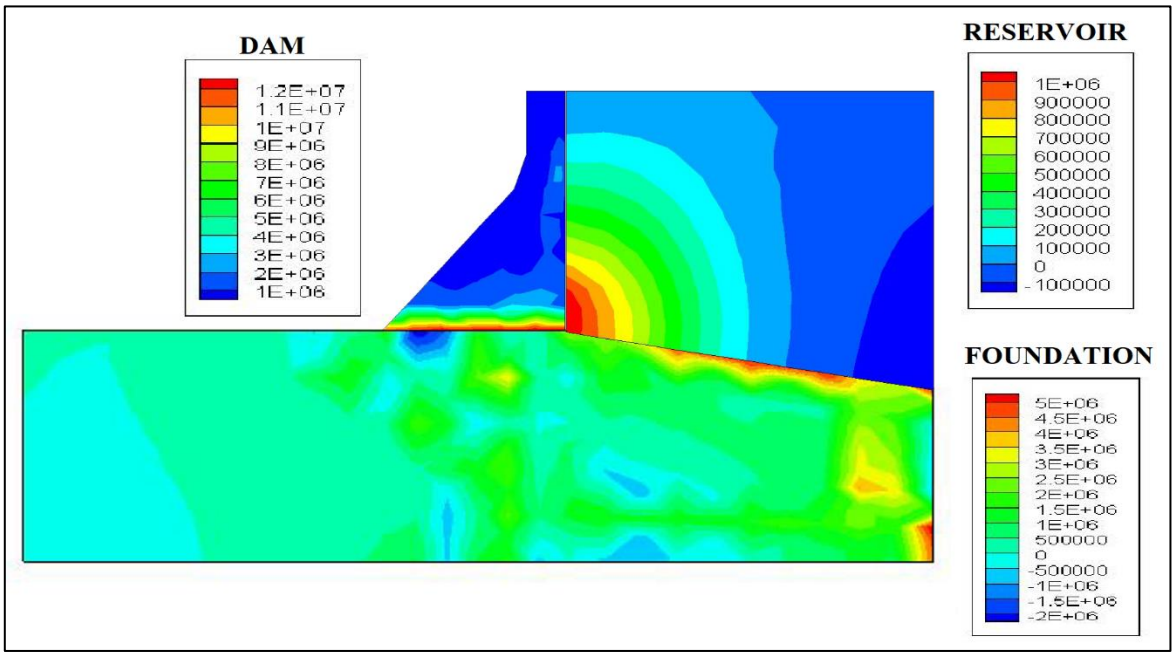

Fig. 4.127: Contour of pressure and stresses for bed slope -10^0 at 2.52 sec. due to North–South component of El-Centro earthquake

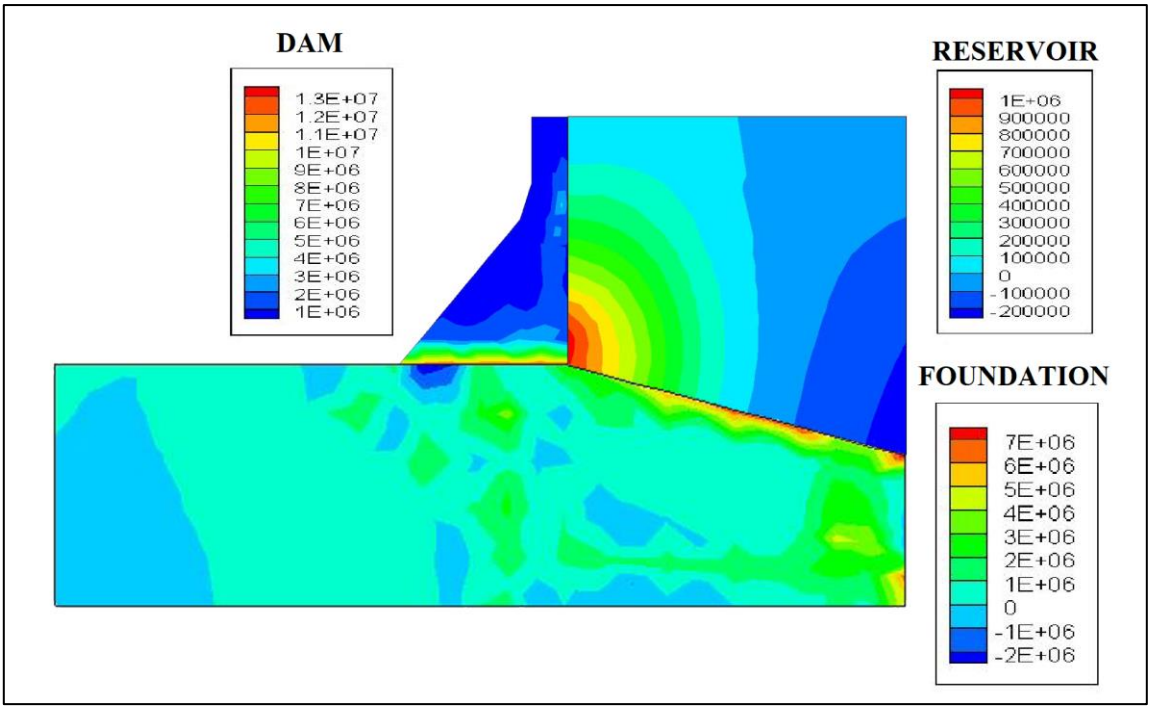

Fig. 4.128: Contour of pressure and stresses for bed slope -15^0 at 2.52 sec. due to North–South component of El-Centro earthquake

CHAPTER 5

SUMMARY AND CONCLUSIONS

5.1 SUMMARY

In Article 4.2 (section 1), variation of the hydrodynamic pressure of an unbounded reservoir adjacent to a concrete gravity dam has been studied for different geometrical parameters of the reservoir. The concrete gravity dam has been assumed as rigid. Case studies revealed that the hydrodynamic pressure at the heel of the gravity dam has steadily increased as the anticlockwise inclination of the reservoir bed went on increasing. However, the trend was reversed as the bed sloped increasingly in the clockwise sense. The length of inclination of the reservoir bed has also been found to influence corresponding hydrodynamic pressure. The hydrodynamic pressure is found to increase at the heel of the dam with an increase of the inclined length for anticlockwise slopes. However, this pressure decreases with the increase of inclined length for clockwise slopes. Significant differences have also been observed in the velocity distribution for different inclined lengths of the reservoir.

In Article 4.3 (section 2), dynamic analysis of dam-reservoir coupled systems have been studied. Here, the dam and the reservoir are coupled to a single system by the direct coupling approach. This method is state-forward and it provides response of the coupled system directly. The hydrodynamic pressure at the heel of the dam is found to increase when the dam-reservoir interaction is accounted. Similar to the analysis of the reservoir, the geometrical parameters of the reservoir have great influence on the behaviour of dam-reservoir coupled system. The hydrodynamic pressure and stresses in the gravity dam increase with gradual increment of slope of the reservoir bed if aligned anticlockwise. These responses have shown a decreasing trend with clockwise increment of reservoir bed slope. The length of inclination of the reservoir bed also has an impact on the pressure coefficient of the reservoir and the stresses of the dam. It has been observed that if the inclined length of the reservoir is increased and oriented in anticlockwise sense, the corresponding hydrodynamic pressure coefficient and stresses at the heel of the dam increase monotonically, whereas, they decreased with the increase of the inclined length of the reservoir for clockwise alignment. The hydrodynamic pressure also increases with the increase of the reflection coefficient of the reservoir bottom. It is also

interesting to note that the maximum stress in the dam occurred at the notch of the dam when it is subjected to the earthquake excitation.

In Article 4.4 (section3), the hydrodynamic pressure and responses of the concrete gravity dam have been studied by simultaneously considering dam-reservoir and dam-foundation interactions. Here, the maximum hydrodynamic pressure and maximum stress in the structure occurred at the heel of the dam. Following previous trend, the hydrodynamic pressure and stresses of the dam increase with the increase of slope angles of the reservoir bed for positive (anticlockwise) slopes. However, the hydrodynamic pressure and stresses of the dam decrease with the increase of slope angles of the reservoir bed for negative (clockwise) slopes. The stress in the foundation near the heel of the dam decreases with the increase in positive bed slope and the stress in the foundation near the heel of the dam increases with the increase in negative bed slope. Like dam-reservoir coupled systems, hydrodynamic pressure increases with the increase of the reflection coefficient.

From the present study, it is clear that when the bed slope of the reservoir is in the positive (anticlockwise) direction responses of dam and reservoir at the at the heel of the dam always increased due to an increase in slope angle and inclined length. The reservoir bed reflects the energy wave towards the gravity dam and amplifies the responses of the reservoir and the dam. From the present study, it is further observed that when the bed slope and length of the reservoir bed is incrementally increased for negative (clockwise) inclination, the hydrodynamic pressure and stresses at the heel of the dam is noticed to have decreased. Due to the inclination in negative (clockwise) direction, the reservoir bed reflects the wave further going away from the gravity dam, thus reducing the responses of the reservoir and gravity dam.

The stress of the foundation under the heel decreased with the increase of bed slope in the case of anticlockwise slope. When the reservoir bed slope is anticlockwise**,** the stiffness contribution of the foundation increases due to the increase in the volume of the soil foundation. As a result, the stresses in the foundation under the heel of the dam is reduced with anticlockwise increment of reservoir bed slope. The reverse condition occurred when the reservoir bed is aligned in clockwise direction.

In the first section of the present work, the reservoir has been analyzed considering the dam as rigid. In the following section, the dam and the reservoir are modeled using finite element technique and solved considering the fluid-structure interaction (FSI). The dam-

reservoir system has been analyzed by direct coupling approach since the sub-systems vibrate simultaneously as a single unit due to the external ground acceleration with inclined reservoir bed. Responses at the heal of the dam are improved by accounting for the fluid-structure interaction. In the last section of the work, dam-reservoir-foundation coupled systems are analyzed through direct coupling approach including fluid-structure interaction (FSI) and soil-structure interaction (SSI) along with inclined reservoir base due to dynamic excitation. A special numerical technique has been used to solve the problem. Here "added motion" approach has been used to solve the soil-structure interaction part. Free field responses have been determined by solving the foundation alone. Then added response has been determined by analyzing the fluid-structure-soil coupled system. Thereafter, the absolute responses of the coupled systems have been determined by the sum of free field responses and added responses. The whole procedure is simple and effective to solve the three sub-domains simultaneously. Finally, the responses of the dam, reservoir and the foundation have been observed for the inclined reservoir base.

5.2 CONCLUSIONS

Based on the numerical results and the observations from the present study specific conclusions are given below.

- The hydrodynamic pressure at the heel of the dam increases with the increase of bottom slope of the reservoir for positive (anticlockwise) slope angles. The main reason behind that the reservoir bed reflects the disturbing waves the towards the gravity dam for anticlockwise slope. However, the hydrodynamic pressure at the heel of the dam decreases with the increase of the reservoir bottom slope for negative (clockwise) slope angles. Because, when the reservoir bed is aligned in the negative (clockwise) direction energy content of the disturbing forces is reflected outward in the form of waves.
- The hydrodynamic pressure is also influenced by the inclined length of the reservoir bed. The pressure coefficient increases at the base of the dam with an increase in the inclined length of the reservoir for positive (anticlockwise) slopes. However, the pressure coefficient decreases at the base of the dam with an increase in the inclined length of the reservoir for negative (clockwise) slopes.

- It has been observed that hydrodynamic pressure on the concrete gravity dam increased if dam-reservoir interaction is included.
- Maximum hydrodynamic pressure occurs on the heel of the gravity dam. However, the maximum stress in the structure occurs at the notch of the dam when dam-reservoir interaction is considered.
- Stresses on the heel of the gravity dam are increased with the increase of slope angles of the reservoir bed for positive (anticlockwise) slopes. However, for negative (clockwise) bed slope, stresses at the same location decreased with the increase of bed slope.
- Principal stresses at the heel of the dam are increased with the increase of inclined length for positive (anticlockwise) slopes. However, the reverse trend is observed for negative (clockwise) slopes.
- Hydrodynamic pressure increases with the increase of the reflection coefficient of the reservoir bottom. The rate of increment is high up to 0.5 and the rate of increment is comparatively low beyond 0.5.
- Maximum stress of the dam and maximum hydrodynamic pressure occurred at the heel of the dam when dam-reservoir-foundation interaction is considered.
- Hydrodynamic pressure on the dam increases with the increase of the reflection coefficient at the reservoir bottom when dam-reservoir-foundation interaction is considered
- The maximum stress in the dam increases with the increase of reservoir bed slope for positive (clockwise) slope with horizontal direction when it is subjected to earthquake excitation and vice versa.
- The stress of the foundation under the heel of the dam decreases with an increase of slope angle for positive (anticlockwise) bed slope. However, stress at this location increases with the increase of the negative (clockwise) slope.
- Hydrodynamic pressure and stresses at the heel of the dam reduced due to negative (clockwise) slope of the reservoir bed. So, dredging can be planned accordingly for the safety and stability of the gravity dam
- Fluid-structure interaction (FSI) interaction has major impact on the dam-reservoir-foundation coupled problem. Interaction between dam and reservoir enhance the responses of the both systems. In the present study, dam-reservoir system has been analyzed by direct coupling approach.

- In the present study, added motion approach has been followed to solve the dam-foundation system. Both soil-structure and fluid-structure interaction have been included simultaneously for the analysis of dam-reservoir-foundation system through direct coupling approach to get more realistic result.

5.3 SCOPE OF FURTHER RESEARCH

The recommendation for future scope of research on this area of work is as follows:

- More studies are required on hydrodynamic pressure and responses of the gravity dam considering the surface wave.
- Hydrodynamic study is required for the different inclinations of the dam-reservoir interface with different truncation lengths of the reservoir.
- Studies are also required on dynamic analysis of dam-reservoir systems with inclined dam-reservoir interface and inclined reservoir bed.
- Dynamic analysis of the dam-reservoir-foundation coupled system with the nonlinearity of soil is required.
- Damage and safety analysis of concrete gravity dam including dam-reservoir-foundation interaction is required.
- Aging of concrete gravity dam may be included in the analysis.

REFERENCES

- Altunisik AC, Sesli H **(**2015) Dynamic response of concrete gravity dams using different water modelling approaches: Westergaard, Lagrange and Euler. Computers and Concrete 16 (3): 429-448
- Antes H, Estorff OV (1987) Analysis of absorption effects on the dynamic response of dam reservoir systems by boundary element methods. Earthquake Engineering and Structural Dynamics 15: 1023-1036
- Attarnejad R, Bagheri A (2011) Dam-reservoir interaction including the effect of vertical component of earthquake acceleration on hydrodynamic pressure. Advanced Materials Research 255-260: 3493-3499
- Avelis J, Francisco J, Sesma S (1986) Hydrodynamic pressures on dams with nonvertical upstream face. Journal of Engineering Mechanics 112: 1054-1061
- Aviles J, Li X **(**1998) Analytical numerical solution for hydrodynamic pressures on dams with sloping face considering compressibility and viscosity of water. Computers & Structures 66 (4): 481-488
- Aviles J, Suarez M **(**2010) Effects of surface waves on hydrodynamic pressures on rigid dams with arbitrary upstream face. International Journal for Numerical Methods in Fluids 62: 1155–1168
- Bathe KJ, Hahn WF (1979) On transient analysis of fluid-structure systems. Computers & Structures 10:383-391
- Bathe KJ (2009) Finite element procedures. PHI Learning Private Ltd.
- Behroozi AM, Vaghefi M (2020) Radial basis function differential quadrature for hydrodynamic pressure on dams with arbitrary reservoir and face shapes affected by earthquake. Journal of Applied Fluid Mechanics 13 (6): 1759-1768
- Bouaanani N, Poultre P, Proulx J **(**2003) A closed-form formulation for earthquake-induced hydrodynamic pressure on gravity dams. Journal of Sound and Vibration 261: 573-582
- Bougacha S, Tassoulas JL (1991) Effects of sedimentary material on the response of concrete gravity dams. Earthquake Engineering and Structural Dynamics 20: 849-858

- Burman A, Nayak P, Agrawal P, Maity D (2012) Coupled gravity dam–foundation analysis using a simplified direct method of soil–structure interaction. Soil Dynamics and Earthquake Engineering 34: 62-68
- Calayir Y, Dumanoglu AA, Bayraktar A **(**1996) Earthquake analysis of gravity dam-reservoir systems using the Eulerian and Lagrangian approaches. Computers & Structures 59 (5):877-890
- Cetin M, Mengi Y (2003) Transmitting boundary conditions suitable for analysis of dam-reservoir interaction and wave load problems. Applied Mathematical Modelling 27: 451-470
- Chandrasekhar R, Humar JL (1993) Fluid-foundation interaction in the seismic response of gravity dams. Earthquake Engineering and Structural Dynamics 22: 1067-1084
- Chavez JW, Fenves GL (1995) Earthquake analysis of concrete gravity dams including base sliding. Earthquake Engineering and Structural Dynamics 24: 673-686
- Chen BF, Hung TK (1992) Dynamic pressure of water and sediment on rigid dam. J. Eng. Mech. 119: 1411-1433
- Chen HC, Taylor RL (1990) Vibration analysis of fluid-solid systems using a finite element displacement formulation. International Journal for Numerical Methods in Engineering 29: 683-698
- Chopra AK, Chakrabarti P (1981) Earthquake analysis of concrete gravity dams including dam-water-foundation rock interaction. Earthquake Engineering and Structural dynamics 9: 363-383
- Cho Y S, Liu PF (2002) Hydrodynamic pressures acting on rigid gravity dams during earthquakes. Journal of hydraulic research 40 (2): 175-181
- Chwang AT (1979) Hydrodynamic pressure on an accelerating dam and criteria for cavitation. Journal of Engineering Mathematics 13 (2): 143-152
- Chwang AT (1981) Effect of stratification on hydrodynamic pressures on dams. Journal of Engineering Mathematics 15 (1): 49-63.
- Clough RW, Penzin J (1993) Dynamics of Structures, 2nd edn. McGraw-Hill, Inc.

- Cook RD, Malkus DS, Plesha ME, Wilt RJ (2007) Concepts and applications of finite element analysis, 4th edn. Wiley-India
- Coskun SB (2007) An exact truncation boundary condition for incompressible fluid domains in dam-reservoir interaction analysis. Engineering Structures 29: 635-639
- Das YC, Aki FA (1988) Hydrodynamic pressure on dams. International Journal of Modelling & Simulation 8 (1): 33-37
- Dastgerdi RH, Beyrag BS, Kazemi K, Malinowska A (2022) Improving seismic performance of concrete gravity dams considering hydrodynamic effect and soil-structure interaction. International Journal of Engineering Research & Technology 11 (9): 65-74
- Eftekhari SA, Jafari AA (2018) A Ritz procedure for transient analysis of dam-reservoir interaction. Iran. J. Sci. Technol.: Trans Civ. Eng
- El-Aidi B, Hall JF (1989) Non-linear earthquake response of concrete gravity dams Part 2: Behaviour. Earthquake Engineering and Structural Dynamics 18: 853-865
- Fenves G, Chopra AK (1987) Simplified earthquake analysis of concrete gravity dams. J. Struct. Eng. 113: 1688-1708
- Fenves G, Loli LMV (1988) Nonlinear dynamic analysis of fluid-structure systems. J. Eng. Mech. 114: 219-240
- Gao Y, Jin F, Wang X, Wang J (2011) Finite element analysis of dam-reservoir interaction using high-order doubly asymptotic open boundary. Mathematical Problems in Engineering 2011: 1-23
- Gao Y, Jin F, Xu Y (2019) Transient analysis of dam–reservoir interaction using a high-order doubly asymptotic open boundary. J. Eng. Mech. 145 (1): 04018119-1-14
- Gill S (1951) A process for the step-by-step integration of differential equations in an automatic digital computing machine. Mathematical Proceedings of the Cambridge Philosophical Society 47: 96-108
- Gogoi I, Maity D (2005) seismic safety of aged concrete gravity dams considering fluid-structure interaction. Journal of Earthquake Engineering 9 (5): 637-656

- Gogoi I, Maity D (2006) A non-reflecting boundary condition for the finite element modeling of infinite reservoir with layered sediment. Advances in Water Resources 29: 1515-1527
- Gogoi I, Maity D (2010) A novel procedure for determination of hydrodynamic pressure along upstream face of dams due to earthquakes. Computers and Structures 88: 539-548
- Golchin S, Atternejad R, Vahdani S (2018) Numerical uncoupling of domains in dam-reservoir problem. Shock and Vibration 2018: 1-11
- Ghorbani MA, Khiavi MP (2011) Hydrodynamic modeling of infinite reservoir using finite element method. International Journal of Civil, Environmental, Structural, Construction and Architectural Engineering 5 (8): 324-328
- Ghaemian M, Ghobarah A (1998) Staggered solution schemes for dam-reservoir interaction. Journal of Fluids and Structures 12: 933-948
- Ghaemian M, Ghobarah A (1999) Nonlinear seismic response of concrete gravity dams with dam–reservoir interaction. Engineering Structures 21: 306-315
- Gorai S, Maity D (2019) Seismic response of concrete gravity dams under near field and far field ground motions. Engineering Structures 196 (109292): 1-16
- Guan F, Moore ID, Lin G (1994) Transient response of reservoir-dam-soil systems to earthquakes. International Journal for Numerical and Analytical Methods in Geomechanics 18: 863-880
- Guttierrez JA, Chopra AK (1978) A substructure method for earthquake analysis of structures including structure-soil interaction. Earthquake Engineering and Structural Dynamics 6: 51-69
- Haghani M, Neya BN, Ahmadi MT, Amiri JV (2020) Combining XFEM and time integration by α-method for seismic analysis of dam-foundation-reservoir. Theoretical and Applied Fracture Mechanics 109 (102752): 1-17
- Hall JF, Chopra AK (1982) Two-dimensional dynamic analysis of concrete gravity and embankment dams including hydrodynamic effects. Earthquake Engineering and Structural Dynamics 10: 305-332

- Hatami K (1997) Effect of reservoir bottom on earthquake response of concrete dams. Soil Dynamics and Earthquake Engineering 16: 407-415
- Heydari MM, Mansoori A (2011) Dynamic analysis of dam-reservoir interaction in time domain. World Applied Sciences Journal 15 (10): 1403-1408
- Hojati M, Lotfi V (2011) Dynamic analysis of concrete gravity dams utilizing two-dimensional modified efficient fluid hyper-element. Advances in Structural Engineering 14 (6): 1093-1106
- Humar J, Roufaiel M (1983) Finite element analysis of reservoir vibration. J. Eng. Mech. 109 (1): 215-230
- Humaish AH, Shamkhi MS, Al-Hachami TK, Sc B (2018) Seismic performance of concrete dam-reservoir system. International Journal of Engineering & Technology 7 (4): 4873-4879
- Hung TK, Chen BF (1990) Nonlinear hydrodynamic pressure on dams. J. Eng. Mech. 116: 1372-1391
- Jain A K (2000) Fluid mechanics, 8th edn. Khanna Publishers
- Khiavi MP, Sari A (2021) Evaluation of hydrodynamic pressure distribution in reservoir of concrete gravity dam under vertical vibration using an analytical solution. Mathematical Problems in Engineering 2021: 1-9
- Kontoe S, Zdravkovic L, Potts DM (2009) An assessment of the domain reduction method as an advanced boundary condition and some pitfalls in the use of conventional absorbing boundaries. Int. J. Numer. Anal. Meth. Geomech. 33: 309-330
- Krishnamoorthy C S (2004) Finite element analysis: Theory and Programing, 2nd edn. Tata McGraw-Hill
- Kucukarslan S, Coskun SB, Taskin B (2005) Transient analysis of dam–reservoir interaction including the reservoir bottom effects. Journal of Fluids and Structures 20: 1073-1084
- Kucukarslan S (2005) An exact truncation boundary condition for incompressible-unbounded infinite fluid domains. Applied Mathematics and Computation 163: 61-69
- Li X, Romo OMP, Avails LJ (1996) Finite element analysis of dam-reservoir systems using an exact far-boundary condition. Computers & Structures 60 (5): 751-762

- Lotfi V, Roesset JM, Tassoulas JL (1987) A technique for the analysis of the response of dams to earthquakes. Earthquake Engineering and Structural Dynamics 15: 463-490
- Loli LMV, Fenves GL (1989) Effects of concrete cracking on the earthquake response of gravity dams. Earthquake Engineering and Structural Dynamics 18: 575-592
- Maity D, Bhattacharya SK (1999) Time-domain analysis of infinite reservoir by finite element method using a novel far-boundary condition. Finite Elements in Analysis and Design 32: 85-96
- Maity D, Bhattacharya SK (2003) A parametric study on fluid-structure interaction problems. Journal of Sound and Vibration 263: 917-935
- Mandal KK, Maity D (2015) Seismic response of aged concrete dam considering interaction of dam and reservoir in coupled way. Asian Journal of Civil Engineering (BHRC) 17 (5): 571-592
- Mandal KK, Maity D (2016) Transient response of concrete gravity dam considering dam-reservoir-foundation. Journal of Earthquake Engineering 00: 1-23
- Mandal KK, Maity D (2017) Performance of aged dam-reservoir-foundation coupled system with absorptive reservoir bottom. ISET Journal of Earthquake Technology 54 (1): 1-16
- Mandal KK, Maity D (2017) Seismic response of a dam-reservoir-foundation coupled system with long term ageing of dam. Dam Engineering XXVII (3): 1-30
- Mandal A, Maity D (2019) Seismic analysis of dam-foundation-reservoir coupled system using direct coupling method. Coupled Systems Mechanics 8 (5): 393-414
- Mandal KK, Aziz M (2019) An Eulerian approach for dynamic analysis of reservoir adjacent to concrete gravity dam. SN Applied Sciences 2019 (1): 709
- Medina F, Dominguez J, Tassoulas JL (1990) Response of dams to earthquakes including effects of sediments. J. Struct. Eng. 116: 3108-3121
- Miquel B, Bouaanani N (2010) Simplified evaluation of the vibration period and seismic response of gravity dam–water systems. Engineering Structures 32: 2488–2502
- Mohammadnezhad H, Ghaemian M, Noorzad A (2019) Seismic analysis of dam-foundation-reservoir system including the effects of foundation mass and radiation damping. Earthq Eng & Eng Vib 18(1): 203-218

- Mohammadnezhad H, Saeednezhad N, Sotoudeh P (2020) The effect of earthquake frequency content and soil structure interaction on the seismic behavior of concrete gravity dam-foundation-reservoir. Numerical Methods in Civil Engineering 4 (4):1-20
- Mohammadi LK, Amiri JV, Neya BN, Davoodi M (2009) Evaluation of Eulerian and Lagrangian method in analysis of concrete gravity dam including dam water foundation interaction. International Journal of Civil, Environmental, Structural, Construction and Architectural Engineering 3(10): 427-433
- Muller WC (1981) Simplified analysis of linear fluid-structure interaction. International Journal for Numerical Methods in Engineering 17: 113-121
- Neya BN, Ardeshir MA (2013) An analytical solution for hydrodynamic pressure on dams considering the viscosity and wave absorption of the reservoir. Arab. J. Sci. Eng. Vol 38: 2023-2033
- Olson LG, Bathe KJ (1985) Analysis of fluid-structure interactions: a direct symmetric coupled formulation based on the fluid velocity potential. Computers & Structures 21 (l/2): 21-32
- Papazafeiropoulos G, Tsompanakis Y, Psarropoulos PN (2011) Dynamic interaction of concrete dam-reservoir-foundation: analytical and numerical solutions. Computational Methods in Applied Sciences 21: 455-488
- Pelecanos L, Kontoe S, Zdravkovic L (2013) Numerical modelling of hydrodynamic pressures on dams. Computers and Geotechnics 53: 68-82
- Rasa AY, Budak A, Duzgun OA (2022) An efficient finite element model for dynamic analysis of gravity dam-reservoir-foundation interaction problems. Latin American Journal of Solids and Structures 19 (6): 1-21
- Saini SS, Bettes P, Zienkiewicz OC (1978) Coupled hydrodynamic response of concrete gravity dams using finite and infinite elements. Earthquake Engineering and Structural Dynamics 6: 363-374
- Samii A, Lotfi V (2007) Comparison of coupled and decoupled modal approaches in seismic analysis of concrete gravity dams in time domain. Finite Elements in Analysis and Design 43: 1003-1012

- Samii A, Lotfi V (2013) A high-order based boundary condition for dynamic analysis of infinite reservoirs. Computers and Structures 120: 65-76
- Sandberg G (1995) A new strategy for solving fluid-structure problems. International Journal for Numerical Methods in Engineering 38: 357-370
- Seghir A, Tahakourt A, G Bonnet (2009) Coupling FEM and symmetric BEM for dynamic interaction of dam-reservoir systems. Engineering Analysis with Boundary Elements 33: 1201-1210
- Sesli H, Altunisik AC (2015) Dynamic response of concrete gravity dams using different water modelling approaches: Westergaard, Lagrange and Euler. Computers and Concrete 16 (3): 429-448
- Sharan SK (1985) Finite element modeling of infinite reservoirs. Journal of Engineering Mechanics 111 (12): 1457-1469
- Sharan SK (1987) Time-domain analysis of infinite fluid vibration. International Journal for Numerical Methods in Engineering 24: 945-958
- Sharan SK (1992) Efficient finite element analysis of hydrodynamic pressure on dams. Computers and structures 42 (5): 713-723
- Sharma V, Fujisawa K, Murakami A (2019) Space-time finite element procedure with block-iterative algorithm for dam-reservoir-soil interaction during earthquake loading. Int. J. Numer. Methods Eng. 120: 263-282
- Sommerfeld A (1949) Partial Differential Equations in Physics, Academic Press. New York
- Tsai CS, Lee GC (1989) Hydrodynamic pressure on gravity dams subjected to ground motions. Journal of Engineering Mechanics 115 (3): 598-617
- Tsai CS, Lee GC, Ketter RL (1990) A semi-analytical method for time-domain analyses of dam-reservoir interactions. International Journal for Numerical Methods in Engineering 29: 913-933
- Tsai CS, Lee GC (1991) Time-domain analyses of dam-reservoir system II: Substructure method. Journal of Engineering Mechanics 117 (9): 2007-2026

- Tsai CS (1992) Semi-analytical solution for hydrodynamic pressures on dams with arbitrary upstream face considering water compressibility. Computers & Structures 42 (4): 491-502
- Tarinejad R, Pirboudaghi S (2015) Legendre spectral element method for seismic analysis of dam-reservoir interaction. International Journal of Civil Engineering, Transaction A: Civil Engineering 13 (2): 148-159
- Valliappan S, Zhao C (1992) Dynamic response of concrete gravity dams including dam-water-foundation interaction. International Journal for Numerical and Analytical Methods in Geomechanics 16: 79-99
- Vani KM, Babu KS (2017) The effect of reservoir compressibility on the earthquake performance of gravity dams. International Journal of Advances in Mechanical and Civil Engineering 4 (5): 57-62
- Wang X, Jin F, Prempramote S, Song C (2011) Time-domain analysis of gravity dam–reservoir interaction using high-order doubly asymptotic open boundary. Computers and Structures 89: 668-680
- Wang YY, Li JY, Ning BK, Zhang P (2017) Seismic response analysis of reservoir water-gravity dam-foundation system. Key Engineering Materials 737: 494-499
- Wang M, Chen J, Wu L, Song B (2018) Hydrodynamic pressure on gravity dams with different heights and the Westergaard correction formula. Int. J. Geomech. 18 (10): 04018134-1-9
- Wepf DH, Wolf JP, Bachmann H (1988) Hydrodynamic-stiffness matrix based on boundary elements for time-domain dam-reservoir-soil analysis. Earthquake Engineering and Structural Dynamics 16: 417-432
- Yang R, Tsai CS, Lee GC (1993) Explicit time-domain transmitting boundary for dam-reservoir interaction analysis. International Journal for Numerical Methods in Engineering 36: 1789-1804
- Yang Li, Zhao Mi, Xu CS, Du X Li, Li Z (2018) Earthquake input for finite element analysis of soil-structure interaction on rigid bedrock. Tunnelling and Underground Space Technology 79: 250-262

- Zhang X, Li Ze, Wu L, (2012) Dynamic finite element analysis of RCC gravity dam. Advanced Material Research 346: 75-79
- Zhao C (1994) Effects of reservoir bottom sediments on hydrodynamic pressure of gravity dams. Compurers & Strucrures 52 (2): 297-307
- Zienkiewicz OC, Bettess P (1978) Fluid-structure dynamic interaction and wave forces: An introduction to numerical treatment. International Journal for Numerical Methods in Engineering 13: 1-16
- http://www.vibrationdata.com/elcentro.htm